Understanding the role of the transcription factor MGA in primordial germ cell differentiation

Dissertation

for the award of the degree
"Doctor of Philosophy"
Division of Mathematics and Natural Sciences
of the
Georg-August-Universität Göttingen

Within the doctoral program
'International Max Planck Research School for Genome Science'
Göttingen Graduate Center for Neurosciences, Biophysics, and Molecular Biosciences (GGNB)

submitted by

Erica Calabrese

from Bologna, Italy

Göttingen, 2023

Thesis Advisory Committee

Dr. Ufuk Günesdogan
Göttingen Center for Molecular Biology, Department of Developmental Biology, Göttingen, Germany

Prof. Dr. Henning Urlaub
Max Planck Institute for Multidisciplinary Sciences, Bioanalytical Mass Spectrometry Group, Göttingen, Germany

Dr. Johannes Söding
Max Planck Institute for Multidisciplinary Sciences, Quantitative and Computational Biology, Göttingen, Germany

Members of the Examination Board

Dr. Ufuk Günesdogan (1st reviewer)
Göttingen Center for Molecular Biology, Department of Developmental Biology, Göttingen, Germany

Prof. Dr. Henning Urlaub (2nd reviewer)
Max Planck Institute for Multidisciplinary Sciences, Bioanalytical Mass Spectrometry Group, Göttingen, Germany

Further members of the Examination Board

Dr. Johannes Söding
Max Planck Institute for Multidisciplinary Sciences, Quantitative and Computational Biology, Göttingen, Germany

Prof. Dr. Heidi Hahn
University Medical Center Göttingen, Department of Human Genetics, Section of Developmental Genetics, Göttingen, Germany

Prof. Dr. Argyris Papantonis
University Medical Center Göttingen, Institute of Pathology, Göttingen, Germany

Prof. Dr. Elisabeth Heßmann,
University Medical Center Göttingen, Department of Gastroenterology, Gastrointestinal Oncology and Endocrinology, Göttingen, Germany

Date of oral examination: January 20, 2023

Science does not know its debt to imagination.

-Ralph Waldo Emerson

Acknowledgements

This long journey could not have been completed without the valuable contributions and unwavering encouragement of many people. Therefore, I would like to extend my heartfelt gratitude to all of them.

First and foremost, I would like to thank my supervisor Dr. Ufuk Günesdogan for giving me the great opportunity to carry out my PhD in his lab under his supervision. I'm really grateful that he gave me enough freedom to explore and develop my interests and ideas. He guided and encouraged me to be a better scientist. Thanks a million!

I also would like to express my gratitude to my TAC members, Prof. Dr. Henning Urlaub and Dr. Johannes Söding, as every meeting with you gave me new insight into my project and allowed me to explore new angles with your advice. A special thanks to Prof. Dr. Henning Urlaub and Dr. Ralf Planz for the collaboration and experimental support, which was essential for the completeness of my project. I would like to thank Prof. Dr. Heidi Hahn, Prof. Dr. Argyris Papantonis and Prof. Dr. Elisabeth Heßmann, who agreed to serve on my examination board.

I would like to express my gratitude to my PGC celebrities, Xiaojuan and Cera. Xiaojuan, or as I like to call her, my "Pretty woman in the morning," meeting you was one of the best parts of my PhD journey. We started this journey together, and you have become a dear friend over the years. I am grateful for the time we have spent together, the laughs, the movies, and how much I have learned from you, both scientifically and personally. As we started this journey together, it is only fitting that we finish it together while watching "Mouse hunt". Cera, you were the first person I met from the lab, and from that moment, I have appreciated your great support and friendship. We have spent countless hours in the lab together, including too many hours in cell culture, and I cherished our fun nights. I hope to see you soon. Finally, Dominik, you are a great colleague and friend, always smiling and ever helpful. Your presence always reassures me, and I value the good memories we have shared, except maybe for your love for Pfeffy. I would also like to thank all the other members of the lab, including Julia, Oleksandr and Carmela, for the good times we shared together.

I would also like to express my gratitude to everyone in the Department of Developmental Biology, particularly Prof. Ernst Wimmer, as well as the technicians and secretaries for creating such a great environment. I am grateful for my great moments with Salim, Ting, Costanza, Bibi, Georg, Gordon, Hassam, Hazem, and Noel over the last four years. I loved being part of the International Max Planck Research School for Genome Science (IMPRS-GS) in such an inspiring environment for learning and seeking advice. I would like to extend special thanks to the program coordinator, Dr. Henriette Irmer, and Frauke Bergmann, for their constant support, as well to all the members of this amazing program.

I would like to thank all my friends. My LAMA lab - Marti, Ila, Lory, and Michy - whom I met during university as we shared our passion for science. Since then, I consider you my "soul friends." Even with the distance between us, your messages and our “Skyppate” were moments of intense laughter, and it was always comforting to know we were there for each other. I cannot forget to mention my “Marpie”-Ludo and Lety. You are incredible friends, and I am always happy to share moments with you. Lastly, Niki and Je, we have known each other since we were little. Over the years, we have shared many moments in our lives, good and bad, but importantly, we have grown up together. I am very happy that you will also be part of this moment.

Finally, I would like to thank my family, with special thanks to my GrandMa. Thank you for your unconditional love and for always making me feel special. To my sister, Chiara, you are my source of inspiration. Every day, thinking about you helps me overcome the impossible. And to my lovely mom, Gigla, "Your heart is my home." I am grateful for your love and support throughout the years. You have always believed in me and encouraged me to keep going. Thank you from the bottom of my heart.

Summary

One of the most crucial cell lineage decisions in mammalian embryos is the differentiation of a few pluripotent epiblast cells into primordial germ cells (PGCs). PGCs are unique for their ability to mature into either sperm or egg, enabling species survival and transmitting genetic and epigenetic information. Remarkably, the spatiotemporal coordination of signal pathways induces a mesoderm T-box factor, T, to initiate the PGC gene expression program, diverging from the mesodermal formation. Although significant progress has been made in identifying the signal pathways, transcription factors, and chromatin remodelers involved in PGC specification, the precise molecular mechanisms leading to this exclusive lineage choice remain unknown. Therefore, it is becoming increasingly evident that novel factors are responsible for this critical cell fate determination and need to be identified.

One ideal candidate for investigating the control of gene expression during PGC differentiation is the transcription factor MGA (Max's giant-associated protein). MGA stands out as a unique transcription factor, harbouring three distinct domains (T-box, bHLH/Zip, DUF4801) and is associated with three diverse families of developmental proteins: T-box factors, MAX-interacting proteins, and Polycomb repressive complex 1.6 (PRC1.6). During early mouse development, MGA expression is observed in the epiblast cells of both pre- and post-implantation embryos, and its abrogation leads to early embryonic lethality. Therefore, considering MGA's structural properties and its essential role in the survival of epiblast cells, which give rise to various fetal cell lineages, including PGCs, it is reasonable to propose that MGA has the potential to influence the development of multiple tissues and exhibit tissue-specific functions. However, despite these properties, the specific role of MGA in PGC differentiation has never been explored.

In this study, I aim to reveal the role of the transcription factor MGA during PGC differentiation.

For this purpose, I used a well-established *in vitro* model that mimics early mouse PGC development by progressively differentiating embryonic stem cells (ESCs) into epiblast-like cells (EpiLCs) and subsequently inducing the formation of PGC-like cells (PGCLCs). Then, I employed a combination of genetic and proteomic approaches to explore the function of MGA in the context of PGC differentiation.

In Chapter 1, I present the main findings of my study. Using an auxin-inducible degron system, I show that depletion of MGA impairs PGCLC induction, further evidenced by a significant increase in the expression of meiotic genes and reduced expression of PGC markers. Indeed, CUT&RUN sequencing analysis from ESCs towards PGCLCs reveals that MGA dynamically binds to and thereby controls the expression of crucial genes involved in pluripotency, epiblast development, and germ cell formation. Furthermore, motif analysis indicates that MGA works in conjunction with pluripotency and T-box factors. Notably, among all MGA domains, the T-box domain is essential in regulating the expression of PGC-specific genes, as its deletion leads to their premature expression.

Interestingly, the MGA interactome analysis uncovers a highly dynamic network of interaction partners during PGCLC differentiation. Indeed, despite the presence of PRC1.6 members and the confirmation of

pluripotency factors only in ESCs, the data also reveal an unexpected interplay between MGA and RNA-binding proteins, suggesting that MGA may play a more complex role in regulating gene expression.

In Chapter II, I investigate the structure and function of MGA's Domain of Unknown Function 4801 (DUF4801) during PGCLC differentiation. I show that deletion of the DUF4801 domain has a significant impact on MGA's canonical binding sites, resulting in the loss and gain of genes involved in neurogenesis and endoderm fate. Consequently, despite the significant alterations observed in the transcriptome of PGCLCs, the lack of a severe phenotype strongly suggests the involvement of compensatory mechanisms in response to the deletion of the DUF4801 domain. Thus, my data suggest that the DUF4801 domain may have an impact on controlling gene expression and regulating cellular processes.

Table of Contents

Thesis Advisory Committee ***2***

Acknowledgements ***4***

Summary ***6***

Introduction ***9***

1. Primordial germ cell development **10**

1.1 Specification of primordial germ cells 11

1.2 Migration and proliferation: Phase I of epigenetic reprogramming 12

1.3 Colonization of the genital ridge: Phase II of epigenetic reprogramming 14

1.4 Sex determination and Meiosis 15

2. MGA: a dual transcription factor **17**

2.1 MGA is a unique member of the T-box gene family 17

2.2 MGA and BMP signalling 19

2.3 MGA acts as repressor of germ cell fate 20

2.4 MGA and cancer 22

3. Aim of this thesis **23**

Results ***24***

Chapter I- MGA coordinates cell-state transitions of developing mouse primordial germ cells **25**

Abstract 26

Introduction 27

Results 29

Discussion 45

Materials and Methods 48

Chapter II - Structure and function of DUF4801 domain of MGA **71**

Abstract 72

Introduction 73

Results 74

Discussion 80

Material and methods 82

Discussion ***88***

Literature ***93***

Abbreviations ***107***

Curriculum Vitae ***108***

Introduction

Numerous cell fate decisions and lineage choices are made during embryogenesis to form a whole organism. This process depends on the spatiotemporal coordination of signal pathways, sequence-specific transcription factors, and chromatin-modifying proteins, which establish a read-out of a specific gene expression program. However, such networks often induce a cellular state to differentiate into multiple different cell lineages within the same spatial and temporal windows throughout development. Therefore, understanding the molecular mechanisms that ensure the correct cell identity remains an important question in developmental biology.

In the following chapters, I will provide an overview of murine germ cell development, starting from the induction of germ cell fate in the embryo to the colonization of the genital ridge. I will highlight the unique features of germ cells with a particular focus on the signalling pathways, transcription factors, and epigenetic reprogramming involved. Then, I will discuss the role of the transcription factor MGA, which is the focus of this work, and its potential involvement during this early cell fate decision.

1. Primordial germ cell development

In mammals, the fusion of sperm and oocyte results in the generation of the zygote, a single totipotent cell, which initiates a cascade of cell divisions leading to the formation of the early blastocyst at embryonic day (E) 3.5 (Zernicka-Goetz, Morris, and Bruce 2009). Two cell populations are distinguished in the early blastocyst: the pluripotent inner cell mass (ICM) and the outer layer trophectoderm (TE). Subsequently, in the late blastocyst (E4.5), the ICM segregates into the pre-implantation epiblast (EPI) and the primitive endoderm (PE) lineages (Zernicka-Goetz, Morris, and Bruce 2009; Tang et al. 2016). The TE and PE give rise to the extra-embryonic components, including the future placenta and yolk sac, whereas the EPI generates the future foetus (Tang et al. 2016). Following implantation, the epiblast cells in the posterior region of the embryo give rise to a small cluster of cells known as primordial germ cells (PGCs), which possess the unique ability to generate gametes and pass on genetic and epigenetic information from one generation to the next (Surani 2007) (Figure1). Their differentiation is crucial to ensure the survival of species. PGC specification from epiblast cells results from a combinatorial action of signalling pathways, transcription factors, and chromatin remodelers. However, even though many of these factors were previously identified, the molecular mechanisms responsible for the unique biology of PGCs still need to be better understood.

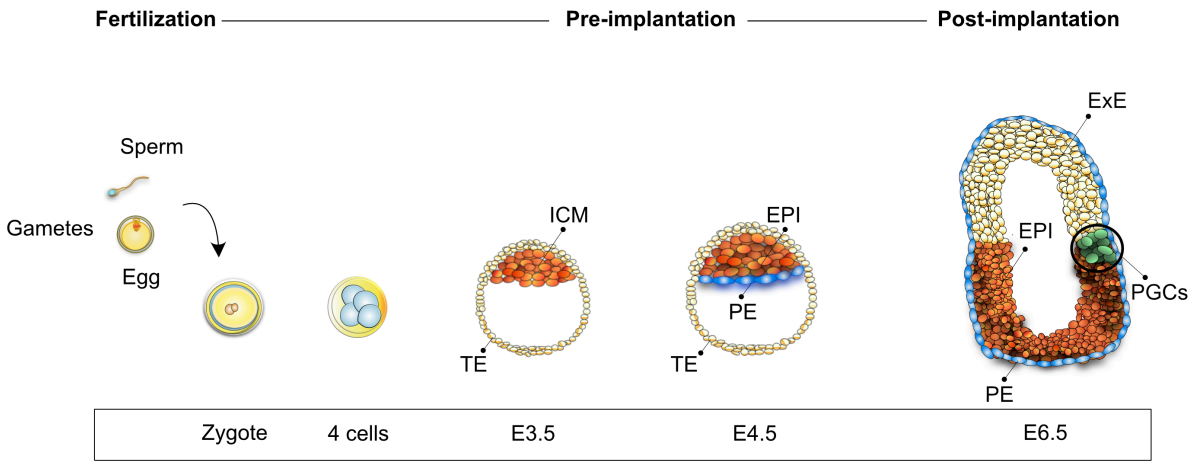

Figure 1. The origin of the mouse germline. Germ cell development in mice starts with the fertilization of the zygote, which undergoes cell division to form a blastocyst (E3.5). Then, at E4.5, the ICM segregates into EPI and TE. After implantation, the EPI gives rise to PGCs (green). EPI, epiblast; TE, trophectoderm; ICM, inner cell mass; PE, primitive endoderm; ExE, Extra embryonic ectoderm; PGCs, primordial germ cells.

1.1 Specification of primordial germ cells

The specification of PGCs between species can be categorized into two different modes: pre-formation and epigenesis. The pre-formation mechanism is based on the localization of maternal inheritance of key factors, known as germplasm in the oocyte, which drive germ cell formation in the embryo. Germ plasm or equivalent was identified in organisms such as *Caenorhabditis elegans*, *Drosophila melanogaster*, *Danio rerio* and *Xenopus laevis* (Extavour and Akam 2003). In contrast, mammals do not 'pre-determine' PGC fate but induce PGCs through extracellular signalling.

PGCs in mouse embryos were discovered as a cluster of 40 alkaline phosphatase (AP)-positive cells, originating from post-implantation epiblast cells most proximal to the extraembryonic ectoderm at E6.5 (Chiquoine 1954; Ginsburg, Snow, and McLaren 1990; Lawson and Hage 1994). The molecular network that drives PGC development includes the transcription factor BLIMP1 (encoded by Prdm1) (Mitinori Saitou, Barton, and Surani 2002; Ohinata et al. 2005). Its expression starts at around E6.25 in the proximal epiblast cells, followed by PRDM14 and AP2γ (encoded by Tfap2c) (Ohinata et al. 2005; Yamaji et al. 2008; Kurimoto et al. 2008). Conditional knockout of any of these factors in the germline results in impaired development of PGCs, demonstrating that these factors are required for PGC fate (Ohinata et al. 2005; Vincent et al. 2005; Yamaji et al. 2008; Weber et al. 2010; Kurimoto et al. 2008).

At least two signalling pathways are involved in the specification of PGCs: the BMP pathway and WNT signalling. BMP4 and BMP8b are expressed in the extraembryonic ectoderm (ExE), and their secretion toward the adjacent epiblast induces PGCs (Lawson and Hage 1990; Lawson et al. 1999). Mice lacking BMP4 and BMP8b show a complete loss of PGCs, demonstrating their essential role in PGC specification (Lawson et al. 1999; Yamaji et al. 2008; Ohinata et al. 2009; Ying, Qi, and Zhao 2001). BMP signalling acts through BMP receptors (ALK2) and/or BMP signal-transducing proteins (SMAD1, SMAD4, SMAD5) (Mitinori Saitou and Yamaji 2010). In addition to BMP signalling, WNT signalling is also involved in PGC specification, expressed in the posterior endoderm and the epiblast around E5.5-6.5. WNT3A has been proposed as essential for the epiblast's responsiveness to BMP4 (Ohinata et al. 2009; Tanaka et al. 2013).

It is technically challenging to study early PGC development, mainly due to the limited cell numbers, ~40 cells per embryo shortly after specification. Thus, an *in vitro* system was established to overcome these limitations, recapitulating PGC differentiation *in vivo*. Mouse embryonic stem cells (mESCs), derived from the pre-implantation epiblast, can differentiate into epiblast-like cells (EpiLCs), resembling cells of the early post-implantation epiblast (Hayashi et al. 2011). EpiLCs can be further differentiated into PGC-like cells (PGCLCs), which can give rise to functional sperm and egg (Hayashi et al. 2011; 2012; Hikabe et al. 2016). This *in vitro* system has provided a solid platform for characterizing the signalling principles of PGC specification (Hayashi et al. 2011; 2012), leading to new discoveries on how PGCs are specified.

It has been shown that BMP4 signalling is necessary to directly or indirectly activate WNT3 signalling, creating an appropriate context for PGC specification (Aramaki et al. 2013). WNT3A, in turn, induces the expression of the mesodermal transcription factor T (also known as Brachyury) (Aramaki et al. 2013).

T belongs to the T-box family of transcription factors required for the expression of mesodermal genes to promote the differentiation of epiblast cells into mesodermal somatic cells at E6.5 (Herrmann et al. 1990; Papaioannou 2014a). Unexpectedly, in this developmental context, T is required to activate the two germline determinants, BLIMP1 and PRDM14, binding their putative enhancers (Aramaki et al. 2013).

BLIMP1 induces the expression of AP2γ, whose expression is maintained by PRDM14. The co-expression of these three genes is sufficient to induce PGCs *in vitro,* suggesting that they are key determinants of PGC fate (Magnúsdóttir et al. 2013). This tripartite genetic network controls subsequent events required for PGC development, including the repression of somatic genes, the transient re-establishment of pluripotency, and epigenetic reprogramming (Kurimoto et al. 2008; Yamaji et al. 2008; Magnúsdóttir et al. 2013).
The re-establishment of pluripotency involves the expression of OCT4 (encoded by Pou5f1), SOX2, and NANOG in PGCs. While OCT4 expression persists throughout early embryonic development in the epiblast and PGCs, SOX2 and NANOG are first downregulated in post-implantation epiblast cells and later re-expressed in PGCs (Kurimoto et al. 2008; Yabuta et al. 2006). Consistently, conditional knockout results in the loss of PGCs through defects in apoptosis and proliferation, strongly indicating their function in maintaining PGCs (Campolo et al. 2013; Kehler et al. 2004; Yamaguchi et al. 2009; Chambers et al. 2007).
Interestingly, the overexpression of Nanog in EpiLCs is sufficient to induce PGCs by directly activating Prdm1 and Prdm14 expression independently of BMP4 (Murakami et al. 2016). *In vivo*, this could mean cooperation between BMP4 and NANOG in PGC specification (Murakami et al. 2016). However, the direct role of pluripotency factors in PGCs is still unclear.

In summary, PGC specification relies on the action of two different signalling pathways, BMP and WNT, which induce the expression of the germline determinants BLIMP1, PRDM14 and AP2γ. These three factors control the molecular events required for early PGC development. However, further work is needed to better understand the underlying molecular mechanisms.

1.2 Migration and proliferation: Phase I of epigenetic reprogramming

After PGCs are specified, they proliferate and migrate towards the developing gonads. Their migration starts from the extraembryonic mesoderm to the developing hindgut endoderm, and then finally, they reach the genital ridges by E10.5 (Molyneaux et al. 2001; Seki et al. 2007; Richardson and Lehmann 2010). During their migration, PGCs require the presence of different signals, such as the receptor tyrosine kinase C-KIT and its ligand STEEL, to guarantee their survival, proliferation and motility (Richardson and Lehmann 2010). Migration is accompanied by the first wave of epigenetic reprogramming, which entails changes in histone modifications and DNA methylation.
The first described chromatin changes that PGCs encounter at E8.0 are the global loss of the repressive histone mark H3 lysine 9 dimethylation (H3K9me2), immediately followed by a global increase of H3 lysine

27 trimethylation (H3K27me3) (Hajkova et al. 2008; Seki et al. 2005; 2007). The erasure of H3K9me2 is potentially triggered by the downregulation of GLP, known as G9a-like protein, that forms a complex with the histone methyltransferase G9a that methylates H3K9, leading to transcriptional repression (Tachibana et al. 2005). During these changes, there is a transcriptional quiescence until the complementary enrichment of H3K27me3 levels (Seki et al. 2007). In addition, PGCs exhibit an increase in the histone modifications H3 lysine 4 di-, tri-methylation (H3K4me2/3) and H3 lysine 9 acetylation (H3K9ac), as well as the repressive histone H2A/H4 arginine 3 symmetrical methylation (H2A/H4R3me2s) (Hajkova et al. 2008). The latter is due to the translocation of the protein arginine methyltransferase PRMT5 from the cytoplasm to the nucleus, where it interacts with BLIMP1 (Ancelin et al. 2006).

Notably, in concomitance with global changes in histone modifications, global DNA demethylation occurs from E8.5 onwards (Seki et al. 2005; Guibert, Forné, and Weber 2012). Whole genome bisulfite sequencing (WGBS) has revealed that methylation levels in PGCs decrease to 30% at E9.5 compared to 70% at the developmental stage E6.5, with reductions occurring in the gene body, promoters, and intergenic regions (Seisenberger et al. 2012). However, at this stage, methylation levels remain stable at retrotransposons, imprinting control regions, and germline-specific promoters in PGCs (Seisenberger et al. 2012; Guibert, Forné, and Weber 2012). Therefore, PRMT5 protects genomic integrity during DNA demethylation by repressing transposable elements (S. Kim et al. 2014) (Figure 2).

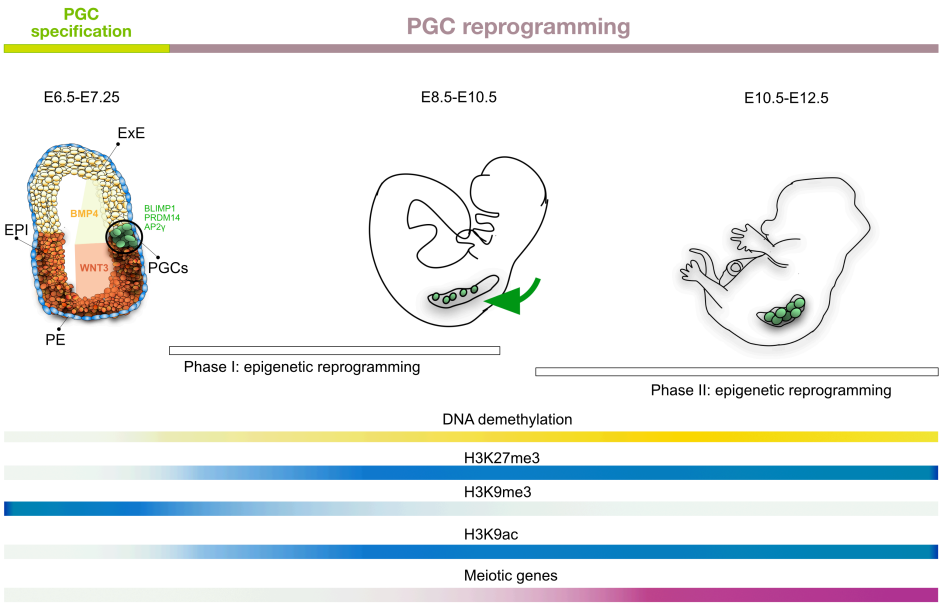

Figure 2. Epigenetic reprogramming in PGCs. A summary of the main signalling, transcriptional, and epigenetic events occurring in PGCs from E6.5 to E12.5. PGC specification occurs from E6.5 to E7.25 and results from the interplay of two signalling pathways: BMP4 secreted from ExE (yellow) and WNT3 from EPI (orange), which leads to the expression of germline tripartite factors BLIMP1, PRDM14, and AP2γ (green). After their specification, PGCs migrate (indicated by the green arrow) and proliferate during PGC reprogramming phase I (E8.5-E10.5) and phase II (E10.5-E12.5), driven by different histone modifications and changes in DNA demethylation.

1.3 Colonization of the genital ridge: Phase II of epigenetic reprogramming

The second phase of epigenetic reprogramming occurs around E11.5 when most PGCs reach the genital ridges and colonize them. The developmental stages between E10.5 and E13.5 are subject to a transient change and loss of histone modifications, primarily associated with further extensive global DNA demethylation. DNA demethylation occurs mainly at germline promoters, repetitive elements and imprinted genes (Hajkova et al. 2002; Seisenberger et al. 2012; Guibert, Forné, and Weber 2012; Hill et al. 2018). Indeed, the methylation level reached by PGCs at this developmental stage is one of the lowest points observed at any time during development (Hill, Amouroux, and Hajkova 2014). The erasure of DNA methylation at imprinted genes is necessary to properly establish parental identity, as these genes are expressed from only one parental allele (Bartolomei and Ferguson-Smith 2011).

In somatic cells, methylation of imprinted genes is maintained, except in PGCs where, at E13.5, the differentially methylated regions of genes, including Igfr2 or H19, are hypomethylated and subsequently re-established after sex-determination (Sato et al. 2003).

Two parallel mechanisms have been proposed to coordinate the global loss of DNA methylation: a passive mechanism, which involves the downregulation of DNA methyltransferases, and an active mechanism, which involves the active removal of methyl groups from DNA (Hackett et al. 2012). The passive demethylation mechanism is mainly attributed to the regulation of DNA methyltransferases, including DNMT1 (DNA methyltransferase 1). DNMT1 maintains a DNA methylation pattern during DNA replication by methylating cytosines in the newly synthesized DNA strand (Sharif et al. 2007). Although DNMT1 is expressed in PGCs, its recruiting factor UHRF1 is downregulated, suggesting that the inefficient localization of DNMT1 contributes to global DNA demethylation in PGCs (Sharif et al. 2007; Bostick et al. 2007). Additionally, the expression of the two *de novo* DNA methyltransferases (DNMT3A and DNMT3B) is repressed in PGCs from their specification until E13.5 (Kagiwada et al. 2012). This suggests that passive DNA demethylation contributes to the global DNA demethylation in PGCs.

The active DNA demethylation mechanism in PGCs is associated with the enzymatic activity of two families of enzymes. The family of ten-eleven translocation (TET1, TET2, and TET3) enzymes catalyses the oxidation of 5-methylcytosine (5mC) to 5-hydroxymethylcytosine (5hmC) and/or other derivatives (Hackett, Zylicz, and Surani 2012). These cytosines can be removed enzymatically and replaced by an unmethylated cytosine during DNA replication, as they are only poorly recognized by DNMT1 (Hackett et al. 2013; Tang et al. 2016). However, it has been proposed that TET enzymes might have only a minor role in PGCs (Hill et al. 2018; Yamaguchi et al. 2012). TET1 loss does not impair genome-wide DNA methylation in PGCs; instead, it increases methylation levels on the promoters of key germline genes, including meiotic genes and imprint control regions (Hill et al. 2018; Yamaguchi et al. 2013). These data suggest that TET proteins may play a role in demethylating specific loci instead of promoting global DNA demethylation (Hill et al. 2018).

In addition, the activation-induced cytidine deaminase (AID) family can deaminase 5hmC and be followed by T: G base excision repair by glycosylases (Popp et al. 2010). In PGCs, loss of AID leads to hypermethylation

compared to wild-type embryos (Popp et al. 2010). However, the methylation level still decreases significantly in AID mutants, suggesting that the AID demethylation process works with other active and or passive mechanisms (Matsui and Mochizuki 2014).

The loss of DNA methylation is associated with the activation of a set of germline reprogramming-responsive genes. The expression of meiotic genes, such as Ddx4, Scp3 and Dazl, is induced in PGCs between E10.5 and E11.5 (Maatouk et al. 2006) (see Figure 2). Their expression depends on the methylation level of their promoter regions. Accordingly, embryos lacking DNMT1 prematurely upregulate these methylation-dependent genes (Maatouk et al. 2006). Notably, recent studies in mESCs have reported that the promoter regions of these meiotic genes are bound by transcription factors of the Polycomb repressive complex 1.6 (PRC1.6), which I will describe in detail in section 2.3 (Stielow et al. 2018; Mochizuki et al. 2021). This might suggest that their upregulation during DNA demethylation in PGCs requires a simultaneous depletion of polycomb marks. Further investigation is needed to clarify how these results relate to the process of hypomethylation.

The second wave of epigenetic reprogramming is also associated with changes in histone modifications. During E10.5 and E11.5, the histone marks of H3K9me3 and H3K27me3, along with linker histone H1, are transiently lost but are subsequently re-established at E12.5 (Hajkova et al. 2008).

In summary, developing PGCs erase or change epigenetic information, including DNA methylation and histone modifications. DNA demethylation in PGCs is complex and likely involves a combination of active and passive processes.

1.4 Sex determination and Meiosis

Once the global wave of DNA methylation and chromatin reorganization is completed, PGCs acquire the ability to differentiate into either sperm or oocytes. This developmental process is initiated by the expression of DAZL, an RNA-binding protein, which licenses the PGCs to become gametogenesis-competent cells and triggers the onset of meiosis, a specialized cell division process that produces haploid gametes (Gill et al. 2011; Nicholls et al. 2019). Nevertheless, the timing of meiotic onset differs between the sexes, marking the beginning of sexual differentiation.

The male genital ridges initiate the development of testicular structures required for spermatogenesis via SRY, a sex-determination gene located on the Y chromosome (Koopman et al. 1991). Downstream genes, including Sox9, are upregulated by SRY and promote the differentiation of somatic precursor cells into Sertoli cells, which direct germ cell development towards the male program (Sekido et al. 2004; Sekido and Lovell-Badge 2008). FGF9, a ligand produced by Sertoli cells, suppresses meiosis by breaking down retinoic acid and inducing the expression of the germ cell-specific gene Nanos2, an RNA-binding protein (Atsushi Suzuki and Saga 2008; Barrios et al. 2010). Then starting at E13.5, Nanos2 binds to meiosis-specific mRNAs, such as Stra8 and Sycp3, and represses meiotic initiation (Atsushi Suzuki et al. 2010). Between E12.5 and E14.5, male

germ cells enter G1/G0 mitotic arrest, and after birth, XY germ cells resume mitotic proliferation and develop into spermatogonial progenitor cells (Western et al. 2008). These cells ultimately enter meiosis at puberty to complete gametogenesis (Hajkova et al. 2002).

The process of female sex specification is distinct from that of males and is initiated by the WNT/β-catenin signalling pathway (Maatouk et al. 2008). In females, the absence of SRY expression in the gonad results in the differentiation of somatic cells into pre-granulosa cells, which produce two signalling factors, WNT4 and RSPO1 (Maatouk et al. 2008; Vainio et al. 1999; Parma et al. 2006). These factors promote the female differentiation program by downregulating Sox9 in surrounding somatic cells (Chassot et al. 2008; Y. Kim et al. 2006). By E13.5, female germ cells begin downregulating pluripotency markers and entering meiosis, expressing genes essential for this process between E12.5 and E16.5 (Pesce et al. 1998). Stra8 is one of the first genes expressed and is essential for entering meiosis as mice are infertile in its absence (Baltus et al. 2006; Anderson et al. 2008). At E13.5, two proteins involved in meiotic prophase I, Sycp3 and Rec8, are expressed, marking the start of this phase (Syrjänen, Pellegrini, and Davies 2014). During meiotic prophase I, female germ cells condense, pair, and recombine their homologous chromosomes until they arrest in the diplotene stage (X. Wang and Pepling 2021). At puberty, they resume meiosis, complete the first division, separate the homologous chromosomes, and then arrest again in metaphase II. The second meiotic division is only completed after fertilization, resulting in haploid germ cells (Handel and Schimenti 2010).

2. MGA: a dual transcription factor

The cooperation of different families of transcription factors is the driving force in establishing gene expression during PGC differentiation. Transcription factors bind specific DNA sequence motifs embedded in chromatin, such as promoters and enhancers, via specific domains. Therefore, the amino acid sequence homology of the protein domains has been used to classify them into different families and unveil their putative functions. The transcription factor MGA (Max's giant associated protein), which is the focus of this thesis, has a complex structure and belongs to three families of proteins. These families are known to control gene expression during cell differentiation towards PGCs, which will be described in the next sections.

2.1 MGA is a unique member of the T-box gene family

Members of the T-box gene family are transcription factors which control a cascade of gene expression events required for various developmental processes and lineage specification (Papaioannou 2014b). All members harbour a conserved T-box domain, which binds DNA sequences known as T-box binding elements (TBE). Subsequently, they may act as transcriptional activators, repressors, or both. Moreover, the T-box domain not only binds DNA but also facilitates the interaction with chromatin remodelers such as histone methyltransferases, demethylases, acetyltransferases and deacetyltransferases, regulating the permissiveness of the chromatin environment (Beisaw et al. 2018; Istaces et al. 2019; M. D. Lewis et al. 2007; Miller et al. 2008; Miller, Mohn, and Weinmann 2010). Studies *in vivo* highlighted the importance of these proteins in diverse processes, including cell proliferation, migration, cell fate and tissue morphogenesis, as their loss often results in embryonic lethality (Papaioannou 2014a). As an example, the founding member of this family, T/Brachyury, was discovered in mouse by the short-tailed heterozygous phenotype, while homozygous mutants were not viable (Stott, Kispert, and Herrmann 1993). T is required for the proper specification of mesoderm during gastrulation (Kispert 1995). However, as described in section 1.1, in the post-implantation epiblast, T also activates the expression of crucial germline determinants to ensure PGC specification (Aramaki et al. 2013). It is important to note that embryos lacking T show an initial expression of BLIMP1, although they failed to express PRDM14 and do not form PGCs (Aramaki et al. 2013). This led to the hypothesis that another T-box factor, expressed from E6.25 onward, could also be required for the initial up-regulation of germline determinants (Aramaki et al. 2013). Several lines of evidence suggest that one possible T-box factor involved in this context could be MGA.

MGA is a very large and complex transcription factor of ~300 kDa characterized by two heterotypic DNA binding domains (Hurlin et al.,1999). Therefore, MGA belongs not only to the T-box gene family but also to

the conserved family of the MAX interacting network. The MAX interacting network comprises the MYC family of oncoproteins and a group of MYC antagonists such as MNT and MXD1-4. These proteins control many aspects of cell behaviour, including cell proliferation and tumorigenesis (Hurlin and Huang 2006; Amati et al. 1993). To act as transcription factors, these proteins heterodimerize with the small basic helix-loop-helix leucine zipper (bHLH/Zip) protein, MAX, which is required for their specific DNA binding to E-box sequences (Hurlin and Huang 2006). MGA was first identified in a screening for interaction partners of MAX in mice, as it harbours the same bHLH/Zip DNA-binding dimerization domain in the C-terminal region (Hurlin et al., 1999). The bHLH/Zip domain makes MGA unique among the T-box genes, which generally only have a single central T-box domain suggesting it might control gene expression of various biological processes.

In mouse embryos, MGA expression is along with some members of the T-box family, such as T, EOMES and TBX3, as well as MAX (Figure 3) (Papaioannou 2014b; Shen-Li et al. 2000). During mouse pre-implantation at E3.5, the ICM is characterized by the expression of MGA, TBX3, and MAX, while the TE expresses EOMES and MAX (Yoshikawa et al. 2006; Shen-Li et al. 2000; Russ et al. 2000; Showell, Binder, and Conlon 2004; 2004). Following implantation at E6.5, MGA is highly expressed only in epiblast cells, and its expression overlaps with T and EOMES in the posterior proximal epiblast, which is the embryonic location where PGC specification occurs (Yoshikawa et al. 2006; Shen-Li et al. 2000; Russ et al. 2000; Showell, Binder, and Conlon 2004; Papaioannou 2014b). T and EOMES are also expressed in ExE, while TBX3 is presented in extraembryonic endoderm (ExEn). MAX expression is maintained in all embryonic and extraembryonic structures (Russ et al. 2000; Shen-Li et al. 2000). At E7.5, MGA expression is still limited to epiblast cells, while EOMES was found in the chorion, T in the core of the allantois, primitive streak and node, TBX3 in the developing yolk sac and MAX is still widely expressed in all tissues (Burn et al. 2018; Papaioannou 2014b; Shen-Li et al. 2000).

During organogenesis (E8.5-E10.5), MGA and MAX are widely expressed in various structures such as the nervous system, reproductive systems, heart, and limbs (Hurlin et al., 1999). MGA's constant expression in epiblast cells, the precursors of PGCs and other somatic cell types, indicates that MGA plays a crucial role in early embryonic cell fate decisions and potentially has a role in PGCs specification.

Deletion of Mga causes peri-implantation lethality in embryos between E3.5 and E6.5. Although Mga null embryos develop into a blastocyst with PE, the epiblast cells undergoes apoptosis (Washkowitz et al. 2015; Burn et al. 2018). Interestingly, the Mga mutant phenotype is similar to the deletion of pluripotency factors, such as Pou5f1 (encoded by OCT4) and Sox2 (Nichols et al. 1998; Avilion et al. 2003), which are also essential in maintaining PGCs as discussed in section 1.1. Despite this, Mga mutants still express pluripotency genes. However, the increase in apoptosis leads to embryonic lethality caused by the defective development of the ICM and EPI (Washkowitz et al. 2015). Similarly, *in vitro*, mESCs lacking Mga display a growth defect, exhibiting impaired self-renewal and spontaneous differentiation to primitive endoderm (Washkowitz et al. 2015; Qin et al. 2021).

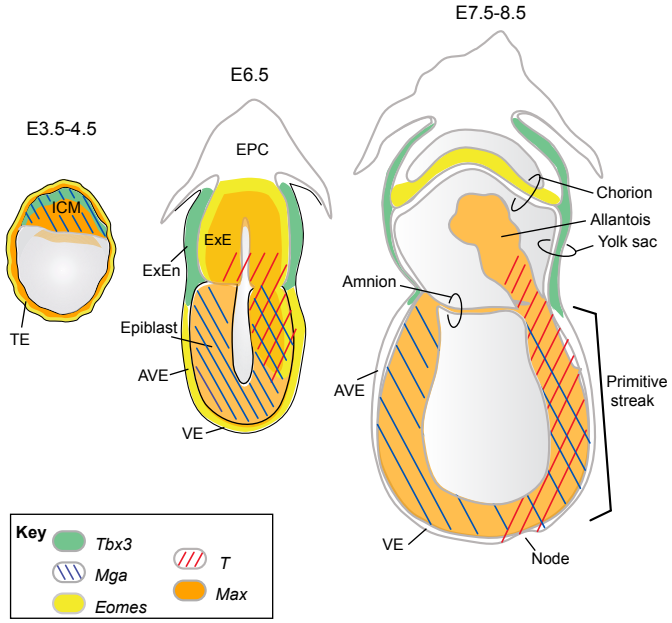

Figure 3. Expression profile of T, TBX3, EOMES, MGA and MAX during mouse pre- and post-implantation embryo development. The figure depicts the expression pattern in various embryonic structures such as AVE (anterior visceral endoderm), EPC (ectoplacental cone), ExE (extraembryonic ectoderm), ExEn (extraembryonic endoderm), ICM (inner cell mass), TE (trophectoderm), and VE (visceral endoderm). This figure is adapted from Papaioannou 2014.

2.2 MGA and BMP signalling

The Mga gene is highly conserved among vertebrates and its mRNA is maternally deposited in zebrafish oocytes, where it is expressed during embryogenesis in the anterior regions (Rikin and Evans 2010). Depletion of Mga through morpholino-mediated gene knockdown revealed its essential role in organogenesis, as it led to defects in brain, heart, and gut development (Rikin and Evans 2010). During zebrafish embryonic gastrulation, it was discovered that MGA forms a complex with SMAD4 and MAX to modulate BMP signalling (Sun et al. 2014). Additionally, MGA is localized not only in the nucleus but also in the cytoplasm, where it associates with BS69, a protein that selectively recognizes the histone variant H3.3 lysine 36 trimethylation (H3.3K36me3), thereby modulating RNA Polymerase II elongation (Guo et al. 2014). MGA antagonizes BS69 to promote BMP signalling activity (Sun et al. 2018).

These findings suggest that MGA may play a crucial role in controlling BMP signalling, which is also essential for PGC specification in mice. Furthermore, the presence of MGA in the cytoplasm suggests that it may have an independent role in addition to its DNA-binding activity.

2.3 MGA acts as repressor of germ cell fate

MGA, together with MAX, was purified with epigenetic factors such as PCGF6, RING1A/B, YAF2, L3MBTL2, CBX3, and the transcription factor E2F6 (Gao et al. 2012). Components of this complex were classified as members of the non-canonical Polycomb repressive complex 1.6 (ncPRC1.6) (Ogawa et al. 2002; Gao et al. 2012). In detail, Polycomb group (PcG) proteins play a fundamental role in controlling gene expression during development. The first PcG gene was discovered in *Drosophila,* and it was shown to be required for stable repression of Hox genes (Lewis,1947; E. B. Lewis 1978). Mutations in PcG genes lead to a homeotic transformation of anterior segments into posterior ones, demonstrating the essential role of Polycomb in preventing incorrect body segmentation (E. B. Lewis 1978). Subsequent genetic screening has expanded the list of annotated PcG genes that exhibit similar homeotic transformations (Jurgens,1985; Duncan,1982;Kennison 1995). In mammals, the number of PcG orthologs has increased, although their major role as regulators during development is conserved across species (Schuettengruber et al. 2017).

PcG proteins exert different molecular activities in two large multiprotein complexes: Polycomb repressive complex 1 (PRC1) and PRC2 (Margueron and Reinberg 2011). In mammals, the different complexes are defined by conserved core subunits that post-translationally modify histones. PRC1 catalyses mono-ubiquitination of Lys 119 of H2A (H2AK119ub1) through E3 ligase activity, whereas PRC2 has a methyltransferase activity and catalyses H3K27me1/2/3. Furthermore, PRC1 and PRC2 core components interact with a heterogeneous group of auxiliary proteins, forming different sub-complexes (Blackledge and Klose 2021). As a result of their highly variable composition, they have been classified as canonical PRC1 (cPRC1) and non-canonical PRC1 (ncPRC1) (Gao et al. 2012; Hauri et al. 2016).

One unconventional PRC1 variant is the ncPRC1.6 complex, considered a germ-cell-specific epigenetic regulatory complex (Bajusz et al. 2019).Therefore, at least five of its subunits, including MGA, have already been connected to repress meiotic genes (Bajusz et al. 2019).

Meiosis is a crucial event of sexual reproduction. While somatic cells and germ cells undergo mitosis to increase their cell number, only germ cells switch their cell division from mitosis to meiosis to generate haploid cells (Ginsburg, Snow, and McLaren 1990b). As mentioned in section 1.3, meiotic genes, such as Dazl, Sycp3 and Ddx4, are transcriptionally activated after erasing genomic DNA methylation in PGCs between E10.5 and E11.5 (Maatouk et al. 2006). PGCs are licensed by DAZL, an RNA-binding protein, to become sexually differentiating germ cells. However, the expression of meiotic genes in PGCs is also associated with global chromatin reorganisation. Deletion of RING1B, a component of the PRC1.6 complex, induces precocious up-regulation of a subset of female meiotic prophase genes such as Stra8, Sycp3, Rec8, and Hormad2, in PGC development between E10.5 and E11.5, which are normally expressed from E13.5.

Therefore, RING1B is a regulator that coordinates the timing of sexual differentiation of female PGCs (Yokobayashi et al. 2013).

Consistently, knockout of PCGF6, L3MBTL2, MAX, E2F6 or MGA in mESCs showed upregulation of meiotic genes. However, the high expression level of these genes were not as strong as those associated with MGA-null ESCs (Maeda et al. 2013; Ayumu Suzuki et al. 2016; Endoh et al. 2017; Qin et al. 2021; Dahlet, Truss, Frede, Adhami, et al. 2021). Studies on genomic binding sites have revealed that MGA and E2F6 are essential for PRC1.6 occupancy at meiosis-related genes (Endoh et al. 2017; Stielow et al. 2018; Dahlet, Truss, Frede, Adhami, et al. 2021). Indeed, both MGA domains are directly involved in distinct binding sets of meiotic genes. In particular, the bHLH/Zip domain is required for repressing Meiosin, which, together with Stra8, is required for meiosis entry in the late stage of PGC development (Uranishi et al. 2021).
The importance of the PRC1.6 complex in repressing meiotic genes in mESCs is well-established. Additional studies on some members of this complex were conducted during different stages of germ cell differentiation, which are listed below.

1) PGCF6: The genetic ablation of PCGF6 showed a severe phenotype only in mESCs and EpiLCs, including growth defects and cell death, which were not reported in PGCLCs (Endoh et al. 2017). PCGF6 is also highly expressed in the testis, and its knockdown alters male germ cell differentiation (J. Sun et al. 2015). In addition, PCGF6 interacts with the testis-specific protein HSPA2, suggesting an important role in modulating male germ cell proliferation and differentiation (J. Sun et al. 2015).
2) L3MBTL2: In testis, L3MBTL2 is highly expressed, and its mutation leads to decreased sperm counts, abnormal spermatozoa, and increased germ cell apoptosis in mice (Meng et al. 2019). Surprisingly, this was not accompanied by a significant change in the transcriptional activity linked to spermatogenesis but by DNA damage and synapsis during meiosis I (Meng et al. 2019).

3) CBX3 (HP1): Loss of CBX3 results in impaired cell cycle progression and, consequently, a lower number of PGCs, while the gene expression profile in germ cells is unaffected (Abe et al. 2011).

In view of these current findings, the role of each component of PRC1.6 is crucial in maintaining the germline. For this reason, I hypothesize that MGA could also play an important role in the development of PGCs.

2.4 MGA and cancer

The role of MGA has also been investigated in the context of tumorigenesis. Its genetic alterations are prevalent in various tumours, such as chronic lymphocytic leukemia, lung cancer, and colorectal cancer (Cancer Genome Atlas Network et al. 2018). In colorectal cancer, MGA acts as a tumour suppressor with members of the ncPRC1.6 complex (Mathsyaraja et al. 2021). Notably, using protein domain databases, a third conserved domain between 1040-1080 ammino acid (aa) of an unidentified function named DUF4801 was revealed, in addition to its N-terminal T-box domain and C-terminal bHLH/Zip. The DUF4801 domain was identified as a linker between MGA and PRC1.6 members (Mathsyaraja et al. 2021). Therefore, during malignant progression, MGA perturbation leads to the upregulation of growth and pro-invasive PRC1.6, MYC and E2F targets. However, most of these studies are associated with the bHLHL/Zip domain activity, not the T-box domain, suggesting that further studies need to be considered to better understand the role of MGA as a tumour suppressor (Mathsyaraja et al. 2021).

3. Aim of this thesis

During development, transcription factors are crucial in orchestrating specific gene expression programs to ensure the correct cell-lineage fate to form a complex multicellular organism. Specifically, in the early post-implantation embryo, epiblast cells differentiate into primordial germ cells (PGCs), essential for reproduction. PGC specification occurs through a remarkable act of the mesoderm T-box factor, T, which initiates the PGC genetic program instead of activating mesodermal fate. However, the molecular mechanism that drives this cell fate decision remains poorly understood, suggesting the presence of new factors that need to be identified.

One transcription factor that may shed some light on how PGC are specified is MGA.
MGA is a unique transcription factor with complex structural properties, as it is part of three families of developmental proteins such as T-box, MAX-interacting proteins and Polycomb repressive complex (PRC1.6). As part of these, it has been suggested that MGA controls different biological processes. Specifically, in the post-implantation embryo, MGA is expressed in epiblast cells where PGCs occur with T-box members such as T and EOMES. Its abrogation demonstrated that it is crucial for the survival of the epiblast cells. However, previous studies only focused on its role as a repressor of meiotic genes and safeguarding pluripotency in embryonic stem cells, leaving its role in other developmental processes completely unknown.

Based on these initial observations, in this thesis, I set out to analyse the role of MGA in PGC differentiation. To achieve this goal, I used an *in vitro* system to recapitulate mouse PGC differentiation *in vivo*. Then, to understand how MGA regulates cell state transition, I applied genetic and proteomic approaches to identify its genomic binding sites and interactors partners.

Results

Chapter I: MGA coordinates cell-state transitions of developing mouse primordial germ cells

Page 25

Chapter II: Structure and function of DUF4801 domain of MGA

Page 71

Chapter I- MGA coordinates cell-state transitions of developing mouse primordial germ cells

In this manuscript, I presented the majority of data gathered during my PhD. I investigated the role of the transcription factor MGA using an *in vitro* system to recapitulate PGC differentiation *in vivo*. Several genetic and proteomic approaches were used to identify MGA binding sites and interactome. We investigate how the absence of MGA, using an auxin-inducible system, affects phenotype and transcriptome during PGC differentiation.

Authors

Erica Calabrese, Xiaojuan Li, Ralf Pflanz, Henning Urlaub, Ufuk Günesdogan

Status

in preparation for submission at '*Molecular cell*, *Nature Communications*'

My contributions

- Contribution to the conceptualisation of the project[1]
- Preparation and conduction experiments[2]
- Preparation or modification of figures
- Data analysis[3]

[1] Together with Dr. Ufuk Günesdogan

[2] Excluding of mass spectrometry data performed in collaboration with Prof. Dr. Henning Urlaub and Dr. Ralf Planz

[3] Excluding of T-box RNA-seq, CUT&RUN ESCs-EpiLCs, Auxin RNA-seq ESCs and EpiLCs bioinformatic analysis performed by Xiaojuan Li

Title: MGA coordinates cell-state transitions of developing mouse primordial germ cells

Authors: E. Calabrese[1], X. Li[1], R. Pflanz[2], H. Urlaub[1,2], U. Günesdogan[1,3,*]

Affiliations:

[1] University of Göttingen, Göttingen Center for Molecular Biosciences, Department of Developmental Biology; Justus-von-Liebig Weg 11, 37077 Göttingen, Germany

[2] Max Planck Institute for Multidisciplinary Sciences, Department for Bioanalytical Mass Spectrometry; Am Fassberg 11, 37077 Göttingen, Germany

[3] Max Planck Institute for Multidisciplinary Sciences, Department for Molecular Developmental Biology; Am Fassberg 11, 37077 Göttingen, Germany

[*] Corresponding author: ufuk.guenesdogan@uni-goettingen.de

Abstract

Primordial germ cells (PGCs) possess a unique ability to ensure lifelong reproduction and heredity through their differentiation into germ cells. However, despite the remarkable role of the mesoderm T-box factor T in PGC specification, the molecular mechanism underlying this lineage choice remains poorly understood.

Our study demonstrates that the transcription factor MGA, a member of the T-box factors and part of the polycomb repressive complex 1.6 (PRC1.6), plays an essential role in targeting and initiating the cell state transition required for PGC specification. During the differentiation of PGC-like cells (PGCLCs), MGA ensures cell fate transitions by regulating specific cell-type genes and interacting dynamically with proteins such as the core of pluripotency, PRC1.6 factors, and potentially RNA-binding proteins.

Using the auxin-inducible degron system during PGCLC differentiation, we demonstrate that MGA stably represses meiotic genes conjunction with PRC1.6 members. Notably, the absence of MGA led to impaired PGCLC development, as evidenced by a notable increase in the expression of meiotic genes and a reduction in the expression of PGC targets, including Prdm1, Prdm14, and Nanog. These targets, along with T-box factors, are directly regulated by MGA.

Our findings shed light on the role of MGA during PGCLC differentiation and undercover its significance in inducing PGC specification.

Introduction

The family of T-box transcription factors are required for early cell fate decisions and for defining specific gene expression patterns during various stages of development (Papaioannou 2014a). The T-box domain recognizes DNA sequences known as T-box binding elements (TBEs). Despite the presence of the T-box domain, the T-box factors differ in many aspects, such as their structure, interactors and transcriptional activity (Beisaw et al. 2018; Istaces et al. 2019; M. D. Lewis et al. 2007; Miller, Mohn, and Weinmann 2010; Miller et al. 2008; Wehn et al. 2020).

One of the early cell fate decisions during development regulated by a T-box factor is the specification of primordial germ cells (PGCs). In the post-implantation mouse embryo, the specification of primed pluripotent epiblast cells to PGCs is mediated by graded BMP and WNT signalling inducing the T-box factor T (also known as BRACHYUURY) (Aramaki et al. 2013; Ohinata et al. 2009). Strikingly, instead of activating mesodermal genes, T activates the expression of key germline determinants such as BLIMP1 (encoded by *Prdm1*) and PRDM14, which shortly after induce the expression of AP2ɣ, encoded by *Tfap2c* (Aramaki et al. 2013; Magnúsdóttir et al. 2013). Following the specification, PGCs regain a pluripotency network, suppress somatic lineage genes, undergo epigenetic remodelling, and develop germ cells (M. Saitou and Yamaji 2012). The genome-wide epigenetic changes include global DNA demethylation, which results in the expression of DNA methylation-dependent genes, such as *Dazl* and *Mvh* (Hackett, Zylicz, and Surani 2012; Hackett et al. 2012). In particular, the expression of DAZL, an RNA-binding protein, is essential to lead the acquisition of meiotic and gametogenic competence for sperm or oocytes, respectively (Gill et al. 2011; Nicholls et al. 2019).
Although much progress has been made in identifying signal pathways, transcription factors, and chromatin remodelers involved in PGC specification, the precise molecular mechanisms leading to this exclusive lineage choice remain unknown. Prevailing PGC specification models suggest that another T-box factor binds to the regulatory region of BLIMP1 and PRDM14, as T mutant embryos still showed their weak activation (Aramaki et al. 2013). One less characterised member of the T-box gene family, the transcription factor MGA (Max's giant associated protein), could play a role in this process.

MGA is a transcription factor of ~300 kDa characterised by the presence of two heterotypic DNA binding domains, T-box and basic helix-loop-helix leucine zipper (bHLH/Zip), and interaction with different groups of proteins (Hurlin et al., 1999.; Gao et al. 2012), indicating involvement in distinct biological process. MGA heterodimerises with MAX, which is required for genomic binding to the E-box motif via their bHLH/Zip domains to regulate genes involved in cell renewal and proliferation (Shen-Li et al. 2000,Blackwood & Eisenman,1991). In mouse embryonic stem cells (ESCs), both domains bind to largely distinct sets of genes associated with meiosis. In particular, the bHLH/Zip domain is required for repressing *Meiosin*, which

together with *Stra8* is required for meiosis entry (Uranishi et al. 2021). MGA and MAX, together with RYBP, PCGF6, E2F6, L3MBTL2, CBX3, RING1A/B, WDR5, HDAC1 and HDAC2, are part of the non-canonical Polycomb repressive complex, PRC1.6. In ESCs, MGA depletion leads to a loss of expression of pluripotency genes and up-regulation of mesoderm and germ cell genes, including *Dazl* and *Mvh* (Washkowitz et al. 2015; Qin et al. 2021). The disruption of other core subunits of PRC1.6, such as PCGF6, MAX, L3MBTL2 and E2F6, shows a similar phenotype but less severe than MGA (Endoh et al. 2017; Maeda et al. 2013; Ayumu Suzuki et al. 2016; Qin et al. 2012; Dahlet, Truss, Frede, Al Adhami, et al. 2021; Qin et al. 2021). In ESCs, a particular set of germline genes is repressed via RING1A-dependent H2AK119ub1 and SETDB1-mediated H3K9me3 deposition. In epiblast-like cells (EpiLCs), which are induced from ESCs and represent the post-implantation epiblast (Hayashi et al. 2011), deposition of H3K9me3 and *de novo* DNA methylation is dependent on MGA binding, suggesting that PRC1.6 engagement at germline gene promoters anticipate DNA methylation (Mochizuki et al. 2021).

MGA expression is first detected in the inner cell mass of pre-implantation embryos (Washkowitz et al. 2015). After implantation, MGA is expressed in the epiblast of the post-implantation embryo together with other T-box members such as T and EOMES (Papaioannou 2014a). Null mutations in *Mga* lead to the loss of epiblast cells, causing peri-implantation lethality (Washkowitz et al. 2015; Burn et al. 2018; Qin et al. 2021). However, the potential role of MGA during PGC specification and subsequent differentiation has never been explored.

Here, we aimed to investigate the function of MGA during the *in vitro* differentiation of ESCs to PGC-like cells (PGCLCs) using genetic and proteomic approaches. Our results show that MGA dynamically maintains the correct cell-type specific gene programs during PGC differentiation through its binding sites and interactions with different proteins. We demonstrate that MGA is critical to ensure PGC specification by targeting their determinant genes through its T-box domain, cooperating with T-box factors. Therefore, using an auxin-inducible degron system, the deletion of MGA results in impaired PGCLCs with misregulation of germ cell genes. MGA acts with pluripotency factors and members of PRC1.6 to maintain pluripotency and repress meiotic genes. Moreover, at the late stage of PGCs, the MGA interactome revealed high enrichment of RNA-binding proteins, leading to the assumption of its possible role not only in controlling DNA but also RNA.

Results

MGA is expressed during PGC differentiation *in vitro* and *in vivo*

We first investigated the expression pattern of MGA in PGCs using a combination of *in vitro* and *in vivo* analyses. The *In vitro* system, designed to replicate early mouse PGC development, is achieved by differentiating ESCs, harbouring a transgenic Blimp1-mEGFP reporter (Ohinata et al. 2005), into EpiLCs and subsequently inducing the formation of PGC-like cells (PGCLCs) within embryoid bodies (Hayashi et al. 2011) (Supplementary Fig. 1A). For subsequent analyses, the resulting PGCLCs were sorted by fluorescence-activated cell sorting (FACS) based on the mEGFP reporter (Supplementary Fig. 1B).

Immunofluorescent stainings revealed that MGA is expressed in the nuclei of ESCs and EpiLCs (Supplementary Fig. 1C). As PGCLCs underwent differentiation, MGA progressively colocalizes with PGC markers, SOX2 and AP2ɣ, in the early and late days of PGCLC differentiation (Supplementary Fig. 1C). However, it is worth noting that MGA expression is not restricted exclusively to PGCs, as we can also detect its expression in somatic cells (Supplementary Fig. 1C). Consistently, performing RNA-seq on ESCs, EpiLCs, and PGCLCs at day 6 (d6) of differentiation showed that MGA transcripts were highly abundant in all three cell types (Supplementary Fig. 1D), indicating a consistent expression pattern of MGA through PGCLC differentiation. *In vivo*, d6 PGCLCs correspond to early PGCs at the onset of epigenetic reprogramming at ~E9.5 (Hayashi et al. 2011). Therefore, we confirmed MGA expression in late PGCs by staining embryonic gonads at E10.5 and E11.5 (Supplementary Fig. 1E). In addition, published single-cell RNA-seq data from E6.5 to E12.5 PGCs confirmed the expression of MGA in early and late PGCs *in vivo* (Supplementary Fig. 1F) (Magnúsdóttir et al. 2013).

Thus, our results demonstrate that MGA is progressively expressed during PGC differentiation, including the developmental time window when epigenetic reprogramming occurs.

MGA directly controls expression of cell-type specific genes in PGCLC differentiation

To understand MGA's regulatory events during cell state transitions from ESCs towards PGCLCs, we conducted a genomic binding analysis using CUT&RUN (Skene and Henikoff 2017) in ESCs, EpiLCs, and d1 PGCLCs. Our analysis revealed that MGA binds promoter, intronic and intergenic regions predominantly in all three cell types (Fig. 1A). Notably, a subset of MGA-bound sites is unique to each cell type (Fig. 1B). This is particularly evident at the transcription start sites (TSSs) +/-1kb of PGCLCs showing a dynamic binding pattern (Fig. 1C).

Next, we performed Gene ontology (GO) analysis with genes bound by MGA. Genes associated with MGA-bound promoters were associated with GO terms such as *stem cell population maintenance* and *regulation of meiotic cell cycle* in all three cell types (Supplementary Fig. 2A), consistent with previous studies in ESCs (Stielow et al. 2018; Qin et al. 2021; Uranishi et al. 2021). Interestingly, in d1 PGCLCs, MGA is associated with genes involved in the *regulation of Wnt signalling pathway* and *regulation of stem cell differentiation*. In contrast, genes within the GO term *Germ cell development* and *regulation of reproductive processes* were enriched in ESCs and EpiLCs, but not in d1 PGCLCs. Additionally, MGA-bound intergenic regions revealed enrichment for genes in GO terms such as *mesoderm development, gastrulation* and *cell fate commitment* in all three cell types. However, the GO term *BMP signalling* pathway was only enriched in ESCs and PGCLCs (Supplementary Fig. 2B). This data suggests that MGA is involved in pluripotency maintenance and differentiation processes, including germ cell development, by controlling cell type-specific but also a common set of genes during PGC differentiation.

To identify cell-type specific genes controlled by MGA, we integrated CUT&RUN peaks at promoter regions with RNA-seq data on ESCs, EpiLCs and d6 PGCLCs. Using this approach, we defined sets of differentially expressed genes (DEGs), which were significantly up- or down-regulated in pairwise comparisons between the different cell types (EpiLCs vs ESCs; d6 PGCLCs vs EpiLCs).

We found that MGA binds to approximately 30% of the DEGs for each cell type, indicating its involvement in the differentiation process (Fig. 1D). These genes include those involved in epiblast development, such as *Lin28a, Fgf15, and Dnmt3l*, pluripotency genes, such as *Esrrb, Klf5, and Dppa5a*, as well as key PGC genes, such as *Prdm1, Nanog, Tfap2c, Dazl,* and *Dppa3* (Fig. 1E).

Furthermore, our analysis of the promoter regions of these genes has shown that MGA's occupancy is dynamic, characterized by a pattern of recruitment, displacement, and maintenance of binding sites during the differentiation of PGCLCs. Taken together, these findings suggest that during the transition from ESCs to PGCLCs, the recruitment and displacement of MGA is directly associated with transcriptional upregulation and downregulation of target genes, respectively.

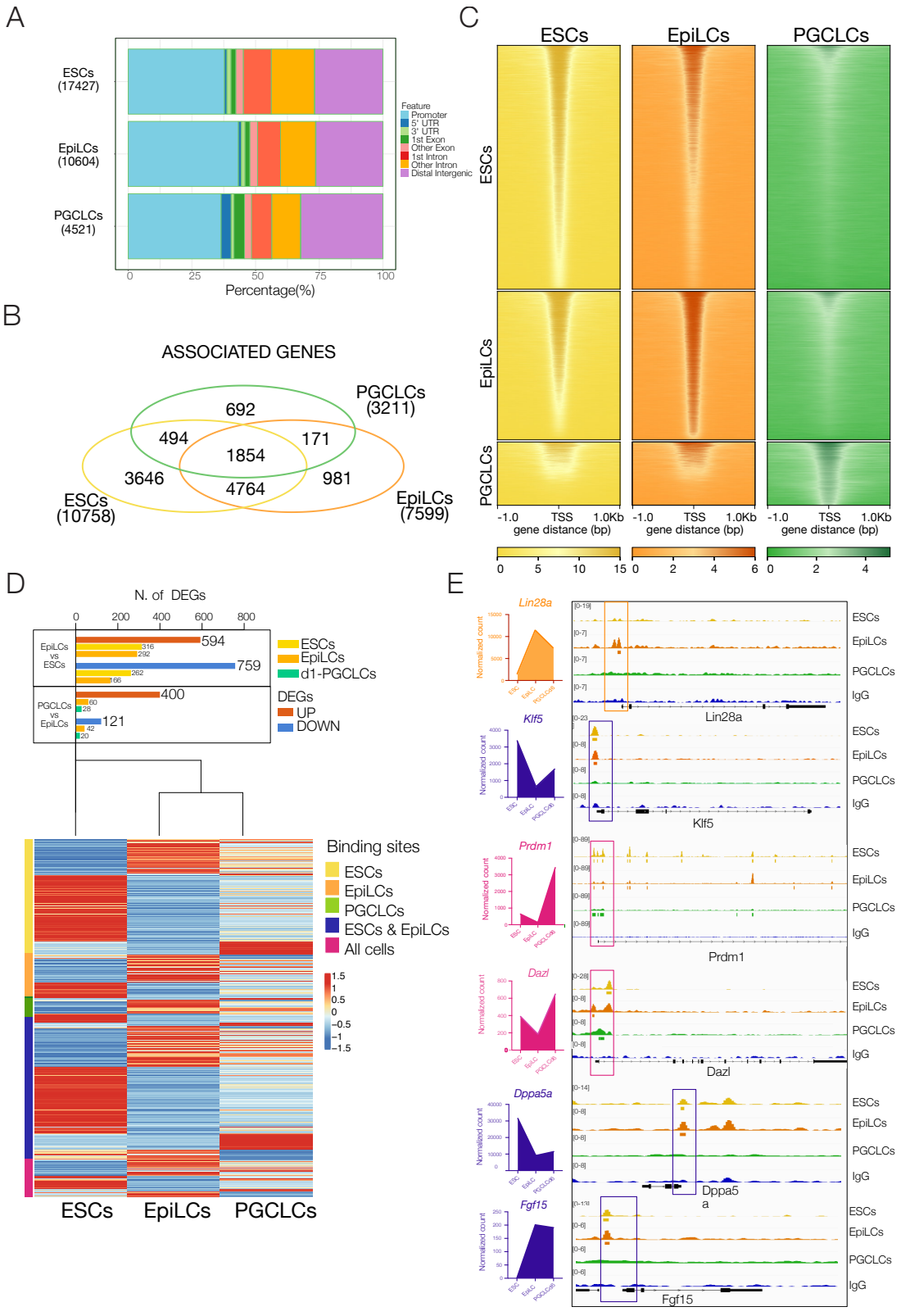

Figure 1. MGA binds genes involved in PGCLC differentiation. A. Genomic distribution of MGA-bound sites in ESCs (n=17,427), EpiLCs (n=10,604), and day 1 PGCLCs (n=4,521). **B.** Overlap of annotated genes bound by MGA in all three cell types, duplicated genes removed. **C.** Heatmaps of average CUT&RUN intensities for MGA over ±1 kb around the transcriptional start site (TSS) during the sequential differentiation of PGCLCs from ESCs. **D.** DEGs bound by MGA in the promoter region (±1 kb TSS). The bar chart in the top panel shows the number of DEGs (UP and DOWN) for each comparison, indicating the number of genes bound by MGA per cell type. **E.** Examples of genomic snapshots of loci bound by MGA in each cell type, with the relative expression during PGCLC differentiation, with colour related to MGA binding sites. IgG track serves as control.

MGA cooperates with pluripotency and T-box factors in controlling PGC fate

We investigated MGA binding sites by motif enrichment analysis and found an expected enrichment of the T-box and E-box motifs in all three cell types (Fig. 2A and Supplementary Fig. 2C). However, the T-box was found more frequently than the E-box motif, which is consistent with our finding that MGA binds many developmental regulators. Moreover, we also found OCT4-SOX2, KLF4, and E2F6 motif enrichment among the top hits (Fig. 2A and Supplementary Fig. 2C), which showed dynamic changes in their frequency during PGCLC differentiation. Most notably, the OCT4-SOX2 motif was lost at the PGCLC stage.

These motifs belong to pluripotency and T-box factors, which might indicate that MGA cooperates with other transcription factors to regulate the expression of the same target genes during PGCLC differentiation. To address this, we used published ChIP-seq datasets from mouse ESCs (Galonska et al. 2015; Tosic et al. 2019; Dahlet et al. 2021). Interestingly, MGA binding sites are mostly co-occupied by pluripotency factors such as OCT4, SOX2 and NANOG (Fig. 2B), which was also the case for MGA-bound DEGs involved in ESC differentiation towards EpiLCs (Supplementary Fig. 2D). This result indicates that MGA might act synergistically with the pluripotency network to control pluripotency transitions.

As a part of the PRC1.6 complex, both MGA and E2F6 share peaks associated with Polycomb target genes and germline genes in ESCs, as previously reported (Fig. 2B) (Dahlet et al. 2021). Comparing the peaks of E2F6 with DEGs showed enrichment only on up-regulated genes in EpiLCs, suggesting a possible cooperation between MGA and E2F6 in repressing genes in ESCs (Supplementary Fig. 2E).

We then analyzed ChIP-seq data of T, which is involved in mesoderm and PGC development, and EOMES, which is required for definitive endoderm development (Tosic et al. 2019). Our comparative analysis showed a strong association of MGA, T and EOMES binding sites (Fig. 2C). Nearly 90% of MGA-associated genes overlapped with T and EOMES target genes, while the remaining 10% corresponded to MGA binding sites on meiotic genes, as revealed by GO analysis (Fig. 2D). In particular, T, EOMES and MGA bound regulatory regions of mesoderm, epiblast, and pluripotency genes (Supplementary Fig. 2F), as well as PGC determinant genes such as *Prdm1*,*Prdm14 and Nanog* (Fig. 2E).

To summarize, our findings suggest that MGA plays a critical role in regulating gene expression during the differentiation of PGCLCs from ESCs. Specifically, MGA binds to regulatory regions of key developmental genes and cooperates with other transcription factors, as pluripotency and T-box factors, to modulate their expression levels. This suggests that MGA is a key regulator of cell fate decisions during early embryonic development.

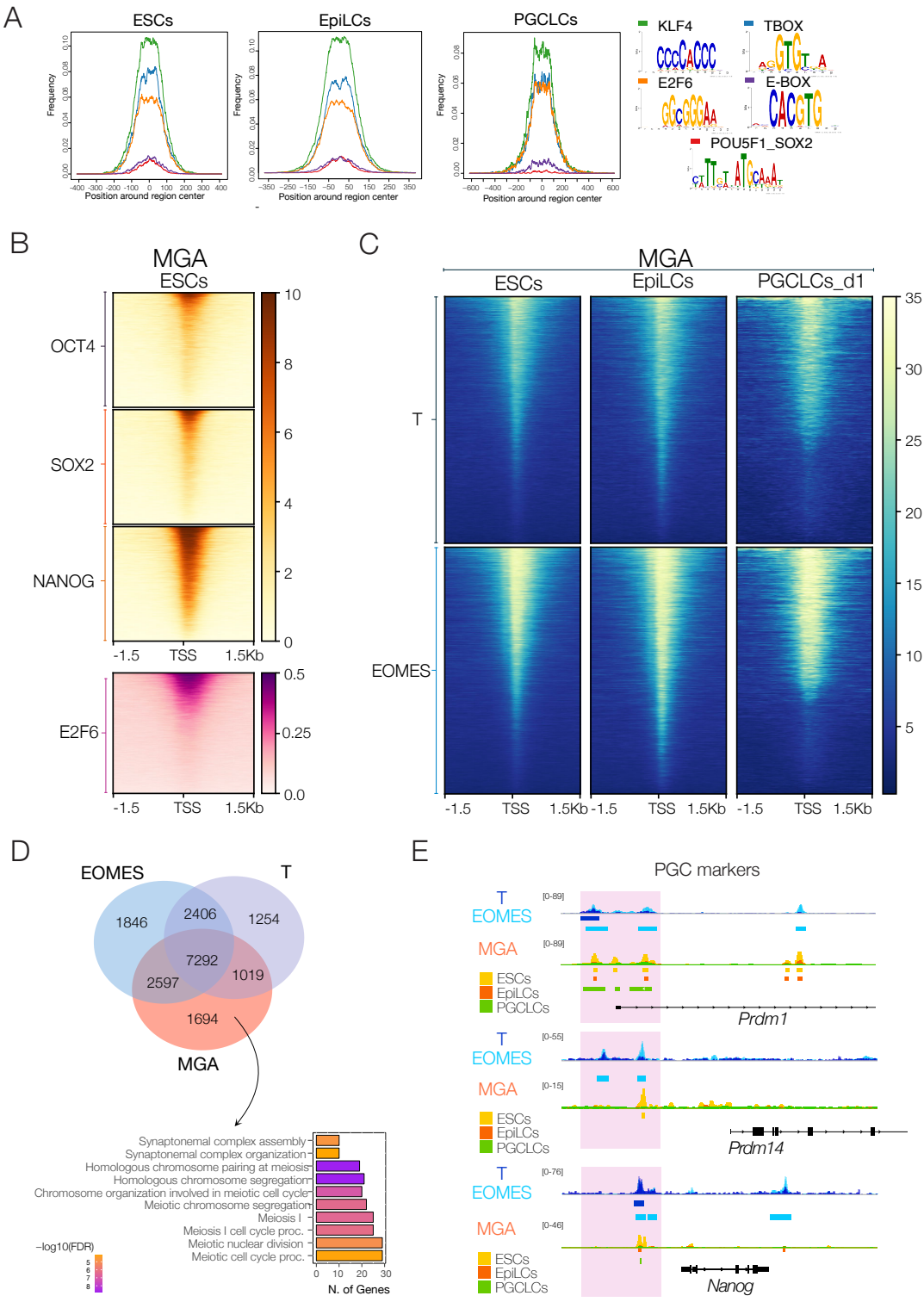

Fig.2 Cooperation between MGA and pluripotency and T-box factors. A. Metaplot of MGA motifs enrichment, comparing the enrichment for high-ranked MGA motifs to the center of the genomic region per cell type (left panel). Legend indicates motif sequences and displays colours (right panel). **B.** Heatmaps of OCT4, SOX2, NANOG and E2F6 ChIP-seq read densities on MGA ESCs genomic loci defined over 1.5 Kb around the annotated TSS. **C.** Heatmaps of T and EOMES ChIP-seq read densities on MGA consensus peaks between cell types. **D.** Venn diagram of annotated genes of T, EOMES and MGA, indicating the number of genes overlapping. The bar plot shows GO analysis of MGA unique genes (lower panel). **E.** Genome tracks of MGA, T and EOMEs over PGC markers such as *Prdm1, Prdm14 and Nanog.*

Deletion of the T-box domain of MGA induces upregulation of PGC genes

The T-box factors bind promoters of developmental genes involved in PGC differentiation. Thus, we asked whether the T-box domain of MGA can directly influence gene expression during PGC differentiation. To explore this, we employed CRISPR/Cas9 to delete the coding sequence of the T-box domain in-frame, thereby creating Blimp1-mEGFP ESCs that express truncated MGA protein. To this end, we generated two different clones and validated the excision of the target region using PCR followed by Sanger sequencing (Supplementary Fig. 3A). Then, we confirmed the expression of the truncated MGA protein using Western blot in two independent clones, named ΔT-box1 and ΔT-box7 (Supplementary Fig. 3B).

To test the requirement of the T-box domain of MGA for PGCLC differentiation, we differentiated ΔT-box ESCs towards PGCLCs. FACS analysis of embryoid bodies at d6 of PGCLC differentiation showed no significant difference in Blimp1-mEGFP+ cells compared to the wild-type (WT) (Fig. 3A). To evaluate the gene expression profile of these cells, we performed RNA-seq on ESCs, EpiLCs and Blimp1-mEGFP+cells at d6 of PGCLCs. Notably, the principal component analysis (PCA) of RNA-seq data indicated a shift in gene expression between ΔT-box and WT cell lines (Supplementary Fig. 3C).

The analysis of DEGs revealed a defined number of up- and down-regulated genes, which were also defined by GO analysis (Fig. 3B and Supplementary Fig 3. E-F). Although we identified approximately 100 significantly upregulated genes in each cell type, only 22 DEGs were shared and were associated with GO terms such as *meiotic cell cycle* and *male sex differentiation* (Supplementary Fig. 3D-3E).

In ΔT-box ESCs cells, we observed upregulation of mesoderm markers such as *Axin2, Sp5, and Cdx2*, which are direct target genes of T (Fig. 3C) (Tosic et al. 2019). Interestingly, slightly below the fold-change of significant DEGs, we also found upregulation of WNT3 and its downstream target T in ΔT-box cell lines. Western blots confirmed the increased levels of T protein (Fig. 3C-D). In EpiLCs, we identified upregulation of PGC markers, including *Prdm14* and *Tfap2c*, which were already upregulated in ΔT-box cells (Fig. 3E). Conversely, epiblast markers, such as *Dnmt3l* and *Otx2*, maintained high expression levels in ΔT-box PGCLCs (Fig. 3E). More than half of these genes were directly bound by MGA in the promoter and distal intergenic regions (Fig. 3F).

These findings suggest that the T-box domain directly controls the expression of specific cell-lineage genes involved in PGC differentiation, resulting in premature expression after its deletion. Moreover, the high expression of T might indicate mutual feedback among T-box factors, as similar phenotypes occur after the deletion of EOMES (Senft et al. 2019).

Based on the genetic background of ΔT-box cells, knowing that T starts PGC specification, we hypothesised that ΔT-box cells could differentiate into PGCLCs directly from ESCs. To test this hypothesis, we differentiated ESCs into PGCLCs using the same cocktails of cytokine but excluded LIF (Supplementary Fig.

3G). To evaluate the differentiation potential of ΔT-box ESCs into PGCLCs, we monitored the mRNA expression and protein levels of PGC markers (Fig. 3G-H).

Interestingly, immunofluorescence analysis revealed that the majority of cells in embryoid bodies were double-positive for the germ cell marker AP2γ and Blimp1-mEGFP, as opposed to the WT (Fig. 3G). Consistently, qPCR analysis showed that *Prdm1, Prdm14 and Tfap2c* were significantly up-regulated in ΔT-box PGCLCs derived directly from ESCs. However, we also found up-regulation of meiotic genes such as *Dazl* and *Sycp3*, which were already up-regulated in ΔT-box ESCs (Supplementary Fig. 3H).

Therefore, further evaluation is needed as the expression of PGC markers might be dependent on a secondary effect rather than the effect of T expression.

In summary, these findings demonstrate that the expression of MGA target genes involved in PGCLC differentiation highly depends on the T-box domain activity. Furthermore, the expression of T, as compensation of the deletion of MGA T-box domain in ESCs, reinforced the idea of the cooperation between MGA and T-box factors in maintaining cell-type programs.

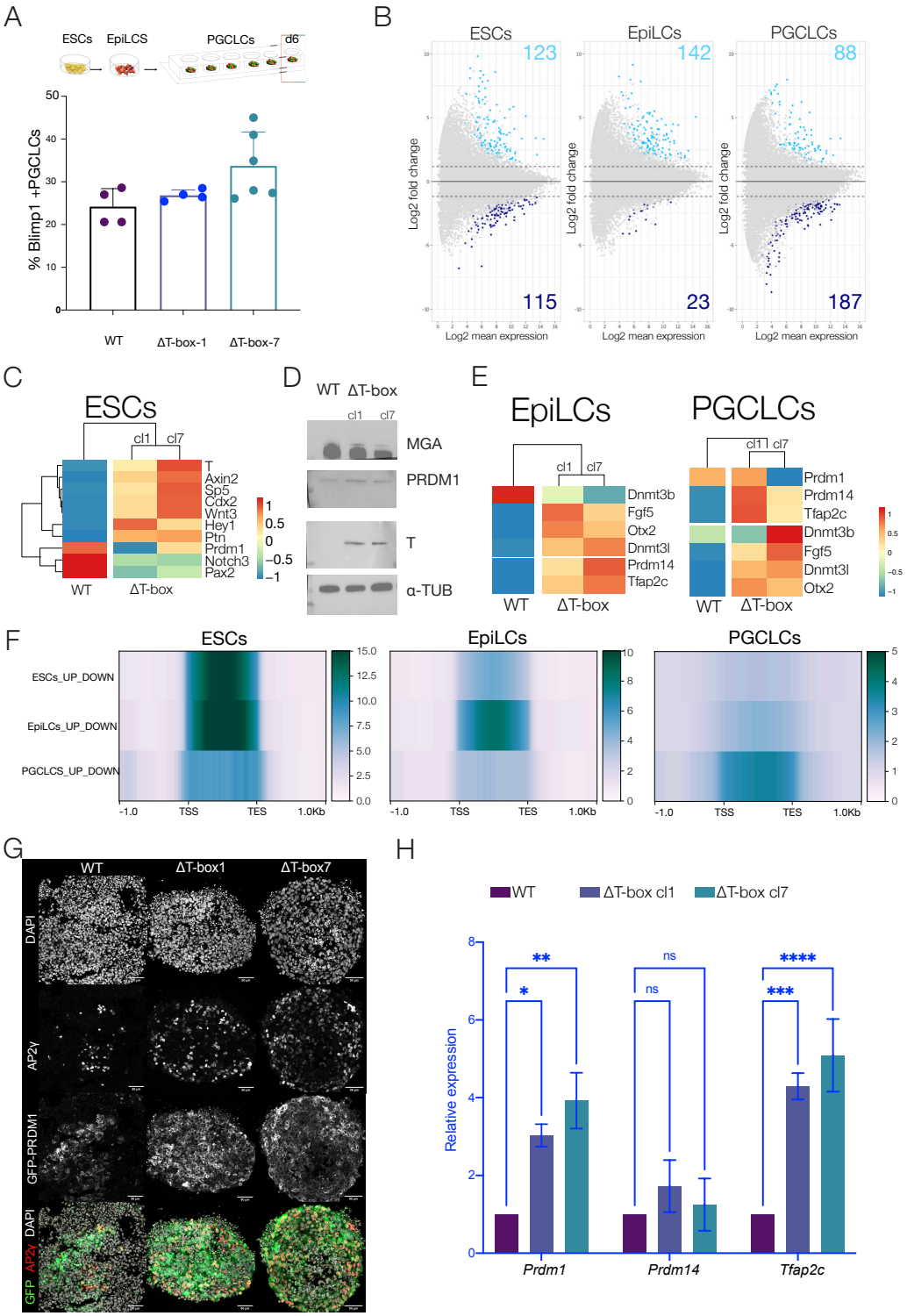

Figure 3. The MGA T-box domain is required to control PGC target genes. A. Quantification of BLIMP1+ cells. FACS result for ΔT-box cells compared to WT, showing no change in the quantification of BLIMP1+ cells number (four independent replicates). Scheme of PGCLC differentiation, highlighting d6 PGCLCs, day we collected the cells (Top panel). **B**. MA plot showing DEGs of ΔT-box cells compared to WT in ESCs, EpiLCs and PGCLCs day6 (Padj < 0.05, fold-change >1.5). **C**. Expression heatmap of genes involved in mesoderm specification resulted from DEGs in ESCs upon T-box domain deletion. Mean expression profile from independent duplicate experiments. **D.** Western blot of BLIMP1, T and α-TUBULIN (α-TUB) in ΔT-box ESCs compared to WT. **E.** Heatmap of DEGs in EpiLCs and PGCLCs upon T-box domain deletion. **F.** MGA CUT&RUN read densities cantered on resulted DEGs of ΔT-box cells. UP-DOWN genes grouped per each cell type. **G.** Immunofluorescence of ESC-PGCLCs cells at day6 stained for BLIMP1-GFP and AP2γ. **H.** Quantitative validation of gene expression changes in ESC- PGCLCs from WT and ΔT-box cell (cl1 and cl7) by independent qRT-PCR experiments. Error bars show s.e.m of triplicate biological experiments.

Dynamic interactome of MGA during PGC differentiation

Given the dynamicity of MGA in controlling different sets of genes together with pluripotency and T-box factors, we aimed to identify MGA's cell-type specific interaction partners. We used mass spectrometry to detect endogenous proteins co-immunoprecipitated with MGA in ESCs, EpiLCs and d6 PGCLCs protein extracts, followed by quantitative MS-based proteomics workflows (Supplementary Fig. 4A). First, we identified the interactors using the label-free quantification (LFQ). Then, using intensity-based quantification (iBAQ), we calculated the stoichiometry of each interactor relative to MGA (Supplementary Fig. 4A) (Smits et al. 2013). This approach allowed us to understand the dynamics of MGA interactors during PGC differentiation. We found that the proteomics of all cell types distinctly separated between MGA and IgG (used as a negative control) using principal component analysis (PCA) (Supplementary Fig. 4B).
Our results showed a strong association of MGA with known members of the PRC1.6 complex, such as PCGF6, L3MBTL2, RING2, and WDR5, along with ATF7ip, SMARCA4, and CEP85, which were maintained in all three cell types (Fig. 4A-B). To confirm our findings, we conducted a Western blot in ESCs and day 6 PGCLCs, which validated the interaction between MGA and L3MBTL2 (Supplementary Fig. 4C). Previous studies have reported that the interaction between MGA and ATF7ip represses germ cell genes together with SETDB1 in ESCs (Tsusaka et al. 2020). Our results showed that this interaction remained stable throughout the differentiation towards PGCLCs. Analysis of the stoichiometry of these factors compared to MGA revealed that PCGF6 was the only stable factor during the differentiation, whereas the abundance of other interactors varied. For example, L3MBTL2 and WDR5 were highly enriched in PGCLCs, and RING2 only in EpiLCs (Fig. 4C).

Analysis of the statistically enriched MGA interactors via GO terms indicated a diverse range of biological processes specific for each cell type (Fig. 4D), indicating different significant hits.
In ESCs, MGA pulled down pluripotency factors, such as ESRBB and TEX10, and we also detected OCT4 and SOX2, although they were below the significance threshold. However, the interaction between MGA and OCT4 was confirmed via Western blot (Supplementary Fig. 4D), consistent with our previous observations of co-occupancy of core pluripotency factors in MGA binding sites. Additionally, previous proteomic studies have shown that MGA is among OCT4's interacting partners (van den Berg et al. 2010; Ding et al. 2015; Buecker et al. 2014; Pardo et al. 2010). Analysis of their stoichiometry seems to indicate a dimeric state when interacting with MGA (Supplementary Fig. 4E). Notably, consistent with our motif analysis of MGA binding sites, the interaction with pluripotency factors was lost at PGC stage (Fig. 4B).

In EpiLCs, we found a significant enrichment of proteins involved in the DNA methylation process, such as DNMT1, TET3 and MEST, along with proteins involved in the regulation of chromosome organization, such as SUMO1 and SPAG5. Previous studies have shown that DNMT1 directly interacts with MAX and SETDB1 to co-repress germ cell genes in ESCs (Tatsumi et al. 2018). Recently, DNMT1 was also reported interacting

with EED to stabilize epigenetic signatures on germ cell genes in EpiLCs (Lowe et al. 2022). Stoichiometry values for DNMT1 and SETDB1 changed very little between ESCs and EpiLCs (Supplementary Fig. 4F). Interestingly, the presence of proteins, such as ATF7ip, SMARCA4, and L3MBTL2, in all cell types could indicate the formation of a complex, different from PRC1.6, to support the repression of germline genes. Indeed, previous publications have already attributed this function to single proteins (Maeda et al. 2013; Qin et al. 2012; Tsusaka et al. 2020).

Altogether, MGA seems to regulate the pluripotent state in ESCs with a core of pluripotency, while in EpiLCs, it might lead DNMT1 to repress germ cells through epigenetic silencing. Therefore, these data reinforce the dynamicity found in MGA binding sites.

Remarkably, mass spectrometry analysis of PGCLCs showed a predominance of RNA-binding proteins and translation factors co-immunoprecipitating with MGA, particularly DAZL. DAZL, known for its role in regulating mRNA translation in germ cells (Gill et al. 2011), has recently been found to bind to chromatin sites of PRC2 to silence developmental genes in ESCs (Rafiee et al. 2020). Interestingly, the majority of DAZL-interacting proteins, such as IGF2BP1 RNP complex, were also found in MGA interactome in PGCLCs. Although MGA was not previously identified in DAZL interactome studies at later PGC stages, a comparison of datasets showed that DAZL and MGA share 30 interaction partners, mostly RNA-binding proteins (Supplementary Fig. 4G). Stoichiometry values derived from iBAQ analysis revealed a DAZL: MGA ratio of 10:1, possibly indicating the formation of a new complex at later stages of differentiation (Supplementary Fig. 4H). These findings suggest that their interaction could depend on binding to common RNA or control of the same DNA targets.

Overall, these results highlight the highly dynamic nature of the MGA interactome and suggest that its role in PGCLC differentiation may be context dependent. Moreover, the interplay between MGA and RNA-binding proteins suggests a potential involvement in RNA regulation, specifically in PGCLCs.

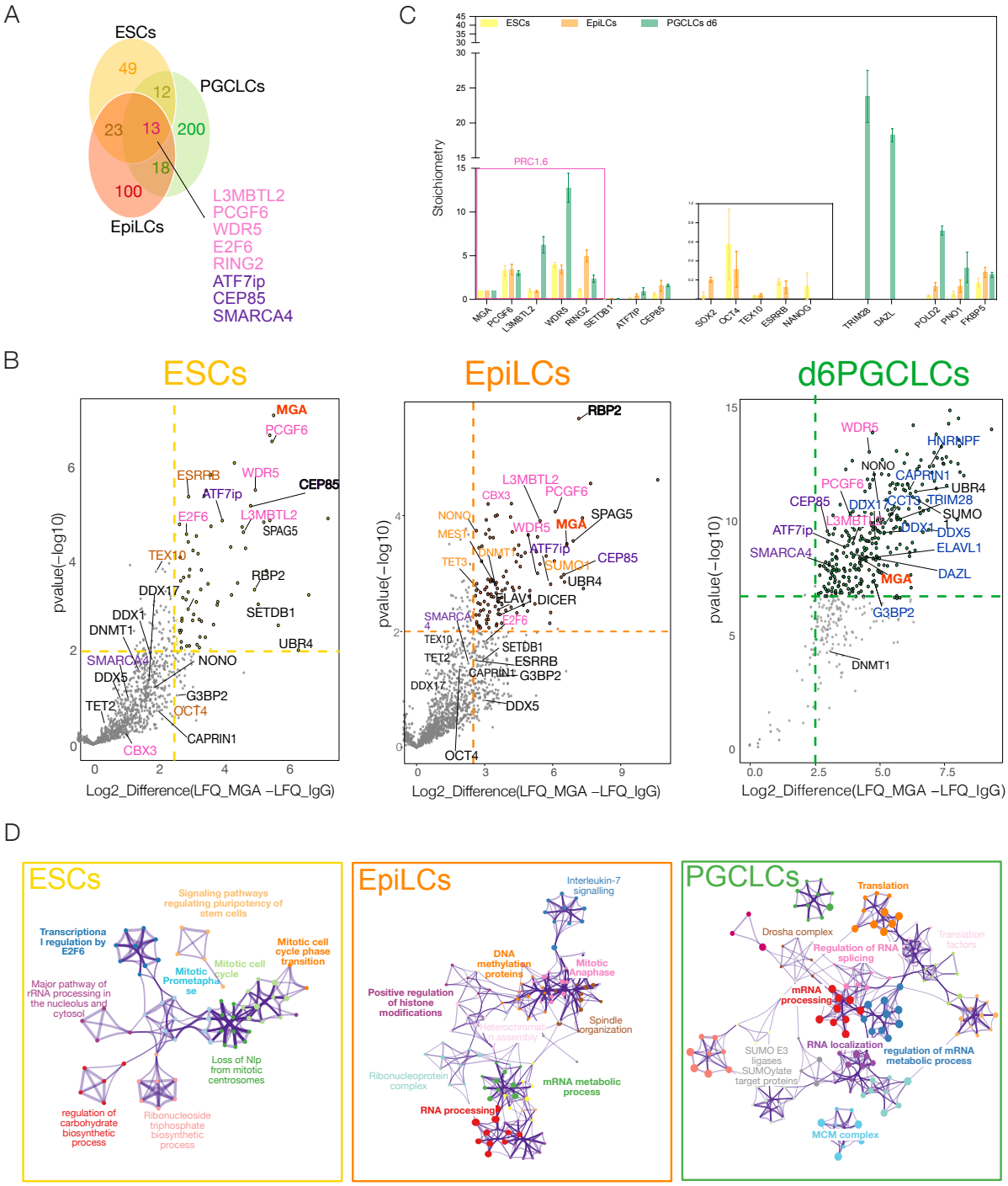

Figure 4. MGA interactome during PGCLC differentiation. A. Venn diagram of the proteins enriched in each cell type, highlighting the shared proteins**. B.** Volcano plot of MGA exhibiting the interaction partners in ESCs, EpiLCs, and PGCLCs on day 6. Statistically enriched proteins in the MGA-pulldowns were identified by a t-test comparing label-free quantification (LFQ) relative to MGA-pulldown with IgG-pulldown. Significantly enriched proteins were represented by different colours indicating different protein groups, including PRC1.6 members (Fuchsia), common proteins (Purple), DNA methylation process (Orange), pluripotency proteins (Brown), and RNA-binding proteins (Blue). **C**. Stoichiometry of MGA interactors during PGCLC differentiation, represented by dividing the iBAQ value of each protein by the MGA value. MGA value is set as 1. Data are shown as the mean of three replicates with standard deviation error bars. **D.** GO analysis of enriched proteins in MGA-pulldown for each cell type.

Depletion of MGA affects PGC specification

MGA controls the expression of many key genes required during PGCLC differentiation and shows a cell type-specific interactome. Thus, we asked whether MGA is required for PGCLC differentiation. Previous knockout studies in ESCs using CRISPR/Cas9 or RNA interference show that MGA is required for the survival of pluripotent stem cells (Washkowitz et al. 2015). Therefore, we harnessed the auxin-inducible degron (AID) system to rapidly deplete MGA at the protein level (Nishimura et al. 2009; Natsume et al. 2016). We generated a stable Blimp1-mEGFP ESC cell line harbouring a transgene for the hormone receptor TIR1. Subsequently, we used CRISPR/Cas9 to knock in a miniAID tag fused to mCherry at the C-terminal of MGA, which is referred to as MGA-AID. The knock-in was verified by PCR and Sanger sequencing (Supplementary Fig. 5A). MGA was efficiently degraded within two hours of auxin addition in ESCs, as shown by Western blot and immunofluorescence staining (Supplementary Fig. 5B-C). After establishing this approach, we conducted various time-course experiments to deplete MGA during PGCLC differentiation through auxin supplementation (Supplementary Fig. 5D). Depletion of MGA in ESCs or EpiLCs after 8-12 hours of auxin treatment results in up-regulation of meiotic genes, but the expression of lineage-specific or pluripotency genes was unaffected (Supplementary Fig. 5E-F). However, depletion of MGA for 96 hours in ESCs resulted in growth defects, reduced proliferation rate, and loss of pluripotency with a reduction of OCT4 expression, as determined by immunofluorescence (Supplementary Fig. 5G).

To determine whether MGA is required for initiating PGCLC differentiation, we treated MGA-AID cells with auxin on d0 and analyzed them on d1 by FACS. Using this approach, we discovered a significant reduction in the percentage of Blimp1-mEGFP+ cells (~5%) in MGA-AID cells treated with auxin compared to controls (~10%) (Fig. 5A). Immunofluorescence staining of Blimp1-mEGFP and MGA confirmed the reduction in PGCLCs upon MGA depletion (Supplementary Fig. 5H). Next, we performed RNA-seq on d1 PGCLCs that were untreated or treated with auxin for 24h. Differential gene expression analysis identified a small number (32) of significantly up-regulated genes. Among them, GO analysis revealed enrichment for genes related to germ cells, such as the *meiotic cell cycle* and *male and female gamete generation* (Fig. 5B). Furthermore, monitoring the expression changes of early PGC genes (318) that were previously defined (Miyauchi et al. 2017), we found that PGC markers such as *Prdm1* and *Prdm14*, pluripotency genes such as *Esrrb* and *Nanog*, and signalling markers such as *Notch1* and *Smad3* showed lower expression levels in MGA-depleted samples (Fig. 5C).

To determine whether the upregulated genes and early PGC genes are direct targets of MGA, we integrated RNA-seq data with the genomic binding sites of MGA in d1 PGCLCs (Fig. 5D). The analysis showed that half of the DEGs (16 out of 32) are predominantly bound by MGA in the promoter region. Genes upregulated without MGA binding are likely regulated by some of the proteins that interact with MGA, which might have lost their genomic binding in the absence of MGA. Moreover, MGA directly binds 49 early PGC genes (Fig.

5D). We then treated PGCLCs from d0 to d3 with auxin to examine whether longer depletion of MGA during PGCLC differentiation enhances the phenotype. Notably, the depletion of MGA led to a significant reduction in PGCLC numbers, as shown by FACS (Fig. 5E). Additionally, the depletion of MGA affected the morphology of the embryo bodies (EBs), which were smaller and poorly defined (Fig. 5F). However, this severe phenotype made transcriptome analysis impossible. We suggest that it might involve severe loss of PGC markers together with high expression of the germ cell genes, as observed in the mild phenotype. Overall, these results demonstrate that MGA is essential in ensuring PGC specification by activating PGC target genes and repressing early expression of meiotic genes.

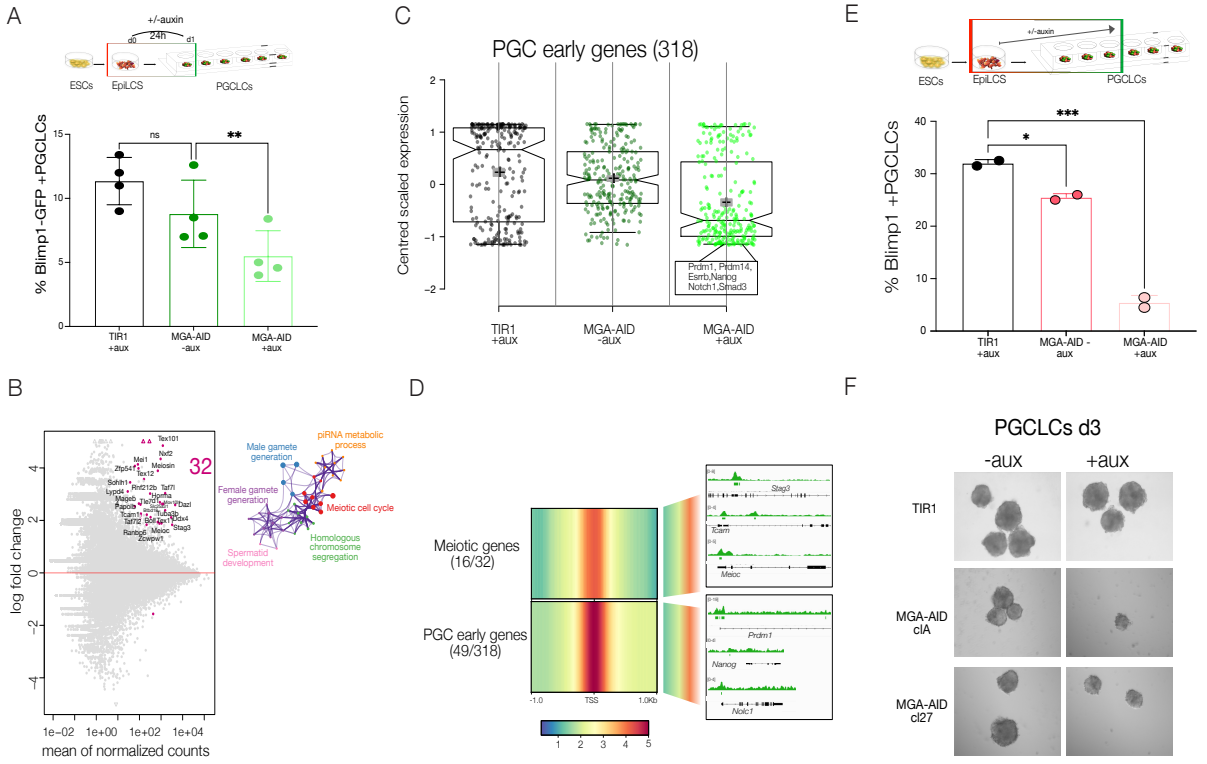

Figure 5. Depletion of MGA results in impaired PGCLCs. **A.** Quantification of Blimp1-mEGFP+ cells in MGA-AID cells after 24h +/- auxin compared to TIR1 (parental cell lines) on day 1 by FACS. The data shows four independent experiments. ns-not significant; ** P<0.01. Two-way ANOVA followed by Sidak's multiple comparison test. Scheme of PGCLC differentiation, highlighting d1 PGCLCs, the day we quantified the cells (top panel). **B.** MA plot depicting 32 DEGs in PGCLCs on day 1 after 24h of auxin treatment (Padj < 0.05, fold-change > 1.5). The upper panel shows the GO analysis of the DEGs, highlighting their biological processes. **C.** Boxplots show normalized counts of the 318 early PGC genes in TIR1 cells and MGA-AID cells +/- auxin after Z-scoring. The lower box indicates genes directly bound by MGA. **D.** MGA CUT&RUN read densities of PGCLCs on day 1 centred on results from DEGs and early PGC genes directly bound by MGA. The right panel shows snapshots of the binding profiles of MGA on meiotic and PGC genes. **E.** Quantification of Blimp1-mEGFP+ cells in MGA-AID cells after 72h +/- auxin compared to TIR1 (parental cell lines) on day 3 by FACS. The data shows four independent experiments. ns-not significant; *** P<0.001 (Two-way ANOVA followed by Sidak's multiple comparison test). Scheme of PGCLC differentiation, highlighting d3 PGCLCs, the day we quantified the cells (top panel). **F.** Brightfield images representing day-3 PGCLCs +/- auxin. They show two MGA-AID clones (clone A and clone n.27) compared to parental cell lines TIR1.

Are meiotic genes coregulated by MGA and DAZL?

Our data suggest that MGA and DAZL interact. As previously described, DAZL is only expressed at a late stage of PGC development, when global DNA demethylation occurs (Maatouk et al. 2006). Thus, to investigate the relationship between MGA and DAZL, we designed a CRISPR-Cas9 targeting strategy to delete the *Dazl* gene in MGA-AID ESCs (Supplementary Fig. 6A). To validate the KO, we used PCR followed by Sanger sequencing to confirm the excision of the target region. At the protein level, we performed staining after depletion of MGA with auxin for 24h. As expected, DAZL was upregulated in the control cell line but not in the DAZL KO, MGA-AID ESCs (Supplementary Fig. 6A-B), referred to as dDAZL hereafter. To explore the potential differences, we evaluated the impairment produced by the loss of DAZL, MGA or both. We analyzed the effect of simultaneous depletion on PGC development by differentiating these cells towards PGCLCs. After treating the resulting EBs with auxin at d5, we quantified Blimp1-mEGFP+ cells at d6 after disrupting DAZL (dDAZL), MGA (dMGA), or both (ddMD). Interestingly, FACS analysis showed a decrease in Blimp1-mEGFP+ cells derived only from dMGA cells and ddMD, while dDAZL was unaffected (Fig. 6A).

To investigate the effect of DAZL and MGA loss on gene expression in PGCLCs, we conducted RNA-seq on Blimp1-mEGFP+ cells isolated via FACS at d6 after their deletion. At first, PCA of the RNA-seq data revealed a significant transcriptional shift in gene expression profiles (Supplementary Fig. 6C).

Then, we performed DEGs analysis between dMGA, dDAZL, and ddMD compared to the matched parental cell lines. We clustered these genes into five groups (Fig. 6B). The first cluster corresponds to DAZL-activated genes (cluster I), while the second cluster corresponds to MGA-DAZL co-activated genes (cluster II), which showed reduced or absent expression in ddMD. The third cluster contains MGA-repressed genes (cluster III), while the fourth cluster contains DAZL-repressed genes (cluster IV). The fifth cluster contains DAZL-MGA co-repressed genes (cluster V), which includes genes that MGA, DAZL or both inversely regulated, resulting in increased expression above parental control levels in dMGA, dDAZL, and ddMD, respectively (Fig. 6B).

However, we observed that among the up- and down-regulated DEGs in dDAZL and ddMD cells, mostly annotated genes were ribosomal pseudogenes, which was expected as DAZL is an RNA-binding protein (Fig. 6C). When considering only defined genes, there was no overlap between the DEGs of dDAZL and dMGA, which is consistent with their opposite phenotypes as evaluated by FACs quantification (Fig. 6D). The up-regulated genes in dMGA were associated with GO terms related to *Male gamete generation* and *meiotic cell cycle* (Fig. 6E), indicating that MGA still acts as a repressor at this stage of differentiation. As most of the meiotic genes were also misregulated in ddMD cells, we speculated whether it was due to the sole deletion of MGA or was connected to the absence of both factors.

To investigate whether DAZL binds to germline genes' RNAs, we examined previously published individual-nucleotide crosslinking and immunoprecipitation (iCLIP) data of DAZL in spermatogonia, which are at a late stage of PGCs (Mikedis et al. 2020; Rafiee et al. 2021). Surprisingly, we found that DAZL binds to genes such as *Ddx4, Sycp3*, *Taf7l*, and *Hormad1* (Fig. 6F), whose translation should be reduced in DAZL's absence (Zagore

et al. 2018). However, we did not observe any changes in the expression of these genes in dDAZL cells. Interestingly, in ddMD cells, the expression of *Ddx4* and *Sycp3* was reduced compared to dMGA, likely as a compensatory effect of DAZL's absence (Fig. 6G).

A previous publication proposed a model where DAZL maintains high mRNA levels for selected targets, thereby preventing the binding of negative regulatory factors (Mikedis et al. 2020). In its absence, the levels of these targets are reduced by negative regulation. Therefore, we speculate that MGA might act as a negative regulator of DAZL to prevent excessive translation of downstream meiotic genes at this time point. However, it is also possible that other RNA-binding proteins in the MGA interactome could play a similar role in this context.

These findings suggest a potential relationship between MGA and DAZL in regulating the late stage of PGCLC differentiation. While our results show that the absence of both proteins directly impacts gene expression, further experiments are needed to confirm this relationship and determine if MGA binds directly to RNA.

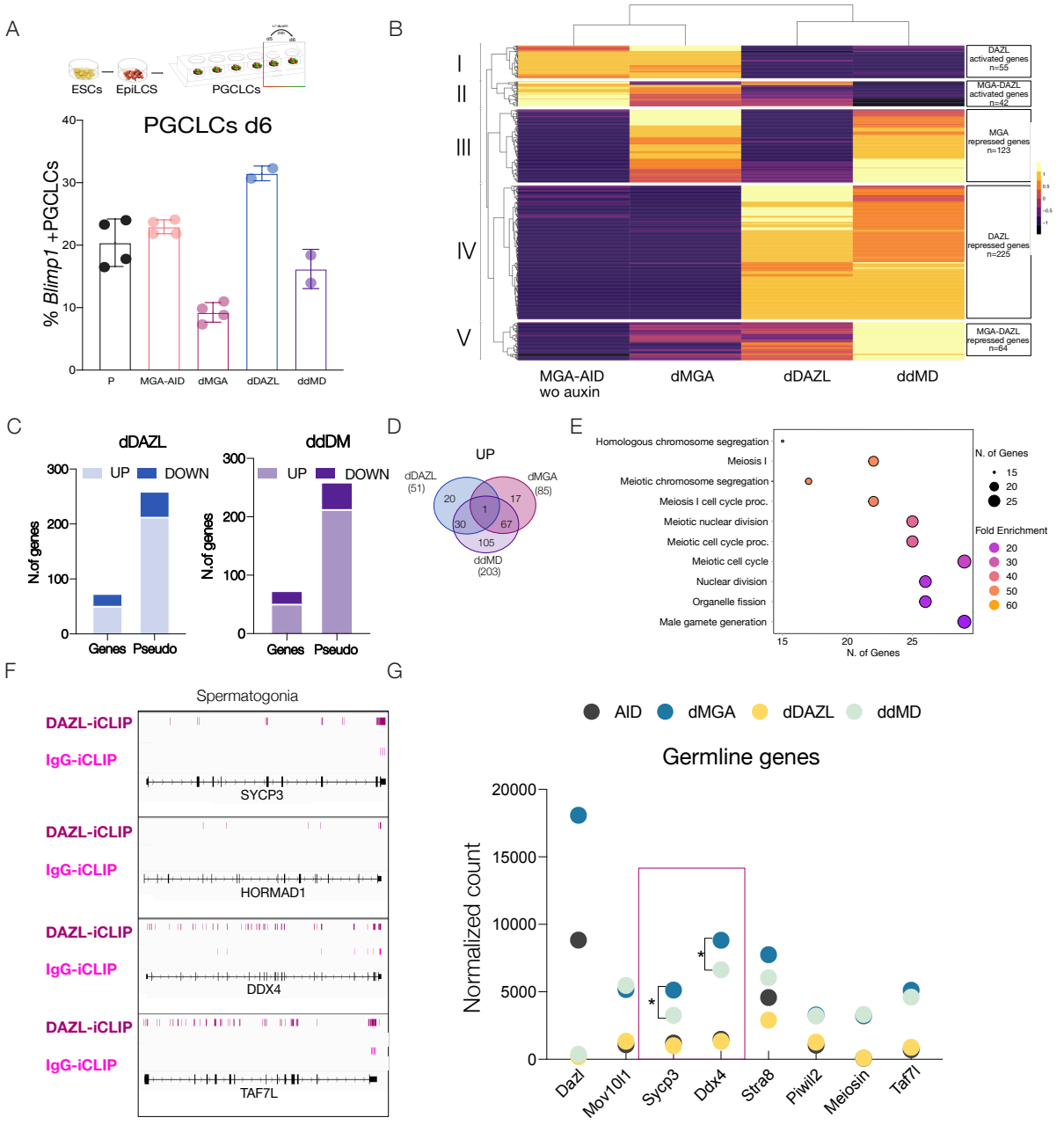

Figure 6. Impact of MGA and DAZL absence on gene expression during day 6 of PGCLC differentiation. A. Quantification of Blimp1-mEGFP+ cells in the parental cell lines TIR1, MGA-AID cells without auxin, dMGA (deletion of MGA), dDAZL (knockdown of DAZL), and ddMD (absence of MGA and DAZL) at day 6 of PGCLC differentiation. The scheme highlights PGCLC differentiation with day 6 PGCLCs quantified (top panel). **B.** Heatmap representing DEGs for each condition using k-means clustering (n=5). Data show the mean of two independent replicates. **C.** Barplot of DEGs in dDAZL and ddMD, indicating the number of genes and pseudogenes found for each cell type. **D.** Venn diagram showing the overlap between up-regulated genes in dMGA, dDAZL, and ddMD. Pseudogenes were excluded. **E.** Dot plot displaying the results of GO analysis of up-regulated genes in dMGA, associated with *male gamete generation* and *meiotic cell cycle*. **F.** Snapshot of iCLIP in spermatogonia for DAZL compared to IgG. **G.** Comparison of normalized counts for meiotic genes between AID (no auxin), dMGA, dDAZL, and ddMD. Data show the mean of two independent experiments. ns: not significant; *p<0.1 via Two-way ANOVA with Sidak's multiple comparison test.

Discussion

Transcription factors and signalling pathways work together during embryonic development to specify PGCs from the mesodermal signalling environment. However, the molecular mechanism driving this cell lineage is not well understood. In this study, we present evidence of the crucial role of the transcription factor MGA in promoting PGC formation, revealing its genomic targets and interaction partners during PGCLC differentiation.

We demonstrate that differentiation into PGCLCs involves the dynamic activity of MGA in maintaining the correct gene programs for the specific cell type (Fig. 7). At first, using an inducible degron system, we confirm the role of MGA as a repressor of meiotic genes and in safeguarding pluripotency (Stielow et al. 2018; Washkowitz et al. 2015; Qin et al. 2021). Indeed, rapid depletion of MGA results in the derepression of meiotic genes in ESCs and EpiLCs, while prolonged deletion leads to an impaired pluripotent state with loss of OCT4 in ESCs. MGA controls promoter regions of genes that maintain stem cell and germ cell development in ESCs and EpiLCs, as evidenced by the enrichment of canonical motifs T-box and E-box, as well as the presence of OCT4-SOX2 motifs. Comparison of the MGA binding site with pluripotency factors (OCT4, SOX2 and NANOG), using previous ChIP-seq data (Galonska et al. 2015), shows a higher overlap that suggests their possible cooperation. Furthermore, we identify MGA interactors in ESCs, including pluripotency factors such as ESRBB, TEX10, OCT4, and SOX2, suggesting that MGA may be part of the core of pluripotency factors in ESCs. This study presents a direct relationship between MGA and pluripotency factors for the first time.
MGA binding sites also overlap with E2F6, and as part of the PRC1.6 complex, MGA guides the complex on the binding sites of meiotic genes together with E2F6, repressing their premature expression in ESCs (Dahlet et al. 2021; Mochizuki et al.2021). In line with that, during PGCLC differentiation, the MGA interactome maintain the presence of PRC1.6 members together with proteins such as ATF7ip and SMARCA4, previously found to influence meiotic gene expression in ESCs (Maeda et al. 2013). DNMT1 and SETDB1, which are involved in silencing germ cell genes through methylation, were also found to sustain the action of these factors in MGA-interactome in EpiLCs. DNMT1 and SETDB1 were previously found to interact with MAX in repressing ESC germ cell genes in ESCs (Tatsumi et al. 2018). In a more recent publication, DNMT1 was shown to interact with EED, a member of PRC2. Their interaction was proposed as essential in maintaining an epigenetic signature on meiotic genes from epiblast through PGC differentiation (Lowe et al. 2022). DNA-methylation establishment may depend on MGA or EED recruitment of DNMT1 rather than MGA binding on their promoter (Mochizuki et al. 2021). Together, this led to an intricate network of proteins implicated in repressing meiotic genes during PGCLC differentiation. In particular, we show how MGA is important in the early step, which precedes PGC specification, as ESCs and EpiLCs, and indicates a context-dependent role of MGA in maintaining their cell-type specific gene program reflected by a combinatorial action with different interactor partners.

One major finding of this study is that MGA plays a direct role in maintaining PGC specification. After MGA deletion, the efficiency of PGCLC formation decreased, and meiotic genes were derepressed. MGA also regulates the expression of PGC markers, including Prdm1, Prdm14, and Nanog, in EpiLCs and d1 PGCLCs by binding to their promoters. Their lower expression upon MGA deletion suggests a context-dependent role of MGA in maintaining the cell-type specific gene program. This phenotype resembles the one observed upon loss of T-box factors, T and EOMES, resulting in the weak activation of BLIMP1 but failure to maintain PGCs (Aramaki et al. 2013; Senft et al. 2019). MGA binding sites overlap with T and EOMES (Tosic et al. 2019), specifically on PGC determinant genes while meiotic genes were controlled only by MGA. Deletion of MGA T-box domain resulted in only changes in the transcriptome but not reduced efficiency of PGCLC formation. Even though PGCLCs have not presented a severe phenotype as it was for the complete deletion of MGA, we observed early up-regulation of genes associated with meiosis and mesodermal differentiation in ESCs and PGC markers in EpiLCs. Moreover, we found an increase in T expression and its target genes in ESCs suggesting a mutual feedback regulation between the T-box factors. A similar result was obtained by a complete loss of EOMES during mesodermal differentiation (Tosic et al. 2019) or the contrary in nascent PGCs with lower expression of T (Senft et al. 2019). Intriguingly, the fact that we influenced T expression only by deleting the T-box domain suggests a strong connection between MGA and T-box factors. Therefore first, we demonstrated that the T-box domain is a key determinant of target genes specific for PGC differentiation. Second, findings of similar phenotypes and target regions of MGA and T-box factors might indicate synergetic action in determining PGC specification achieved by their overlapping expression in the posterior epiblast region where PGCs occur. Their redundant function might ensure continuous activation of PGC determinant genes until their expression is lost during differentiation. However, T and EOMES were not presented in the MGA interactome. Instead, in a previous publication, SMARCA4 was linked to EOMES cell state transition by changing chromatin accessibility (Istaces et al. 2019). Considering this, it would be interesting to study how accessible chromatin is after the deletion of these T-box factors in relation to SMARCA4 in this cell-state transitions from epiblast to PGC.

One intriguing finding was the complete change in the interactome of MGA at day 6 of PGCLCs, with the enrichment of RNA-binding proteins. In particular, we found the presence of DAZL, an RNA-binding protein essential for ensuring meiotic and gametogenic competence (Gill et al. 2011). We investigated the nature of their interaction by disrupting the simultaneous expression of both proteins using an inducible system and CRISPR/Cas9. We found that impairment of either MGA or DAZL alone leads to different phenotypes. Deletion of MGA reduced the number of PGCLCs, resulting in higher expression of meiotic genes. Conversely, deletion of DAZL did not influence the differentiation of PGCLCs but rather genes involved in RNA processing. Instead, the combined loss of both MGA and DAZL seems to result in a compensatory action to restore the expression of some meiotic genes, such as *Ddx4* and *Sycp3*, which were expressed at higher levels in the absence of MGA and bound by DAZL. Therefore, it is tempting to speculate that MGA might act as a negative

regulator of DAZL to avoid excessive translation of downstream meiotic genes at this time point. Future work is needed to test this hypothesis.

In summary, MGA is required to ensure PGC specification, with an expanded role during the differentiation process, relying on controlling cell-type gene expression and interaction with multiple proteins. Our data demonstrate the essential role of MGA in ensuring cell fate transition, providing an exciting glimpse into the complex action of this transcription factor.

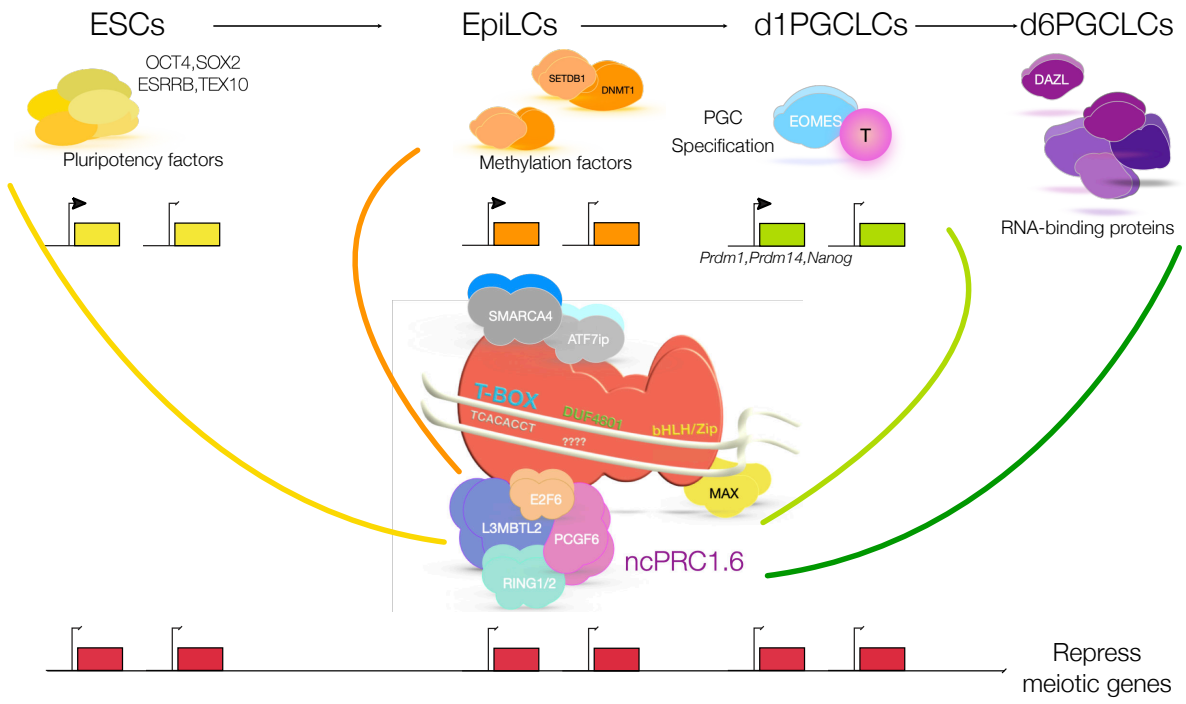

Figure 7. Model depicting the diverse regulatory roles of MGA during the differentiation of PGCLCs. During PGCLC differentiation, MGA maintain the interaction with PRC1.6 members, ATF7ip, and SMARCA4, and represses meiotic genes. In ESCs, MGA interacts with pluripotency factors (OCT4, SOX2, ESRRB, and TEX10) and safeguards pluripotency. In EpiLCs, MGA interacts with methyl proteins, such as DNMT1 and SETDB1. In the early stage of PGCLCs (day 1), MGA induces primordial germ cell (PGC) specification by binding to PGC genes such as *Prdm1, Prdm14, and Nanog*, along with T and EOMES. In the late stage of PGCLCs (day 6), MGA is linked to RNA binding proteins such as DAZL. These findings suggest that MGA plays a critical role in the regulation of various developmental programs during PGCLC differentiation.

Materials and Methods

Mouse embryonic stem cell culture and primordial germ cells like cells induction

Previously established mouse embryonic stem cell (mESC) lines carrying Blimp1-mEGFP were used in this study (Ohinata et al. 2005).The cells were cultured in N2B27 medium (1:1 DMEM/F12 and Neurobasal, 2mM L-glutamine,1x penicllin-streptomycin, 0.1 mM β-mercaptoethanol, 1% B27, 0.5% N2) supplemented with 2i (1 μM PD0325901, 3 μM CHIR99021) and 1000 U/ml mouse leukemia inhibitory factor (mLIF) on fibronectin-coated dishes (Millipore). Media was replaced daily, and cells were passaged using Tryple (Gibco). All ESCs were regularly tested for mycoplasma contamination using Lookout mycoplasma PCR Detection Kit (Sigma).

To induce mPGCLCs following the previous protocol established (Hayashi et al. 2011),mESCs were dissociated and seeded onto fibronectin-coated plates with EpiLC medium (N2B27 medium, 1% KnockOut Serum Replacement (KSR), bFGF (12 ng/ml), Activin A (20 ng/ml)) for 42 hrs. Media was changed every day. The resulting EpiLCs were dissociated and plated into ultra-low cell attachment U-bottom 96-well plates (Corning) at a density of 3000 cell/well in 100 ul PGCLC induction medium (GK15: GMEM, 15% KSR, NEAA, 1 mM sodium pyruvate, 0.1 mM β-mercaptoethanol, 100 U/ml penicillin, 2 mM L-glutamine; supplemented with cytokines: BMP4 (500 ng/ml), LIF (1000 U/ml), SCF (100 ng/ml), BMP8a (500 ng/ml), and EGF (50 ng/ml)). For late-stage analysis, 100 ul of GK15 medium was added on day 4.

For large-scale induction of PGCLCs (for CUT&RUN, RNA-seq, and Mass Spectrometry experiments), 1.5x10^6 cells/well in 1 mL PGCLC induction medium were plated into six-well AggreWell 400 plates (STEMCELL Technologies), which were previously coated with Anti-Adherence Rising Solution (STEMCELL Technologies), and 1 mL of GK15 medium was added after 24 hours. From day 2 on, media was changed by removing 1 mL and adding 1 mL of fresh GK15 medium. After 1-6 days, embryo bodies (EBs) were collected for fluorescence-activated cell sorting (FACS) or immunofluorescence. EpiLCs were also seeded in GK15 medium without cytokines as a negative control.

To deplete MGA-AID cells, auxin (indole-3-acetic acid sodium salt, IAA, Sigma) was used at 100 μM (in H2O) for adherent cells and 500 μM for EBs.

Flow cytometry

To prepare cells for fluorescence-activated cell sorting (FACS), cultured cells or embryoids were first dissociated into single cells using Tryple and suspended in phosphate-buffered saline (PBS, Gibco) with 2% fetal bovine serum (FBS, Gibco), as well as 4′,6-diamidino-2-phenylindole (DAPI) for nuclear staining. The cell suspension was then passed through a 35-μm cell strainer into a Falcon tube (Corning) and sorted using a Sony SH800 cell sorter. PGCLCs were identified and analyzed based on the absence or presence of Blimp1-

mEGFP expression. Gates were set using expression levels in ESC-Blimp1-mEGFP and PGCLCs without cytokines to normalize the data. Negative population mESCs without any fluorescence (mE14) were used to set absolute thresholds. Data were analyzed using FlowJO for further interpretation.

Immunofluorescence

To prepare for fluorescence microscopy, adherent ESCs were grown on fibronectin-coated round slides, placed into 4-well rectangular plates (Thermo Scientific), and washed with phosphate-buffered saline (PBS). The cells were fixed with 4% paraformaldehyde (PFA, Thermo Scientific) in PBS for 20 minutes at room temperature (RT). After washing with PBS, the slides were permeabilized with 0.1% Triton X-100 in PBS (washing buffer or WB) for 30 minutes and then incubated with 2% bovine serum albumin (BSA) and 0.1% Triton X-100 in PBS (permeabilization buffer or PB) for 30 minutes. Primary antibodies (Table 1) were added, and the samples were incubated overnight at 4°C. The next day, the samples were washed with WB three times and incubated with secondary antibodies (Table 1) in PBS for 2 hours at RT. After washing with PBS, the samples were incubated with 4′,6-diamidino-2-phenylindole (DAPI) in PBS for 20 minutes and mounted using Vectashield Mounting Medium (Biozol).

Images were acquired using a Zeiss confocal LSM980 microscope and analyzed using Fiji software. For PGCLCs, EBs were collected on day 1 or day 6 and fixed with 4% PFA in PBS at RT for 20 minutes. After washing with PBS, the EBs were incubated with 10% sucrose solution in PBS at 4°C for 24 hours, followed by 1-hour incubation with 20% sucrose/PBS and embedding in OCT embedding matrix for 30 minutes at 4°C. The EBs were then embedded in a tissue-mould and stored at -80°C until cryosectioning.

The cryosectioned slides (8-µm thickness), made using Leica Cryostat CM3050S, were collected on Superfrost Plus Micro slides (Thermo Scientific) and stored at -80°C. To prevent the sections from drying out, they were circumscribed using ImmEdge Pen (Biozol) and washed with WB three times before incubation with PB for 30 minutes. The slides were then processed as described for adherent cells.

Collection of Genital Ridges from Embryos

All animal experiments were performed following the ethical guidelines of the German animal protection law (TierSchG) and approved by the Niedersächsisches Landesamt für Verbraucherschutz und Lebensmittelsicherheit (LAVES). Mice carrying ΔPE-Oct3/4-GFP (GOF-GFP), previously established (Yeom et al. 1996), were bred and housed in the mouse facility of the Max Planck Institute for Multidisciplinary Sciences (Göttingen, Germany). Genital ridges of male and female siblings were isolated from 10.5 and 11.5 dpc embryos. After fixation with 4% paraformaldehyde, the tissues were embedded in OCT compound and frozen. Sectioning and immunostaining procedures were performed as described above for EBs.

Cleavage under target and release under nuclease (CUT&RUN) procedure

All CUT&RUN experiments were performed using 500,000 cells per biological replicate (ESCs-EpiLCs: triplicates; PGCLCs day1: duplicates) and normalized using IgG from each cell type. ESCs and EpiLCs were dissociated with Tryple and counted using the Invitrogen Countess automated cell counter. PGCLCs day1 were dissociated into a single-cell solution with Tryple and sorted with FACS based on appropriate Blimp1-mEGFP expression until reaching the appropriate number. CUT&RUN was performed as previously described (Skene and Henikoff 2017).Briefly, cells were washed and captured with BioMagPlus Concanavalin A (Polysciences), permeabilized with Wash Buffer (20 mM HEPES pH 7.5, 150 mM NaCl, 0.5 mM spermidine, and 1× complete protease inhibitor cocktail (Roche)) containing 0.065% digitonin (Dig Wash), and incubated with primary antibody (MGA, IgG) overnight at 4°C.

The cell-bead slurry was washed twice with Dig Wash, incubated with Protein AG-Micrococcal Nuclease (pAG-MNase) for 1 hour at 4°C, then washed twice more with Dig Wash. Experiments were carried out in part using pA-MNase provided by Dr. S. Henikoff and the pAG-MNase from EpiCypher. The slurry was then placed on an ice-cold block and incubated with Dig Wash containing 2 mM CaCl2 to activate pAG-MNase digestion for 30 minutes. After adding one volume of 2x Stop Buffer (340 mM NaCl, 20 mM EDTA, 4 mM EGTA, 0.05% Digitonin, 0.05 mg/mL glycogen, 5 mg/mL RNase A) to stop the reaction, fragments were released by a 10-minute incubation at 37°C. Samples were centrifuged for 5 minutes at 16,000xg at 4°C, and the supernatant was recovered. DNA was extracted by spin column (NucleoSpin kit Qiagen), and resulting DNA was quantified and analyzed by TapeStation 2200 (Agilent). The resulting DNA was used as input for library preparation.

Library preparation was carried out following the protocol (https://dx.doi.org/10.17504/protocols.io.bagaibse) modified to preserve short DNA fragments, ideal for studying transcription factor profiles, using NEBNext Ultra II DNA Library Prep Kit (NEB). Fragment size distribution and the absence of adaptor dimers were checked using Agilent TapeStation 2200 and High Sensitivity D1000 ScreenTape. Libraries were sequenced as 100 bp paired-end reads on the Illumina Nova Seq 6000 at the Sequencing Core Facility (Max Planck Institute for Molecular Genetics, Berlin, Germany).

CUT&RUN data analysis

Sequencing data were processed according to the standard CUT&RUN pipeline (https://bitbucket.org/qzhudfci/cutruntools/src/default/). First, paired-end reads were quality-checked using FastQC, and then trimmed for adapter removal using a two-step process with Trimmomatic (Bolger, Lohse, and Usadel 2014) and Kseq trimmer. The trimmed reads were then mapped to the mouse genome (mm10) using Bowtie2 (Langmead and Salzberg 2012), and duplicate reads were removed using Samtools. Peak calling was performed using MACS2 (Li et al. 2009; Zhang et al. 2008), and bed files for each replicate were obtained after removing IgG peaks with BEDTools subtract (Quinlan 2014). Merged peaks from

biological replicates were obtained using an R script that generated consensus non-redundant peaks with an occurrence in at least two samples for triplicates and by concatenating two BED files on the Galaxy platform for duplicates (Afgan et al. 2016). Genomic peak annotation was performed using the ChIPseeker R package (Yu, Wang, and He 2015) with ±1kb around TSS set for the promoter region window. The comparison of Gene-ontology analyses of MGA targets was performed using the Bioconductor package clusterProfiler (Yu et al. 2012), setting the threshold as an adjusted p-value of 0.01, and using ShinyGO 0.76.2 (http://bioinformatics.sdstate.edu/go/) for visualization. Motif discovery and enrichment were performed using TFmotifView (Leporcq et al. 2020). CUT&RUN signals were obtained by merging bam files from each replicate using Samtools merge, and then deepTools bam-Coverage (option --binSize 50 --normalizeUsing CPM --scaleFactor 10 --smoothLength 150 --extendReads 157) was used to generate bigwig files (Ramírez et al. 2016). Heatmaps and profile plots were performed using the functions computeMatrix, followed by plotHeatmap and plotProfile from deepTools. The data were visualized using IGV (Thorvaldsdottir, Robinson, and Mesirov 2013), and Venn diagrams were generated using InteractiVenn (http://www.interactivenn.net).

Construction of T-box deletion, auxin-Inducible MGA Degron and DAZL Knockdown cells

The CRISPR/CAS9 system was to target endogenous genes in our study. All guide RNAs (gRNAs) were designed using either Benchling/CRISPOR software or sequences obtained from CRISPR screening designed by the laboratory of Feng Zhang (Sanjana, Shalem, and Zhang 2014). Next, gRNA oligos with *BbsI* overhangs were annealed and ligated into pSpCas9(BB)-2A-Puro (PX459) V2.0, which was a gift from Feng Zhang (Adgene plasmid # 62988, http://n2t.net/addgene:62988; RRID:Addgene 62988). The gRNA oligos used are listed in Table 2.

To construct the MGA-AID-mCherry targeting vector, we assembled it by serial modification of the base vector pMK292 (mAID-mCherry2-NeoR), which was a gift from Masato Knemaki (Addgene plasmid # 72830; http://n2t.net/addgene:72830; RRID:Addgene_72830). We used Gibson assembly with the following templates: the minimal functional AID tag fused with mCherry was amplified by PCR from pMK292, and homology arms to the last exon and 3'UTRs of MGA were PCR amplified from Blimp1-mEGFP ESCs genomic DNA (1kb each).

Plasmids were transfected into Blimp1-mEGFP cells using lipofectamine 2000 (Invitrogen), following the manufacturer's guidelines. The day after transfection, cells were subjected to puromycin selection (1ug/ml) for 48h to eliminate any non-transfected cells and passed them at a range density. Approximately one week later, colonies were picked and expanded, and PCR screened them followed by Sanger sequencing to determine the desired genomic modification.

To delete the T-box domain, we transfected Blimp1-mEGFP cells with two px459-Cas9-sgRNA targeting MGA's T-box domain in exon 2. Two correctly targeted homozygous clones were used for this study (T-box1 and T-box7).

To knock in the AID-mCherry cassette at the N-terminal of MGA, we first generated TIR1-Blimp1-mEGFP ESCs by transfecting pPB-CAG-OsTir1-V5-T2A-Puro along with the pPBase vector. After evaluating the number of copies of TIR1 for the selected colonies, we then transfected the MGA-AID-mCherry vector together with px459-Cas9-sgRNA targeting MGA last exon. Two correctly targeted homozygous clones were used for this study (clone A and clone 27).

To generate DAZL knockdown (dDAZL cells), one MGA-AID clone was then transfected with px459-Cas9-sgRNA targeting DAZL fifth exon. One correctly targeted homozygous clone was used for this study.

A table of the gene targeting gRNAs, genotyping primers and the editing strategy is shown below.

Target gene	Target site	gRNA sequence (5'-3')	Primer sequence (5'-3')	Strategy
T-box domain (MGA)	Exon 2 (beginning)	FW-CAC CGC CCT TGA TAA CAA TAG TAT G	FW-AGTCATCACCAGGAAAATCTAAAGAGAA	Deletion of T-box domain
		REV-AAA CCA TAC TAT TGT TAT CAA GGG C		
	Exon 2 (end)	FW-CAC CGC CCA TCA TCC CGA AAG CCT T	REV-GGATCAAAATCACCTGAATGTATCTCTG	
		REV-AAA CAA GGC TTT CGG GAT GAT GGG C		
MGA	Exon 24-3'UTR	FW-CACCGAGCTCCATCAAGTTCATCA	FW-ATGCCTACATTGGCACCTGTT	Tagged MGA with AID-mCherry (Auxin degron system)
		REV-AAACTGATGAACTTGATGGAGCTC	REV-CTCACAGCCTGGCTTTTGTATG	
	pMK292-exon24		FW-gactcactatagggcgaattggagctccccgggAGGTATGAGTGGCAACAAA	Generate MGA-AID-mCherry vector
			REV-TTTGCCTGATGAACTTGATGGAGCT	
	Exon24-AIDmCherry		FW AGCTCCATCAAGTTCATCAGGcAAAaaggagaagagtgcttgtcctaaaga	
			REV-GCTTTTGTATGAGGATGAACAAGCTCAttacttgtacagctcgtccatgccg	
	AIDmCherry-3-UTRs		FW-TGAGCTTGTTCATCCTCATACAAAAGC	
			REV-atgtggtatggctgattatgatcagttatctagaATTTTGGCTACGGTCTCTGGTTAGGG	

DAZL	Exon 5	FW- CACCGTGAAACT GGGCCCTGCAAT CAGG	FW GAA CTG GTG TGT CGA AGG GG	Generate frame-shifting indel in coding exon
		REV-AAAC GATTGCAGGGCCCAGTTTCAC	REV- CAG CTC CTG GAT CAA CTT CAC T	

RNA-sequencing procedure

RNA sequencing was performed on two independent cultures of ESCs, EpiLCs, and PGCLCs on day 1 and day 6. ESCs and EpiLCs were dissociated with Tryple, pelleted, and processed. PGCLCs on day 1 and day 6 were dissociated into a single-cell solution with Tryple and sorted with FACS based on appropriate Blimp1-mEGFP expression until 100,000 cells were obtained. All samples were processed as follows: ΔT-box samples were obtained from two independent cultures of ESCs, EpiLCs, and PGCLCs on day 6 for both the wild-type and two ΔT-box clones(ΔT-box1 and ΔT-box7),respectively; MGA-AID samples were obtained from two clones (clA and cl27) from the same passage (ESCs and EpiLCs) or the same PGCLC inductions were used as replicates together with TIR1 cells; dDAZL samples were obtained from two independent cultures. RNA extraction was performed using the RNeasy Mini kit (Qiagen). The RNA integrity number was assessed using RNA ScreenTape (Agilent), and all samples were confirmed to have RIN >8.5. Libraries were prepared from 250ng of total RNA using the NEBNext® Ultra™ II Directional RNA Library Prep Kit for Illumina (NEB). The libraries were sequenced as 100bp single/paired-end reads on the Illumina Nova Seq 6000 at the Sequencing Core Facility (Max Planck Institute for Molecular Genetics, Berlin, Germany).

RNA-seq data analysis

The quality of the library sequence was analyzed using FastQC, and low-quality reads and adaptor sequences were removed using Trimmomatic. RNA-seq reads were aligned to the mouse reference (GRCm38/mm10) genome using STAR (Dobin et al. 2013). Read counts per gene were obtained by HTseq-count (parameters –t exon –s reverse) (Anders, Pyl, and Huber 2015) and normalised using DEseq2 in R (Love, Huber, and Anders 2014). Differential expression analysis was performed using DESeq2 (fold change >1.5, adjusted p-value < 0.05). GO analysis was performed using Metascape (http://metascape.org/gp/index.html). Heatmaps were generated using ComplexHeatmap and pheatmap in R, while Boxplot were created using BoxPlotR (http://shiny.chemgrid.org/boxplotr/).

Reverse-transcriptase quantitative PCR

Total RNAs were reverse transcribed into cDNA using the QuantiTect Reverse Transcription Kit (Qiagen). qPCR was performed with KAPA SYBR FAST (Roche) on a CFX96 touch Real-Time PCR instrument (Bio-Rad). The expression of target genes was normalized using the housekeeping gene, *Arbp*, as indicated in the figure. The primer sequences for qPCR are listed in the table below.

Target genes	Forward primer (5'-3')	Reverse primer (5'-3')
Arbp	CAAAGCTGAAGCAAAGGAAGAG	AATTAAGCAGGCTGACTTGGTTG
Prdm1	GAGGATCTGACCCGAATCAA	CATGGAGGTCACATCGACAC
Prdm14	ACAGCCAAGCAATTTGCACTAC	TTACCTGGCATTTTCATTGCTC
Ap2y	ATCAAGATCGGACACCCAAC	ATGGCGATTAGAGCCTCCTT
Dazl	CCAGAAGGCAAAATCATGCCAA	GGCAAAGAAACTCCTGATTTCGG
Sycp3	TGTGTTGCAGCAGTGGGAACTG	GGCTCTGAACAATTCTAGACTGC

Co-immunoprecipitation (Co-IP) and Western Blotting

Cells were harvested and suspended in lysis buffer (50 mM Tris-HCl [pH 7.5], 150 mM NaCl, 1% NP40, 0.5% NaDeoxycholate, 1× cOmplete protease inhibitor cocktail). The cell suspension was incubated on ice for 10 minutes, followed by incubation for 15 minutes on a rolling wheel at 4°C, and then centrifuged at 16,000 g for 10 minutes at 4°C. The supernatant was collected and quantified using the Qubit Protein assay (Thermo Fisher Scientific).

For immunoprecipitation, the cell lysates were incubated with Dynabeads Protein G (Thermo Fisher) for 1 hour at 4°C to pre-clear the lysate. Then, the cell lysates were incubated with the indicated antibodies for 2.5 hours at room temperature. Protein G-associated Dynabeads were added and incubated overnight at 4°C. After washing three times with lysis buffer and two times with Wash Buffers (50 mM Tris-HCl, pH 7.5, 250 mM NaCl, 0.1% NP-40, 0.05% deoxycholate), 1X protein SDS loading buffer (Bio-Rad) was added and boiled for 5 minutes. The supernatant was cooled on ice for 5 minutes before loading onto a gel for immunoblotting. As a control, immunoprecipitation was performed using IgG. Immunoprecipitated proteins and input were loaded onto a 4-12% SDS-polyacrylamide gel electrophoresis (Bio-Rad) and transferred to a 0.45 µm nitrocellulose membrane (Amersham). The membranes were probed with appropriate antibodies (listed in Table 1).

Mass spectrometry and data analysis

To characterize novel interactor partners of MGA, we performed MGA and IgG immunoprecipitation using $6x10^6$ cells (ESCs, EpiLCs) and $1.5x10^6$ cells (PGCLCs) per biological replicate (ESCs, EpiLCs: triplicates; PGCLC day 6: quadruplicate). Dr. Ralf Pflanz at the Proteomics Facility, part of the Bioanalytical Mass Spectrometry group of Prof. Henning Urlaub in Göttingen, Germany, carried out further processing steps.

Raw files from MS/MS were analyzed with MaxQuant (Cox and Mann 2008) version 2.0.3.0 with default settings and searching against the UniProt mouse proteome (UP_mouse_rev_070219). Additional options for 'match between runs', LFQ, and iBAQ were selected. Statistically enriched proteins were identified using a permutation-based false discovery rate (FDR)-corrected two-sided t-test applied on LFQ, using the Perseus Software protocol which are listed in table 2 (Rudolph and Cox 2019). Stoichiometry calculation was made using the iBAQ value. We subtracted the IgG values from MGA pulldown iBAQ intensity. The relative abundance values were scaled to obtain the abundance of the bait protein, which was set to 1 (Smits et al. 2013). GO analysis was performed using Metascape.

Table 1

A table of the antibodies used for western blot, staining, CUT&RUN and immunoprecipitation with the concentration used is shown below.

Primary Antibody	Western Blot	Staining	CUT&RUN	Immunoprecipitation
MGA Abcam EPR19854	1:1000	1:100/1:500	1:50	1:50
Guinea Pig anti-Rabbit-IgG Antibodies ABIN101961	x	x	1:100	1:50
DAZL Abcam ab34139	1:1000	1:100	x	1:50
L3MBTL2 Active Motif 39569	1:1000	x	x	x
Alpha Tubulin proteintech 66031-1-Ig	1:2000	1:50	x	x
T Abcam ab20680	1:1000	x	x	x
BLIMP1 Cell Signalling 9115	1:1000	x	x	x
Anti-GFP Abcam ab13970	x	1:400	x	x
SOX2 Santa Cruz sc-365823	1:500	1:50	x	1:50
AP2γ Santa Cruz sc-12762	x	1:50	x	x
OCT4 Santa Cruz sc-5279	1:500	1:50	x	1:50
NANOG eBioscience, clone eBioMLC-51, 14-5761	x	1:50	x	x

Secondary Antibody	Western Blot	Staining	CUT&RUN	Immunoprecipitation
Anti-Mouse Cell Signalling 7076	1:2000	x	x	x
Anti-Rabbit Cell Signalling 7074	1:2000	x	x	x
Alexa Fluor 488 anti-Mouse	x	1:400	x	x
Alexa Fluor 555 anti-Rabbit	x	1:400	x	x
Alexa Fluor 405 anti-Mouse	x	1:500	x	x
Alexa-Fluor 488 anti-Chicken	x	1:400	x	x
DAPI	x	1:1000	x	x

Table 2

Proteins specifically associating with MGA identified by mass spectrometry. Proteins are highlighted with different colours same used in volcano plot.

1) ESCs-MGA-IP (5 replicates)

Protein IDs	Significant	pvalue(-log10	Difference	LFQ_ESC_IgG_1	LFQ_ESC_IgG_2	LFQ_ESC_IgG_3	LFQ_ESC_IgG_4	LFQ_ESC_IgG_5	LFQ_ESC_MGA_1	LFQ_ESC_MGA_2	LFQ_ESC_MGA_3	LFQ_ESC_MGA_4	LFQ_ESC_MGA_5
sp|Q80UY2|KCMF1_MOUSE	+	4.864379	7.22539	17.29074	18.17029	19.31948	17.87659	18.47747	21.14383	20.81519	20.11108	21.78568	23.15791
sp|P48725|PCNT_MOUSE	+	3.217146	6.632461	16.90578	18.58159	18.78289	18.94906	18.89322	23.63079	21.3573	23.28799	22.7707	20.14507
sp|P14115|RL27A_MOUSE	+	2.56127	5.695423	17.80792	17.8595	18.04164	18.44245	18.4863	22.44927	20.28704	20.53583	21.17548	20.11057
sp|A2AWL7|MGAP_MOUSE	+	**7.085907**	**5.551546**	**22.5784**	**22.88183**	**23.18884**	**23.87474**	**24.50458**	**30.11458**	**27.51683**	**29.34613**	**29.22617**	**28.00935**
sp|Q99NA9|PCGF6_MOUSE	+	6.524911	5.500742	17.07492	18.37029	18.98438	19.64164	18.2612	25.90896	23.32072	26.94838	26.67936	25.60196
sp|P16460|ASSY_MOUSE	+	4.821072	5.436934	19.10669	18.71021	19.12873	19.06434	19.01927	22.92879	21.00168	21.70514	21.67029	23.08892
sp|Q80WT5|AFTIN_MOUSE	+	6.657309	5.434052	18.27526	18.69169	18.17485	18.30829	18.08298	18.72589	25.59229	24.75445	25.13065	25.80691
sp|Q64378|FKBP5_MOUSE	+	3.737555	5.327825	16.87557	18.90737	18.45806	18.74946	18.82351	24.37789	20.90095	22.54527	22.13665	24.07308
sp|Q7TME2|SPAG5_MOUSE	+	**4.783512**	**5.249745**	**17.78074**	**18.64042**	**18.84328**	**18.71615**	**18.73328**	**24.79223**	**21.70126**	**22.47949**	**22.83103**	**24.35494**
sp|P46061|RAGP1_MOUSE	+	3.015538	5.080585	18.02693	18.19289	18.34735	18.54296	19.10772	23.34584	21.16165	22.18954	21.95656	21.69043
sp|P61965|WDR5_MOUSE	+	5.475254	4.990519	19.0341	18.37037	18.20655	18.90438	18.82156	24.22347	22.043	24.02893	23.79828	24.19588
sp|Q9ERU9|RBP2_MOUSE	+	**3.330141**	**4.963639**	**16.74708**	**17.94639**	**18.09619**	**19.42929**	**19.11728**	**21.02547**	**20.62033**	**20.61072**	**20.53886**	**20.23853**
sp|Q8BMK0|CEP85_MOUSE	+	5.137912	4.845451	17.50936	20.11362	20.5966	20.75418	18.34404	26.58792	24.06093	25.14091	24.0792	24.08797
sp|Q9CQJ4|RING2_MOUSE	+	4.220932	4.689016	17.84619	19.9607	19.53615	19.78483	18.38648	21.34462	21.35127	21.70434	21.11261	21.89353
sp|P59178|LMBL2_MOUSE	+	4.567914	4.622455	17.72537	18.61598	18.04278	18.83809	19.29896	24.64301	23.77957	23.98163	23.64339	23.64384
sp|Q99JY0|ECHB_MOUSE	+	4.680971	4.584631	18.61878	20.31141	20.2383	20.41204	18.92595	21.23064	21.87023	21.82225	22.05778	22.71186
sp|Q5SV85|SYNRG_MOUSE	+	3.473287	4.443975	17.52284	18.61026	18.47269	18.32181	18.25054	21.35456	21.87871	22.32663	22.34384	21.3573
sp|Q8K389|CK5P2_MOUSE	+	6.059588	4.345991	19.28888	20.90932	18.92204	17.44352	19.03564	21.51576	23.21749	21.76596	22.41573	25.20116
sp|Q88RT1|CLAP2_MOUSE	+	3.215924	4.257121	17.05919	20.93207	18.79995	19.47326	17.82302	22.05933	22.32975	21.80923	21.82536	21.37146
sp|Q9D921|SKAP_MOUSE	+	4.248775	4.231905	21.10066	14.79589	15.25978	16.26138	18.97948	24.07194	23.15754	24.09281	23.89597	24.34123
sp|Q7TT18|MCAF1_MOUSE	+	**4.81869**	**3.972414**	**20.12098**	**18.93004**	**19.48911**	**19.1481**	**18.74816**	**23.5798**	**21.08842**	**23.16408**	**22.12626**	**24.14709**
sp|Q8JZU2|TXTP_MOUSE	+	3.069002	3.836668	16.31882	18.49612	19.28862	18.71621	18.52236	22.33189	20.38036	20.93179	21.21282	21.1077
sp|Q6NV72|WDCP_MOUSE	+	3.00261	3.815859	18.90259	18.77355	18.23612	17.40939	18.44921	21.16116	20.77209	20.42491	20.82314	21.24028
sp|Q9CY58|PAIRB_MOUSE	+	2.577674	3.703339	16.92501	17.94148	17.79005	18.9229	18.57468	20.12692	19.58261	20.75116	20.48572	20.34819
sp|Q3UYG1|CC160_MOUSE	+	4.695302	3.625234	18.36438	18.59363	19.15365	18.22234	19.1033	25.09096	22.92586	22.79511	22.96603	23.8866
sp|Q99LC3|NDUAA_MOUSE	+	5.806003	3.616579	24.84891	25.21148	24.7168	24.95553	25.10278	26.26573	25.5813	26.39062	26.03758	26.2325
sp|Q9QWT9|KIFC1_MOUSE	+	3.45476	3.533851	18.32418	19.88832	20.20275	19.98008	19.70198	21.84165	21.06612	21.23468	21.84126	21.41183
sp|Q62158|TRI27_MOUSE;sp|Q9ESN2|	+	5.468193	3.480026	17.72832	18.98479	18.57485	19.77748	17.0559	25.98494	20.63254	23.46688	22.99099	24.44891
sp|Q8R0G9|NU133_MOUSE	+	5.350689	3.417185	24.67098	26.38407	26.57615	25.96838	19.15602	18.85611	18.32464	17.27808	18.05817	17.65093
sp|Q8BM51|ECHA_MOUSE	+	2.648071	3.334945	23.17039	21.94796	21.46558	21.10961	21.1465	18.76435	18.79549	18.92654	18.81285	17.73571
sp|O35654|DPOD2_MOUSE	+	3.755144	3.331898	17.44402	18.46725	18.75192	18.43848	18.26642	21.61405	20.71934	21.36592	21.34186	21.00696
sp|Q07104|GDF3_MOUSE	+	3.333797	3.311195	17.45482	18.80634	19.83542	19.02208	17.2058	21.51716	20.995	20.32499	20.53735	21.34841
sp|Q9R0L6|PCM1_MOUSE	+	2.688287	3.26334	17.30335	18.94982	19.49166	18.22647	17.9825	21.30463	21.30575	22.34865	21.88818	21.24899
sp|Q9JLM4|ZMYM3_MOUSE	+	4.10499	3.228481	17.48729	18.50863	17.71899	18.85577	19.51081	24.0554	21.64759	22.98024	23.12321	23.38732
sp|Q8BX10|PGAM5_MOUSE	+	3.065349	3.175824	17.35867	18.43378	18.39384	17.7171	18.94855	20.48188	21.06362	21.49121	21.08434	20.1149
sp|Q62074|KPCI_MOUSE	+	4.486076	3.175246	18.57724	18.84522	18.76451	19.74801	18.48861	21.76571	20.78556	21.42198	20.46981	21.67405
sp|Q9CPS7|PNO1_MOUSE	+	2.796193	3.093671	17.64821	18.83231	18.41362	18.38858	18.26406	22.69098	20.16668	21.66214	20.83746	20.93575
sp|Q1PSW8|LIN41_MOUSE	+	4.174234	3.073117	17.2727	19.22331	18.70094	19.15321	18.72588	25.46678	22.7233	23.47296	23.62701	24.03473
sp|Q08297|RAD51_MOUSE	+	2.667424	3.061529	18.34456	17.69764	18.67682	18.81059	19.68404	21.39827	19.61585	21.04747	21.18574	20.87725
sp|Q91WG4|ELP2_MOUSE	+	3.763087	2.973619	17.70212	18.65896	19.36065	19.08454	18.28166	23.28968	21.40919	21.7536	20.89903	22.3959
sp|Q9CZH8|CCD77_MOUSE	+	3.621243	2.949246	17.67343	18.3693	17.83508	19.28598	18.16488	20.38648	19.83138	20.42798	20.75385	20.63076
sp|Q61539|ERR2_MOUSE;sp|P62509|(	+	5.332413	2.936009	18.44735	18.16781	19.44704	17.97622	18.4391	24.50367	23.09512	24.00196	23.9832	24.39728
sp|Q9DBE8|ALG2_MOUSE	+	4.360018	2.927506	18.34868	21.54567	21.51658	20.80349	19.57895	24.55298	22.7554	24.62109	23.97272	22.56591
sp|Q3UM18|LSG1_MOUSE	+	3.279385	2.925325	18.82128	18.79945	19.11932	18.00607	18.367	23.55777	22.28176	23.09933	22.46498	23.43924
sp|O88974|SETB1_MOUSE	+	**2.910369**	**2.924483**	**16.91353**	**18.84809**	**19.05765**	**18.6806**	**18.23175**	**22.13931**	**21.35294**	**21.11515**	**21.32948**	**20.66284**
sp|O54917|E2F6_MOUSE	+	4.526082	2.87351	17.36342	20.79939	18.81663	19.42922	18.14665	21.98242	21.92872	21.18538	21.81206	23.11509
sp|Q6ZQ88|KDM1A_MOUSE	+	3.114579	2.859486	18.72604	19.07726	18.72572	19.2002	18.85054	22.26178	20.56514	21.57038	21.66027	21.81535
sp|Q3UJV1|CCD61_MOUSE	+	3.592023	2.784077	18.92852	18.36755	17.38269	18.50854	17.33782	22.52669	20.97778	23.54333	22.88876	21.74809
sp|Q3UMC0|AFG2H_MOUSE;sp|Q9D3R(	+	3.156669	2.758309	17.35169	18.75402	18.52957	18.99436	17.93571	20.24493	20.73438	20.87793	20.76409	20.01468
sp|Q9D1M0|SEC13_MOUSE	+	2.710707	2.733451	17.43469	18.45388	18.98886	18.7186	18.49244	20.26098	20.37241	20.19832	21.74271	19.90686
sp|Q9D753|EXOS8_MOUSE	+	3.519826	2.694489	20.52593	20.35348	19.64679	19.46718	18.18436	22.97325	22.07215	22.25503	21.48729	23.18158
sp|Q9CQU5|ZWINT_MOUSE	+	4.027277	2.676801	17.80386	18.41569	19.31711	19.02877	18.45933	22.86761	20.41833	20.70092	21.49565	22.16886
sp|Q8BSF4|PISD_MOUSE	+	4.737019	2.658635	21.55754	18.34628	17.95775	18.34664	18.76145	25.42089	22.01723	23.67368	23.84575	24.83031
sp|Q4FZF3|DDX49_MOUSE	+	4.505759	2.530143	17.8351	18.32795	19.26318	18.11878	18.92206	23.48013	21.69047	22.10217	22.00683	23.04955
sp|Q9DCE5|PK1IP_MOUSE	+	2.724102	2.479687	17.49553	18.29369	18.37722	18.32973	18.06686	19.51389	20.91335	19.86974	19.14684	20.54066
sp|Q3UA06|PCH2_MOUSE	+	3.130503	2.380051	18.2066	18.46936	18.92172	18.25015	19.30349	21.1332	19.90389	21.55417	20.58371	19.74598
sp|Q8CGY8|OGT1_MOUSE	+	3.192464	2.378401	18.98305	18.88288	17.90351	18.89885	18.42634	22.48895	22.19277	21.34749	21.84	22.62556
sp|Q8K224|NAT10_MOUSE	+	3.248277	2.34962	17.60976	18.41572	18.10866	18.43629	16.71716	21.61441	20.85795	20.5657	20.71154	21.41421
sp|Q91VY9|ZN622_MOUSE	+	2.845555	2.339536	17.49454	18.20889	18.21043	18.47484	17.60196	19.22873	19.74665	20.02052	20.00813	20.64042
sp|Q6NVF9|CPSF6_MOUSE	+	3.897306	2.338703	17.15218	18.22782	19.21715	18.57114	16.78025	23.32113	22.24394	20.20108	20.71925	22.64647
sp|Q922S8|KIF2C_MOUSE	+	2.955484	2.237255	17.17759	18.65023	18.64167	17.82393	17.55497	20.4711	20.4051	19.71089	19.65992	21.34949
sp|Q6P2B1|TNPO3_MOUSE	+	3.296352	2.228093	17.00776	18.7751	18.46344	18.51384	19.62511	21.32965	21.02499	20.7576	21.58049	21.16497
sp|Q8BIX3|AL14E_MOUSE	+	3.71546	2.214132	18.61941	17.85	19.4004	16.55258	19.39455	24.70556	21.23911	22.4039	22.25023	22.50373
sp|Q8C547|HTR5B_MOUSE	+	2.888982	2.182186	18.32147	17.84518	18.51717	18.2852	19.07129	22.39331	21.11343	21.59113	21.68205	22.34633
sp|Q9D0I8|MRT4_MOUSE	+	3.773041	2.140356	17.53542	19.72274	20.47229	19.12168	18.67664	22.83919	21.22647	22.41669	22.77296	22.82945
sp|P11157|RIR2_MOUSE;sp|Q6PEE3|RI	+	2.979951	2.078563	17.77425	19.02162	18.40604	17.98364	18.28256	21.93708	20.69702	20.68398	20.8413	21.67629
sp|O55091|IMPCT_MOUSE	+	2.875296	1.953928	17.53911	19.49798	17.9631	17.6166	18.12802	20.72117	21.08602	21.18749	21.22158	21.16607
sp|Q3URQ0|TEX10_MOUSE	+	3.71968	1.930756	22.4496	20.90984	20.64966	20.09558	18.20766	24.49637	23.02337	23.80528	23.43454	23.86948
sp|Q9JKC8|AP3M1_MOUSE;sp|Q8R2R9	+	3.07743	1.88429	16.74464	19.09455	19.47011	19.4427	18.17532	21.86374	21.21549	21.66813	21.70936	20.13786
sp|P61963|DCAF7_MOUSE	+	2.998458	1.859644	18.46481	18.50536	18.69039	18.28055	18.26267	19.47807	19.33032	19.78069	20.11261	20.81878
sp|A2AN08|UBR4_MOUSE		**2.018348**	**6.315606**	**18.11285**	**24.58159**	**23.96305**	**25.83535**	**22.88142**	**18.17612**	**25.5994**	**26.53726**	**25.65103**	**26.21178**
sp|P20263|POF1_MOUSE		0.890182	1.819274	18.29254	18.8133	21.7432	21.57759	18.53584	17.6356	22.11312	21.39509	21.56481	20.51759
sp|Q921E6|EED_MOUSE		2.224329	1.807505	18.04421	19.00987	18.04036	24.74812	23.62712	18.28914	20.38121	22.30847	23.04243	25.9467
sp|Q88T07|CEP55_MOUSE		1.68623	1.801362	26.29971	19.06163	23.13449	21.61621	17.96614	26.00958	20.52946	25.4197	24.86287	25.18597
sp|Q9D6Z1|NOP56_MOUSE		1.065148	1.801134	17.66565	19.42323	18.63347	18.88551	17.49359	19.74179	20.75858	21.0997	20.48621	18.92413
sp|Q8K3Y3|LN28A_MOUSE		1.558061	1.800281	19.78144	20.71095	20.72983	20.39393	22.06569	22.58854	22.20398	21.83927	21.89152	24.47655
sp|Q8BP48|MAP11_MOUSE		1.064472	1.794736	24.34577	24.00898	23.89078	24.21904	17.8075	25.82982	23.37372	24.95731	24.95593	24.0059
sp|P70398|USP9X_MOUSE		2.597993	1.794429	26.60102	27.72221	27.0878	27.39517	26.62519	26.02766	27.14822	28.18631	27.66878	26.51437
sp|Q6PDQ2|CHD4_MOUSE		1.605852	1.793665	22.27855	22.37875	23.16294	22.52703	19.06445	23.52612	22.45438	21.8514	22.50281	23.8624
sp|P62307|RUXF_MOUSE		1.228441	1.785793	17.78582	22.40234	23.15877	22.94135	18.85508	22.35351	22.3787	22.61901	22.399	23.73655
sp|Q6P3A8|ODBB_MOUSE		1.981534	1.781789	22.43451	20.76838	22.00512	19.73759	24.59366	23.86854	18.67942	22.53969	21.95031	25.90012
sp|Q3TJZ6|FA98A_MOUSE		0.961473	1.775948	20.67219	22.65347	23.089	23.61336	19.23334	22.03999	24.21148	23.63467	23.09347	20.8786
sp|Q91W50|CSDE1_MOUSE		1.973842	1.775764	22.35114	24.47957	25.04689	25.04256	18.61082	25.08489	24.75995	24.92913	24.97705	24.41041
sp|Q99P88|NU155_MOUSE		2.078677	1.771374	17.5386	25.20404	25.10025	25.73624	19.03561	18.02378	25.85369	25.31907	25.6294	26.56758
sp|P31230|AIMP1_MOUSE		0.646786	1.770588	17.39932	22.48424	21.86495	22.16846	19.29239	18.52972	22.10926	21.80865	21.60123	20.81972
sp|P70168|IMB1_MOUSE		0.655372	1.770123	20.42419	23.79054	23.38153	23.57554	19.28449	18.08898	23.08188	22.7615	23.17594	17.35264
sp|Q3U9G9|LBR_MOUSE		1.473152	1.769833	21.79769	18.80883	21.75471	21.29592	17.58902	22.47665	20.60684	22.27421	22.05033	19.1989
sp|Q8CG47|SMC4_MOUSE		1.154976	1.765545	17.3756	18.9159	18.67266	17.87655	19.56284	17.23454	19.15931	17.89131	17.82056	19.51077

2) EpiLCs MGA-IP (3 replicates)

Protein Ids	Significant	pvalue(-log1	Difference	LFQ_EpiLC_IgG_1	LFQ_EpiLC_IgG_2	LFQ_EpiLC_IgG_3	LFQ_EpiLC_MGA_1	LFQ_EpiLC_MGA_2	LFQ_EpiLC_MGA_3
DOPD_MOUSE	+	4.61658688	10.6617285	18.81955147	17.36318398	18.31180191	28.56223679	29.25925636	28.65822983
KCMF1_MOUSE	+	4.55384368	7.68915494	18.9022789	18.0851078	17.80310631	26.22326469	25.74911499	25.88557816
CHIP_MOUSE	+	2.7415183	7.37027486	19.68459702	16.90718842	18.04935646	26.73039627	24.74237061	25.2791996
RAGP1_MOUSE	+	3.95867771	7.32686806	19.30167198	18.243536	19.39508629	25.72517776	26.40666962	26.78905106
RBP2_MOUSE	**+**	**5.67360424**	**7.16579501**	**18.73498726**	**19.22387886**	**18.81690788**	**25.92601204**	**26.22618866**	**26.12095833**
SPAG5_MOUSE	**+**	**3.56227851**	**6.91701508**	**19.16125679**	**18.22177124**	**17.60593414**	**24.85000229**	**24.9343605**	**25.95564461**
AFTIN_MOUSE	+	3.51294491	6.63915507	18.92004585	17.61921883	17.59650612	24.10797119	24.59109306	25.35417175
MGAP_MOUSE	**+**	**3.48410145**	**6.62339528**	**18.56089592**	**18.68721199**	**17.57990646**	**25.8158741**	**24.4582634**	**24.42406273**
UBR4_MOUSE	**+**	**2.85385193**	**6.53383636**	**20.14895058**	**20.56885338**	**22.64662743**	**27.17111969**	**27.58684921**	**28.20797157**
CEP85_MOUSE	**+**	**2.98246108**	**6.50317891**	**18.72481728**	**17.59318924**	**17.36949348**	**23.12941742**	**24.92886162**	**25.13875771**
SUMO1_MOUSE	**+**	**2.93731738**	**6.38932482**	**19.27436256**	**17.15667915**	**17.5198307**	**23.67076874**	**24.36452866**	**25.0835495**
CLAP2_MOUSE	+	2.04299779	6.23827076	19.30665588	15.27953815	17.26554108	22.32846832	23.83701515	24.40106392
PCGF6_MOUSE	**+**	**4.06752149**	**6.1213754**	**18.42327118**	**17.96426201**	**17.53875542**	**24.57010651**	**23.60263634**	**24.11767197**
SYNRG_MOUSE	+	3.21421546	6.08395894	18.81247902	17.83550644	18.7971344	23.57484818	24.73003387	25.39211464
RING2_MOUSE	**+**	**2.32771904**	**5.91979408**	**20.70223999**	**17.46801567**	**18.04773521**	**25.25234222**	**24.43872833**	**24.28630257**
MCAF1_MOUSE	**+**	**2.81527341**	**5.91836294**	**19.4872303**	**17.64792442**	**18.47970963**	**23.40626335**	**24.67168617**	**25.29200363**
PCNT_MOUSE	+	2.14238437	5.8811264	18.34606171	20.09764099	16.30773354	23.5370636	24.87333298	23.98441887
GSH0_MOUSE	+	3.30242589	5.71939214	18.55685616	17.29494858	17.3850174	22.76016045	24.0500946	23.5847435
LMBL2_MOUSE	**+**	**3.90749812**	**5.4538784**	**18.22072601**	**18.8119812**	**17.64989471**	**23.99412155**	**23.54674911**	**23.50336647**
RL36_MOUSE	+	3.16336298	5.4461422	19.76869774	18.96806145	17.80791473	24.39021301	24.33619881	24.15668869
WDR5_MOUSE	**+**	**3.00409955**	**5.34064039**	**19.33665085**	**17.71678925**	**17.87186813**	**24.30089569**	**23.14734077**	**23.49899292**
H32_MOUSE	+	3.63307755	5.33774948	18.74908829	17.62896538	17.45686531	23.3730526	23.45010376	23.02501106
RL7_MOUSE	+	1.98299709	5.31462224	19.27352333	22.14513397	23.08284378	27.23114204	26.74727249	26.46695328
FKBP5_MOUSE	+	3.37689456	5.28241285	18.86065102	20.12148857	20.17596817	24.59559631	24.99804497	25.41170502
CK5P2_MOUSE	+	2.48332287	5.24262746	19.06321907	17.17523766	17.59961319	21.98978043	23.96912575	23.60704613
H11_MOUSE	+	2.4760626	5.22491646	17.57205772	17.16720581	19.61009216	23.73892403	22.62885284	23.6563282
PURA_MOUSE	+	2.70534745	4.9961586	19.17216301	16.94867134	18.41490746	23.39649773	23.42342186	22.70429802
SRRM1_MOUSE	+	2.59781929	4.97811762	19.31382561	16.81764793	18.1520462	23.32223701	23.11909866	22.77653694
U2AF1_MOUSE	+	3.66527257	4.92716726	18.63405228	17.59212494	18.73543739	23.41209221	23.32443619	23.00658798
DPOD2_MOUSE	+	2.35312434	4.89784431	18.79545403	17.14063072	19.44566536	22.40275574	23.60681915	24.06570816
U2AF2_MOUSE	+	1.93896012	4.83501752	18.91314316	21.42183113	17.72529984	24.34170532	24.21378517	24.0098362
NCK5L_MOUSE	+	3.35844773	4.7909406	19.08883667	18.21545601	17.61260986	23.32991982	22.86221123	23.09759331
SNUT1_MOUSE	+	2.45564743	4.70922089	19.64601517	17.32256699	17.52886581	23.20402527	22.82080841	22.60027695
SKAP_MOUSE	+	3.29758259	4.61767324	18.44835281	17.50347137	18.46372795	22.79629898	22.18752289	23.28474998
KIF2A_MOUSE	+	3.11950811	4.5745093	18.268116	18.99476814	17.59426689	22.32819366	23.30187225	22.95061302
TSR1_MOUSE	+	2.75864991	4.53007062	18.70022583	17.40155792	17.57525826	22.62722778	23.08407593	21.55595016
UBC9_MOUSE	+	3.48977552	4.5066274	17.46515656	18.56554985	17.73800278	22.03123474	22.73566437	22.52169228
PNO1_MOUSE	+	3.32848092	4.46100934	17.93741608	18.11243248	17.59237862	22.1634922	23.10184669	21.75991631
EXOSX_MOUSE	+	2.32039044	4.42460442	18.42805672	17.58399773	17.02157402	23.16633034	22.26258659	20.87852478
MEF2D_MOUSE;sp	+	2.1544291	4.42369016	Color2 [A=255, R=1	4	19.94671822	1		23.89892197
SYHM_MOUSE	+	3.20291713	4.3939298	18.84627342	17.54482841	18.11864853	22.3318615	22.29642105	23.06325722
CLU_MOUSE	+	2.17165909	4.38948758	18.67285919	20.66431618	21.25942802	24.18055916	24.32546616	25.25904083
PGAM5_MOUSE	+	3.42012251	4.30949593	18.14195442	17.3527832	17.33651352	22.32385826	22.06601906	21.3698616
RHG29_MOUSE	+	2.55568929	4.30063756	18.71793938	16.87994385	18.45842171	21.95663261	22.94611931	22.0554657
IF2B_MOUSE	+	2.70932477	4.28642591	18.5987339	17.79199028	19.00489616	23.67260361	22.09003448	22.49225998
THOC4_MOUSE;sp	+	2.76153011	4.22520002	4	18.49230003	17.06309891		22.71334839	22.2612381
WDCP_MOUSE	+	2.05155866	4.22488149	20.00613976	17.44912148	17.9667511	23.3823185	21.93081093	22.78352737
CBX3_MOUSE	**+**	**3.7179372**	**4.22261111**	**18.09908676**	**18.41207123**	**18.00570297**	**22.97774506**	**22.01478195**	**22.19216728**
PSMD4_MOUSE	+	4.20598152	4.18266233	18.95907593	18.38945961	18.20957947	22.81971741	22.5572834	22.72910118
KHDR1_MOUSE;sp	+	2.41835049	4.16928355	4	19.56681061	18.82207108		22.26987839	23.45022964
SUH_MOUSE;sp	+	3.97482932	4.14488729	4	18.36063957	18.28832245		22.97999573	22.12136078
SON_MOUSE	+	2.18578946	4.11195755	18.22954178	17.17340851	18.11042404	20.51854897	22.74011803	22.59057999
LUC7L_MOUSE	+	1.98123811	4.04061953	18.83032799	18.33063889	16.56433678	23.03853607	21.65215302	21.15647316
TMM11_MOUSE	+	2.83713278	4.00419617	18.38152885	16.75878716	17.6762867	21.71770477	21.90080261	21.21068382
CNBP_MOUSE		1.9145825	3.96387672	18.68654442	18.21321106	20.72375679	23.96947861	23.2588253	22.28683853
SRSF5_MOUSE	+	2.1948316	3.9635671	19.92101479	20.89548683	18.38638878	23.99412155	23.78925133	23.31021881
SMD3_MOUSE	+	3.03961418	3.95172564	17.23462296	17.64693451	18.42859077	21.73463058	22.19976425	21.23093033
NOB1_MOUSE	+	2.36447098	3.93350538	18.45409584	17.90167999	20.08342743	22.69718742	23.05147171	22.49106026
DDX21_MOUSE	+	2.73525738	3.90571976	19.42481041	18.32781982	17.88010979	22.26490593	22.98231316	22.10268021
SRSF2_MOUSE		1.90375762	3.83568573	17.91196251	17.96323586	20.41905403	23.1043129	22.70227051	21.99472618
S39A7_MOUSE	+	2.94695685	3.82988294	19.00814629	17.93953705	18.20274544	22.4443512	21.56616211	22.62956429
NOG1_MOUSE	+	2.70646874	3.76861827	19.17247391	18.30768967	17.61941719	22.34256172	22.45878983	21.60408401
EMC8_MOUSE	+	2.4656001	3.76219749	18.52657509	16.92974663	18.09870529	21.98060608	20.86725426	21.99375916
CCNB1_MOUSE	+	2.58904554	3.7585481	18.62435532	17.4655571	16.6985054	21.33843231	21.31080055	21.41482925
CDK12_MOUSE	+	2.1440596	3.7505544	19.73575783	17.41963196	17.75734138	21.8911171	22.38606071	21.88721657
RL35A_MOUSE	+	2.05529123	3.74745496	19.05754852	21.61063194	21.08388138	24.1943779	24.52784729	24.27220154
DICER_MOUSE	**+**	**2.29404174**	**3.67201233**	**18.64511299**	**16.90665627**	**17.70597649**	**22.10155678**	**20.63706017**	**21.53516579**
RMXL1_MOUSE	+	3.28614614	3.65982564	17.58579254	17.3586483	18.45462418	21.59900665	21.57911301	21.20042229
EXOS8_MOUSE	+	2.56972915	3.64147059	19.01972961	17.80752945	17.14531326	21.67387581	21.65189171	21.57121658
PRP19_MOUSE	+	2.51157976	3.6112353	19.5657959	19.65847015	18.16633987	23.28093338	22.67415619	22.26922226
ELAV1_MOUSE	**+**	**2.37362593**	**3.60992686**	**18.40230751**	**19.40922546**	**20.41452026**	**22.94904518**	**23.40301704**	**22.70377159**

HTR5B_MOUSE		1.88726154	3.60236677	19.4677639	17.5326786	18.04446411	22.75427818	20.7446003	22.35312843
WNK3_MOUSE	+	2.30273101	3.5954202	19.29206467	17.21456718	17.73704529	21.39937019	21.71762085	21.9129467
PISD_MOUSE	+	2.74293697	3.55810229	19.26364517	17.80336952	17.86763	21.80829239	21.7747879	22.02587128
TRI25_MOUSE	+	4.00772135	3.55450694	19.11874199	18.87729645	18.90888596	22.93387413	22.20997047	22.4246006
NOP2_MOUSE	+	2.12814316	3.53299014	19.60223007	17.34068871	18.95849609	22.54719734	22.13921165	21.81397629
TALDO_MOUSE	+	2.10143685	3.51943207	18.97449875	17.58217621	17.40431976	22.16189384	20.49150085	21.86589622
DNMT1_MOUSE	+	2.84431766	3.514925	19.15879631	19.25847435	17.91040802	22.41758728	22.39183998	22.06302643
SUCB2_MOUSE	+	2.66466605	3.50717481	18.25875282	17.98645401	16.89194489	21.3324337	21.62685013	20.69939232
MEST_MOUSE	+	2.80837395	3.47779592	18.61448288	17.58100319	17.6534462	20.81190109	21.74283409	21.72758484
BYST_MOUSE	+	3.99109639	3.47118441	17.75229645	17.53569412	17.16963005	21.11254311	21.09448814	20.66414261
AT5F1_MOUSE	+	2.43233143	3.46662966	19.4241066	17.83839226	18.41090584	22.65298462	21.52645111	21.89385796
ML12B_MOUSE	+	2.59570949	3.39487394	18.05635834	16.99129105	18.32303047	20.95631409	21.77615547	20.82283211
RTCA_MOUSE	+	3.6186024	3.37957764	18.1959095	17.9691143	17.39465141	21.02519608	21.473629	21.19958305
LSG1_MOUSE	+	2.8693905	3.37275505	18.88176918	19.40804291	20.21299934	22.77517128	23.2095089	22.63639641
HNRPD_MOUSE		1.87306606	3.35786311	18.88443184	16.82100487	17.65238762	22.0777359	21.07750702	20.27617073
RL1D1_MOUSE	+	2.89493839	3.3216114	17.679039	17.99532509	17.43842125	21.13420486	20.32366562	21.61974907
T2EB_MOUSE	+	1.98177931	3.3042558	19.90309525	17.50738525	18.13588715	21.96975899	21.59204102	21.89733505
HSP7E_MOUSE		1.91843997	3.3001194	19.29907036	17.45659447	16.95477676	20.69879913	21.52094841	21.39105225
SSRA_MOUSE	+	2.60189312	3.29609299	18.94052315	18.66926575	17.40090942	21.40857315	21.72250748	21.76789665
SRSF6_MOUSE		1.86096716	3.2881368	19.29615593	21.36072922	21.76267624	24.33681297	24.19633102	23.75082779
DDX49_MOUSE	+	2.64357576	3.28070831	18.62909126	17.11583138	17.32959747	21.00058365	20.9770813	20.9389801
PESC_MOUSE	+	2.8868824	3.27648608	18.65057373	17.58664131	17.47824669	21.00511551	21.50416756	21.0356369
DYL1_MOUSE	+	2.85940659	3.25629234	18.67635536	17.5611763	18.41140556	21.10980606	21.38890076	21.91910744
DLGP5_MOUSE	+	3.62145495	3.23456955	19.79797745	19.83361816	19.66892624	23.42534447	23.03456306	22.54432297
ECHB_MOUSE	+	2.33928743	3.21498044	18.99215317	20.44515991	18.82802773	22.38719177	23.08375168	22.43933868
TMCO1_MOUSE	+	3.75585073	3.19059817	18.81286812	18.40224266	18.12962341	21.43170738	21.60936928	21.87545204
YMEL1_MOUSE	+	2.06584491	3.18849373	18.96538734	19.32054138	20.15276527	23.79064369	22.15548515	22.05804634
EXOS2_MOUSE	+	2.20866702	3.1583271	18.85819054	17.27005768	18.09522057	21.9417038	20.61934662	21.13739967
CKAP2_MOUSE	+	4.20023216	3.15111923	17.39134789	16.81180191	17.2273941	20.39832687	20.22493935	20.26063538
NDUA9_MOUSE	+	2.4626907	3.15011978	19.57715034	17.93442535	18.21523094	21.66570282	21.740942	21.77052116
FBRL_MOUSE	+	2.64760567	3.14600563	19.14769554	18.63257027	20.04046059	22.27690887	22.79409981	22.1877346
GNL3L_MOUSE	+	2.64115788	3.14579264	19.01182747	18.6932621	20.1000824	22.45665932	22.664814	22.12107658
MTCH2_MOUSE	+	2.89832428	3.14402898	17.9082222	17.35104942	18.25613022	20.49306488	21.48035049	20.97407341
SGPL1_MOUSE	+	2.27116817	3.13570595	18.84325409	16.86871719	17.87706184	20.9480648	21.05840874	20.98967743
NPM_MOUSE	+	2.76544164	3.08877945	23.28700829	21.92488098	22.94861794	25.81872749	25.70514297	25.90297508
TRI27_MOUSE;sp	+	2.13965719	3.08835856	4	18.48321342	17.21704102		20.43389893	21.9629631
DIDO1_MOUSE	+	2.20123077	3.07623545	18.47603035	16.99752617	17.30516052	21.34288597	20.61593819	20.04859924
MEP50_MOUSE	+	3.92528573	3.07179832	18.52910233	18.13588333	18.69158745	21.41379738	21.77168846	21.38648224
TMM33_MOUSE	+	3.68128493	3.04577573	18.29094505	17.95749474	18.12707138	21.27719116	21.47975922	20.75588799
FBX22_MOUSE	+	2.00219533	3.02914111	18.81344223	16.98171043	17.39554596	20.3709259	20.44485664	21.4623394
NAT10_MOUSE	+	2.72423404	3.00707881	17.29899406	18.30316544	18.59105492	21.25885391	20.82057571	21.13502121
E2F6_MOUSE		1.82418939	2.98405393	19.54010201	17.34550667	18.29234123	21.53815269	20.69038391	21.90157509
TROAP_MOUSE	+	2.51731806	2.98344167	19.53733826	18.42133522	18.18543816	21.90943527	21.28523064	21.89977074
DYR1A_MOUSE;sp	+	2.3745244	2.94946416	4	18.71510506	17.32423592		20.91466331	20.79114151
RS21_MOUSE		1.83428312	2.93997383	20.00487709	17.59166336	18.67482758	21.75702858	21.92408371	21.41017723
ELP3_MOUSE	+	3.47308065	2.88117854	17.92194557	17.96098328	18.08898163	21.31174469	20.84796906	20.45573235
RLA0_MOUSE		1.94665327	2.8687884	23.72837448	25.30089569	25.83893967	28.03674316	27.83815765	27.59967422
UBE2O_MOUSE	+	3.21259762	2.86349169	17.93568993	17.60186386	16.95231247	20.4488945	20.27980042	20.35164642
ROAA_MOUSE		1.95957431	2.82550875	18.39328003	17.92689896	18.02707863	22.11483192	20.66942787	20.03952408
TET3_MOUSE	+	2.67273403	2.82024002	18.7338829	17.39466667	17.88165092	20.9813385	20.77225304	20.71732903
GDF3_MOUSE		1.97332285	2.8201135	19.49834824	18.0141964	17.64297295	21.19766617	21.65896606	20.75922585
RSMB_MOUSE;sp	+	2.35535587	2.81978099	4	19.36260796	18.73496819		21.51850128	21.65704727
EXOS9_MOUSE	+	2.06462023	2.81634712	19.3006916	18.83514977	17.69370079	21.99206543	20.81636238	21.47015572
PMVK_MOUSE	+	2.47244535	2.80433273	18.68691063	18.12099075	17.41152191	21.26619339	20.39152527	20.97470284
SMD2_MOUSE	+	2.09651373	2.76702372	19.17065048	17.26848412	18.1407299	21.20591927	20.88546753	20.78954887
NOP58_MOUSE	+	2.28596754	2.76040967	18.69968987	17.74523926	19.26677704	21.72008705	20.9392662	21.33358192
VPS4B_MOUSE	+	3.44478845	2.75020917	18.14476967	17.52608681	18.19351006	20.90822601	20.49960136	20.70716667
CAZA1_MOUSE		1.97346707	2.7426815	18.90531731	17.09835625	18.72807503	21.30312729	20.6395359	21.0171299
EXOS4_MOUSE	+	2.07909903	2.73094432	19.60915565	17.78770828	18.31497383	21.50208092	20.99562454	21.40696526
GTPB1_MOUSE	+	2.03255544	2.72808329	17.93639183	19.45500946	19.83343315	21.77390289	21.80455399	21.83062744
FMR1_MOUSE	+	2.49136054	2.70481936	18.76949501	19.00637627	20.01930237	21.67422104	22.3298645	21.90554619
DNJC2_MOUSE		2.00182223	2.66148822	18.53262138	19.96310425	20.42306328	22.39430237	22.10744476	22.40150642
RCC2_MOUSE	+	2.12781339	2.65528361	20.28411293	21.40841675	22.06190681	23.70176315	23.95109177	24.0674324
TRIPC_MOUSE	+	2.82466447	2.65045547	18.9413662	18.99194717	18.72170639	21.94663811	20.87829971	21.78144836
NUBP2_MOUSE	+	2.16596871	2.64924939	19.50900841	18.08821487	18.04970741	20.86135864	21.51629066	21.21702957
ATPD_MOUSE	+	2.71088472	2.63251495	18.65138245	17.71687889	17.94215202	21.1935215	20.44929695	20.56513977

NONO_MOUSE	+	3.73971876	2.63155556	19.51903152	19.06773376	19.37243652	21.8279171	21.78456688	22.24138451
HIRA_MOUSE	+	2.28591994	2.62014325	18.57726097	17.78154755	17.57140923	19.87738609	20.97435379	20.93890762
RFC3_MOUSE	+	2.61743441	2.59665235	17.97568893	18.35216331	18.89495468	20.46353722	21.31589508	21.23333168
CWC22_MOUSE		1.86524175	2.55943044	19.46443939	17.46541977	18.37982941	21.26636505	20.62622643	21.09538841
ELP2_MOUSE	+	2.38205511	2.53295199	18.98376083	18.50392532	17.63197327	20.72800064	21.24214172	20.74837303
AP3D1_MOUSE	+	2.53726493	2.48476982	19.2923069	18.84980202	19.16393471	22.12221527	21.73446465	20.90367317
SC61B_MOUSE	+	2.53962517	2.4836216	18.10457039	17.24526978	18.38258743	20.07077599	20.46901321	20.64350319
TBG1_MOUSE;sp	+	2.25731432	2.43540637	4	18.65612602	18.82596397		20.36996841	21.23432541
MYO9B_MOUSE	+	2.18690916	2.38238398	17.02120399	18.03404999	16.63549805	19.93329811	19.62578011	19.27882576
RFC2_MOUSE	+	3.16182357	2.35842133	18.89457703	19.33293724	19.71538544	21.52453995	21.76255417	21.73106956
TCOF_MOUSE	+	2.34943115	2.34908231	18.90975189	17.59043503	18.00426483	20.50076866	20.72891426	20.32201576
DDX41_MOUSE	+	2.53685214	2.34658051	18.436409	18.25401878	19.15088272	20.71523476	20.73314095	21.43267632
TRBP2_MOUSE	+	2.90567059	2.30510585	18.67405319	18.06248093	17.96382141	20.60774612	20.80278206	20.20514488
MELK_MOUSE	+	2.76176502	2.30014038	19.13614464	18.77622986	18.20246887	20.748209	21.01338577	21.25366974
DJC21_MOUSE	+	3.67285613	2.28212229	18.99835014	19.15288925	18.91843796	21.06131363	21.61701584	21.23771477
UBF1_MOUSE	+	2.27049474	2.27344449	18.55065346	19.63466835	19.78335953	21.8488102	21.58801842	21.3521862
MPIP1_MOUSE;sp	+	2.34121332	2.26911227	4	18.75317383	17.69032097		20.07691956	20.48237038
PMM1_MOUSE	+	2.08321991	2.26083819	18.81152153	17.56939125	18.33868599	20.75417709	20.82888603	19.91905022
SPAS2_MOUSE	+	2.59284906	2.24589666	18.55794716	17.48685265	17.79099083	20.06157684	20.38953018	20.12237358
SOX2_MOUSE;sp	+	2.67294922	2.24576124	18.64822578	20.58801842	17.99599457	20.09352112	17.68462181	20.38458633
MTMR5_MOUSE	+	2.17168245	2.23930486	17.89781189	18.69874573	18.54829788	20.93149567	19.90600967	21.02526474
ARHGC_MOUSE	+	2.43191852	2.23814519	19.2429657	18.28191185	18.58264732	21.32948112	20.9731617	20.51931763
PR38A_MOUSE	+	2.09354493	2.2218984	18.35954475	17.44160271	17.97063446	20.22658539	20.73826408	19.47262764
RRP12_MOUSE	+	2.71514774	2.17904854	19.1470871	18.66017723	18.53004837	20.83738136	21.41183281	20.62524414
CCD47_MOUSE	+	3.77340538	2.16991234	18.31539536	18.0249691	17.97405624	20.27366829	20.48089218	20.06959724
AFG31_MOUSE	+	2.87678203	2.08526611	19.43767166	19.15202141	19.82680893	21.21210861	21.72903824	21.73115349
FOLC_MOUSE	+	2.52336291	2.02305794	18.49145317	17.85420036	18.21076584	19.75403023	20.23724747	20.63431549
PWP3A_MOUSE	+	2.85711724	2.01078033	18.2483902	17.52182961	18.2165947	20.18410492	19.96366882	19.87138176
RBX1_MOUSE	+	2.58068557	1.98654111	18.22340012	17.65926552	18.57178497	20.29423523	19.87073517	20.24910355
DDX47_MOUSE	+	2.36373207	1.97561709	18.53499603	17.66792107	18.11487198	20.30785942	19.62381744	20.31296349
HJURP_MOUSE	+	2.25081453	1.94696299	18.60614014	18.33687782	17.9405632	19.69360352	20.73842812	20.29243851
PSME4_MOUSE	+	3.58661916	1.93106524	18.50156784	18.73780251	18.51148224	20.40748405	20.34765244	20.78891182
TEFM_MOUSE	+	2.41183206	1.90176773	18.84143448	18.69717026	17.92343521	20.63493538	20.37581062	20.15659714
DNJC9_MOUSE	+	2.28543001	1.82427343	18.883564	17.77752495	18.23247528	20.01876068	20.2631588	20.08446503
PDS5B_MOUSE	+	2.19794526	1.82134374	19.40730476	20.09596825	20.049263	21.14519501	22.01338577	21.85798645
AURKA_MOUSE	+	2.37595355	1.80390867	18.52012062	18.71187973	17.77050972	20.03925705	20.01848793	20.35649109
EXOS3_MOUSE	+	2.29181383	1.79384232	18.79178429	17.90615654	18.65461349	20.22776222	20.54349709	19.96282196
GTSE1_MOUSE	+	2.32572897	1.77018483	18.09778404	18.80344391	18.81187057	20.08615112	20.74073601	20.1967659
RU2A_MOUSE	+	2.58311108	1.72907066	17.58222389	17.55879593	18.28915405	19.7302742	19.48006439	19.40704727
ILF3_MOUSE	+	2.39614401	1.60576375	19.54289627	19.43493843	19.79823112	21.64389992	21.16134071	20.78811646
KIF23_MOUSE	+	2.61562083	1.60206286	18.79933167	18.78190422	19.31333923	20.61566925	20.81245041	20.27264404
ECHA_MOUSE	+	2.62406927	1.52130063	21.68897629	22.28025436	21.72899628	23.20445824	23.58955193	23.46811867

3)PGCLCs d6 MGA-IP (3 replicates)

Protein_nam	Significant	pvalue(-log1	Difference	LFQ_IgG_1	LFQ_IgG_2	LFQ_IgG_3	LFQ_IgG_4	LFQ_IgG_5	LFQ_IgG_6	LFQ_IgG_7	LFQ_IgG_8	LFQ_IgG_9	LFQ_MGA_1	LFQ_MGA_2	LFQ_MGA_3	LFQ_MGA_4	LFQ_MGA_5	LFQ_MGA_6	LFQ_MGA_7	LFQ_MGA_8	LFQ_MGA_9
Rps14	+	14.8189415	7.75893868	19.0752964	17.6767788	19.2354965	17.9217835	19.6483402	19.4341641	18.3896751	19.1212673	19.3943653	27.2644558	26.6193295	26.3877182	26.8056278	26.645401	26.4385395	26.850193	26.4714088	26.2449417
Tcp1;TCP1	+	14.4694752	8.0948783	18.1094303	18.1581764	19.3461227	19.8209133	18.3580589	17.4726276	18.4696236	18.8641682	19.0774975	27.0931549	26.8743172	27.1121731	27.1589432	26.2570992	26.997551	26.5092545	26.6747875	25.8532429
Rps23	+	14.2364314	7.70837318	18.8291969	18.1214008	19.4959602	19.8107529	18.455822	19.0248795	19.6229363	17.9269371	18.963129	27.3610172	26.8634872	26.8140888	26.8927288	26.834486	25.5785961	26.6343651	26.1738854	26.4737186
Rpl13a	+	14.1674543	6.32546891	19.5118179	18.6125412	19.6266003	19.2128182	18.1773796	19.9340935	19.4113464	18.458374	19.3033142	25.9024448	25.5160503	25.2374306	26.0969772	25.5777321	24.9282742	25.3343926	25.3661976	25.2180061
HIST2H3A;Hi	+	13.9873814	9.38661618	17.9987984	17.5187397	20.6523399	19.140007	17.7422257	18.6416721	18.6162167	18.5657997	19.4030972	28.8471794	28.1906052	27.5824051	28.3398991	28.2048054	27.6115418	28.3175602	28.1432629	27.521183
Mars	+	13.8480265	4.73304367	18.2349186	18.2925777	18.7577076	18.7570152	18.5466328	19.2807427	19.0895977	18.4690132	18.8476315	23.104393	23.2368393	24.0432682	23.5595264	23.4441738	23.8299713	22.6351795	23.3908691	23.6290093
Rps3a	+	13.7709976	7.2245973	18.7107925	18.221592	19.6012611	20.2779255	17.9586239	19.3844128	18.4197445	19.1491489	18.5595417	26.6875248	26.0391941	25.9987125	26.8371353	26.1957111	25.8431168	26.091198	25.9576817	25.6541443
Rpl8	+	13.5217321	8.11487346	19.8032742	17.6154652	20.4777718	19.4902344	19.5879555	19.3078575	20.0720654	19.8860893	19.9587631	27.9227505	28.293951	27.5314808	28.0489006	28.2848473	27.4773045	26.5827637	27.7390518	27.3522873
Rpl3	+	13.253036	8.13286103	18.3300247	18.4271946	20.0249767	17.86726	19.0809097	19.7885399	17.8782787	17.8238277	19.6411514	27.1639423	27.4181213	26.5560055	27.2620373	27.4190865	26.6343651	26.5236969	27.1069927	25.9736652
Rpl27	+	13.2249838	7.42781088	17.9306202	17.043108	19.7043762	18.7235985	18.0973949	18.1706257	19.6184788	18.4729004	19.6562328	26.3769474	26.0897846	26.0482445	25.8320484	25.8489056	26.1712151	25.9700699	25.9865036	25.9439144
Rpl32	+	13.0374583	5.67028957	19.0181427	18.0430012	18.8842125	19.5914593	19.1961823	19.3352413	17.7625046	18.2426357	19.2069454	24.8451767	24.6575279	23.9184341	24.6297875	24.8986912	24.1148167	24.5628471	24.6350575	24.0505924
Wdr5	+	12.9995681	4.60654407	18.3749485	18.125845	19.5311604	18.3932076	18.3794937	18.4513245	18.6582737	19.5476112	19.2555962	23.1554089	23.5273113	23.4911823	23.3114662	23.5953693	23.4384747	22.9649029	23.6224327	23.069809
Igf2bp1	+	12.9659223	7.14245733	18.9467793	18.0332298	20.1435795	19.7341595	18.1301041	18.7890091	17.548605	17.9292374	18.8555908	26.2065754	25.9817219	25.4902344	26.4132061	25.9456329	25.4219456	25.7812672	25.7592869	25.39254
Pcbp1	+	12.8980946	6.09024048	19.4353409	19.1502609	19.6636124	19.0136795	18.0654373	18.6288338	17.9643173	18.6712418	19.0112362	25.5164414	25.2844677	24.3027096	25.6455116	24.9993801	24.1194153	25.1724167	25.0751667	24.3006153
Rps6	+	12.77706	7.61920272	17.1605396	17.2684479	19.8029938	17.7211533	17.5424595	18.5145741	17.5723286	18.6523171	19.1996727	26.1257153	25.9094658	25.520134	26.4735165	26.1414127	25.4312229	25.7779617	25.5449829	25.0828991
Rpl7	+	12.7338833	7.26187621	19.3334179	19.1684189	20.1397152	19.2448311	17.4928284	20.2697201	18.5465221	18.1458454	19.5186863	27.0108395	26.3754234	25.9052029	26.8749046	26.4104271	26.0277882	26.3302269	26.319603	25.9624558
Rpl24	+	12.6937809	7.45672226	19.0656147	17.4959583	19.9668369	17.9540215	18.219101	18.9358997	19.7704353	17.7254906	19.4225044	26.7189484	26.614563	25.9379787	26.1563797	26.5867767	25.6400871	25.9735565	26.4965725	25.5415001
Ywhaz	+	12.6539573	5.1187333	18.9824028	18.3837986	18.3297977	18.2306671	17.8847542	18.346302	17.6900215	18.323864	19.3708172	23.7999592	23.9630528	23.3085537	24.1069336	23.9191628	23.0465183	22.8807488	23.6481209	22.9379749
Hnrnpu	+	12.6407612	6.62876723	18.6404572	19.9857922	20.426611	18.9236107	20.1294346	19.8176041	17.9923897	18.4650536	19.2811356	25.7691078	26.2212009	25.7716541	25.9220696	26.2168407	25.9575272	25.1789646	26.244978	26.0386505
Srp68	+	12.6104702	3.94503085	19.1623039	18.3488369	19.5865879	19.4740598	18.8095512	19.0482483	18.5779076	19.1501122	19.7931824	22.9560127	23.0436173	22.9167595	23.3517819	23.1199226	22.8571701	22.6441212	22.9359627	22.6269169
Rps16	+	12.5579867	7.7946682	20.5371571	18.0497513	19.1190662	17.3514996	19.2987175	19.5348129	19.1450939	18.1807938	19.1123924	27.6087246	26.6575832	26.5128288	27.1897106	26.7373772	26.1895981	27.1072922	26.6486969	25.8294869
Hnrnph1	+	12.5062135	5.9789558	18.84338	18.5126362	19.2568226	18.5679073	17.540041	19.2409992	18.8193607	19.7381706	19.220274	25.537241	24.9778404	24.5290394	25.69203	24.7926807	24.5528584	24.9308929	24.6801376	23.8574734
Rps11;RPS11	+	12.4888715	7.49766901	18.5349846	17.1745205	19.7146778	17.8521004	17.8563061	19.3181553	18.993557	18.1940041	19.5023365	27.0344372	26.3867321	25.4083061	26.4578247	26.3661308	25.5024567	26.1312809	26.1165237	25.215971
Rps8	+	12.4782362	8.07476574	19.1184292	19.9349213	20.3276711	19.4506912	19.4877377	18.8639927	18.2651444	19.9572239	18.6809158	27.4221382	27.6438885	26.6302033	27.5574226	27.6204491	26.5390759	26.2391243	27.1523819	26.9549351
Rps24	+	12.4695251	7.51969104	17.8554459	17.4329243	20.3779278	18.6222858	18.8182392	19.2286053	18.9724464	17.2494011	18.7262802	26.7010765	26.6515732	25.6602516	26.118227	26.5597153	25.8748093	25.7431946	25.8681603	25.7837677
Rpl35a	+	12.3850964	7.11468527	17.8492565	16.8961105	19.4800549	17.987215	18.8683739	18.7530766	17.8686314	17.8902779	18.9466801	26.7486801	25.2658863	24.7898979	25.700943	25.5184536	24.6635113	25.7546291	25.0402603	25.0895824
Rpl18	+	12.3615154	6.56132974	18.878006	18.2598343	20.415165	19.4152451	18.6264839	18.5811863	17.4891472	19.0957737	19.5685558	26.0849896	25.5815296	25.1844997	26.1770649	25.6385403	25.1033363	25.1381722	25.3546085	25.1186237
Hnrnpf	+	12.3516801	6.96474414	18.272007	20.3722019	20.2147427	18.4329243	17.7448616	19.6441555	18.5640259	18.9840298	19.7432365	26.3584194	26.3449097	25.782568	26.5658855	26.4312706	25.7362423	25.7404175	26.1048756	25.5902939
Rpl5	+	12.2432508	6.4784707	19.6952515	18.5867195	19.2893505	19.0762367	18.0919972	17.8200226	18.7495518	17.7832813	19.6186352	25.9962578	25.5336208	25.2315464	26.082798	24.5440979	24.4953976	25.3686295	25.0882893	24.6766453
Abcf1	+	12.2317332	3.69130156	18.6620922	18.231678	18.8902302	19.8485661	18.9548798	19.3708267	18.8426476	18.6948376	19.619381	22.6104736	22.7713471	22.6783981	22.9959679	22.8648777	22.5318852	22.490963	22.809391	22.5835495
Mcm7	+	12.1487914	6.19983758	18.0422974	18.1996288	19.8036823	18.6264877	20.0154972	18.9095841	17.9913502	18.3469658	19.8118725	25.6216774	24.841341	24.8344631	25.8517189	24.98633	24.7872601	25.1291199	24.8552876	24.6387062
Rpl27a;RPL2	+	12.1109236	8.15362803	18.6083565	19.2009544	19.9930821	19.4566803	16.261898	19.2373447	18.3760109	18.4469376	19.0425415	27.5346012	27.4262238	26.2145634	27.4040566	27.2966671	26.0861645	26.9017315	26.8819199	26.2605305
Rps15a	+	12.0910986	7.05510902	18.1709213	17.7728901	19.3481216	19.4839535	18.46488	19.5495834	17.3377266	17.9075775	20.1313267	26.459671	26.1565933	25.3222714	25.8947887	25.795433	25.2270718	25.8109551	25.5657845	25.4303932
Rbm14	+	12.0262849	5.0892103	19.5488987	17.4264202	19.4341621	18.4239407	18.8040638	19.0820942	18.6115093	19.1423626	19.6206055	23.7085152	24.049263	24.2445965	23.9889317	24.1374302	24.1638451	23.2410946	24.1102829	24.2529907
Asns	+	12.0088139	4.80161667	18.6927757	17.7267723	19.7074146	19.301733	18.5996933	18.7665939	17.8530808	18.0280056	19.1621437	23.5830231	23.7176418	23.4342804	23.8545284	23.4202118	23.2783833	23.0717087	23.2534962	23.4394894
Kpnb1	+	11.9880538	5.36797036	18.2942143	17.8364391	18.9646606	18.7344894	18.5972118	20.3855496	18.7991028	18.8161373	19.3563652	23.7626343	24.4218178	24.5462189	24.3091774	24.544157	24.3292351	23.4124794	24.4400597	24.3301239
Ass1	+	11.9588017	8.30290985	19.3828659	18.8225708	19.7801914	19.8121433	19.1024761	18.3003388	19.0200882	17.5039234	19.5512676	26.4836845	27.3098202	28.8351193	26.66885	27.3924751	28.4642353	25.6455669	27.1213932	28.0809097
Rangap1	+	11.9166866	6.69942602	19.8474693	17.3094597	19.9449062	19.068779	17.456667	19.4678879	18.2014599	19.0450897	18.3677673	25.0006695	25.6864567	25.5738945	25.3910656	25.754961	25.5401421	24.8490486	25.6842365	25.5238457
Iars	+	11.7937815	4.53850471	19.0083141	18.447525	20.4834442	19.2296391	19.3583489	18.8706894	18.5106125	19.9788418	18.7345066	23.8607922	23.6807804	23.5755405	24.2223606	23.611105	23.0182495	23.8232784	23.3991089	23.2772484
Hsp90b1	+	11.777876	4.74276818	17.7696915	18.6920548	19.1501541	18.833601	17.963131	19.9359818	18.1328125	18.469904	19.0154781	23.6321201	23.6740055	23.3968906	23.7471447	23.5034885	22.9547348	23.1197643	23.6103172	23.0092564
Rpl18a	+	11.7186135	7.15257221	17.8817177	19.1519966	20.8557625	18.6404781	17.8110409	19.6029739	17.9801407	19.3150101	18.364584	26.8189716	26.1145001	25.501606	26.4675598	26.2833214	25.5256691	26.1167412	25.9565525	25.1919327
Hsp90aa1	+	11.629354	5.51689318	18.5377102	17.5422115	19.7226925	19.0532265	18.283123	18.2887077	19.058321	17.9153996	19.4217835	24.1454601	24.6457596	23.6207562	24.694767	24.7553692	23.6447144	23.7020798	24.5761166	23.6901913
Rpl28	+	11.5925874	6.10213958	20.2295704	17.9610291	19.8273373	18.0943165	17.7462597	18.7455692	18.2261772	18.2995262	18.7589188	25.4392052	25.1096058	24.3280697	25.0508003	25.0219994	24.0579624	24.6681728	24.9604912	24.1716538
Hnrnpa3	+	11.5848379	5.73100683	19.3859139	17.7064552	19.688448	18.6652241	17.8513355	19.2527466	19.5298691	17.8456917	18.6975842	24.1739426	24.3589058	25.5868626	24.6360531	24.4319878	24.591322	23.8262901	24.3088303	24.2881355
Rps7	+	11.5709649	6.68058417	19.594698	18.7008686	19.8199635	18.9222374	17.6856022	19.2582455	18.9820519	17.978735	17.95327	26.7054329	25.7241116	25.4235497	26.2317658	25.4596405	24.9420357	25.6192169	24.6865635	24.2286129
Prpf19;PRPF	+	11.5686526	5.66612795	18.9925537	19.8801289	19.0795555	18.4469242	19.8777027	18.4349785	18.3058624	18.8701668	19.8829422	25.4068813	24.4966183	24.68046	25.9335728	24.6978455	24.2015743	25.1474018	24.1982803	24.0033321
Taldo1;TALD	+	11.5677945	4.63053131	19.0544376	18.0969639	19.2197132	19.0588074	19.1190395	19.3344669	19.4372997	18.1918812	19.7448559	23.307581	23.6711998	24.2944584	23.2727013	23.7134533	24.180027	22.7049313	23.7231751	24.0647202
Eef2	+	11.5589415	6.11686431	18.28792	18.0632057	20.0154858	18.7319794	19.4728355	18.5500069	18.8996697	19.2127533	19.5234394	25.5468369	25.5859184	24.509903	25.9066715	25.7709236	23.9458351	25.2196693	25.3245392	23.9987774
Rpl6	+	11.5423713	5.90438122	18.8357887	18.9971771	20.7767639	18.8270874	18.8929119	18.5147476	18.6945076	19.1371326	18.7746925	25.831831	25.0743084	24.4373951	25.8275738	24.8671703	24.4328175	25.3155499	25.0351925	23.7684021
Ap2m1	+	11.5377377	5.42441305	19.4950886	17.3591614	19.6264114	18.3799744	17.2704277	19.0966206	17.7012806	17.7822533	18.977972	23.9091225	23.9833756	23.579113	24.0848064	23.7888527	23.4247036	23.3387852	23.9757004	23.424448
Rps4x	+	11.5187588	7.6324518	19.7014504	17.1541653	19.0011597	19.5250034	17.9439106	19.6034756	19.5001488	18.5207806	20.9000168	27.2283936	27.1492844	26.5536785	27.6341572	26.9873924	26.4729443	25.8837166	26.4804211	26.1521893
Gnl3	+	11.434383	4.62622685	18.1783085	18.5791664	18.9445095	17.7229214	17.6881599	18.579958	18.0133152	18.3219986	19.9226017	23.3870602	23.1388683	22.8061485	23.620533	23.2268658	22.9197979	23.0104694	22.7959423	22.6812954
Caprin1;CAPI	+	11.4114881	6.18018765	18.2493362	17.7150192	20.742794	19.365221	18.0757599	18.0804615	19.4200287	18.7259045	18.795351	24.9060059	25.4282551	24.6799221	25.4051933	25.4312553	24.5164108	24.5578327	25.2194481	24.6472416
Rpl7a	+	11.3936729	7.22934702	18.2093926	18.0895519	19.786232	18.5375557	19.3769531	18.6754532	17.6277123	16.9589977	20.0554905	26.6570377	26.1873894	25.1651497	26.6257515	25.9734459	24.8845081	25.8316631	25.8242016	25.2323151
Cct6a	+	11.3799343	5.62435362	18.6687374	18.2319355	19.0662289	18.6966915	17.155714	18.5524178	17.6497707	18.7933025	19.8248367	24.8624954	24.3454342	23.7685032	24.8773632	24.1923466	23.3338814	24.0323772	24.0980434	23.748373
Ddx3x;DDX3>	+	11.3455108	5.95275434	19.6003799	19.5796108	19.2091637	19.5217056	21.60779	19.4636726	18.4519558	20.6141415	19.4873581	25.2804375	26.1994782	25.7428341	25.5950279	26.2526302	25.7342529	24.9114571	25.7928047	25.6016445
Atp5c1	+	11.2976842	6.01996697	18.8423462	18.2697048	20.3559933	19.1201916	18.5746613	18.461813	18.2184601	18.5633564	19.1729221	25.0865898	25.2516918	24.8879032	25.2713471	25.38867	24.7787132	22.9012814	25.1165237	25.0764313
Aco2	+	11.2675121	4.44215711	18.8680611	17.6245232	19.4955158	18.2088795	17.6134872	19.3249245	18.8681088	18.9495602	18.6608238	23.0719223	23.1448841	22.6964455	23.2989388	23.4548798	22.7617016	22.6875668	23.5000877	22.9768715
Ubr4	+	11.2562137	6.42375247	19.9128761	17.6325016	20.6112957	18.7636681	18.9387341	19.2962875	18.6581955	17.776062	19.4443283	24.4957638	25.6122589	25.8797016	25.2607994	25.6446037	25.8534813	24.716753	25.5046101	25.8797493
Paics	+	11.2126985	5.40560044	19.1512489	17.9339905	18.8831539	18.5913353	18.5206089	20.5960236	19.2074337	18.8523617	20.0474224	24.6076107	24.2921429	25.296772	24.8256588	24.4645081	24.7591343	24.1733322	23.8780193	24.1368046
Sumo1	+	11.1708005	6.21302266	18.466898	18.6450481	19.6344414	18.6611023	17.2066498	20.087265	19.5216847	17.8216496	18.8913231	24.4557571	25.1564579	25.4219132	24.6796532	25.3394642	25.2610149	23.8244457	25.4544411	25.2601185
Rps3	+	11.0794776	7.34401427	19.7979469	16.9129982	20.1524277	19.7737026	18.1588326	20.0075798	19.5831051	17.9154778	20.0184879	26.6028614	26.7060928	26.7770596	27.0822296	26.6590805	26.6805668	25.4115105	26.3813782	26.1159077
Rpl13	+	11.0196875	6.30693542	20.2684097	18.6311493	20.691061	18.6191616	18.2321091	19.0757752	19.8719521	18.3166485	19.6858444	25.8851357	25.6850395	25.3731842	27.0239029	25.3245392	25.2133045	24.8615494	25.7436047	25.0442696
Cct5	+	10.8966249	5.26960543	18.8643341	17.6729469	19.1590729	18.0534859	17.0023079	19.0680924	19.3928986	18.7142716	19.8460026	24.1531372	23.6332283	23.9186173	24.4275188	24.0119705	23.8116665	23.7730389	23.661665	23.8090191
Rpl23a	+	10.8628454	6.87661828	18.9936237	17.2006817	20.5825234	19.1087723	17.2351246	17.9309139	18.7573776	18.3099403	19.5443821	26.3651295	26.1315155	25.323473	25.5755405	25.858469	24.7274914	25.5030632	25.2612667	24.8069553
Dhx15	+	10.8465117	6.56376182	17.8983784	16.7455635	19.2377129	18.1788101	20.4608402	19.3536358	17.3101769	18.3739586	18.9743309	25.3526917	25.0115871	24.9162483	25.5760307	25.2848568	24.67729	24.8428764	25.1776352	24.7680473
Abcf2	+	10.8174152	4.45086204	19.7532005	17.4804096	19.2498055	19.1409836	19.641119	19.8919029	18.7473126	18.5454044	18.9322491	23.5377731	23.3651962	23.3455696	24.1616955	23.6695805	23.546278	23.1580315	23.2685661	23.387455
Igf2bp3	+	10.7760244	4.55077532	19.1353474	17.4243031	18.9442444	18.7862778	17.1330929	19.0455017	18.8890896	18.4452744	19.1394043	23.2775326	23.276823	22.9633865	23.6276741	23.5085735	22.8169861	22.7886734	22.8935814	22.7462826
Rpl21	+	10.7753758	7.26347711	19.3353424	17.614357	21.0208778	18.0678005	19.3100414	19.2280426	17.2451115	19.2198486	20.0959969	27.0636311	25.7627373	25.5349579	27.1740761	26.381609	26.1163654	26.0523758	26.2924061	26.1305542
Ddx21	+	10.7159988	4.79274432	19.9738922	18.7612267	18.9822807	17.3405113	18.2792931	18.3441811	18.2570114	19.3606968	19.4386272	23.1135292	23.2937584	23.0695629	23.613018	23.4031467	23.1956253	22.8588963	23.3792801	22.9456024
Clint1	+	10.685654	3.47176213	19.3054676	18.663866	19.8706055	19.4459686	18.240118	18.9738865	19.5639324	19.1096687	19.9375992	23.0040169	22.7105541	22.5668125	23.0288754	22.9288254	22.559782	22.3150387	23.0314026	22.2116642
Rrbp1	+	10.6829335	4.76202075	19.6488552	17.4551506	19.7994728	17.9540482	18.5176907	18.1501961	18.8699703	18.1077442	18.8012562	22.4705048	23.6436138	23.5043373	23.3932285	23.6532688	23.5706844	22.9238472	23.4015846	23.6015015
Rplp0	+	10.5968592	5.58210924	18.2677136	20.662056	20.457859	18.5972462	18.3620853	19.6142311	18.2911873	18.5104427	19.5935173	24.9796734	25.1712341	24.9743004	25.0417652	25.0185642	24.5595837	24.4800663	24.4742603	23.895874
Pabpc1	+	10.5415232	5.5768013	19.619772	21.0838814	19.9633694	18.9698582	21.3851128	19.1388798	18.9936085	18.9575138	21.143549	27.0683556	26.7116165	25.6910706	27.2850685	27.1403389	25.570076	26.5599346	26.7945156	25.6257801
Rps9	+	10.5110259	5.76454777	17.8366089	18.2126408	19.7188072	19.3113728	18.0469399	19.1274872	19.6439095	18.4565716	20.027401	25.7280369	24.5497494	24.0905514	25.8682537	24.7465286	23.8077412	25.0309906	24.1593876	24.2814293
Rpl4	+	10.4998463	6.14957386	18.8216324	18.3318806	20.3661518	19.3937779	17.8265171	18.0830135	19.3924847	19.423914	19.2380333	26.0341644	25.4159641	24.3761025	26.3208256	25.413578	24.0333023	25.516531	25.1402035	23.9728985
Eef1g	+	10.4798737	5.4891563	17.9354782	17.4812603	19.4479828	18.1213436	17.7538471	19.504633	18.6273823	20.1551151	19.1717396	24.4021702	24.552742	23.739027	24.7816181	24.7086735	23.7363453	23.7431431	24.3402805	23.597189
Rps2;RPS2	+	10.450673	6.92212656	20.4585037	17.1266441	19.7765865	19.0932121	17.429203	19.5812988	19.4779644	17.7216167	19.2497196	26.3945541	26.1673145	25.0032024	26.5158253	26.1989365	25.2857037	26.0839558	25.6817989	24.882597
Cfl1	+	10.4429257	5.33190134	19.2543144	17.9822044	20.2716351	19.1867542	17.8812523	18.8715801	17.9237137	18.2419643	19.7381191	24.8376904	24.3769646	24.1772919	24.6989594	24.1339073	23.2572422	24.2978916	24.1769123	23.3817902
Rpl10	+	10.4180695	6.71917449	19.2381935	16.5831814	19.8338394	18.9483776	18.5302239	19.9554768	18.3037834	19.1853809	19.8834801	26.6246376	26.1512604	25.1893711	26.7423973	25.5853157	24.6244412	25.5779896	25.4839153	24.9551792
Npepps	+	10.3873299	3.97461234	17.8279629	17.8955555	19.6068478	18.2319431	19.65868	18.3578739	17.8041954	18.8630734	18.3888378	22.3130741	22.3269062	22.9000092	22.6743069	22.5545464	22.5778008	21.9710579	22.5042648	22.5845146
Tdh	+	10.3600641	4.4362562	18.6455665	17.7558594	20.2333794	18.951252	18.7563076	18.3494568	19.3253365	17.9105568	19.6592598	23.2612667	23.5068817	23.7504196	23.1776123	23.4746933	23.1672955	22.7625942	23.0521355	23.3603802
Tufm	+	10.30729	3.87178781	20.1749268	18.7045803	19.0592575	17.9216309	18.5671902	18.4603901	18.6366501	18.6096172	19.3703518	23.1354904	23.0138626	22.7609711	23.1602802	22.841898	22.61232	22.0569553	22.6028385	22.166069
Ldha	+	10.3021429	6.60424317	19.3764267	18.4826641	19.6271362	18.1522102	16.2002392	18.2244606	17.6152744	19.2191773	19.6944733	25.905983	25.1498451	25.2125244	25.8667221	25.1860123	24.6971569	25.1191387	25.0213203	23.8715477
Cad	+	10.2832215	5.4898279	19.0008602	16.9967461	19.2625237	18.6287022	18.8899136	19.2484074	18.8820343	17.6467724	20.2767601	24.3780232	24.6103172	23.8762398	24.8172894	24.7463245	23.740572	24.3275909	24.3788166	23.3659973
Rtcb	+	10.2783711	4.6927912	19.1880932	18.2418575	19.672884	18.2938652	18.0436115	18.9829445	18.2549057	18.1964359	19.1234264	23.8874397	23.4336453	23.1184654	24.8095589	23.1496372	22.3006439	23.6180687	23.0461693	22.8695164
Hspa9	+	10.2442812	5.40134663	19.1706638	16.7177486	18.246151	19.2388821	19.3855972	19.197897	19.3698406	18.4981976	18.6024113	23.9016857	24.7770596	23.5567226	24.1659164	25.1075726	23.8678761	23.1160545	24.6074982	23.9391232
Hspa5	+	10.2164932	3.19210328	19.4477863	19.9516258	19.8946533	20.4849072	20.5598297	20.5709858	19.6309605	21.2022762	20.8511753	23.215683	23.3405514	23.5993481	23.9527817	23.6072712	23.4993572	23.2261162	23.4422779	23.439743
Fxr1	+	10.2085389	5.68804084	20.3469429	18.2386913	19.649931	17.9141979	17.8877754	20.3618088	18.6614227	19.0591164	19.1808415	24.6238289	25.2155266	24.4152546	25.0955906	25.5426235	24.1481018	24.1601563	25.3607159	23.9312973
Pcgf6	+	10.1924332	3.86539163	18.9490833	17.8334484	19.5640678	19.2100868	18.7800026	19.064045	18.7541847	18.2249794	19.8020897	22.662035	22.3848763	23.4540005	22.5891399	22.5399761	23.4493485	22.2380638	22.5109901	23.1420822

Hspa14	+	10.166435	4.20196639	18.4400311	18.7388287	18.9783096	18.4673023	18.3656216	18.4109173	17.6118107	18.796402	19.8553562	23.4434166	22.5147018	22.8463249	23.7743454	22.7580261	22.5269051	23.0562267	21.7487831	22.8135471
Ahcy	+	10.1367941	4.42219946	20.150177	18.4106484	19.1580524	18.3727684	18.7602806	19.8818321	18.2068672	18.7615414	20.3178654	23.4808674	23.322237	24.1999283	23.7315884	23.3631916	23.8971691	23.4380951	23.0254326	23.3613186
Rpl30	+	10.10605	5.67769453	19.4319172	21.0701218	20.0923767	18.8471584	17.2201481	18.9071293	19.0985298	18.7141991	19.7655907	25.7147369	24.7897987	24.7741947	25.335825	24.9519367	24.7294121	25.0309067	24.5030022	24.4166088
Cltc	+	10.105689	5.74093225	18.5688248	19.8356247	18.6337071	18.9757671	18.4910698	19.838398	17.1814842	19.5950871	19.9810867	24.7079353	25.4855747	23.8843689	25.0718556	25.6940498	24.043684	24.4364433	25.4623261	23.983202
Rps18	+	10.0685141	4.94692167	18.8023224	18.106308	19.825964	19.3566265	18.1019745	18.2732716	19.0620117	17.5687981	19.7417374	24.7890015	23.6278954	23.2502766	24.3241615	23.5123177	23.2403374	24.2202969	23.3988476	22.9981747
Pcbp2	+	10.0352248	5.13971286	18.7526035	18.8733482	20.0388966	17.6109619	18.7304535	18.4411221	19.1852303	17.6908779	20.0414295	24.4077549	24.3403492	23.1589241	24.3245049	24.4838219	22.9792118	23.9562435	24.3757057	23.5958233
Stub1	+	10.0338849	5.82394727	20.5140476	18.6845608	20.0573959	18.6398506	17.14328	18.7823792	18.4925499	18.2448845	17.7815132	24.0878029	25.2537136	24.4071083	24.3143749	25.3879471	24.288065	23.9181614	25.0606461	24.038168
Rpl14	+	10.0315951	8.04709646	18.7698727	17.7098141	19.8724785	19.9262142	22.2428093	18.1096954	19.2288933	22.0089817	19.244627	28.2228317	27.8380985	28.5408573	27.7679348	27.6796951	27.1418018	27.4472675	27.2105751	
Trim28	+	10.0298632	5.70019701	19.5003204	18.7768269	19.4223309	18.7214508	17.2811699	20.5655842	18.7830086	18.2865906	18.6895866	24.8037567	25.208437	23.5073643	25.0605621	25.4186363	23.7503166	24.496069	25.2286873	23.8548126	
Aimp2	+	10.0008949	5.46021673	17.2141399	17.6508217	19.3024578	20.3800564	19.0533638	19.1920052	19.9478188	17.9955883	19.7602215	24.3124371	24.5398464	24.6279526	24.4545651	24.4750023	24.5428009	23.8789539	24.4529972	24.3538685	
Gars;GARS	+	9.9796704	4.92946434	19.1068611	17.0669613	20.3786068	19.29426	18.2505703	18.3340988	17.7898064	19.2153454	18.8027153	23.7843666	23.7747479	23.884182	23.6784191	23.93643	23.6055775	23.0194054	23.3346996	23.5865765	
Impdh2	+	9.96219	4.16654205	19.4532318	18.2477551	20.1331577	18.0639992	18.9913616	19.0664425	18.3852882	19.8163319	19.3880692	23.6530514	22.9765396	22.9342709	24.1929493	23.0051823	22.7763958	23.4872627	22.8505268	23.1683369	
Hnrnpc	+	9.92841498	6.00556988	19.0609932	18.0763187	20.2862988	18.9912548	19.1103478	18.6569405	19.015543	18.2422981	21.4856167	25.7768078	25.7172241	25.0413895	25.8151646	25.2634163	24.1203651	25.2882061	25.6732235	24.2799435	
Aimp1	+	9.92833567	4.09045665	18.7147694	17.3929977	19.7348976	18.0403996	18.7345161	19.1480198	18.7532139	19.3991776	19.4673214	23.5577736	22.7457905	22.9269619	23.4719677	22.7862225	22.3593617	23.0501938	22.8408623	22.460289	
Nup107	+	9.92563237	4.2690612	19.4595261	18.6152897	19.5187435	19.7314472	17.1979675	18.3538799	18.5718536	19.140028	19.193243	22.7787228	23.3381062	23.4429092	23.2131481	23.3359261	23.272131	22.1943016	23.3617191	23.2665653	
Nono	**+**	**9.90034453**	**5.06479157**	**19.9190998**	**17.0798168**	**19.2130451**	**18.2805729**	**17.0905838**	**19.2333965**	**18.1029739**	**19.4481068**	**19.1635113**	**23.7280617**	**23.9769249**	**23.5792294**	**23.9924812**	**23.5036087**	**23.6209793**	**23.4882431**	**23.6630783**	**23.5616245**	
Tardbp	+	9.89585932	4.66701826	18.5122089	16.9776745	19.8695259	17.9729118	18.6155338	19.3076248	19.0412388	18.1246662	19.3063736	23.6588364	23.6681728	23.0392571	23.9115944	23.6156025	22.9038754	23.1319008	23.1217403	22.6799431	
Cct3	+	9.8811593	5.21867265	18.9711227	19.3581448	19.5691299	19.1610718	17.7447262	19.6131878	19.7021217	19.3441048	20.0563583	23.4396172	25.2781353	24.9109078	23.739542	25.2761841	25.0038891	23.022625	25.0937386	24.723383	
Cdk1	+	9.87830662	4.76716317	18.5618095	17.438427	18.7164078	19.4944954	17.2406311	19.2543316	19.5115566	18.1437588	19.9397106	23.3519154	23.6701202	23.5262375	23.6190777	23.9983463	23.4859123	23.0834274	23.3446217	23.1259384	
Dars	+	9.81025004	6.09669516	18.8229561	15.86656	19.4090614	19.988472	18.8190327	19.0807724	17.9684544	18.881876	18.560566	25.3512764	24.3860073	24.4253445	25.7108021	24.5602264	24.2728424	24.9514046	24.2256756	24.384428	
Rbbp4	+	9.76148633	4.70388158	18.6707478	18.3329449	20.2420216	18.7752724	18.4789677	18.8524971	17.1171513	17.9340763	19.4631214	23.6476822	23.6590538	22.9165592	23.8563328	23.7074623	22.717413	23.3412304	23.6470223	22.7089787	
Rpl15	+	9.73802646	4.75754653	19.4116764	18.2563953	19.8098469	19.0438976	19.2006455	18.6589832	19.7839584	18.852005	20.8983231	23.9787579	25.1651115	23.9420795	23.902422	24.9066944	24.24757	23.0172997	23.955534	23.6181812	
Nedd4	+	9.73419348	4.34452396	17.1787567	19.7055225	19.7665081	18.69067	18.4643154	18.4378376	18.390789	19.2552624	19.5191784	23.0261593	23.6275616	22.9665585	23.237524	23.6927471	23.0072727	22.4476337	23.5346909	22.969408	
Ranbp2	+	9.703542	5.65687837	18.1231461	17.79883	20.3093338	18.3175736	17.4764671	18.9635086	18.6904049	20.0055084	19.1320763	23.397543	24.7764568	25.0215321	23.7139778	24.7691078	24.9341354	23.2853146	24.6642723	25.1664143	
Mcm5	+	9.69199548	5.1439671	20.4307556	20.3353825	20.188139	19.0404949	20.8909683	18.9479218	18.2882881	18.7123585	19.9891968	25.3896885	24.9357109	24.094101	25.8325558	24.9764004	24.040678	24.7823677	24.9530487	24.1146584	
Phgdh	+	9.68933425	3.95971002	19.1462803	18.6210136	20.3587608	18.5451355	17.9260368	19.5652866	18.0109749	19.5655098	19.5609093	23.2110252	22.7499085	23.0404778	23.3723888	22.9963474	23.0560284	22.6623173	22.7581883	23.0906162	
Rpl26	+	9.66384009	5.81109874	18.8046036	17.8251934	19.1567707	19.4258442	17.3422756	20.3200741	16.9323616	18.6800995	19.6400719	24.6506424	25.2624855	24.1082096	24.3461781	25.1712723	24.0670204	23.9157028	25.034689	23.8709831	
Gdi2	+	9.66091311	4.84614754	18.3796749	17.657217	19.2892914	18.4596729	16.8463154	18.3704605	18.3189926	17.2402725	19.5624352	23.578537	23.9015026	22.9648857	23.5546169	23.4707279	22.602499	22.7254429	22.3774014	22.5640469	
Aldh16a1	+	9.63631294	3.25560909	19.34301	18.5225792	19.6042805	18.5168514	17.8110924	18.7888794	18.7272358	17.9818535	19.5977154	21.9922733	21.9341984	22.2457714	22.4017677	22.0491314	21.9681778	21.4438458	22.1463146	22.0124989	
Ldhb	+	9.6319215	5.5627149	18.2376328	18.4001026	20.3236122	18.8825111	17.2727127	19.8092632	19.2244759	18.0663681	20.4851761	24.4966183	25.2316914	24.2214031	24.4823456	25.1202469	24.4833298	23.8563328	24.9960213	23.8782997	
Nop2	+	9.61050882	4.23709488	18.2808189	18.8309898	20.4809399	17.7604961	18.7595768	18.3618164	17.9128895	17.5620861	18.8612557	22.516964	23.2009602	22.9721623	22.9895382	22.6577892	22.9261303	22.2817268	22.5701981	22.8292542	
Ddx5	+	9.58157275	6.92611864	19.4376049	18.4328384	19.5807552	18.447916	22.0381508	20.1752358	19.0137882	22.5013027	19.2530975	27.077755	26.9431305	26.5436993	27.3512764	27.1092873	26.4665947	26.6680374	26.7287121	26.3272648	
Hdac1	+	9.57836975	4.7431789	18.3268108	17.8286743	20.3639565	19.4419804	19.1481152	19.7740593	17.2730904	19.0360279	19.0003414	23.0539093	24.0435181	23.8246403	23.2298603	23.9455662	23.9140606	23.2553711	23.740469	23.8742714	
Rpn1	+	9.57559147	4.03017044	18.3173809	19.5733166	19.9085369	18.3682766	17.8188057	18.6556454	18.733448	19.1743317	18.5354919	23.6100922	22.2952728	22.6411686	23.7798653	22.6779671	22.6308975	23.0758915	21.9825573	22.6630554	
Rars	+	9.56945611	5.81382985	16.9614067	17.9432392	20.30867	18.1809902	16.7863064	18.6730919	17.6612091	18.9539337	20.1194248	24.2560196	24.2712765	24.2228031	24.5768089	24.3804035	24.1744766	23.8230858	24.039423	24.1684437	
Mybbp1a	+	9.55293867	4.93534512	19.6972694	16.9948978	19.9744721	18.9003105	18.3189144	19.0716705	18.3318386	19.1894131	19.5617924	24.0544071	24.1731033	22.9678249	24.4834538	24.3704605	23.1275768	23.8999367	24.1804066	23.2015152	
Gart	+	9.53314962	3.68900172	19.0604916	18.8717022	19.1634579	18.0150585	20.0943298	18.4163895	18.1567593	18.0798206	19.2172089	22.4497261	22.8920441	22.3091087	22.838728	22.955286	22.1940918	22.3058853	22.7147522	21.6166115	
Rbmxl1;Rbm	+	9.5233798	4.96576712	20.3046207	18.5171528	19.5573616	18.3967171	18.7180023	19.4966946	16.9802647	18.5821419	19.1533508	24.350029	24.1002903	23.3678646	24.5911503	24.1851807	23.1142292	23.8362446	23.8458462	23.0073757	
Cep85	+	9.52297967	2.96805573	19.4455814	18.916996	18.463316	19.0283871	18.8412437	19.0753708	19.4636917	18.2010784	19.8701248	21.8363419	21.9482079	22.3351364	22.5902824	22.1086254	22.1602325	21.6951504	21.8107262	22.0335884	
Hnrnpm	+	9.47527946	6.70607588	20.1883469	18.243824	21.0980854	18.9297314	17.9691029	18.5703068	17.2353058	21.4019756	20.2037277	26.2395439	25.7761555	26.1463337	26.4884434	25.8451042	26.0767765	25.9027443	25.7347431	25.9852448	
Srrm2	+	9.46579131	3.74355825	18.9218578	19.0961247	19.7618637	18.4890499	17.5379505	19.5528565	18.2732277	18.4464111	18.7218552	22.407095	22.7987137	22.0399933	23.3382416	22.7465076	21.7741852	22.6179123	22.6765041	22.0940685	
Ddx1	+	9.46423838	5.19300503	19.2141953	18.2986889	20.0098934	16.7530232	17.569582	19.55163	18.612875	18.0233612	18.4559097	24.0707932	23.9604912	23.3899498	24.3395329	24.0587063	22.766058	23.7335548	24.0146122	22.8925057	
Atp5a1	+	9.4623362	5.03307046	21.0904865	22.0218792	20.7572727	22.443922	24.0142708	21.3972302	21.6245308	20.7138939	20.950346	27.2042446	26.6564922	26.8486424	27.2152119	26.7559547	26.5213165	26.5833378	26.4280624	26.0982037	
Kars	+	9.44847058	5.44584041	20.1236267	16.8985863	19.5777817	19.3939343	16.7233887	18.683485	18.824049	18.5629635	19.4767456	24.4214973	24.2123756	23.9635811	24.5866909	24.3843613	23.775753	23.9473515	24.0721836	23.9133301	
Eif2s3x;Eif2s	+	9.44344259	4.63428561	18.5691109	18.1891995	19.0731545	18.1818333	17.0474911	19.6065693	18.813715	18.2197495	19.1531601	24.3408909	22.6948109	23.050909	24.1847267	23.488121	22.6254673	23.2063961	22.358799	22.6124325	
Eprs	+	9.43047703	5.18193054	18.0744305	17.7198296	19.5420227	19.1063671	17.4895382	20.4652844	18.8206234	17.8713036	19.8726692	24.1493416	24.2840443	23.4792652	24.544569	24.4111233	23.3104954	23.7964973	24.2480049	23.3761025	
Pdia6	+	9.39213108	3.199376	19.3475704	18.9029179	20.0969544	19.1099873	17.9658337	18.1270046	18.9771614	18.7534485	19.4828091	22.3236656	22.2175922	22.1711502	22.4776115	22.4949455	21.7589817	22.0898418	22.3139591	21.7103233	
Srpk1	+	9.37293226	3.03753514	19.9692116	18.8309631	18.8088436	18.3606949	18.1946049	18.9545078	20.0025635	18.9940796	19.5375938	22.1977558	21.7987537	22.2325115	22.3989525	22.3620682	22.0667419	21.740284	22.0792007	22.1146107	
Etfb	+	9.32759584	3.81204796	18.5280228	17.551014	19.2123165	19.4721413	19.4818306	19.6974144	17.7773018	19.2164059	19.4785519	22.8915806	23.2159786	22.8333149	23.0965004	22.8871422	22.7108288	22.2150459	22.5560665	22.3169727	
Sdha	+	9.3092996	3.54695447	20.2027874	17.7430573	19.4690781	19.1357307	18.8746014	18.6037369	18.3697662	18.8700447	18.6641655	22.7263584	22.9367523	22.1835003	22.8153267	22.8054218	21.7899475	22.1790409	22.3927307	22.0264797	
Dstn	+	9.29331777	4.29808935	17.5795097	17.5248604	19.8505478	19.2859573	18.3332157	19.5927467	18.4129448	17.0664406	18.0588951	19.155714	22.2515049	22.5400944	23.488121	22.6854515	22.8099995	22.8240757	22.2104759	22.455082	22.6983547
Ddx17	+	9.23719936	4.83356433	19.2499352	17.6060181	20.1676083	18.7711296	17.6387043	18.2350807	18.5415916	19.2545338	20.3925476	23.3378334	24.1465473	23.8291969	23.7225494	24.191143	23.7758541	22.6274948	24.0792828	23.6493263	
Psmd11	+	9.22305031	4.00158352	19.3682442	18.1106319	19.8322792	19.066021	18.8777351	18.4129448	17.0664406	18.0588951	19.155714	22.2515049	22.5400944	23.488121	22.6854515	22.8099995	22.8240757	22.2104759	22.455082	22.6983547	
Cct4	+	9.20667894	4.96365717	19.7945328	18.5427475	19.9281197	17.4463139	17.2215977	18.6086235	18.8104134	19.8933468	19.537632	24.4021702	23.7858639	23.3046608	24.8294392	23.9402885	23.419054	23.8606968	23.4677467	23.4463215	
Rpl19	+	9.20384584	3.86322975	18.842968	18.1242905	19.5408363	18.9827023	17.2924748	18.256712	18.2297936	18.86829	20.2351818	22.6098442	22.684639	22.6543407	22.9788094	22.6594448	22.5951862	22.1807709	22.4248066	22.354475	
Ckb	+	9.19290036	4.72368516	17.9861507	18.8790264	19.011116	19.4449558	17.6457157	18.9845181	18.2665596	16.6579762	20.145155	23.2974014	23.3208599	23.7915382	23.4952145	23.5102654	23.2741242	23.0404282	23.1789951	22.6255131	
Vdac2	+	9.18795371	4.36473317	19.9057884	18.3138771	19.2690525	18.769422	16.883503	19.2415257	18.9459763	18.8359318	19.8460674	23.0257378	23.8627796	23.8102932	23.0058003	23.5417957	23.1814842	22.4600391	23.3088303	23.096983	
Usp10	+	9.13428608	4.25820669	18.911829	18.2988987	20.5221176	19.2020969	18.1323376	18.5806408	17.2784786	19.6863079	19.3590965	22.83638	23.0859413	23.1799812	23.8200684	22.9411659	23.0829563	22.9841404	23.2507381	23.1142921	
Psmd2	+	9.10578407	4.47688972	18.5109425	18.6325684	20.0380249	20.0542584	17.2626343	19.5291023	18.8336163	17.5418205	19.3019352	23.7578621	23.1092796	23.2007656	23.9387646	23.3654633	22.9254608	23.3020115	23.3379688	23.0593338	
Acly;ACLY	+	9.08697645	4.53651089	19.4617748	17.5374355	19.8830414	18.0857716	17.6025887	18.8600597	18.2924194	18.8601112	20.2621498	23.4410114	23.502882	22.7347965	23.9684238	23.6150398	22.6642723	23.2930565	23.5339775	22.9204903	
Trim71;TRIM	+	9.08462112	3.8154174	19.0906601	18.4341106	20.0323906	19.9928894	17.4791737	19.1955891	19.1301689	18.3747845	19.3408489	22.7473908	23.0904064	22.6387844	23.0741291	23.3428593	22.4611645	22.3185997	23.2741242	22.4619141	
Myef2	+	9.08267561	4.59537591	19.0605869	18.0333977	20.5732956	17.9277878	19.0716629	18.1950874	17.2063656	19.4898319	18.8309174	23.8887405	23.1471081	23.5006943	23.8929138	23.1318378	23.334837	23.3189316	22.8404007	22.6918526	
Rps6ka1	+	9.06481455	2.98475329	18.9546547	19.6573124	19.1876316	17.9484043	18.4184475	19.4983368	18.7530041	19.8194752	19.5452938	22.2864723	21.8981094	22.1407719	22.7783432	21.8919697	22.1309433	21.8590469	21.6709423	21.9887409	
Phb2	+	9.01865858	6.29185719	17.9581776	20.6506214	20.4041557	17.1893234	21.4685669	19.2653217	18.0055161	19.1610165	19.4901886	25.9973126	25.9378223	25.4328804	26.2241478	26.0088749	25.1404362	25.4996014	25.3549786	24.6235485	
Rcc2	+	9.0019457	4.8711213	19.837389	17.5630055	19.3138332	19.1902275	17.2774983	19.2508488	19.387291	18.4935627	19.3728523	24.5018501	23.7685032	23.0000324	24.9185257	23.8225994	22.5826092	24.2166748	23.547102	23.1687031	
L3mbtl2	+	8.98871749	3.976781	17.8827953	18.0420647	20.1933346	17.7150211	18.7761154	18.5955257	19.0259094	17.8783436	19.7850819	22.5058155	22.687973	22.8995304	23.0693512	22.8258228	22.6568089	21.8702679	22.6935978	22.4760532	
Dhx9	+	8.98521368	4.87663057	19.904129	16.5450993	19.8344479	18.5610695	18.0080967	19.0292091	17.6966305	18.0656338	18.974741	23.4987488	23.6579647	23.0747166	23.7136631	23.9854622	22.727335	23.3229237	23.7851658	22.7427521	
Qars	+	8.98490828	4.72458564	17.6042175	17.4334183	20.6202736	18.1321583	18.429224	19.1964397	18.2907105	17.8405514	19.9733028	23.262413	23.3792801	23.3042412	23.7976856	23.4919167	23.2826309	22.8355331	23.5197735	23.1680927	
Ptbp1	+	8.94325956	5.81001112	19.9517708	15.5218754	19.2469215	19.8739166	18.6072407	18.2324314	18.1655769	18.3635674	19.4711475	24.4490967	24.7470417	24.3444176	24.7455044	24.856144	24.2293472	24.2609787	24.4510479	23.6409702	
Nufip2	+	8.90111375	3.76669481	18.2956677	18.0363789	19.528101	18.8183899	16.862608	19.3147621	18.9475613	18.5212593	19.1901703	22.5184059	22.2504635	22.4328556	23.3560867	21.9810944	22.2258797	22.3993435	22.1490479	22.1019745	
Atf7ip	+	8.83342905	3.64378548	19.9833107	17.3565083	19.8260689	18.9695435	18.6773148	18.7856674	18.649704	18.3823128	19.6928501	22.6829891	22.6410141	22.1996441	22.9357472	23.0420322	22.416893	22.5027599	22.7114162	21.9848537	
Prdx1	+	8.80780371	5.33759223	19.6520023	16.568161	20.3980904	20.2617626	17.9167023	20.0758133	19.5842152	19.1647701	19.4532871	25.3062954	24.819191	24.386797	24.8486176	24.7210369	24.327179	24.0027313	24.6510258	24.0502605	
Cct8	+	8.79300816	4.40892665	19.8435402	17.6221294	19.4514237	20.542593	18.0391064	19.7711964	19.062542	17.9689903	20.0066185	23.8575687	23.6609039	23.3442154	24.0544891	23.7092514	23.1258297	23.5192928	23.5951405	23.121788	
Mcm4	+	8.77741789	4.88578055	17.9683571	17.5179825	19.3836231	18.8763409	19.0665569	19.8249588	18.2371464	18.1939545	19.8340149	24.7324162	23.7002831	23.323473	24.9881096	23.5951405	22.3800468	24.039423	23.563139	22.5529289	
Gnb2l1	+	8.77079032	6.07900408	20.3786717	19.8277397	19.3158283	20.3059673	16.9473763	20.9084454	21.3562756	18.3521347	21.4349175	26.1905022	25.8777142	26.2617683	26.3046951	26.018755	25.9667301	25.8552399	25.5219002	25.5410881	
Rps13	+	8.75948281	5.67463854	19.2855835	16.9444618	19.9181919	17.9196491	18.9656677	17.7983875	18.4292755	19.9336834	20.4624882	25.7294121	23.840189	24.0801773	25.5653477	24.0856972	23.8412457	25.3401108	23.8125477	23.4344082	
Slc25a13;SLC	+	8.75394893	4.50628154	19.8392849	16.1071091	19.0565586	19.2717247	17.7358933	17.9117794	18.5374394	18.7030201	18.9830093	22.9995174	22.9270172	23.1955643	23.299778	23.0956631	22.9113197	22.7341557	22.7221947	22.8171425	
Snrpd3	+	8.6950223	4.14319844	18.6164875	17.8009701	19.3658714	18.3685398	16.862812	19.4639416	18.0540791	18.3430996	20.0405369	23.3610516	22.6537495	22.5442276	22.5705452	23.121851	22.0434017	22.6270943	22.6844235	22.5987797	
Phb	+	8.67764601	6.39801237	17.9418564	21.0474014	20.1237412	18.541132	21.6641846	18.6480541	18.4078693	17.8545094	20.2516499	26.6144218	25.693306	26.4428463	26.784441	25.4314137	26.1836853	24.7603016	24.7855644	25.3665295	
Hnrnpa0	+	8.67387528	4.43845092	18.2381401	17.5433159	20.3630619	19.2012978	17.9128742	18.3190613	18.298933	18.9509754	20.4191647	23.3575649	23.7074623	23.0470676	23.4899578	23.7350025	22.9498653	23.24683	23.3190689	22.3400631	
Eif2b4	+	8.6689056	3.3473888	18.3681507	17.5223885	19.7991524	20.0914249	18.7815743	18.8357506	18.8063622	19.4300175	19.3498745	22.3207493	21.6455326	22.424345	22.8266964	22.4360104	22.3028202	22.572073	22.2331276	22.3498402	
Mov10	+	8.61482547	4.12739669	18.8926811	16.9165344	20.1331215	17.6839256	18.5344296	19.4047222	18.7511196	18.1829453	19.6932907	22.7340927	23.1713638	22.7352505	23.1686573	23.0477829	22.4282875	22.4957027	22.9493294	22.6088734	
Rpl22	+	8.5879848	6.187134	22.2812176	18.2706051	20.3794193	20.6429215	18.7059727	19.785286	17.1323547	18.8690453	20.0261726	26.4706192	25.805481	25.7535591	25.796051	25.8975372	25.8544807	25.8542652	25.516592	24.8286152	
Npm1	+	8.58445256	5.43651348	17.7690945	18.4707928	20.3503285	18.2638512	17.8369122	19.2676621	18.9877796	18.5113277	21.7842064	24.0274086	25.1001701	24.3266316	24.3619213	25.1790791	23.972374	24.2442341	24.8475189	24.1112385	
Trim25	+	8.56695974	3.60255941	19.5545235	18.0864239	19.9009075	19.5380917	17.8849297	18.1397133	18.3222332	17.5435925	19.2765122	22.0909081	22.2457428	22.5098076	22.4507828	22.3761292	22.5414658	21.6175079	22.2997494	22.5378685	
Larp4	+	8.55324229	3.91071638	20.1383667	17.6465702	19.7734718	19.2954483	18.1877098	19.0227547	18.4132881	18.324379	19.445055	23.5845146	22.8660851	22.3933582	23.8334484	22.7800465	22.6393585	22.8806171	22.386797	22.0792656	
Arf1;Arf3;Arf	+	8.53401376	4.68398794	19.2316914	19.1048088	20.6070728	18.4456596	17.764513	18.901041	18.0422688	18.7244339	20.2207699	24.2356415	23.8985519	24.1123524	23.915247	24.2929859	23.2540741	23.776556	23.8616428	21.851099	
Csde1	+	8.53289746	4.33603435	18.464735	19.3610497	20.0610619	18.6136627	17.4608555	19.1981678	17.8872395	18.6624813	19.9684391	23.3256702	23.5711479	22.938261	24.0787125	23.9266911	22.5612755	23.000309	23.3924427	21.9074917	
Kif2c	+	8.51663987	3.15536202	19.6282368	18.2096863	19.7977829	18.8507195	17.6804161	18.2349358	18.6246384	18.6450634	19.8731117	22.1440449	22.1796475	21.7395001	22.2290249	22.1467819	21.7128868	21.7247162	22.2604618	21.8075848	
Dazl	+	8.46729429	4.01300409	18.8343239	16.5491314	19.7045937	19.4804592	18.7536049	18.6996479	19.3945522	18.7708073	18.7329769	23.0308971	23.2364006	22.47855	23.5733452	22.6500282	22.1315708	23.1635685	22.5252323	22.2475414	

Mthfd1	+	8.42514277	4.89025307	19.2127895	17.4503746	20.474926	18.8599262	20.8834553	19.4146233	17.3017559	19.8234234	18.9064694	24.2350578	24.2252331	23.972023	24.6764298	24.3303299	23.5697575	23.8197765	24.1194954	23.3919182
Rpl10a	+	8.42073054	6.18061977	18.8905716	17.791956	20.2262859	17.8336601	18.0703239	18.79566	18.9660378	18.0125122	19.2230358	25.7135582	25.234911	25.1618099	26.2857037	25.1649189	21.3474827	25.205719	24.5143662	24.8071518
Pno1	+	8.40894494	3.72452121	17.7495441	19.1221905	19.1775913	17.8327446	17.9444656	18.8967533	18.1920414	18.7804527	20.0630932	22.4174843	22.6208687	23.1225777	22.7490902	21.6801586	22.6256905	21.8581753	21.3622818	22.8432407
Igf2bp2	+	8.39883525	3.30813768	18.4882107	18.6137829	19.9532986	19.0546627	18.8074322	18.7704105	17.1027947	19.2131367	19.4845524	22.3907642	22.6894455	22.1117172	22.4357815	22.2685947	21.9945183	21.8532715	21.9783745	21.539053
Snrnp200	+	8.39098876	4.50549401	18.1996517	16.5614739	19.5681114	18.1110973	19.0881958	18.9093075	17.2253628	16.9693279	18.6628571	22.5352593	22.9649391	21.9754028	23.4426575	23.2739811	22.2404251	22.6117573	23.0202026	21.7802067
Psmd3	+	8.38642646	3.98097971	18.7946739	17.2685528	20.4870396	18.3883686	18.7887478	18.7956257	17.8962936	19.5045528	19.8412609	22.5912418	22.8564091	23.4087277	22.9601021	22.8260956	23.0485649	22.1835308	22.6113529	23.1079083
Mri1	+	8.3712769	3.2927759	19.3286686	18.1069965	19.5610981	18.8249378	18.1822147	19.2965546	18.3232594	17.1404953	19.4377689	22.0965481	22.1298103	21.7035809	22.4285431	22.2244091	21.4069653	21.9759636	22.0854721	21.7856846
Ddx39a	+	8.36633861	4.93047863	19.7839069	18.74263	20.221695	17.8463478	17.3488922	18.8735657	20.0675583	17.9225617	20.8754482	24.1290417	24.4277744	23.5494556	24.6069336	24.3413677	23.616724	23.6860294	24.2200756	23.4795113
Ogt	+	8.34812577	4.23520915	18.5615234	17.0347118	19.0866833	20.3096752	17.5153961	18.5734386	19.8181515	18.5011845	19.197279	22.5397396	23.2218151	22.9756126	22.7985554	23.4841919	23.1296063	22.1011086	23.3955841	23.0687122
Ruvbl2	+	8.33303161	4.23790847	19.2667198	18.6619721	19.5820522	19.2795448	18.1772423	19.5527706	19.8361569	17.4967537	20.2385807	22.910532	24.3631916	23.1693001	23.3699951	24.3163776	23.0276108	22.3817902	24.0111179	22.683054
Hnrnpk	+	8.32515016	5.00539017	19.2057667	19.2529202	19.7151451	20.8078194	19.921711	20.567091	20.8449841	18.6262608	21.186163	26.302412	25.2146378	24.1001301	26.2465916	25.4517708	23.8020325	25.6195526	24.6998062	23.739439
Elavl1;ELAVL	+	8.32270024	4.39134534	18.3985081	17.7614384	21.2459621	18.1848583	18.5139751	19.2837811	18.6758575	18.686266	19.5181637	23.4399967	24.0645561	22.5416775	23.5682507	24.0954704	22.908556	23.1740189	23.3629246	22.6354675
Aldh18a1	+	8.32014053	3.3441018	20.0312405	19.0784187	19.5626049	17.2761517	18.237936	19.6476307	18.8699036	19.2566605	18.619976	22.187582	22.1373043	22.7224445	22.4071732	22.2023373	22.5592213	21.6747379	22.3346729	22.4519653
Capza2	+	8.31721646	4.75691054	19.5755215	16.9039536	19.7959652	19.5428391	17.4602108	18.36516	19.5218735	17.1033917	19.4881172	23.7431431	23.5135231	23.4157066	23.9466381	23.5802631	23.0298195	23.5788822	23.1935806	22.5676708
Mga	+	8.31145908	4.28493055	18.5604897	17.2346439	20.0753326	18.5806656	17.8280392	18.1204796	19.0343304	18.7918568	18.6353035	21.5636044	23.6093025	23.4772892	21.9532967	23.5230084	23.1502571	21.803648	23.0776863	23.2674236
Iif2	+	8.28019184	4.34254498	18.1587238	16.7548256	19.9017658	17.9704189	17.8573189	19.6339207	18.6931515	18.2083168	20.0676708	22.9461021	22.9573765	23.5732307	23.0794773	22.9689503	23.1052246	22.4262905	22.9664536	22.305912
Pfkp	+	8.26183838	3.16034126	18.8633118	19.6960793	19.6011944	18.7265301	17.7989445	18.0867367	17.6039867	17.9949722	19.1500454	21.9682484	21.4631367	21.7617436	22.3821068	21.4031715	22.0664139	21.8734264	21.4739265	21.5726986
Fbl	+	8.25774638	4.86143345	19.7716866	17.1843491	20.485714	19.035244	17.4979992	19.9678993	17.1674061	17.5715809	18.707962	23.6448819	23.6978455	23.4284153	23.5819893	23.6587257	23.3974133	23.2424316	23.4612637	23.2097759
Larp1	+	8.22566092	4.48064444	17.7131271	17.3176956	18.6286449	18.4370937	16.2307358	19.3454971	18.9314518	18.2314396	19.3191395	22.7081356	23.0572853	22.5472908	23.4857884	23.4484654	21.7588596	22.7586765	23.0531979	21.6629257
Eftud2	+	8.17037498	4.23678144	19.9090061	16.8973866	19.4839897	19.4761257	18.5189133	19.9932156	18.2779961	17.9784393	19.160574	23.0154457	23.6744366	22.7918167	23.4045754	23.6282311	22.6756439	22.6243973	23.7254639	22.2866688
Psmd5	+	8.16584689	2.90309715	18.4337444	17.7726917	18.8672257	19.8400059	18.1463528	19.5001011	18.7855053	18.6750107	19.1698322	21.4875317	22.0136242	21.7915783	21.9406643	20.9574375	22.3853493	21.6545162	21.9634228	21.1242199
Hace1	+	8.13659326	3.04097875	18.3672562	18.3912258	19.5046101	17.8405781	17.1401138	18.1368179	17.3081265	17.573822	19.2077808	20.9096909	21.4902763	21.220459	21.2570133	21.3327084	21.304409	20.8859139	21.2471352	21.191534
Eif3f	+	8.11321966	4.23661995	18.1241703	16.6414738	18.5115204	18.4804249	16.9487286	19.321785	19.0493527	19.6990337	19.6071453	23.0475178	22.9842453	22.5487728	23.0845795	23.1535225	22.2061882	22.3863239	22.8559151	22.2461491
Lars	+	8.06820316	3.88103379	18.3785286	17.8198357	19.1199284	18.191391	18.6670837	19.3575039	19.4571343	17.0522995	20.590559	22.815424	22.37854	22.4223957	23.027071	22.7532578	22.1531982	22.8105488	22.5151596	22.687973
Upf1	+	8.05761504	3.32439317	18.9431629	18.6788311	19.7691517	20.3733788	18.2292881	19.0793781	19.3734131	19.323122	19.9395237	23.2568111	22.8335838	22.5423164	23.6447144	22.505888	21.5678806	22.5627422	22.8569412	21.8579102
Pold2	+	8.04474132	4.98287794	19.3606892	17.1947823	20.4657955	19.1599121	16.3617001	19.3005886	17.9452515	18.3087559	20.1035652	23.6208687	23.8786736	23.7340717	23.9728108	24.0704651	23.629343	23.0847092	23.6238842	23.4321156
Slc25a5	+	8.03313535	5.68199094	21.8490772	22.0849209	20.3919811	18.4427872	20.6320972	22.3044376	18.9394016	22.2517643	21.9076748	26.8876247	26.7926559	26.8842506	27.3560715	27.230135	26.5509529	25.445406	26.1945095	26.6004543
Pold1	+	8.03150609	3.04230775	17.9124508	17.9995976	19.9361324	19.4483528	18.5261688	18.7666836	18.8081513	17.8930206	19.352766	21.3374519	22.1981449	21.7816486	22.1368046	22.3685303	21.421526	21.4958	22.0362415	21.2479458
L1td1	+	8.03075091	4.05074056	18.1113777	17.9331513	18.9593506	19.4123077	19.224287	18.7151833	18.1736755	16.9314518	19.5787067	22.3438892	23.5781918	21.9394817	22.8898354	23.5638371	21.9673328	22.1517429	23.3253975	21.7364483
Mcm3	+	8.02941933	5.18360647	18.6841927	17.5757313	19.4308987	20.1279488	18.0263481	21.1053944	16.7412949	18.494297	19.2847347	24.5880642	24.0996494	23.8622112	24.9580593	24.1092472	23.5218105	23.9996376	23.9397507	23.0448685
Gfm1;GFM1	+	8.00732839	2.68463792	17.930727	18.3160725	19.7507515	19.4779873	18.1077652	19.3267441	19.1406689	18.5987396	19.3198547	21.8729	21.2640762	21.5721893	22.2698498	21.1151505	21.6789131	21.6433277	21.2524567	21.4621887
Suz12	+	8.00031354	2.67450015	19.6681995	18.4078484	18.9081898	19.419878	19.0480633	19.6212807	19.4447327	18.2979832	19.0735073	21.553093	22.1948433	21.9014282	21.9522305	22.2734413	21.5160027	20.4985428	22.2879944	21.782608
Rnf2	+	7.9997476	4.29661179	19.1414738	18.4110603	20.3445377	17.9171066	19.1877785	18.7398453	16.6570282	18.0368767	19.7394009	22.9402885	22.579113	23.841053	23.1341267	22.8780556	23.3923111	22.3439713	22.3956871	23.3400078
Srsf1	+	7.99657537	5.32074399	18.9388104	19.5819511	20.2068462	19.1611996	17.7147903	19.5316124	18.9596825	17.7540913	19.7509975	25.4457531	24.9825058	23.2263508	25.8557644	25.2680664	23.3524551	23.6030884	25.2674942	22.485199
Prep	+	7.99012142	2.82649337	18.7426033	17.6218853	19.223629	18.7629528	18.9602242	19.0309467	19.3334522	18.8042412	20.133112	21.5738545	22.3058567	21.3684769	22.0332184	22.5022736	21.2864723	21.4945793	21.9716187	21.5151367
Smarca4	+	7.9510595	3.18618435	18.7658978	18.2205086	19.7129269	19.574749	18.515192	19.809824	18.8292217	19.1886654	19.3951607	22.9872665	22.6179562	21.8902264	23.3627911	22.4066544	21.6510582	22.4578133	22.280283	21.0337563
Atxn2l	+	7.92380481	4.01173486	19.1925049	18.988699	19.0554504	20.1373825	17.939249	18.7583275	17.4065228	18.2410908	20.0913258	23.3073025	22.9477787	23.0133686	23.8590851	22.5586853	21.8974819	23.5685997	22.8387661	21.9250984
Aars;AARS	+	7.88438097	3.62624359	18.954443	19.1183128	18.3355846	18.3678112	18.4074669	18.7066269	19.6415596	18.239151	19.0340462	22.2102966	23.3663979	22.2751465	22.4605408	23.3505688	22.1089115	21.6288967	23.417511	20.6229248
Ppp1ca	+	7.88149225	4.17946879	19.7356091	17.447506	19.3854542	19.4455681	18.4251308	18.2637405	17.1611614	17.324913	20.012558	22.740715	23.0042744	22.940361	23.2402058	23.0242672	22.7166176	22.297205	23.0215416	21.8316727
Fyttd1	+	7.87588449	3.61035474	19.1196766	18.2813759	21.0282383	18.4202213	18.1487064	19.2002029	19.201561	18.7542191	20.0862961	23.1285534	23.1617413	22.232893	23.3396015	22.9286442	22.2134152	22.7156334	22.8526058	22.1606026
Mcmbp	+	7.87470967	2.91238552	18.1849289	18.4953003	18.9234943	19.9811821	18.2156525	18.9589825	17.5573273	18.0223198	19.278225	21.5255432	21.5549202	21.5655575	22.2452202	21.998106	21.2717323	21.4152947	21.2332726	21.0192356
Khsrp;KHSRP	+	7.85395298	3.3263624	19.3767452	17.4015045	19.154213	18.926548	18.3248844	19.905201	18.9859028	18.9398327	19.8469734	22.6437454	22.77318	21.7390881	23.0273075	22.662035	21.5555286	22.2484379	22.5947762	21.5549679
Parp1	+	7.83932729	4.0875793	19.6387692	17.182581	20.833458	18.8071556	19.5246944	19.6194916	18.0637245	19.3707466	19.3348122	22.6251564	23.5483971	23.7952099	23.1482868	23.3661308	23.7813683	22.1990147	23.1424255	23.5576572
Dnajc21	+	7.82250447	3.22377777	19.5509281	17.6539078	19.1716404	18.3856258	17.4328671	18.6040878	17.3323288	18.4069138	19.7415543	21.8562393	21.6230125	22.0751247	21.5338345	21.8463631	21.7090206	21.1745682	21.6270733	21.8486176
Eif3d	+	7.81866913	4.60169559	18.3585053	18.329422	19.022644	20.1864262	17.8736172	18.7824955	20.3203869	19.4554024	19.3238869	22.8488674	25.0113735	23.0938435	23.307581	25.0355701	23.3571625	22.5071716	24.9536247	22.9528523
Top2a	+	7.81535421	4.21375487	17.664259	18.423914	19.8621407	19.9857521	16.9811745	19.1566258	18.0807514	19.8582783	20.0894108	22.567091	23.4665012	23.2324104	23.0161438	23.6206436	23.1521626	22.5048943	23.37994	23.0863133
Mtco2	+	7.80573101	3.85210631	19.3365898	18.6335926	18.9329338	18.5083103	18.6281471	18.8872261	18.9782009	18.0274468	19.2684727	23.1279545	22.7619057	22.5041428	23.1522236	23.0338745	20.0332279	22.7633038	23.6463642	22.84688
Serpinh1;SEF	+	7.80417019	3.42709965	19.2526226	18.0412731	20.0713368	18.0977993	18.6605129	18.9144363	18.3837833	16.7632771	19.3619709	22.1821365	22.2938423	21.9131298	22.371006	22.277874	21.89678	21.894598	22.0121574	21.5493851
Copb1	+	7.79523203	2.99808396	18.3306923	17.7668457	19.5074978	19.7241764	18.0153561	19.6100388	17.9433994	19.8048801	19.3515549	21.9525147	21.9514122	21.8936367	21.8959293	22.0240135	21.7245483	21.7001133	22.0344276	21.8606014
Rpa1	+	7.78400021	3.1565573	19.3378048	18.6359615	19.7829094	17.6080723	17.8209591	19.0730114	19.1517906	18.0685234	18.8804607	21.5182133	22.8190346	21.4698582	21.8433361	22.6078587	21.5696888	21.2811031	22.1245842	21.534832
Eif4g1	+	7.78332491	4.94319471	19.9589653	17.1097374	19.1857967	20.1015873	17.0768719	18.2129383	19.0393028	18.9486198	20.6140919	24.4673729	24.0329666	23.1884136	24.9817219	23.9484215	22.9251156	24.2784538	23.8153839	23.098814
Rsl1d1	+	7.76515819	3.32518281	17.6756516	17.0891323	19.4147701	18.9818611	19.1918373	18.8312492	18.2268963	18.6180458	19.6059284	22.7628994	21.9257507	21.6579208	22.8209248	21.6071587	21.4969215	21.8622303	21.6987572	21.729454
Pdhb	+	7.76193601	3.6608518	18.8230534	17.333168	19.5257282	19.405098	17.5081387	19.9794464	18.0854969	17.7881565	19.7083645	22.216526	22.8237457	22.2739525	22.4159641	22.7504807	22.0944557	21.9991379	22.4555817	22.0744724
Mcm6	+	7.722328	4.99639172	18.9191418	16.9815693	21.5126877	19.0117168	17.9902725	19.1064282	17.7295704	19.1347961	19.8636017	24.6227684	23.7842674	23.3085537	25.1277027	23.840765	23.3247109	24.1972313	23.8037071	23.2076035
Nup98	+	7.6863548	3.12593587	19.0454292	18.8334465	19.9391651	19.9243832	18.2442951	19.5622292	19.0356827	18.3505573	19.5041485	21.5412769	22.6441422	22.9681416	21.9231758	22.8597488	22.5750561	20.9543972	22.6971874	22.4096336
Hadh	+	7.68382783	5.09008302	20.4560757	18.197546	19.9132061	18.8321877	18.0592747	19.4110794	17.4796181	17.1465282	19.1833115	24.3811302	24.3656635	23.7488842	24.342453	24.4415169	20.9613762	23.8305512	23.954113	23.4638863
Dync1h1	+	7.60552471	3.17094273	19.0250397	18.1780987	19.0863056	18.0735588	18.5058479	19.9407997	17.5116501	17.2402535	19.3738613	21.3805752	21.6548214	21.8113918	22.2600308	21.5254002	21.2606926	22.043869	21.5827923	21.9543266
Farsa	+	7.60047635	4.77072907	18.7079315	17.4473076	20.9292984	19.2774696	16.4105587	19.904768	17.8441029	19.5087032	19.4452725	24.0356541	23.4835758	23.4472046	24.2379761	23.625	23.4886112	23.315342	23.3400078	23.4386025
TUBA3;TUBA	+	7.59873499	6.22792689	19.0100784	17.2107964	20.2000332	19.1888371	18.559021	18.6002579	18.1698055	18.4693432	19.513916	25.6942101	25.6877918	25.8080368	26.1692276	24.1059742	25.5508347	25.3273163	25.7575836	20.8724556
Prrc2c	+	7.59195813	2.67479134	18.1471329	19.0342236	19.6595116	19.6392212	18.9047604	18.8796978	18.5792255	17.9569798	18.790802	20.9676151	21.7358704	21.5590363	22.8613415	21.4119892	21.1961651	21.2110996	21.363512	21.3580475
Cdc5l	+	7.52841172	3.59155994	19.9566898	18.4003525	19.0685387	18.2146816	17.991457	19.2100506	18.2379074	17.7424011	19.944149	22.0297184	23.1872501	21.79982	22.8767834	23.1015892	21.6228352	21.7327271	23.1022625	21.6372814
Cope	+	7.51688811	3.24609884	18.7967949	18.5996113	20.7519131	19.678503	17.7905808	18.7319088	19.2358646	17.9009781	19.7696896	22.5964375	22.0566578	22.4304314	22.7345066	22.0952931	21.9472809	22.2892056	22.2870636	22.0338574
Ppp2r1a	+	7.50932571	3.62556415	17.7192745	17.7922649	20.0058174	18.5439911	18.614378	18.899334	18.2964363	17.4116802	19.5246887	21.8520527	22.6339817	22.7265663	22.0721836	22.6185169	22.3489208	20.4811554	22.2431011	22.4614639
Eif4a3	+	7.49403949	4.08641879	17.6176624	17.8872585	18.3490219	19.0719662	16.4276638	17.9956741	19.043005	17.6548634	19.7942925	21.6942577	21.9147358	23.5660458	22.4316311	22.2580776	23.0477161	21.3012314	21.6416092	22.7638722
Pfkl	+	7.49112201	3.80776787	18.7236385	17.1424923	19.8226032	19.672102	18.8729973	18.3893681	19.6024914	19.6353245	21.0030251	22.822094	23.3911305	22.7208176	22.9598904	23.7278557	22.6611862	22.5573998	23.372654	22.9209251
Psmc6	+	7.46205893	3.0991088	18.4813671	18.8809795	19.6460686	19.1991425	17.344101	18.3313408	18.989027	18.2874489	20.1381531	22.2531223	21.9674397	22.3620415	22.1849823	21.7089787	22.5021038	21.7276268	21.149044	21.3342686
Nup85	+	7.44909573	3.08877076	19.384161	18.3681755	18.6307983	18.1501255	18.3783855	19.2673035	18.606514	18.16078	19.464941	22.1569367	22.2842426	22.5192699	22.1897869	22.3067188	22.0828114	21.1083374	21.4925289	20.0694885
Trap1	+	7.40662185	4.28566848	18.6931019	17.0326481	19.6138783	18.6263142	17.0158806	17.6408272	18.9113159	17.9390163	20.9164581	22.318573	23.0221176	22.5536079	22.8441029	23.4412651	22.8244648	22.2559185	23.1336422	22.5667648
Syncrip;SYNC	+	7.38269854	3.27739398	17.8679924	18.2073898	20.4430981	18.5558453	18.4061203	18.0366974	19.237339	18.050808	20.0723267	22.0844326	22.3078594	22.001236	22.5040455	22.328085	21.5042648	21.7680588	22.3706074	21.5055733
Atp5o	+	7.3451699	4.80026669	18.6910553	18.6443272	19.2391911	18.2059116	18.7427654	19.0730972	18.4335098	20.0821209	19.8594303	24.6952992	24.7121944	23.751442	24.4213677	24.1858597	24.1480236	20.3037167	23.8454628	24.1104431
Fkbp5	+	7.33289282	3.82462162	18.4710674	19.4202538	19.8657951	18.5305576	17.9571476	19.1910801	18.1176128	19.448328	19.5822773	23.2795181	22.7323341	23.3164482	23.3442154	23.1009808	23.248394	22.8963547	22.8209248	20.2665443
Mcm2	+	7.32257185	4.32537121	18.8437977	17.4906635	20.8873444	18.4867077	17.731451	18.3752918	18.0025959	19.2270565	19.8760395	22.8187828	24.12076	22.4276981	23.2076778	24.1333599	22.4539509	22.4172535	24.0248756	22.2449303
Cct2;CCT2	+	7.31897388	5.21720791	18.5958767	15.6659632	20.0007668	19.7102394	17.9687958	19.4025383	18.9551163	18.3501911	19.6669388	24.8248329	24.2202969	23.8277435	25.2153053	24.2515469	22.4129448	24.409441	23.5286236	22.5805626
G3bp2	+	7.29884788	4.74756898	18.8595161	19.8076668	20.0482864	19.9151459	18.0737629	19.8337212	18.611208	18.1121388	19.3686733	22.621315	25.1956177	24.2195587	22.9266911	25.3336773	24.0136757	21.7336369	25.1591549	24.154913

Supplementary Figure 1

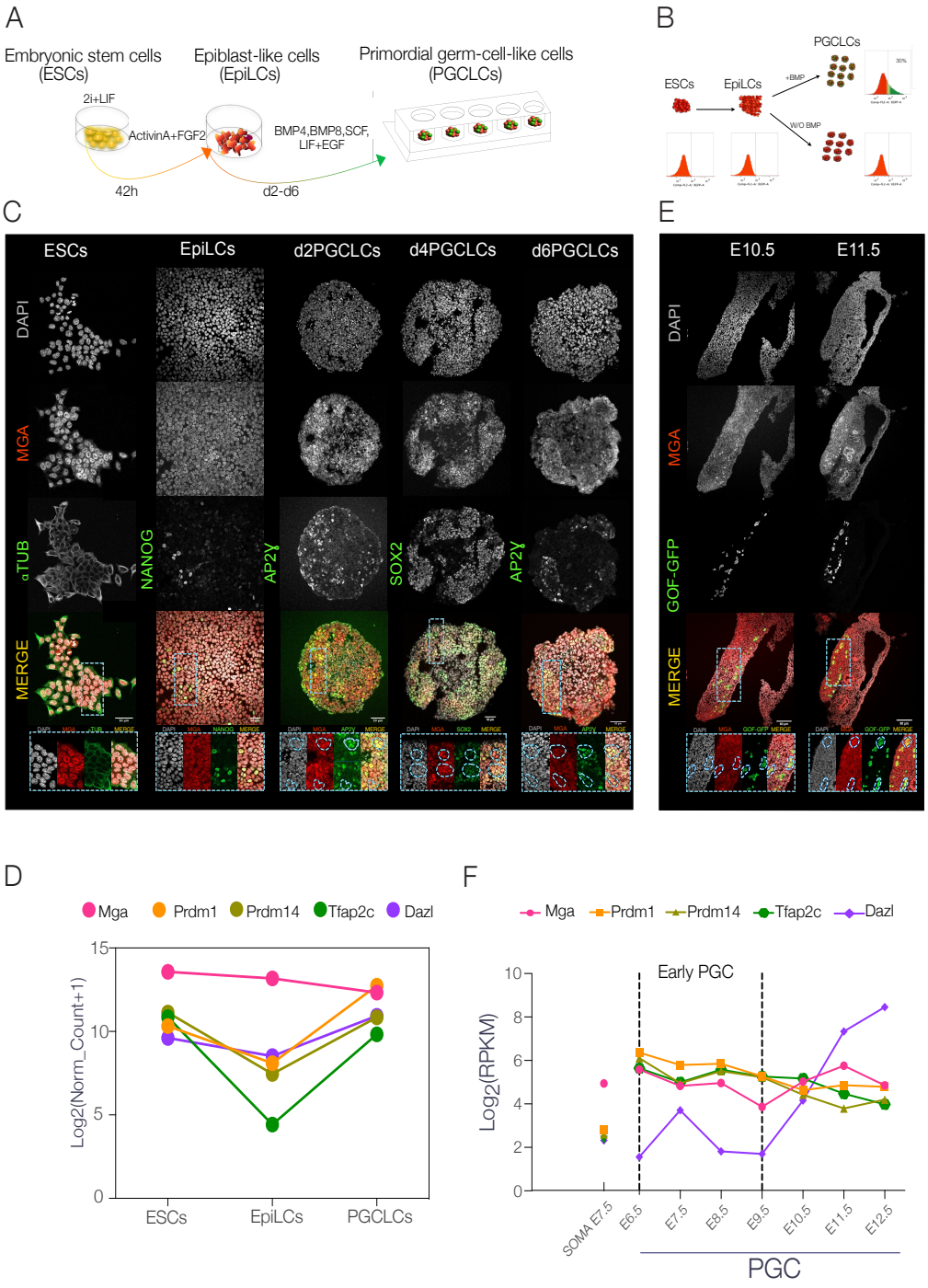

Supplementary Figure 1. MGA expression during PGC differentiation *in vitro* and *in vivo*. A. Schematic representation of the culture protocol used for PGCLC differentiation. **B.** Representative flow cytometry profile of BLIMP1-GFP during *in vitro* cell fate transition from ESCs to PGCLCs, with BLIMP1+ cells (green) and BLIMP1- cells (red). **C.** MGA immunofluorescence (IF) staining was performed throughout PGCLC differentiation *in vitro* and counterstained with αTUBULIN (ESCs), NANOG (EpiLCs), AP2γ (d2-d6) and SOX2 (d4). The bottom magnifications of the image show that MGA is primarily expressed within the nuclei of ESCs and EpiLCs. In contrast, the magnifications in PGCLCs at d2, d4, and d6 display the overlap area between MGA and PGC markers, as well as a somatic area, indicated by the dashed square. Scale bars, 50 µm. **D.** Expression levels of MGA and representative early (*Prdm1, Prdm14, Tfap2c*) and late (*Dazl*) PGC markers during PGCLC differentiation. The average of two replicates is shown. **E.** Staining of MGA in the genital ridge of ΔPE-Oct3/4-GFP (GOF-GFP) cells at E10.5 and E11.5 counterstained with GFP. The bottom magnifications show the zooming of the overlap area between MGA and GFP indicated by the dashed square. Scale bars, 80 µm. **F.** Expression levels of MGA with early PGC markers (*Prdm1, Prdm14, and Tfap2c*) and the late PGC marker (*Dazl)* transcripts during PGC specification assayed by single-cell RNA-seq (Magnúsdóttir et al. 2013).

Supplementary Figure 2

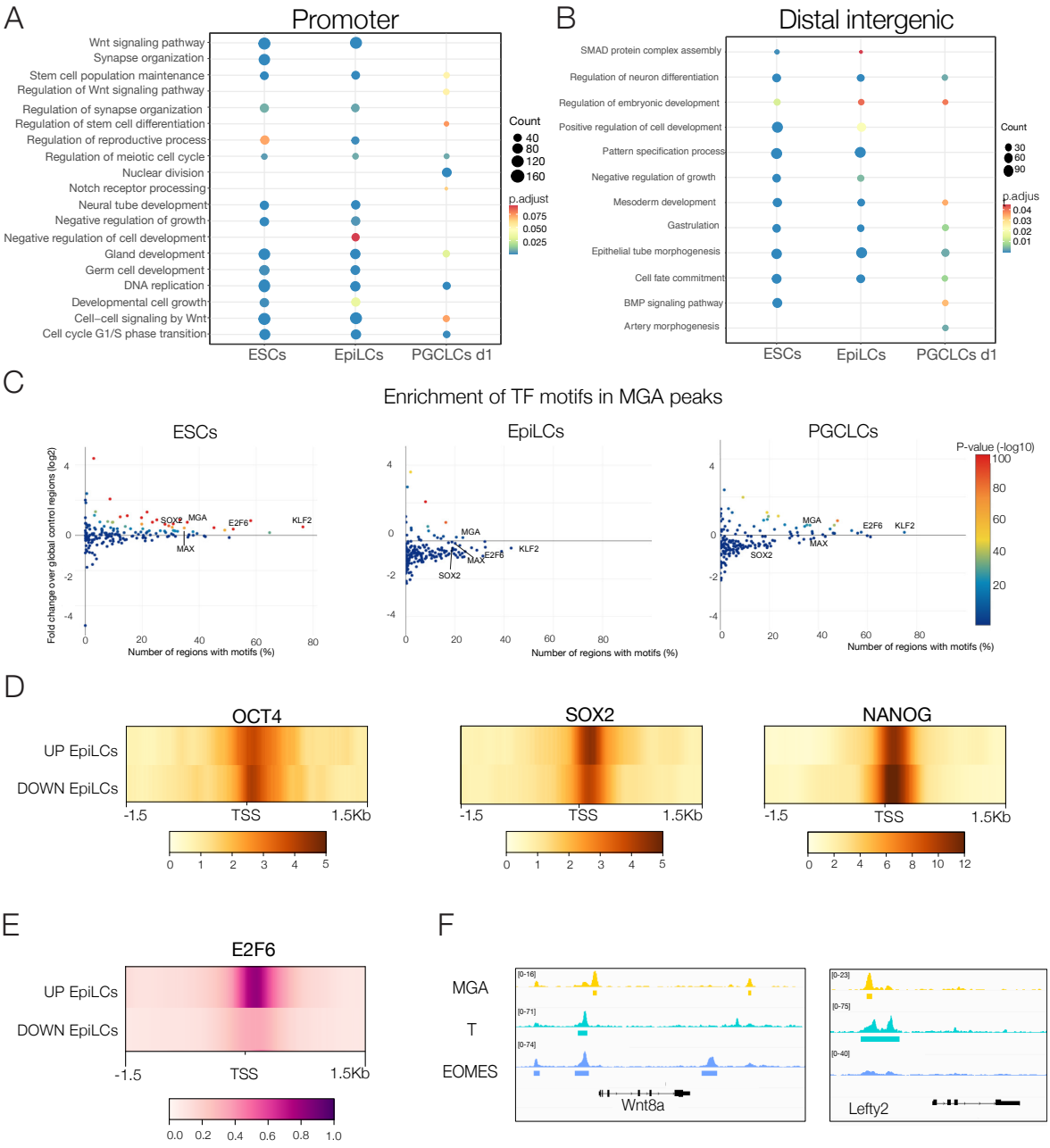

Supplementary Figure 2. Analysis of MGA binding sites during PGCLC differentiation. A-B. Comparison of GO enrichment analysis of MGA binding sites in the promoter (**A**) and distal intergenic (**B**) regions of selected biological processes across all cell types. **C.** Scatterplots showing the enrichment of MGA motifs in each cell type. The x-axis represents the number of regions with one motif %, while the y-axis represents the fold change over the global control regions. The color scale is associated with P-values, with motifs of higher frequency highlighted. **D-E.** Heatmaps displaying ChIP-seq read densities for pluripotency factors (**D**) and E2F6 (**E**) centered on differentially expressed genes bound by MGA during the transition from ESCs to EpiLCs. The analysis considers a region 1.5 kb upstream and downstream of the transcription start site (TSS). **F.** Coverage tracks of MGA, T, and EOMES at the loci of *Wnt8a* and *Lefty2*.

Supplementary Figure 3

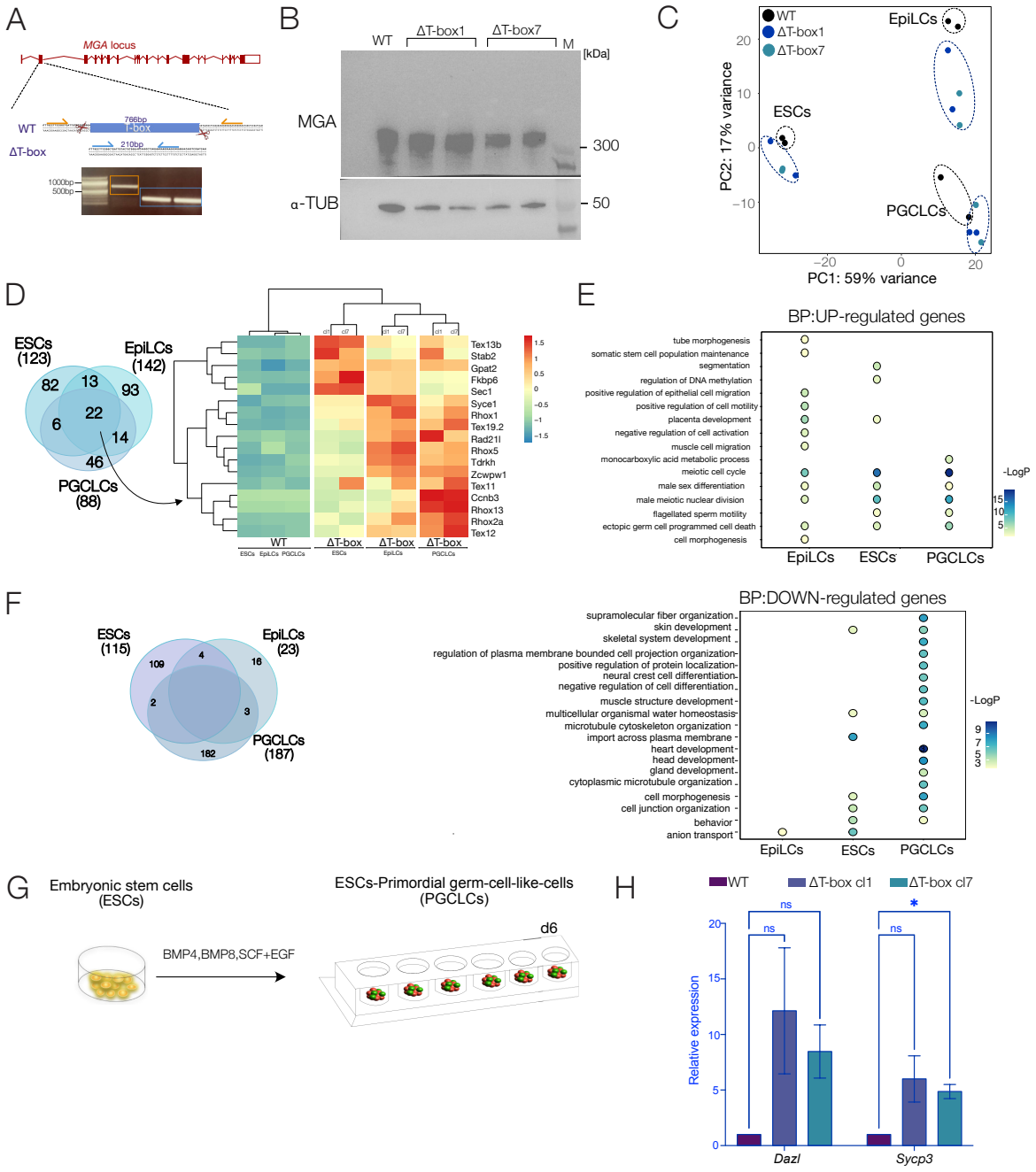

Supplementary Figure 3: Deletion of T-box domain. A. Position of T-box domain in MGA coding sequence, highlighting the position of the gRNAs used to delete this region. PCR was performed to confirm the deletion. A band was observed at 766 bp in the wild-type, while in the two selected clones, a band was observed at around 210 bp. **B**. Western blot shows no change in protein levels after deletion of T-box domain. The two clones and wild-type were loaded twice each. α-tubulin was used as a loading control. **C.** PCA plot of RNA-seq comparing ESCs, EpiLCs, and d6 PGCLCs transcriptome of ΔT-box cells clone 1 and clone 7, compared to the wild-type cell line. **D.** Comparison of the up-regulated genes identified in each cell type of ΔT-box cells. The arrow indicates the 22 genes shared between cell types. The expression is shown via Heatmap, mean of the normalized count of two independent experiments. **E.** Comparison of GO terms identified per up-regulated gene in ΔT-box cells during PGCLC differentiation. **F.** Comparison of down-regulated genes identified in each cell type of ΔT-box cells, with the results of GO analysis for the biological processes shown in the right panel. **G.** Scheme used to differentiate ΔT-box cells from ESCs to PGCLCs. **H.** qPCR of meiotic genes such as *Dazl* and *Sycp3* in ESCs-PGCLCs from WT and ΔT-box cell (cl1 and cl7). Error bars show s.e.m of triplicate biological experiments. * P<0.01, not significant (ns). Two-way ANOVA followed by Sidak's multiple comparison test.

Supplementary Figure 4

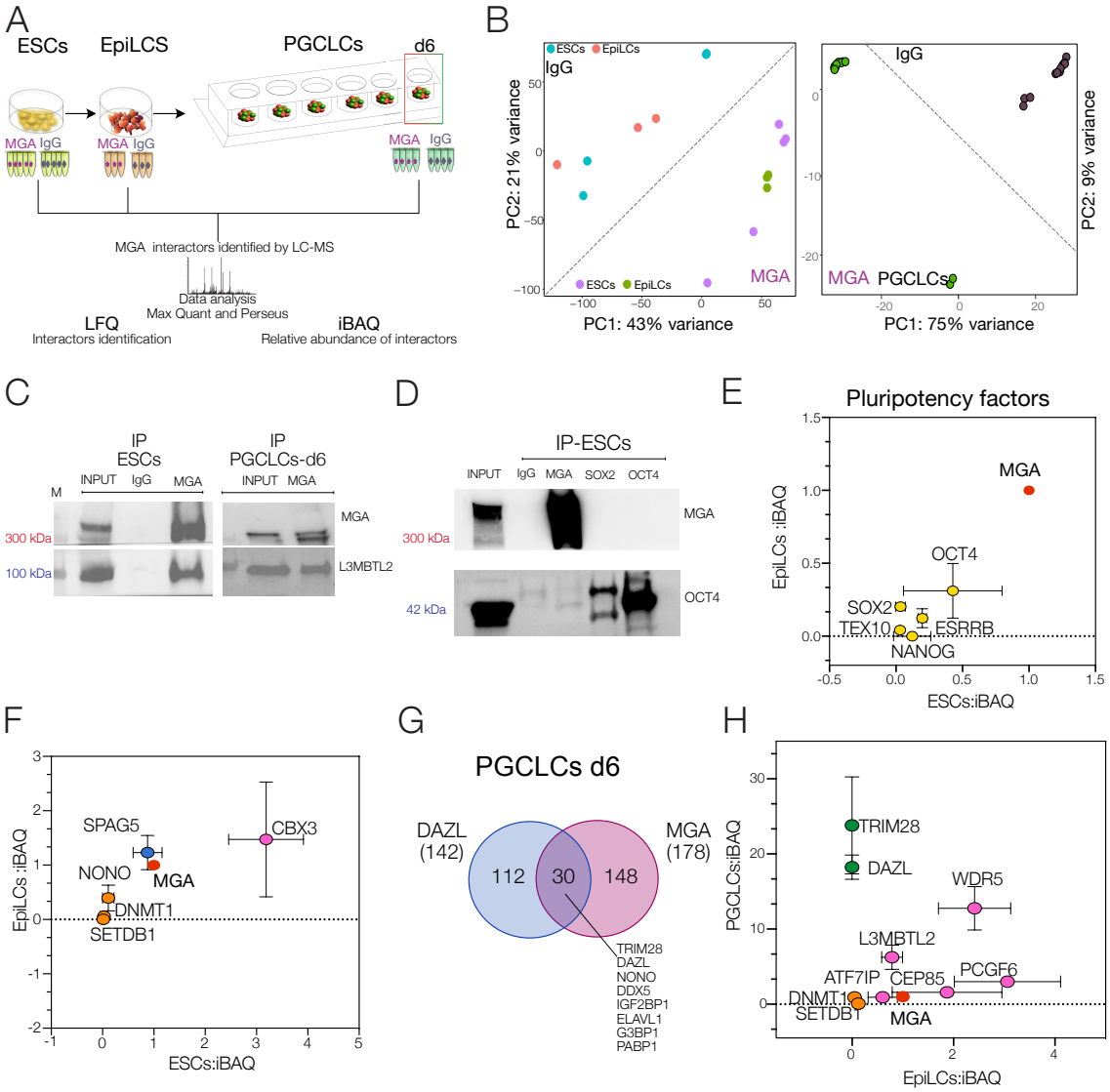

Supplementary Figure 4. Comprehensive analysis of MGA interactome during PGCLC differentiation. A. MS-based proteomics workflows during PGCLC differentiation. Protein extracts from ESCs, EpiLCs, and PGCLCs are subject to MGA and IgG immunoprecipitation. Five replicates for ESCs, three replicates for EpiLCs, and four replicates for PGCLCs. Pull-downs are analyzed by LC-MS. The data analysis was performed using MaxQuant, identifying proteins, and statistical analysis using Perseus. Label-free quantification (LFQ) was used to identify statistically enriched proteins in the MGA-IP by permutation-based FDR-corrected t-test. iBAQ intensities are used to calculate stoichiometry. **B.** Quality control of LFQ values of each interactome performed via PCA analysis. **C.** Co-immunoprecipitation of MGA in ESCs and PGCLCs (IP-d6). Western blot was performed on input, IgG-IP, and MGA-IP using MGA and L3MBTL2 antibodies. **D.** Co-immunoprecipitation of MGA, SOX2, and OCT4 in ESCs. Western blot was performed on the input, IgG-IP, MGA-IP, SOX2-IP, and OCT4-IP using MGA and OCT4 antibodies. **E-F-H**. Stoichiometry determination of the statistically significant interactors in MGA-IP. **(E)** Pluripotency factors. iBAQ-ESC vs iBAQ-EpiLCs. **(F)** Proteins involved in methylation. iBAQ-ESC vs iBAQ-EpiLCs. **(H)** DAZL-PRC1.6 proteins iBAQ-EpiLCs vs iBAQ-PGCLCs. **G.** Comparison of proteins enriched from MGA-IP in PGCLCs day 6 with published mass spec data (Chen et al. 2014) of proteins enriched in DAZL-IP.

Supplementary Figure 5

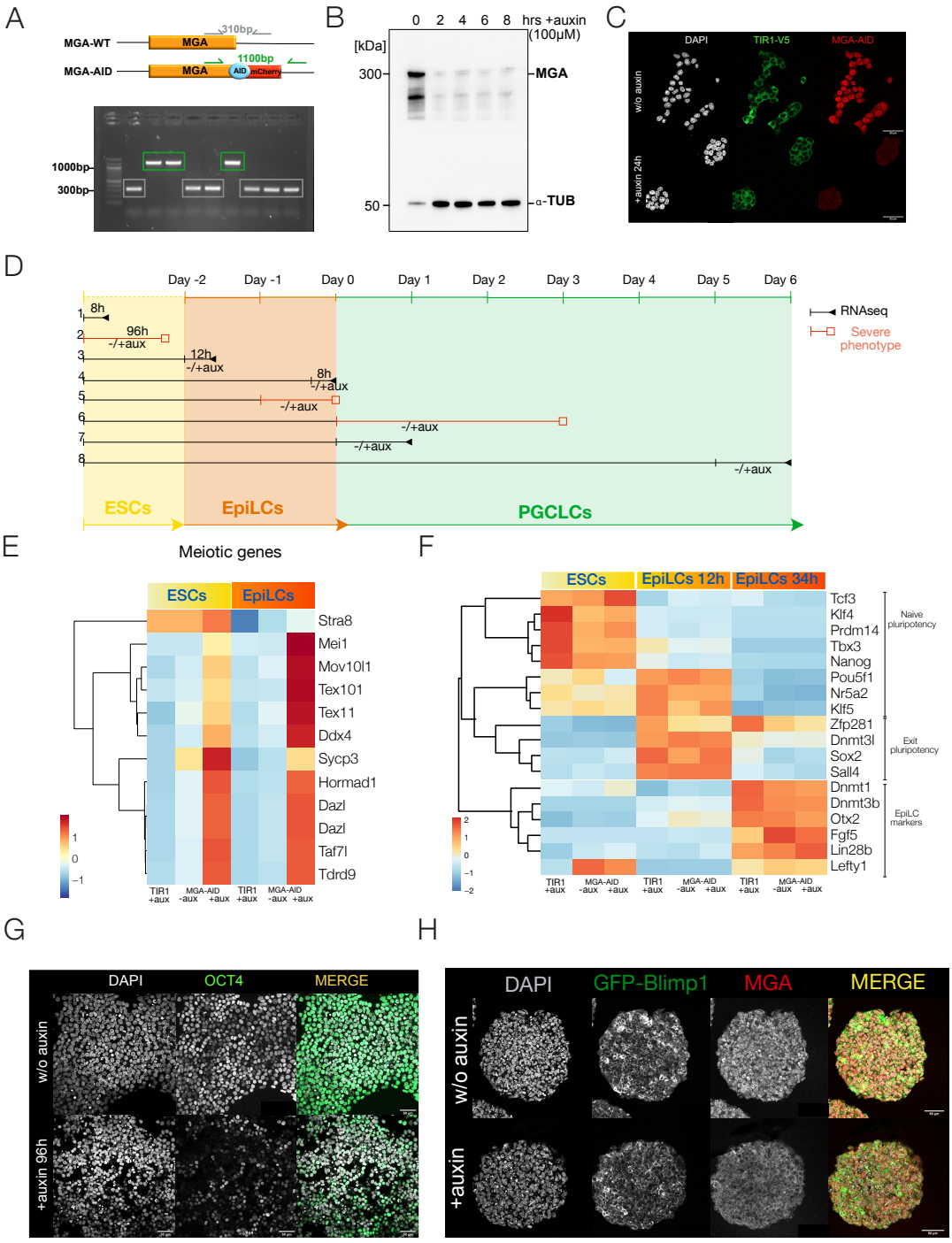

Supplementary Figure 5. Extended analysis of MGA depletion in PGCLC differentiation. A. Targeting strategy of MGA-AID. CRISPR/Cas9 is used to tag AID-mcherry at the C-terminal locus of MGA. PCR showed positive insertion with a size of 1100 bp. **B**. In ESCs, Western blot analysis of MGA-AID cells treated with auxin for the indicated times. .α-tubulin was used as a loading control. **C.** Staining of ESCs after 24h of treatment with auxin in TIR1 (parental cell line) and MGA-AID cells. **D.** A schematic representation of the *in vitro* differentiation scheme for MGA-AID cells from ESCs to PGCLCs. Auxin was added to deplete MGA at the indicated time points. Cells were also collected for RNA-seq (dashed line). The red square indicates a severe phenotype. **E.-F.** Expression Heatmaps of lineage-specific genes **(E)** Meiotic genes and **(F)** naïve pluripotency, exit pluripotency, and EpiLC markers of ESCs and EpiLCs after MGA-AID cells treated with auxin. Mean of the normalized count of two different biological experiments. **G.** Staining in ESCs of MGA-AID cells treated with auxin for 96h and stained with OCT4. **H.** Immunofluorescence of PGCLCs day 1 of MGA-AID cells +/- auxin after 24h. Cells were stained for GFP-BLIMP1, PGC marker, and MGA.

Supplementary Figure 6

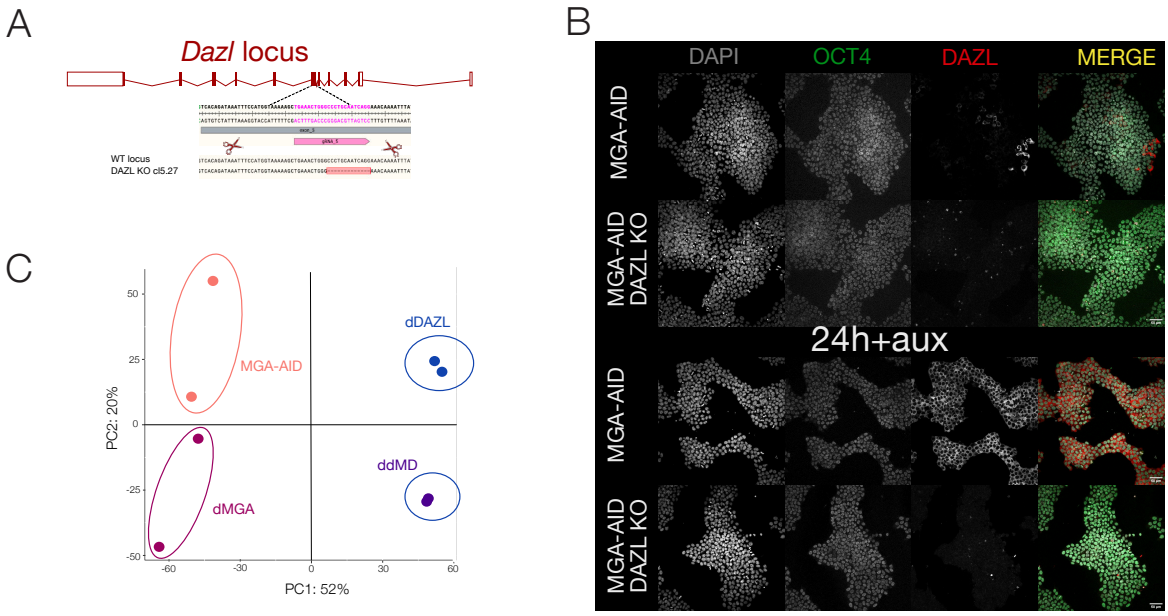

Supplementary Figure 6. DAZL knockdown in MGA-AID cells. A. Schematic representation of DAZL coding sequence indicating the gRNA used for DAZL knockdown. **B.** Validation of DAZL knockdown via immunofluorescence in the presence of auxin. The positive clone for DAZL knockdown did not show any DAZL expression after adding auxin. **C.** PCA plot of RNA-seq comparing the transcriptome of PGCLCs at day 6 from MGA-AID, dMGA (without MGA), dDAZL (without DAZL), and ddMD (without both DAZL and MGA) cells.

Chapter II - Structure and function of DUF4801 domain of MGA

In this manuscript, we investigated the role of the DUF4801 domain of MGA. Given that MGA has been identified as essential in promoting PGCs, we were interested in understanding the functional properties of the DUF4801 domain, which have not been fully studied. To this end, we utilized structural prediction tools and genetic approaches to explore the structure and function of this domain in the context of PGC differentiation.

Authors

Erica Calabrese, Ufuk Günesdogan

Status

Preliminary results that require more additional experiments to validate the major finding

My contributions

- Contribution to the conceptualisation of the project[1]
- Preparation and conduction experiments
- Preparation or modification of figures
- Data analysis

[1] Together with Dr. Ufuk Günesdogan

Title: **Structure and function of DUF4801 domain of MGA**

Authors: E. Calabrese[1], U. Günesdogan[1,3,*]

Affiliations:

[1] University of Göttingen, Göttingen Center for Molecular Biosciences, Department of Developmental Biology; Justus-von-Liebig Weg 11, 37077 Göttingen, Germany

[3] Max Planck Institute for Multidisciplinary Sciences, Department for Molecular Developmental Biology; Am Fassberg 11, 37077 Göttingen, Germany

[*] Corresponding author: ufuk.guenesdogan@uni-goettingen.de

Abstract

The transcriptional MAX-giant associate protein (MGA) contains a domain that has not been thoroughly characterized- the domain of unknown function 4801 (DUF4801). In this study, using the HHpred tool, we predicted the structural properties of this domain and identified the presence of two unknown zinc fingers, suggesting new protein-, RNA-, and DNA-binding capabilities of MGA. To investigate the role of the DUF4801 domain, we deleted it and examined its effect during the differentiation of mouse primordial germ cell-like cells (PGCLCs) *in vitro*. Our results show that deleting the DUF4801 domain affects MGA's canonical binding sites, resulting in the loss and gain of genes involved in neurogenesis and endoderm fate. These changes in gene expression are evident in the transcriptome of PGCLCs, although no severe phenotype was observed. This could be attributed to the weakened binding of MGA to DNA. Overall, our findings demonstrate that the deletion of the DUF4801 domain alters the genome-wide DNA binding and transcriptional profile of MGA.

Introduction

The driving force determining proteins' functional and structural properties derives from a small unit of 30-100 amino acids defined as a domain (Janin and Wodak 1983). Typically, most proteins contain one or several domains, indicating a significant complexity in their function and evolution (Dawson et al. 2017). To track down their functions, computational methods based on the sequence-based domain concept classify different proteins based on their homology regions (Y. Wang et al. 2021). Despite identifying many protein domains with putative functions (*e.g.*, helix-turn-helix domain, T-box domain, methyltransferase-like domain), more than 3000 domains still lack confirmed functions and are known as domains of unknown function (DUFs) (Bateman, Coggill, and Finn 2010). Since their first classification a decade ago, many studies have explored the functions of DUFs in bacteria and plants, but only a few in mammalian cells. In mammals, DUF domains are mainly involved in binding RNA and DNA or mediating protein interactions (Burgute et al. 2014; Huang et al. 2020; H. Wang et al. 2014; Al Chiblak et al. 2019).

One transcription factor characterized by the presence of the DUF4801 domain is the MAX giant-associated (MGA) protein (Mathsyaraja et al. 2021). According to its characterized domains, MGA is a member of two highly conserved families of transcription factors: MAX interacting proteins (bHLH/zip domain) and the T-box family (T-box domain) (Hurlin et al., 1999). Moreover, structural studies have reported its belonging to the non-canonical Polycomb repress complex 1.6, PRC1.6, based on its interaction with different proteins (Gao et al. 2012). Therefore, MGA has been studied in various biological processes, such as mouse embryonic stem cell development, germ cell development, and crucially, tumour progression (Stielow et al. 2018; Washkowitz et al. 2015; Burn et al. 2018; Qin et al. 2021; Mochizuki et al. 2021; Mathsyaraja et al. 2021). While previous studies have dissected the activity of MGA's DNA-binding domains in gene expression regulation during development (Uranishi et al. 2021), the DUF4801 domain was only suggested as a mediator of protein interaction in lung cancer cells (Mathsyaraja et al. 2021). However, a recent publication has suggested the DUF4801 domain as a DNA-chromatin binding region, opening up a potential transcriptional role never investigated before (Rafiee et al. 2021).

As MGA is known to play a crucial role during the early development in dynamically regulate the expression of cell-type-specific genes, including pluripotency, meiotic, and germ genes, we utilized mouse primordial germ cell-like cells (PGCLCs) as an *in vitro* differentiation model system (Hayashi et al. 2011). In particular, we focused how the deletion of the DUF4801 domain influences MGA binding sites, which are critical for the transcriptional regulation of genes involved in PGCLC differentiation. By analyzing MGA binding sites, we determined which genes are directly regulated by DUF4801 domain and how it influences their regulation. Our research aims to provide insights into the specific mechanisms by which MGA and its DUF4801 domain regulate gene expression during PGCLC differentiation.

Results

Analysis of DUF4801 structure

To comprehensively understand the role of the DUF4801 domain, we first started by characterizing its structure. The DUF4801 domain is a conserved region of MGA protein located between amino acids (aa) 1040-1080. To predict the structure of DUF4801 domain, we relied on its primary sequence and its homology with known proteins. We used the HHpred tool to predict the structure, which listed MGA with a probability of 99.5% as its exclusive domain. However, the DUF4801-MGA alignment showed the same arrangements of cysteins, CxxxxCxxxCxC, indicating the presence of two zinc fingers of the same unknown type that could suggest its ability to bind DNA, RNA, or protein (Fig. 1A). We also found that part of this region has structural similarity with the CCCH zinc finger domain of the RNA-binding protein ZC3H14, which is known to bind RNA and regulate RNA metabolism primarily involved in neurogenesis (Rha et al. 2017; Morris and Corbett 2018, 3) with a probability of 37% (Supplementary Fig. 1A). Furthermore, we used the AlphaFold2 structural modelling tool to confirm the presence of the only predicted helix, which had high confidence. However, the confidence in other predicted regions was very low (Fig. 1B).

By using these structural hunting strategies, we were able to gain insights into the structure of DUF4801 domain, which opens up avenues for further characterization of this domain and its possible functions. based on its sequence.

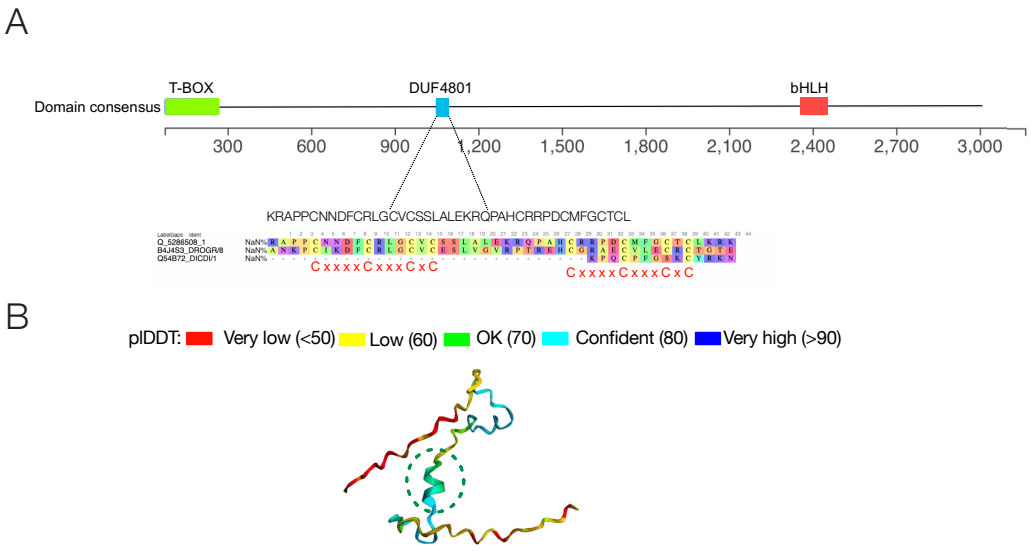

Figure1. Summary of DUF4801 domain. **A**. Overall structure of MGA protein, including a schematic alignment of DUF4801 domain based on HHpred result. The corresponding HHpred alignment of the DUF4801 domain shows a high structural homology with CCCH zinc finger domain, with the arrangement of cysteins highlighted red. **B**. Alphold2 structure prediction of DUF4801 domain with highlight of predicted helix.

Deletion of DUF4801 domain influenced MGA binding sites and gene expression in ESCs

To characterize the functional activity of the DUF4801 domain, we utilized CRISPR/Cas9 system to delete its coding sequence and produce a truncated MGA ΔDUF4801 protein in ESCs. We validated the excision of the target region using PCR followed by Sanger sequencing in two clones, referred to as ΔDUF4801-cl8 and ΔDUF4801-cl16 (Supplementary Fig. 1B). The absence of this domain did not affect MGA protein expression, as demonstrated by staining and western blot (Supplementary Fig. 1C-D).

Considering its potential role as a DNA-chromatin binder (Rafiee et al. 2021) and its structural properties, we investigated whether its deletion could impact MGA binding sites. Thus, we performed a CUT&RUN analysis on ΔDUF4801 clones in ESCs and compared them to the wild-type. Our analysis of the binding sites revealed that the deletion of DUF4801 domain caused MGA to bind more promoter regions, with a frequency of 49.2% compared to 37.7% in the wild-type (Fig. 2A). Although MGA still bound a large subset of genes in DUF4801 cells, it lost 4000 genes and gained 2000 genes, primarily in the promoter regions (Fig. 2B). Indeed, heatmaps of MGA binding loci from wild-type and ΔDUF4801 cells, partitioned into 4 distinct clusters, showed gained peaks of ΔDUF4801 cells in cluster 2 (Fig. 2C).
Gene ontology analysis on unique MGA peaks in ΔDUF4801 cells revealed that most genes were associated to *tissue development*. We found genes linked to *endoderm fate*, such as *Sox17, Sox2, Tbx21*, and *Pou6f1*, and to *neurogenesis*, such as *Creb1* and *Gabra4* (Fig. 2D, Supplementary Fig. 2A-B). Interestingly, MGA lost binding sites in some target genes known to play an important role in pluripotency, such as *Dppa5a* and *Prdm14*, as also shown by the L2 database (Supplementary Fig. 2C-2D).

Based on that, we conducted RNA-seq analysis to investigate the effect of the absence of the DUF4801 domain on gene expression in ESCs and to correlate the binding sites changes. The analysis revealed that the absence of the DUF4801 domain led to the significant upregulation of 97 genes and downregulation of 261 genes (Fig. 2E). The high number of downregulated genes suggests that the domain may act as a transcriptional activator. GO analysis showed that *negative regulation of ERK1 and ERK2 cascade*, such as *Dusp6, Chrna9, Dynlt1b*, and *histone H3 acetylation*, as *Lef1, Dmrtc2, Sumo2* related terms were significantly enriched among upregulated genes, while downregulated genes were linked to *tube morphogenesis,* such as *Stra6, Hoxa5, and Itga5* genes, and *cell adhesion* terms such as *Dsp, Fat2, Cebpb* (Supplementary Fig. 2F-H). These results indicate that the DUF4801 domain controls different signalling pathways.

We also checked the expression of unique genes bound in ΔDUF4801 cells. Although many of them were not significant in the differentially expressed genes (DEGs) analysis, they showed lower expression than in the wild-type cells. However, genes related to endoderm fate and neurogenesis, already downregulated in ESCs to maintain the pluripotency state, showed an even more significant reduction in absence of DUF4801

domain. When we compared the DEG list with the CUT&RUN binding sites, we found that only half of the genes were directly influenced by the DUF4801 domain suggesting that change in gene expression may depend on a secondary effect relate to change of MGA structure (Fig. 2G).

Taken together, these data showed for the first time how DUF4801 domain is important to bind specific regions, and how its deletion destabilizes canonical MGA binding sites leading to influence several genes' expression in ESCs.

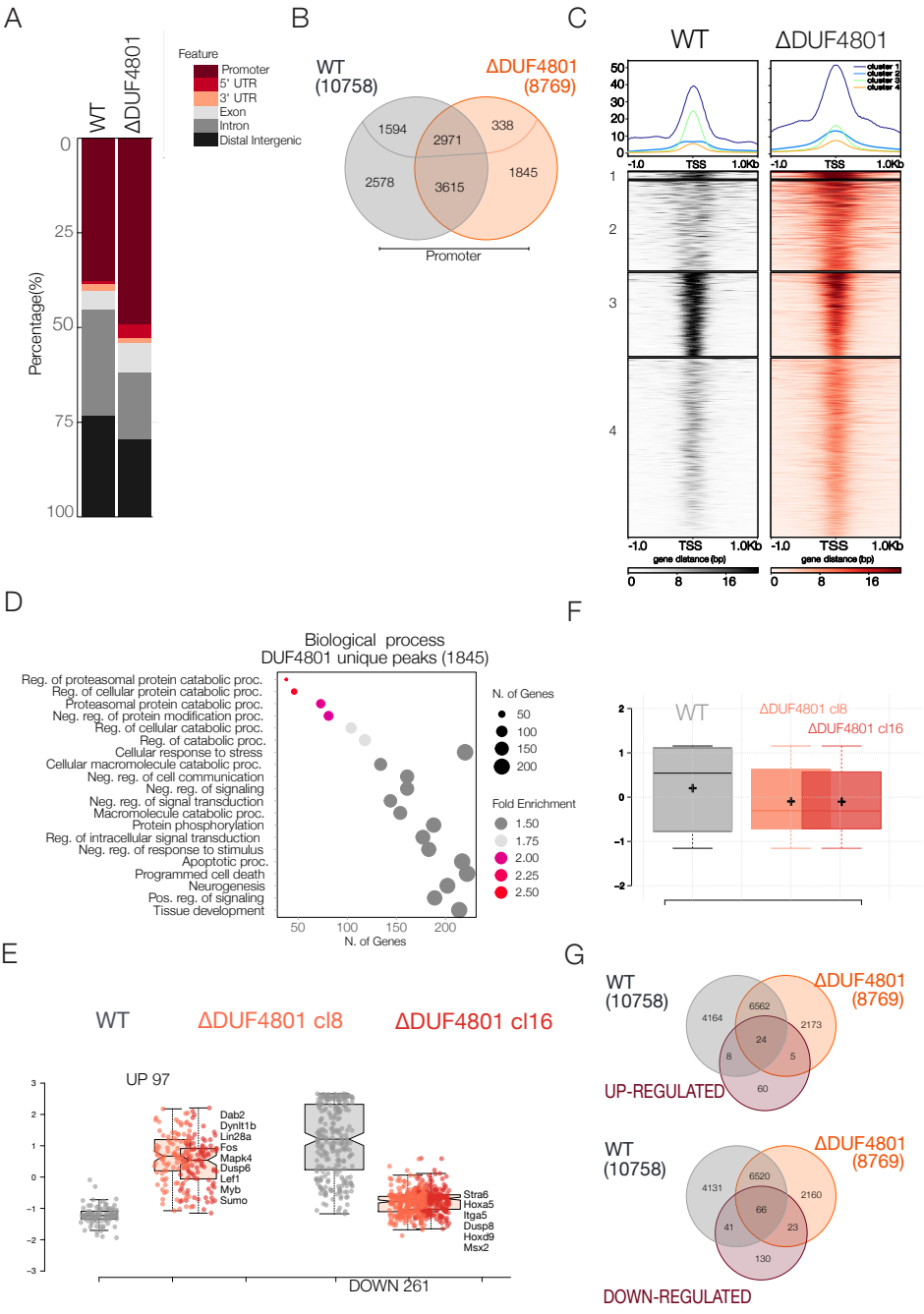

Figure 2. ΔDUF4801 influences MGA binding sites and gene expression in ESCs. A. Genomic distribution of MGA wild-type and ΔDUF4801 peaks in the genome. Promoters are defined as the region around ±1 kb from mm10-annotated TSS. **B.** Overlap of

genes associated with the region bound by MGA wild-type and ΔDUF4801 cells, highlighting those bound in the promoter region, shows 6,586 genes shared, 4,172 lost after deletion, and 2,183 gained genes. **C.** Heatmap analysis of MGA bound loci in wild-type and ΔDUF4801 over ±1 kb around the TSS. Peaks are separated into four clusters by k-means clustering. Profile plots (top panel) show the average signals per each cluster, highlighting cluster 2 as the one with the most difference. **D.** GO analysis for biological processes associated with genes bound only in the ΔDUF4801 clones in the promoter region. **E.** Boxplot showing significantly DEGs in both clones ΔDUF4801, cl8, and cl16, compared to wild-type in ESCs. Data points are shown using a jittered plot. Important genes are highlighted. **F.** Boxplot showing the expression levels of 2,160 unique genes bound in the ΔDUF4801 cells compared to wild-type. Medians are represented by the + symbol. **G.** Venn diagrams of DEGs, up and downregulated, intersected with MGA binding sites in ΔDUF4801 cells and wild-type.

ΔDUF4801 in PGCLCs affect the transcriptome but not the phenotype

Since ΔDUF4801 cells were generated from a transgenic ESC line harbouring a PGC-expressed reporter gene such as Blimp1-mEGFP (Ohinata et al. 2005), we evaluated how the deletion influenced PGCLC differentiation. Firstly, EpiLCs and PGCLCs did not present any abnormalities in their morphology. Indeed, quantification of Blimp1+ cells of ΔDUF4801 clones at day 6 of PGCLC differentiation, evaluated by fluorescence-activated cell sorting (FACS), showed no significant difference compared to wild-type cells (Fig. 3A). However, we did not exclude changes in gene expression during PGCLC differentiation. Therefore, we performed RNA-seq experiments in ΔDUF4801-cl8, ΔDUF4801-cl16, and wild-type cells in EpiLCs and d6 PGCLCs.

Interestingly, integrating the data from ESCs, principal components analysis (PCA) from RNA-seq profiles showed that ΔDUF4801 cells in ESCs and EpiLCs clustered closely with wild-type while in PGCLCs diverged (Fig. 3B). However, analysis of cell-type-specific genes showed no changes in PGC markers, as for other cell-type-specific genes for ESCs and EpiLCs, confirming the morphology of cells and FACS data. Nevertheless, these data indicated that changes in the transcriptome were related to the misregulated gene expression of other classes of genes (Fig. 3C). DEGs in EpiLCs showed the same number (59) of up and downregulated genes, respectively. In PGCLCs, we found 150 high-express genes and 250 down-expressed genes (Fig. 3D). Overlap of DEGs showed a larger number of exclusive genes per each cell type, indicating that the DUF4801 domain has different targets during PGC differentiation. This finding was confirmed by the comparison of GO terms in each cell type (Supplementary Fig. 2E-G). Interestingly, a higher number of down-regulated genes in PGCLCs boosted our hypothesis of the DUF4801 domain as a potential transcriptional activator. Closer inspection of ΔDUF4801 PGCLCs revealed up-regulation of meiotic genes, such as *Ddx4*, *Mov10l1, Sycp3,* and *Hormad2*. Notably, transcriptional regulation of this class of genes has always been attributed to MGA canonical domains in ESCs (Uranishi et al. 2021; Mochizuki et al. 2021). Therefore, this result might indicate a dynamic regulation of these genes during PGC differentiation involving different MGA domains. By contrast, down-regulated genes, such as *Wnt8a*, *Brd9*, and *Tfap2a*, are linked to GO terms, such as *skeletal system development*.

We then assessed whether other transcriptional regulators could control the DEGs in PGCLCs. To this end, we used the DEG list and looked for putative transcription factors that were enriched using in silico ChIP

analysis of public ChIP-seq datasets from various mouse cell types, using the ChEA 2022 database. In up-regulated genes, we found enrichment for transcription factors such as SUZ12 and EZH2, which are part of the PRC2 complex, as well as the zinc finger protein EGR1 (ZNF268) and SOX17. Different proteins targeted other down-regulated genes, such as ZFp281, YY1, and DMTR1. Moreover, SETDB1, NANOG, and OCT4 were also listed, but with a lower fold-change (Supplementary Fig. 3).

However, only about 30 genes of the DEGs were considered potential targets for different transcription factors, which indicated that the rest of the genes were a direct consequence of the loss of the DUF4801 domain.

Our results indicate that the removal of just 40 amino acids from the MGA protein leads to significant changes in gene expression during PGCLC differentiation. Despite this, we observed that the cells did not exhibit severe phenotypic effects, suggesting that the deletion did not affect essential genes. Additionally, the fact that other factors controlled only a small fraction of the differentially expressed genes suggests that the absence of a severe mutant phenotype did not arise from the loss of interaction partners.

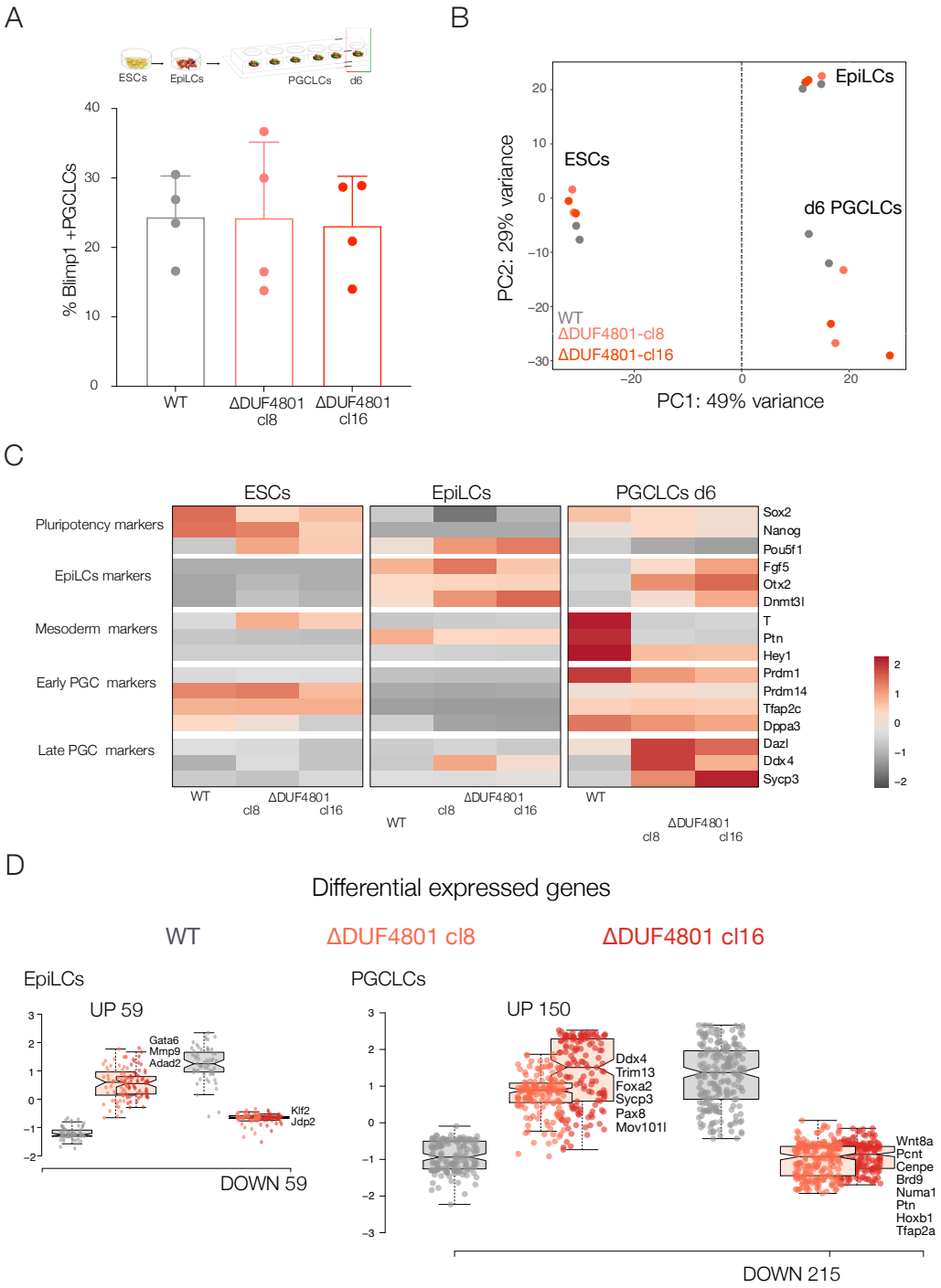

Figure 2. ΔDUF4801 influences gene expression in PGCLCs. A. FACS results of ΔDUF4801 cells compared to wild-type cells show no changes in the quantification of BLIMP1+ cells in independent replicates. A scheme of PGCLC differentiation is shown, highlighting d6 PGCLCs (top panel). **B**. PCA plot of RNA-seq data generated from ESCs, EpiLCs, and d6 PGCLCs. **C** Heatmap showing changes in the mean expression profile of selected genes from duplicate independent WT, ΔDUF4801 cl8, and cl16 during PGCLC induction by RNA-seq. **D.** Boxplot showing significantly DEGs in both ΔDUF4801 clones, cl8 and cl16, compared to wild-type cells in EpiLCs and PGCLCs. Data points are shown using a jittered plot. Some of the important genes are highlighted.

Discussion

Transcription factors are known to play a primary role in driving gene expression in specific cell types and developmental patterns. It is therefore paramount to identify the different domains that compose these factors in order to elucidate their function in orchestrating different expression programs (Lambert et al. 2018). Different computational approaches have been established over the last few decades to predict protein domains and their putative functions based on sequence homology or their structure (Y. Wang et al. 2021). Among these, the conserved protein domain of unknown function (DUF) has not been extensively characterized yet. In this study, we examined the DUF4801 domain, which is part of the transcription factor MGA, to provide insight into its role during PGC differentiation.

Deletion of the DUF4801 domain in ESCs, using CRISPR/Cas9, revealed that its absence affects MGA binding sites and several gene expressions. CUT&RUN data showed that the MGA without DUF4801 domain lost known target genes such as pluripotency genes and bound to new DNA sequences of genes involved in endoderm fate and neurogenesis. Even though these genes are down-regulated in the wild-type to maintain pluripotency, their expression levels are even lower in the absence of DUF4801 domain.

As MGA is a member of the PRC1.6 complex, it is possible that a change in its structure can also affect other members of this complex, as MGA functions as a scaffold protein (Qin et al. 2021; Mathsyaraja et al. 2021). Furthermore, such structural changes may lead to counteracted transcription initiation. Previous studies have shown that Polycomb target genes are expressed at low levels, implying that Polycomb members primarily regulate transcription burst frequency rather than block it (Paula Dobrinić et al. 2021).

Therefore, the new binding of MGA to these target regions may further compromise their transcription.

The intersection of MGA binding sites, from wild-type and ΔDUF4801 condition, with DEGs in ESCs revealed that only a fraction of these genes was directly influenced by MGA due to loss of binding sites, reduction of DNA-binding affinity, or gained binding. The remaining genes were affected by the change in MGA structural properties. Indeed, our structural analysis of the DUF4801 domain predicted that the amino acid residues are characterized by a repetitive cysteine sequence, indicating the presence of two novel Zinc fingers. As well-known, Zinc finger proteins are mainly involved in transcriptional and post-transcriptional regulation interacting through DNA, RNA and other proteins. Therefore, we cannot exclude that change in the binding site and gene expression could indicate its function as a DNA-binding domain or as a scaffold to support MGA binding to the DNA or as an interaction domain.

In this study, we also investigated how ΔDUF4801 influences PGCLC differentiation. We found changes in gene expression, with a high number of down-regulated genes mostly involved in different developmental processes. Interestingly, we observed up-regulation of meiotic genes known to be directly controlled by T-box and bHHL/zip domains in ESCs (Uranishi et al. 2021; Mochizuki et al. 2021). This data might indicate cooperation between MGA domains in repressing these genes, or that the absence of the DUF4801 domain allows MGA canonical domains to bind less tightly, leading to increased expression. However, genes directly

involved in the induction of PGC differentiation were not found to be deregulated, and the phenotype did not present any abnormalities. Moreover, we investigated whether other transcription factors could regulate DEGs in PGCLCs, but we found only a small fraction of genes enriched for members of the PRC2 complex or pluripotency factors, reinforcing the idea that observed gene expression changes are related to the change in MGA structure

In summary, our findings expand previous studies on the role of the DUF4801 domain, showing changes in MGA binding sites and gene expression during PGCLC differentiation for the first time. Moreover, these data suggest that MGA is an even more unique and complicated transcription factor, controlling different biological processes. Therefore, future studies are needed to address the molecular mechanism that drives the action of the DUF4801 domain.

Material and methods

Structural bioinformatics

The putative structural and functional features of the DUF4801 domain of MGA were identified by analyzing its amino acid sequence for remote protein homology. This was done using the HHPred web server (Soding, Biegert, and Lupas 2005) available through the MPI Bioinformatics Tool kit https://toolkit.tuebingen.mpg.de/tools/hhpred (Zimmermann et al. 2018) and PSI-Blast tool (EMBL) (Madeira et al. 2022). Additionally, AlphaFold (Jumper et al. 2021) generated a three-dimensional model using a high accuracy structure prediction method in the ColabFold notebook (Mirdita et al. 2022).

Cell culture

Mouse embryonic stem cells were cultured in N2B27 supplemented with 2i/LIF. N2B27 medium was prepared by combining 50% Neurobasal and 50% DMEM/F12, along with 1% B27, 0.5% N2, 2 mM L-glutamine, 1x Pen/strep, and 0.1 mM 2-mercaptoethanol. These cells were grown on dishes that were treated with 0.1% gelatin for 10 minutes.

Epiblast-like cells (EpiLCs) were cultured in N2B27 medium supplemented with 1% KnockOut Serum Replacement, FGF2 (12 ng/ml), and ActivinA (20 ng/ml). They were grown on dishes coated with Fibronectin in PBS for 30 minutes at room temperature.

PGCLCs (Primordial Germ Cell Like-Cells) were cultured in GK15 medium supplemented with BMP4 (500 ng/ml), LIF (1000 U/ml), SCF (100 ng/ml), BMP8a (500 ng/ml), and EGF (50 ng/ml). They were cultured in ultra-low cell attachment U-bottom 96-well plates at 3000 cells per well (Corning) or in six-well AggreWell 400 plates at 1.5 x 106 cells per well (STEMCELL Technologies). PGCLCs were obtained using a cell line carrying the fluorescent reporter Blimp1-mEGFP, which was previously established (Ohinata et al. 2005). Cells were dissociated into a single-cell suspension using 3% fetal bovine serum in PBS. PGCLCs were then sorted based on Blimp1-mEGFP fluorescence using the FACS (fluorescent-activated cell sorting) Sony SH800 and collected for further analysis (RNA-seq). The data was analyzed using FlowJo software.

Generation of DUF4801 domain deletion in mESCs

The CRISPR/Cas9 was used to delete the DUF4801 domain of MGA, and the respective gRNA were designed using Benchling. We designed two gRNAs to target the DUF4801 region as follows:

FW gRNA1	CACCGTCGACGGCAGTGAGCAGGT
REV gRNA1	AAACACCTGCTCACTGCCGTCGAC

FW gRNA2	CACCGCAACAATGACTTCTGTCGCC
REV gRNA2	AAACGGCGACAGAAGTCATTGTTGC

Then, oligos were annealed and ligate in pSpCas9(BB)-2A-Puro (PX459) V2.0 was a gift from Feng Zhang (Adgene plasmid # 62988, http://n2t.net/addgene:62988; RRID:Addgene 62988).
mESCs were transfected with the plasmid using Lipofectamine 2000 (Invitrogen) and selected with puromycin (1ug/ml) for 48h. We then expanded the cells and picked single colonies. Deletion was evaluated by PCR and Sanger sequencing. We generated two different clones, named cl8 and cl16.

CU&RUN sequencing and analysis

For each experiment, 500,000 cells were used and performed per clone (cl8 and cl16) in duplicate. CUT&RUN, a targeted in situ genome-wide profiling technique, was performed following protocol version 1 https://www.protocols.io/view/cut-run-targeted-in-situ-genome-wide-profiling-wit-14egnr4ql5dy/v1?version_warning=no (Skene and Henikoff 2017). DNA was used as input for library preparation, which was performed using the NEB Next Ultra II Library Prep Kit (NEB) following the modification suggested in a publication (https://dx.doi.org/10.17504/protocols.io.bagaibse) to analyze transcription factor profiles. The final samples were sequenced as 100 bp paired-end reads on an Illumina Nova Seq 6000 at the Sequencing Core Facility (Max Planck Institute for Molecular Genetics, Berlin, Germany).

Libraries were then analysed using the standard CUT&RUN pipeline. Peaks were called using MACS2. Genomic annotation was performed on merged consensus peaks of biological replicates using the ChIPseeker R package (Yu, Wang, and He 2015). Heatmaps were generated using the merged bigwig files obtained using Samtools merge and then Deeptools bam-Coverage (Ramírez et al. 2016).

Gene ontology was performed on selected peaks using the web tool ShinyGO 0.76.2 (http://bioinformatics.sdstate.edu/go/) with standard parameters. InteractiVenn (http://www.interactivenn.net) was used to generate a Venn diagram, and IGV was used to generate gene coverage (Thorvaldsdottir, Robinson, and Mesirov 2013).

RNA-sequencing procedure and analysis

To perform RNA sequencing, we used two independent cultures of ESCs, EpiLCs, and PGCLCs from day 6 of both the ΔDUF4801 cl8 and clone 16, as well as wild-type cells. Total RNA was extracted using the RNeasy Mini Kit (Qiagen) and evaluated for quality using RNA ScreenTape (Agilent). We generated libraries using RNA and the NEBNext® Ultra™ II Directional RNA Library Prep Kit for Illumina (NEB), and then sequenced the

samples as 100bp single/paired-end reads on the Illumina Nova Seq 6000 at the Sequencing Core Facility (Max Planck Institute for Molecular Genetics, Berlin, Germany).

We aligned the RNA sequencing reads to the mouse reference (GRCm38/mm10) using STAR (Dobin et al. 2013) and obtained mRNA read counts per genes using HTseq-count (Anders, Pyl, and Huber 2015). To identify differentially expressed genes, we performed normalization and pairwise comparison using DESeq2 (fold change >1.5, adjusted p-value < 0.05).

We then used various tools to complete further analysis: we used pheatmap to generate heatmaps in R, BoxPlotR (http://shiny.chemgrid.org/boxplotr/) to create boxplots, and GO analysis was conducted using (http://metascape.org/gp/index.html).

Immunofluorescence staining

Immunofluorescence staining was performed as follows. Cells growing on round slides were fixed in 4% paraformaldehyde for 30 minutes, washed three times with PBS, and permeabilized with 0.2% Triton X-100 and 3% BSA for 30 minutes at room temperature. The cells were then incubated overnight with anti-MGA antibody (Abcam EPR19854). The next day, after washing with PBS, the secondary antibody (Alexa Fluor 555 anti-rabbit) was applied for 1 hour. Subsequently, DAPI was applied for 20 minutes, and the coverslips were mounted on slides. The slides were analysed using a Zeiss confocal LSM980 microscope, and the images were processed using Fiji software.

Western Blot

Cells were lysed on ice using 50 mM Tris-HCl (pH 7.5), 150 mM NaCl, 1% SDS, 0.5% NaDeoxycholate, and 1× Complete protease inhibitor cocktail. Whole-cell extracts were resolved by 4-12% SDS-PAGE and transferred to 0.45 µM nitrocellulose membranes at 60V for 4 hours in a cold room. The membranes were then probed with the following antibodies: anti-MGA (Abcam EPR19854) and Alpha Tubulin (Proteintech 66031-1).

Supplementary Figure 1

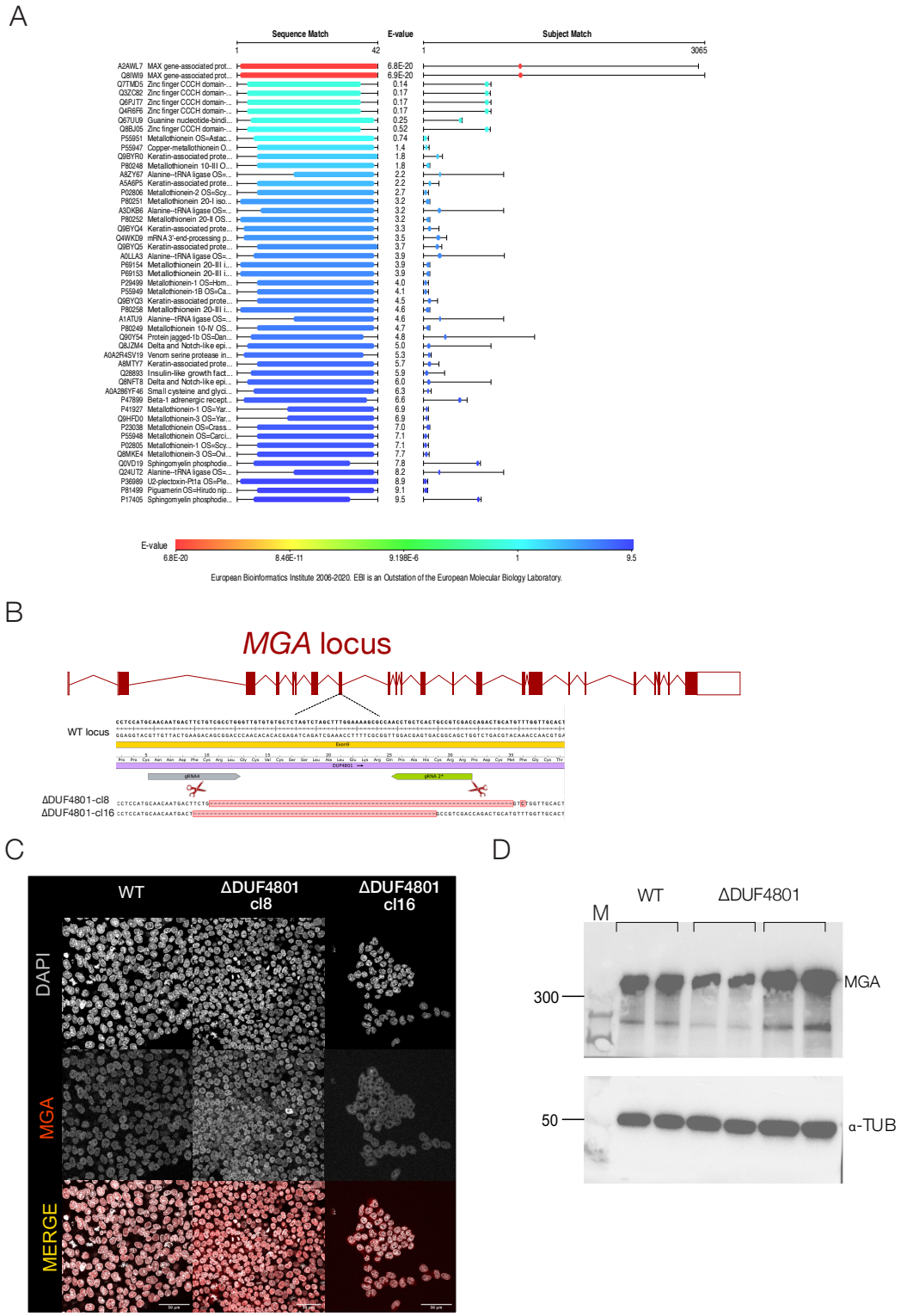

Supplementary Figure 1. Sequence homology and verification of DUF4801 domain deletion. A. Sequence alignment of DUF4801 domain to different protein sequences, showing the protein with the highest similarity to the DUF4801 domain. In contrast, subject match shows the position of the domain in the respective proteins. **B** Position of DUF4801 domain in the MGA coding sequence, highlighting the position of the two gRNAs used to delete this region and generating two different clones, cl8 and cl16. **C-D.** No change in MGA protein expression was observed after the deletion of DUF4801 compared to wild-type in ESCs. Staining in ESCs (**C**) and Western blot (**D**). Each clone and wild-type were loaded twice, and α-tubulin was used as a loading control.

Supplementary Figure 2

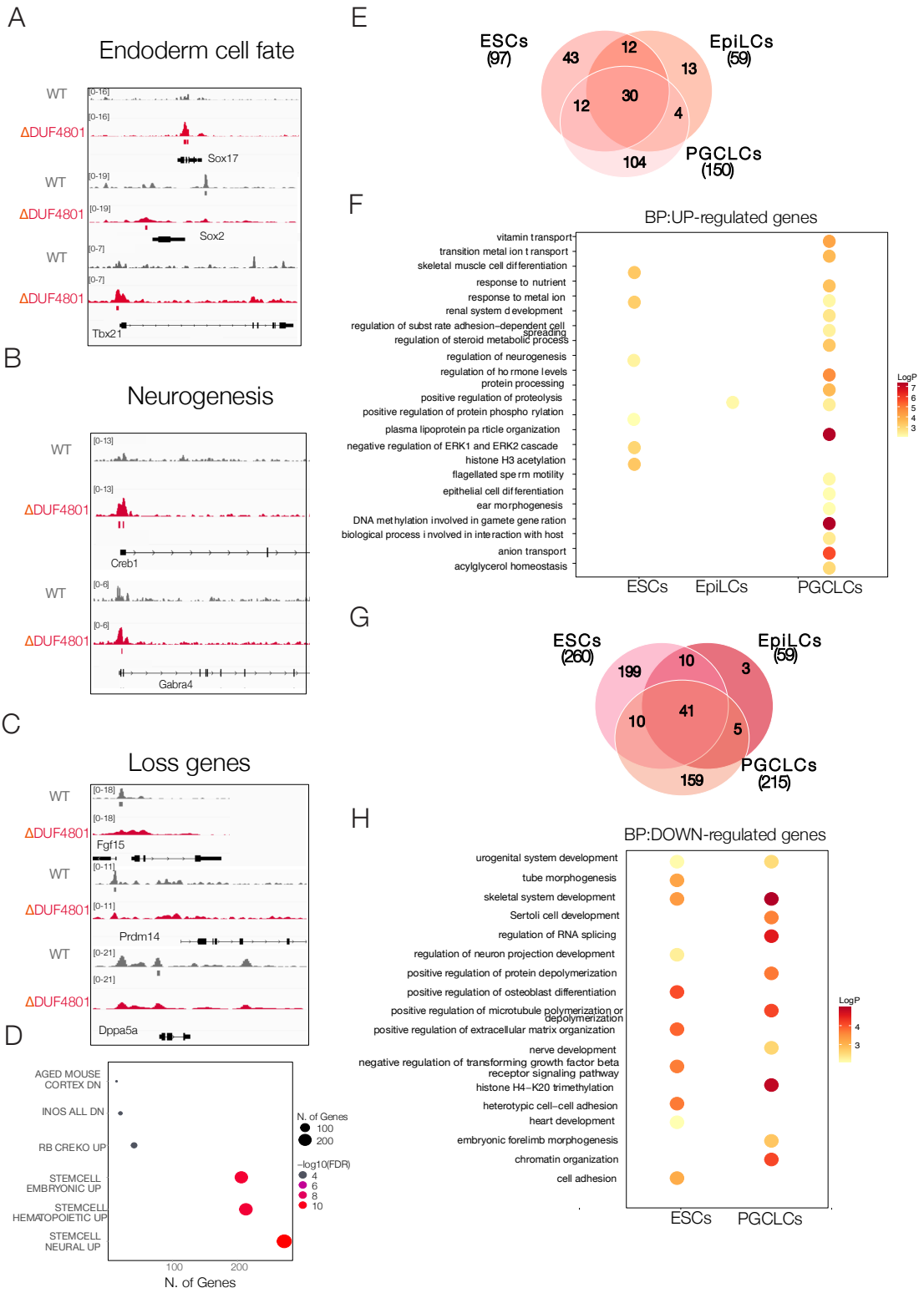

Supplementary Figure 2. Deletion of DUF4801 domain alters binding sites and gene expression in ESCs. A-B-C. CUT&RUN coverage tracks of wild-type and ΔDUF4801 for endoderm genes (**A**), neurogenesis genes (**B**), and genes with lost binding in DUF4801 cells. Tracks represent the merging of three replicates for wild-type and two clones for DUF4801 cells. **D.** GO analysis of lost genes using the L2L database compared to differentially expressed genes from public data. **E.** Overlap of up-regulated genes between ESCs, EpiLCs, and PGCLCs in ΔDUF4801 cells. **F.** Comparison of GO terms associated with each up-regulated DEG per cell type. **G.** Overlap of down-regulated genes between ESCs, EpiLCs, and PGCLCs in ΔDUF4801 cells. **H.** Comparison of GO terms associated with each down-regulated DEGs per cell type.

Supplementary Figure 3

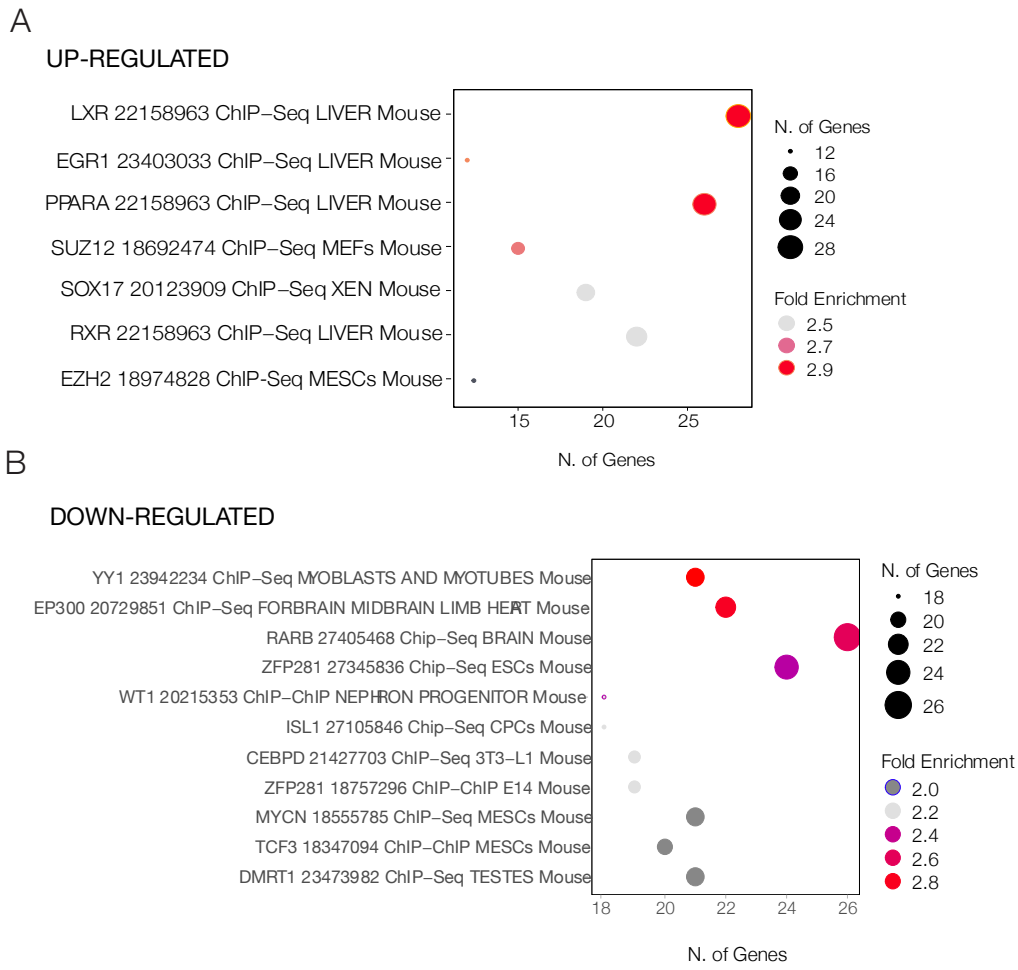

Supplementary Figure 3. The transcription factors that target the differentially expressed genes of PGCLCs ΔDUF4801. A. The dot plot demonstrates the enrichment of transcription factors for up-regulated genes. **B.** The dot plot shows the enrichment of transcription factors for down-regulated genes.

Discussion

One of the driving questions in developmental biology is how PGCs maintain their unique cell identity in an environment where mesodermal fate occurs. Up to date, we know that the influence of a temporally and spatially restricted expression of specific signalling pathways and transcription factors drives this cell fate decision. Despite these findings, the molecular mechanism governing PGC cell fate decision remains ill-defined, suggesting the presence of new factors that need to be characterized.

Here, we investigate the role of transcription factor MGA during PGC differentiation.

MGA is a unique transcription factor with complex structural properties, owning three heterotypic domains (T-box, bhLH/zip and DUF4801), and belonging to three families of proteins essential for the development such as T-box factors, MAX-interacting proteins and PRC1.6 complex (Hurlin et al., 1999; Gao et al. 2012). In early development, MGA is crucial for the survival of epiblast cells in the pre-and post-implantation of the embryo (Washkowitz et al. 2015). Given that these cells can generate all fetal cell lineage, it is reasonable to suggest that MGA may influence the development of multiple tissues and have a tissue-specific function.

However, all previous studies on MGA have focused exclusively on its role as a member of the PRC1.6 complex, acting to repress germ cell genes and safeguard pluripotency in ESCs (Stielow et al. 2018; Endoh et al. 2017; Qin et al. 2021; Burn et al. 2018).

On the other hand, this thesis aims to explore MGA's role during PGC differentiation by identifying its genomic binding sites and interactors partners and examining the functions of its two domains (T-box and DUF4801). Through a combination of genomic and proteomic characterization of MGA during ESCs differentiation to PGCCLs in vitro (Hayashi et al. 2011), we have made several key observations regarding MGA biology.

MGA acts as repressor of meiotic genes during PGCLC differentiation

Previous studies have only described the role of MGA as a repressor of meiotic genes in ESCs (Stielow et al. 2018; Endoh et al. 2017). In our study, we found that the role of MGA as a repressor of germ cell genes during PGC differentiation, with the assistance of the PRC1.6 complex. Germline genes, such as *Dazl, Ddx4, Mael*, and *Mov10l1*, are expressed during the late stage of PGCs when epigenetic reprogramming occurs at E9.5 (Hackett et al. 2012). Therefore, strict temporal regulation of these genes is necessary for normal development, as the premature expression can lead to a precocious meiosis pathway deleterious for the cells (Yokobayashi et al. 2013; Hargan-Calvopina et al. 2016). Our data extends the function of MGA as a repressor of these genes also to EpiLCs and PGCLCs stage. We employed an auxin-inducible degron system

and observed significant up-regulation of meiotic genes after performing a time course MGA depletion during PGCLC differentiation.

By integrating the up-regulated genes with our analysis of MGA binding sites obtained through CUT&RUN experiments, we demonstrated that MGA binds to their promoter regions. However, in PGCLCs, we found that only half of the genes were directly targeted by MGA, indicating that their overexpression was due to the loss of MGA interactors. We found a higher frequency of E2F6 motif in MGA binding sites, which we confirmed by finding co-occupancy of E2F6 on these sites, a relation previously described only in ESCs (Dahlet, Truss, Frede, Adhami, et al. 2021). Our analysis of MGA interactome during PGCLC differentiation indicated the constant presence of PRC1.6 members and auxiliary proteins such as ATF7ip and SMARCA4. Interestingly, ATF7ip and SMARCA4 in MGA interactome during PGCLC differentiation gained our attention, suggesting cooperation with MGA and PRC1.6 members in repressing germline genes. Indeed, the absence of these two proteins resulted in higher expression of meiotic genes in ESCs (Maeda et al. 2013). In addition to its transcriptional regulatory function, ATF7ip has been found to interact with SETDB1, a histone methyltransferase, recently involved in the repression of germline genes in a combinatorial action with PRC1.6 complex during PGCLC differentiation (Mochizuki et al. 2021). The binding of MGA to germline gene promoters appears necessary for DNA methylation, highlighting the complex interplay among ATF7ip, SETDB1, PRC1.6, and MGA in regulating germline genes. Interestingly, this combination of proteins may form a new complex with the only function to repress meiotic genes, with MGA serving as a scaffold protein that tethers them together. Mechanistically, this role as a scaffold protein has been proposed for MGA only as part of the PRC1.6 complex, as its deletion resulted in a more severe phenotype and reduced expression of PRC1.6 members (Qin et al. 2021).

In summary, our findings have extended the role of MGA as a repressor of meiotic genes during PGCLC differentiation. MGA binds to their promoter regions along with PRC1.6 complex members, and its absence resulted in their derepression. The stable presence of PRC1.6 members, ATF7ip and SMARCA4 in MGA interactome during PGCLC differentiation suggests the possibility of a new complex, formed by MGA, specialized in repressing meiotic genes.

The dynamic interactome and genomic targets of MGA during PGCLC differentiation

Having described these stable interactors during PGCLC differentiation, we also found a context-dependent role of MGA sustained by an interactome and highly cell-type-specific genomic binding sites. The binding profile of MGA during PGCLC differentiation is highly dynamic, regulating genes involved in cell state transition. Interestingly, MGA has a dual function switching on and off specific genes following the differentiation of PGCLCs from ESCs. Changes in MGA interactome also contributed to this re-arrangement of MGA binding sites.

Therefore, following through the differentiation process, only in ESCs, MGA was linked to proteins involved in maintaining pluripotency, such as TEX10, ESRRB, SOX2 and OCT4. Even though OCT4 and SOX2 interaction with MGA was consistent with previous studies in ESCs (van den Berg et al. 2010; Buecker et al. 2014), it was interesting to find the presence of TEX10 and ESRRB proteins, recently indicated as part of the core pluripotency circuity (Ding et al. 2015; Martello et al. 2012). Therefore, we investigated how MGA establishes and maintains pluripotency by cooperating with these factors. Consistent with our CUT&RUN experiments in ESCs and previous ChIP-seq data (Galonska et al. 2015), we demonstrated that SOX2, NANOG and OCT4 occupied a higher number of MGA target genes involved in ESC differentiation towards EpiLCs. These data were consistent with our discovery of the OCT4-SOX2 motif among MGA motifs with a frequency rate comparable to the canonical E-box motif. Accordingly, with their correlation, we showed that a more persistent depletion (96h) of MGA induced loss of OCT4 expression with growth defects of ESCs. This data adds another brick in sustaining MGA's role in maintaining pluripotency and orchestrating the expression of specific genes together with the principal core of this circuitry.

In EpiLCs, MGA's interactome enriched proteins involved in DNA methylation, such as DNMT1 and SETDB1. Recently, these proteins were linked with MAX in repressing germ cell genes in ESCs (Tatsumi et al. 2018). However, based on our findings, we cannot exclude that the presence of SETDB1 was indirectly linked with the presence of ATF7ip. Instead, DNMT1 was proposed to maintain epigenetic signatures on meiotic genes in EpiLCs with EED (Lowe et al. 2022). Therefore, MGA might recruit DNMT1 close to the promoter regions of germ cells to methylate, indicating an even more fine-tuning of these instruct signals.

Continuing with the differentiation, we found a broad spectrum of RNA-binding proteins characterizing MGA interactome, but only in PGCLCs. Enriching these proteins adds another layer of complexity to MGA biology, indicating its potential ability to control RNAs, which has not been investigated before. The nature of these interactions may be related to typical protein-protein interaction or binding of the same RNAs. Notably, we observed enrichment of DAZL, an RNA-binding protein, essential for PGC differentiation into gametes (Gill et al. 2011).To understand their interaction, we used the inducible depletion of MGA combined with CRISPR/Cas9 to simultaneously deplete both proteins and investigate their phenotype. Depletion of both proteins resulted in a reduced number of PGCLCs and a change in the transcriptome. However, this phenotype reflects a compensatory trend of both proteins' impairment alone, presenting two different phenotypes. Specifically, we observed higher expression of meiotic genes and a lower number of PGCLCs in the absence of MGA, while in the absence of DAZL, only misregulation of genes related to RNA pathways was observed.

Interestingly, we found that the expression of some meiotic genes, such as *Ddx4* and *Sycp3*, seems restored without both proteins. As DAZL represses their translation by binding their RNAs and we only observed their high expression in the absence of MGA, we attempted to speculate that the nature of their interaction was related to avoiding excessive translation of meiotic genes. However, it remains an open question which needs further investigation. In the future, it would be interesting to perform iCLIP on MGA to assess its direct

binding on RNA. Additionally, it would be valuable to define the interaction with other RNA-binding proteins found in the MGA interactome.

MGA induces PGC specification in a synergetic action with T-box factors

As previously mentioned, our primary focus regarding MGA was on its role in ensuring PGC specification. The discovery of an intricate network of proteins and dynamic binding sites of MGA involved in cell-type-specific gene programs reinforced the idea of its involvement in this cell fate decision.

The T-box factors have been implicated in various developmental processes, mainly in maintaining the mesodermal program (Papaioannou 2014a). Notably, one member, T, is also responsible for initiating PGC specification, as its downstream targets are two germline determinants, BLIMP1 and PRDM14 (Aramaki et al. 2013). As MGA belongs to this family of factors, the presence of the T-box domain as a sign of high similarity between these proteins could reflect similar modes of action and functional redundancy. Moreover, the expression of MGA, T and EOMES in the posterior epiblast, where PGC specification occurs, indicates a possible functional correlation (Papaioannou 2014a). Therefore, we correlated MGA binding sites with these proteins and showed an interplay of MGA with T and EOMES in controlling genes involved in PGC specification and maintaining cell identity as pluripotency or mesodermal genes. It is worth noting that MGA exclusively controls meiotic genes, suggesting the only clear distinction with the T-box factors.

Depletion of MGA during the transition from EpiLCs to PGCCLs resulted in impaired PGCLCs accompanied by derepression of meiotic genes and decreased expression of PGC markers such as *Nanog, Prdm1 and Prdm14*, which are direct targets of MGA. This supports the idea of their combinatorial action, as similar phenotypes were also observed in the absence of T and EOMES in this early stage of PGC (Aramaki et al. 2013; Senft et al. 2019).

To gain further insight, we deleted the T-box domain of MGA and focused on changes in the transcriptome during PGCLC differentiation. Even though it did not result in a severe phenotype as a reduced number of PGCCLs, we found a significant premature expression of cell-type specific genes, such as mesodermal and meiotic genes in ESCs, and PGC markers in EpiLCs. Moreover, the absence of the T-box domain promoted higher expression of T as a compensatory effect, as a similar result was found in the absence of EOMES (Senft et al. 2019). These findings support the idea of a synergetic action between MGA and T-box factors to ensure PGC specification, even though the enrichment of T-box factors in MGA interactome was not identified. Nevertheless, T-box factors have been recently connected with chromatin remodellers, i.e. demethylases and acetyltransferases, which regulate the permissiveness of the chromatin environment (Istaces et al. 2019; Beisaw et al. 2018).

In particular, SMARCA4, a stable component of MGA interactome, was previously linked to EOMES in controlling chromatin state (Istaces et al. 2019). Intriguingly, the accessibility of definitive endoderm

enhancers depends on the binding of T and EOMES (Tosic et al. 2019), indicating that ensuring germ layer segregation might depend on the asymmetry of the chromatin landscape.
In the future, it would be interesting to investigate how chromatin accessibility changes after deleting these factors during the cell state transition from epiblast to PGC and the nature of their interaction.
In summary, our data presented for the first time a relation between MGA and T-box factors establishing its role in PGC. We showed that MGA is essential to ensure PGC specification, regulating the expression of PGC genes such as *Prdm1 and Prdm14,* and how its absence led to impaired PGCLCs.

Functional properties of MGA DUF4801 domain

Having described the role of the T-box domain during PGCLC differentiation, we sought to assess the role of the DUF4801 MGA domain, which has been poorly understood in terms of its functional properties. While previous studies have suggested that it may play a role in protein interaction or DNA-chromatin binding, little is known about its specific functions (Mathsyaraja et al. 2021; Rafiee et al. 2020). To better understand its role, we utilized CRISPR/Cas9 to delete this domain and evaluated its effects on gene expression and MGA binding sites. Our findings revealed that deleting the DUF4801 domain altered the canonical MGA binding sites, resulting in the loss and acquisition of new target genes. Surprisingly, we also found that MGA was binding to regulatory regions of genes that were not expressed in ESCs, such as *Sox17* and *Sox2*, which are involved in endoderm development, and *Creb1* and *Gabra4*, which are involved in neurogenesis. Interestingly, the expression of these genes was even lower in the DUF4801-deleted cells compared to wild-type cells. Therefore, we hypothesize that the deletion of the DUF4801 domain may have influenced the structural properties of MGA, potentially impacting other members of the PRC1.6 complex. Additionally, previous research has shown that Polycomb members can counteract transcription initiation, regulating the burst frequency of transcription instead of blocking expression (Paula Dobrinić et al. 2021). This could potentially explain our findings.
To better understand the DUF4801 domain's functional role, it would be interesting to study how chromatin accessibility changes after its deletion, as this could explain changes in gene expression. However, the presence of two Zinc fingers of unknown type within the domain makes it challenging to determine its exact function. Further studies are therefore needed to elucidate the DUF4801 domain's precise role in gene regulation and protein interaction.

Literature

Abe, Kanae, Chie Naruse, Tomoaki Kato, Takumi Nishiuchi, Mitinori Saitou, and Masahide Asano. 2011. 'Loss of Heterochromatin Protein 1 Gamma Reduces the Number of Primordial Germ Cells via Impaired Cell Cycle Progression in Mice1'. *Biology of Reproduction* 85 (5): 1013–24. https://doi.org/10.1095/biolreprod.111.091512.

Afgan, Enis, Dannon Baker, Marius van den Beek, Daniel Blankenberg, Dave Bouvier, Martin Čech, John Chilton, et al. 2016. 'The Galaxy Platform for Accessible, Reproducible and Collaborative Biomedical Analyses: 2016 Update'. *Nucleic Acids Research* 44 (W1): W3–10. https://doi.org/10.1093/nar/gkw343.

Al Chiblak, Mohannad, Felix Steinbeck, Hans-Jürgen Thiesen, and Peter Lorenz. 2019. 'DUF3669, a "Domain of Unknown Function" within ZNF746 and ZNF777, Oligomerizes and Contributes to Transcriptional Repression'. *BMC Molecular and Cell Biology* 20 (1): 60. https://doi.org/10.1186/s12860-019-0243-y.

Amati, Bruno, Mary W. Brooks, Naomi Levy, Trevor D. Littlewood, Gerard I. Evan, and Hartmut Land. 1993. 'Oncogenic Activity of the C-Myc Protein Requires Dimerization with Max'. *Cell* 72 (2): 233–45. https://doi.org/10.1016/0092-8674(93)90663-B.

Ancelin, Katia, Ulrike C. Lange, Petra Hajkova, Robert Schneider, Andrew J. Bannister, Tony Kouzarides, and M. Azim Surani. 2006. 'Blimp1 Associates with Prmt5 and Directs Histone Arginine Methylation in Mouse Germ Cells'. *Nature Cell Biology* 8 (6): 623–30. https://doi.org/10.1038/ncb1413.

Anders, S., P. T. Pyl, and W. Huber. 2015. 'HTSeq--a Python Framework to Work with High-Throughput Sequencing Data'. *Bioinformatics* 31 (2): 166–69. https://doi.org/10.1093/bioinformatics/btu638.

Anderson, Ericka L., Andrew E. Baltus, Hermien L. Roepers-Gajadien, Terry J. Hassold, Dirk G. De Rooij, Ans M. M. Van Pelt, and David C. Page. 2008. '*Stra8* and Its Inducer, Retinoic Acid, Regulate Meiotic Initiation in Both Spermatogenesis and Oogenesis in Mice'. *Proceedings of the National Academy of Sciences* 105 (39): 14976–80. https://doi.org/10.1073/pnas.0807297105.

Aramaki, Shinya, Katsuhiko Hayashi, Kazuki Kurimoto, Hiroshi Ohta, Yukihiro Yabuta, Hiroko Iwanari, Yasuhiro Mochizuki, et al. 2013. 'A Mesodermal Factor, T, Specifies Mouse Germ Cell Fate by Directly Activating Germline Determinants'. *Developmental Cell* 27 (5): 516–29. https://doi.org/10.1016/j.devcel.2013.11.001.

Avilion, Ariel A., Silvia K. Nicolis, Larysa H. Pevny, Lidia Perez, Nigel Vivian, and Robin Lovell-Badge. 2003. 'Multipotent Cell Lineages in Early Mouse Development Depend on SOX2 Function'. *Genes & Development* 17 (1): 126–40. https://doi.org/10.1101/gad.224503.

Bajusz, Izabella, Surya Henry, Enikő Sutus, Gergő Kovács, Melinda Katalin Pirity, Melinda Katalin Pirity, and Melinda K. Pirity. 2019. 'Evolving Role of RING1 and YY1 Binding Protein in the Regulation of Germ-Cell-Specific Transcription.' *Genes* 10 (11): 941. https://doi.org/10.3390/genes10110941.

Baltus, Andrew E, Douglas B Menke, Yueh-Chiang Hu, Mary L Goodheart, Anne E Carpenter, Dirk G De Rooij, and David C Page. 2006. 'In Germ Cells of Mouse Embryonic Ovaries, the Decision to Enter Meiosis Precedes Premeiotic DNA Replication'. *Nature Genetics* 38 (12): 1430–34. https://doi.org/10.1038/ng1919.

Barrios, Florencia, Doria Filipponi, Manuela Pellegrini, Maria Paola Paronetto, Sara Di Siena, Raffaele Geremia, Pellegrino Rossi, Massimo De Felici, Emmanuele A. Jannini, and Susanna Dolci. 2010. 'Opposing Effects of Retinoic Acid and FGF9 on *Nanos2* Expression and Meiotic Entry of Mouse Germ Cells'. *Journal of Cell Science* 123 (6): 871–80. https://doi.org/10.1242/jcs.057968.

Bartolomei, M. S., and A. C. Ferguson-Smith. 2011. 'Mammalian Genomic Imprinting'. *Cold Spring Harbor Perspectives in Biology* 3 (7): a002592–a002592. https://doi.org/10.1101/cshperspect.a002592.

Bateman, Alex, Penny Coggill, and Robert D. Finn. 2010. 'DUFs: Families in Search of Function'. *Acta Crystallographica Section F Structural Biology and Crystallization Communications* 66 (10): 1148–52. https://doi.org/10.1107/S1744309110001685.

Beisaw, Arica, Pavel Tsaytler, Frederic Koch, Sandra U Schmitz, Maria-Theodora Melissari, Anna D Senft, Lars Wittler, et al. 2018. 'BRACHYURY Directs Histone Acetylation to Target Loci during Mesoderm Development'. *EMBO Reports* 19 (1): 118–34. https://doi.org/10.15252/embr.201744201.

Berg, Debbie L.C. van den, Tim Snoek, Nick P. Mullin, Adam Yates, Karel Bezstarosti, Jeroen Demmers, Ian Chambers, and Raymond A. Poot. 2010. 'An Oct4-Centered Protein Interaction Network in Embryonic Stem Cells'. *Cell Stem Cell* 6 (4): 369–81. https://doi.org/10.1016/j.stem.2010.02.014.

Blackledge, Neil P., and Robert J. Klose. 2021. 'The Molecular Principles of Gene Regulation by Polycomb Repressive Complexes.' *Nature Reviews Molecular Cell Biology*, August, 1–19. https://doi.org/10.1038/s41580-021-00398-y.

Bolger, Anthony M., Marc Lohse, and Bjoern Usadel. 2014. 'Trimmomatic: A Flexible Trimmer for Illumina Sequence Data'. *Bioinformatics* 30 (15): 2114–20. https://doi.org/10.1093/bioinformatics/btu170.

Bostick, Magnolia, Jong Kyong Kim, Pierre-Olivier Estève, Amander Clark, Sriharsa Pradhan, and Steven E. Jacobsen. 2007. 'UHRF1 Plays a Role in Maintaining DNA Methylation in Mammalian Cells'. *Science* 317 (5845): 1760–64. https://doi.org/10.1126/science.1147939.

Buecker, Christa, Rajini Srinivasan, Zhixiang Wu, Eliezer Calo, Dario Acampora, Tiago Faial, Antonio Simeone, Minjia Tan, Tomasz Swigut, and Joanna Wysocka. 2014. 'Reorganization of Enhancer Patterns in Transition from Naive to Primed Pluripotency'. *Cell Stem Cell* 14 (6): 838–53. https://doi.org/10.1016/j.stem.2014.04.003.

Burgute, Bhagyashri D., Vivek S. Peche, Anna-Lena Steckelberg, Gernot Glöckner, Berthold Gaßen, Niels H. Gehring, and Angelika A. Noegel. 2014. 'NKAP Is a Novel RS-Related Protein That Interacts with RNA and RNA Binding Proteins'. *Nucleic Acids Research* 42 (5): 3177–93. https://doi.org/10.1093/nar/gkt1311.

Burn, Sally F., Andrew J. Washkowitz, Svetlana Gavrilov, and Virginia E. Papaioannou. 2018. 'Postimplantation Mga Expression and Embryonic Lethality of Two Gene-Trap Alleles'. *Gene Expression Patterns* 27 (January): 31–35. https://doi.org/10.1016/j.gep.2017.10.006.

Campolo, Federica, Manuele Gori, Rebecca Favaro, Silvia Nicolis, Manuela Pellegrini, Flavia Botti, Pellegrino Rossi, Emmanuele A. Jannini, and Susanna Dolci. 2013. 'Essential Role of Sox2 for the Establishment and Maintenance of the Germ Cell Line'. *Stem Cells* 31 (7): 1408–21. https://doi.org/10.1002/stem.1392.

Chambers, Ian, Jose Silva, Douglas Colby, Jennifer Nichols, Bianca Nijmeijer, Morag Robertson, Jan Vrana, Ken Jones, Lars Grotewold, and Austin Smith. 2007. 'Nanog Safeguards Pluripotency and Mediates Germline Development'. *Nature* 450 (7173): 1230–34. https://doi.org/10.1038/nature06403.

Chassot, A.-A., F. Ranc, E. P. Gregoire, H. L. Roepers-Gajadien, M. M. Taketo, G. Camerino, D. G. De Rooij, A. Schedl, and M.-C. Chaboissier. 2008. 'Activation of -Catenin Signalling by Rspo1 Controls Differentiation of the Mammalian Ovary'. *Human Molecular Genetics* 17 (9): 1264–77. https://doi.org/10.1093/hmg/ddn016.

Chen, Hsu-Hsin, Maaike Welling, Donald B. Bloch, Javier Muñoz, Edwin Mientjes, Xinjie Chen, Cody Tramp, et al. 2014. 'DAZL Limits Pluripotency, Differentiation, and Apoptosis in Developing Primordial Germ Cells'. *Stem Cell Reports* 3 (5): 892–904. https://doi.org/10.1016/j.stemcr.2014.09.003.

Chiquoine, A. Duncan. 1954. 'The Identification, Origin, and Migration of the Primordial Germ Cells in the Mouse Embryo'. *The Anatomical Record* 118 (2): 135–46. https://doi.org/10.1002/ar.1091180202.

Ciruna, Brian G., and Janet Rossant. 1999. 'Expression of the T-Box Gene Eomesodermin during Early Mouse Development'. *Mechanisms of Development* 81 (1–2): 199–203. https://doi.org/10.1016/S0925-4773(98)00243-3.

Cox, Jürgen, and Matthias Mann. 2008. 'MaxQuant Enables High Peptide Identification Rates, Individualized p.p.b.-Range Mass Accuracies and Proteome-Wide Protein Quantification'. *Nature Biotechnology* 26 (12): 1367–72. https://doi.org/10.1038/nbt.1511.

Dahlet, Thomas, Matthias Truss, Ute Frede, Hala Al Adhami, Anaïs F. Bardet, Michael Dumas, Judith Vallet, et al. 2021. 'E2F6 Initiates Stable Epigenetic Silencing of Germline Genes during Embryonic Development'. *Nature Communications* 12 (1): 3582–3582. https://doi.org/10.1038/s41467-021-23596-w.

Dahlet, Thomas, Matthias Truss, Ute Frede, Hala Al Adhami, Anaïs F. Bardet, Michael Dumas, Judith Vallet, et al. 2021. 'E2F6 Initiates Stable Epigenetic Silencing of Germline Genes during Embryonic Development'. *Nature Communications* 12 (1): 3582. https://doi.org/10.1038/s41467-021-23596-w.

Dawson, Natalie, Ian Sillitoe, Russell L. Marsden, and Christine A. Orengo. 2017. 'The Classification of Protein Domains'. In *Bioinformatics*, edited by Jonathan M. Keith, 1525:137–64. Methods in Molecular Biology. New York, NY: Springer New York. https://doi.org/10.1007/978-1-4939-6622-6_7.

Ding, Junjun, Xin Huang, Ningyi Shao, Hongwei Zhou, Dung-Fang Lee, Francesco Faiola, Miguel Fidalgo, et al. 2015. 'Tex10 Coordinates Epigenetic Control of Super-Enhancer Activity in Pluripotency and Reprogramming'. *Cell Stem Cell* 16 (6): 653–68. https://doi.org/10.1016/j.stem.2015.04.001.

Dobin, Alexander, Carrie A. Davis, Felix Schlesinger, Jorg Drenkow, Chris Zaleski, Sonali Jha, Philippe Batut, Mark Chaisson, and Thomas R. Gingeras. 2013. 'STAR: Ultrafast Universal RNA-Seq Aligner'. *Bioinformatics* 29 (1): 15–21. https://doi.org/10.1093/bioinformatics/bts635.

Endoh, Mitsuhiro, Takaho A. Endo, Jun Shinga, Katsuhiko Hayashi, Anca M. Farcas, Kit-Wan Ma, Kit Wan, et al. 2017. 'PCGF6-PRC1 Suppresses Premature Differentiation of Mouse Embryonic Stem Cells by Regulating Germ Cell-Related Genes'. *ELife* 6 (March). https://doi.org/10.7554/elife.21064.

Extavour, Cassandra G., and Michael Akam. 2003. 'Mechanisms of Germ Cell Specification across the Metazoans: Epigenesis and Preformation'. *Development* 130 (24): 5869–84. https://doi.org/10.1242/dev.00804.

Galonska, Christina, Michael J. Ziller, Rahul Karnik, and Alexander Meissner. 2015. 'Ground State Conditions Induce Rapid Reorganization of Core Pluripotency Factor Binding before Global Epigenetic Reprogramming'. *Cell Stem Cell* 17 (4): 462–70. https://doi.org/10.1016/j.stem.2015.07.005.

Gao, Zhonghua, Jin Zhang, Roberto Bonasio, Francesco Strino, Ayana Sawai, Fabio Parisi, Yuval Kluger, and Danny Reinberg. 2012. 'PCGF Homologs, CBX Proteins, and RYBP Define Functionally Distinct PRC1 Family Complexes'. *Molecular Cell* 45 (3): 344–56. https://doi.org/10.1016/j.molcel.2012.01.002.

Gill, Mark E., Yueh-Chiang Hu, Yanfeng Lin, and David C. Page. 2011. 'Licensing of Gametogenesis, Dependent on RNA Binding Protein DAZL, as a Gateway to Sexual Differentiation of Fetal Germ Cells'. *Proceedings of the National Academy of Sciences* 108 (18): 7443–48. https://doi.org/10.1073/pnas.1104501108.

Ginsburg, M., M.H. Snow, and A. McLaren. 1990a. 'Primordial Germ Cells in the Mouse Embryo during Gastrulation'. *Development* 110 (2): 521–28. https://doi.org/10.1242/dev.110.2.521.

———. 1990b. 'Primordial Germ Cells in the Mouse Embryo during Gastrulation'. *Development* 110 (2): 521–28. https://doi.org/10.1242/dev.110.2.521.

Guibert, Sylvain, Thierry Forné, and Michael Weber. 2012. 'Global Profiling of DNA Methylation Erasure in Mouse Primordial Germ Cells'. *Genome Research* 22 (4): 633–41. https://doi.org/10.1101/gr.130997.111.

Guo, Rui, Lijuan Zheng, Juw Won Park, Ruitu Lv, Hao Chen, Fangfang Jiao, Wenqi Xu, et al. 2014. 'BS69/ZMYND11 Reads and Connects Histone H3.3 Lysine 36 Trimethylation-Decorated Chromatin

to Regulated Pre-MRNA Processing'. *Molecular Cell* 56 (2): 298–310. https://doi.org/10.1016/j.molcel.2014.08.022.

Hackett, Jamie A., James P. Reddington, Colm E. Nestor, Donncha S. Dunican, Miguel R. Branco, Judith Reichmann, Wolf Reik, M. Azim Surani, Ian R. Adams, and Richard R. Meehan. 2012. 'Promoter DNA Methylation Couples Genome-Defence Mechanisms to Epigenetic Reprogramming in the Mouse Germline'. *Development* 139 (19): 3623–32. https://doi.org/10.1242/dev.081661.

Hackett, Jamie A., Roopsha Sengupta, Jan J. Zylicz, Kazuhiro Murakami, Caroline Lee, Thomas A. Down, and M. Azim Surani. 2013. 'Germline DNA Demethylation Dynamics and Imprint Erasure Through 5-Hydroxymethylcytosine'. *Science* 339 (6118): 448–52. https://doi.org/10.1126/science.1229277.

Hackett, Jamie A., Jan J. Zylicz, and M. Azim Surani. 2012. 'Parallel Mechanisms of Epigenetic Reprogramming in the Germline'. *Trends in Genetics* 28 (4): 164–74. https://doi.org/10.1016/j.tig.2012.01.005.

Hajkova, Petra, Katia Ancelin, Tanja Waldmann, Nicolas Lacoste, Ulrike C. Lange, Francesca Cesari, Caroline Lee, Genevieve Almouzni, Robert Schneider, and M. Azim Surani. 2008. 'Chromatin Dynamics during Epigenetic Reprogramming in the Mouse Germ Line'. *Nature* 452 (7189): 877–81. https://doi.org/10.1038/nature06714.

Hajkova, Petra, Sylvia Erhardt, Natasha Lane, Thomas Haaf, Osman El-Maarri, Wolf Reik, Jörn Walter, and M.Azim Surani. 2002. 'Epigenetic Reprogramming in Mouse Primordial Germ Cells'. *Mechanisms of Development* 117 (1–2): 15–23. https://doi.org/10.1016/S0925-4773(02)00181-8.

Handel, Mary Ann, and John C. Schimenti. 2010. 'Genetics of Mammalian Meiosis: Regulation, Dynamics and Impact on Fertility'. *Nature Reviews Genetics* 11 (2): 124–36. https://doi.org/10.1038/nrg2723.

Hargan-Calvopina, Joseph, Sara Taylor, Helene Cook, Zhongxun Hu, Serena A. Lee, Ming-Ren Yen, Yih-Shien Chiang, Pao-Yang Chen, and Amander T. Clark. 2016. 'Stage-Specific Demethylation in Primordial Germ Cells Safeguards against Precocious Differentiation'. *Developmental Cell* 39 (1): 75–86. https://doi.org/10.1016/j.devcel.2016.07.019.

Hauri, Simon, Federico Comoglio, Makiko Seimiya, Moritz Gerstung, Timo Glatter, Klaus Hansen, Ruedi Aebersold, Renato Paro, Matthias Gstaiger, and Christian Beisel. 2016. 'A High-Density Map for Navigating the Human Polycomb Complexome'. *Cell Reports* 17 (2): 583–95. https://doi.org/10.1016/j.celrep.2016.08.096.

Hayashi, Katsuhiko, Sugako Ogushi, Kazuki Kurimoto, So Shimamoto, Hiroshi Ohta, and Mitinori Saitou. 2012. 'Offspring from Oocytes Derived from in Vitro Primordial Germ Cell–like Cells in Mice'. *Science* 338 (6109): 971–75. https://doi.org/10.1126/science.1226889.

Hayashi, Katsuhiko, Hiroshi Ohta, Kazuki Kurimoto, Shinya Aramaki, and Mitinori Saitou. 2011. 'Reconstitution of the Mouse Germ Cell Specification Pathway in Culture by Pluripotent Stem Cells'. *Cell* 146 (4): 519–32. https://doi.org/10.1016/j.cell.2011.06.052.

Herrmann, Bernhard G., Siegfried Labeit, Annemarie Poustka, Thomas R. King, and Hans Lehrach. 1990. 'Cloning of the T Gene Required in Mesoderm Formation in the Mouse'. *Nature* 343 (6259): 617–22. https://doi.org/10.1038/343617a0.

Hikabe, Orie, Nobuhiko Hamazaki, Go Nagamatsu, Yayoi Obata, Yuji Hirao, Norio Hamada, So Shimamoto, et al. 2016. 'Reconstitution in Vitro of the Entire Cycle of the Mouse Female Germ Line'. *Nature* 539 (7628): 299–303. https://doi.org/10.1038/nature20104.

Hill, Peter W. S., Harry G. Leitch, Cristina E. Requena, Zhiyi Sun, Rachel Amouroux, Monica Roman-Trufero, Malgorzata Borkowska, et al. 2018. 'Epigenetic Reprogramming Enables the Transition from Primordial Germ Cell to Gonocyte'. *Nature* 555 (7696): 392–96. https://doi.org/10.1038/nature25964.

Hill, Peter W.S., Rachel Amouroux, and Petra Hajkova. 2014. 'DNA Demethylation, Tet Proteins and 5-Hydroxymethylcytosine in Epigenetic Reprogramming: An Emerging Complex Story'. *Genomics* 104 (5): 324–33. https://doi.org/10.1016/j.ygeno.2014.08.012.

Huang, Chuyu, Yan Chen, Huaiqian Dai, Huan Zhang, Minyu Xie, Hanbin Zhang, Feilong Chen, Xiangjin Kang, Xiaochun Bai, and Zhenguo Chen. 2020. 'UBAP2L Arginine Methylation by PRMT1 Modulates Stress Granule Assembly'. *Cell Death & Differentiation* 27 (1): 227–41. https://doi.org/10.1038/s41418-019-0350-5.

Hurlin, Peter J., and Jie Huang. 2006. 'The MAX-Interacting Transcription Factor Network'. *Seminars in Cancer Biology* 16 (4): 265–74. https://doi.org/10.1016/j.semcancer.2006.07.009.

Hurlin, Peter J, Eirıkur Steingrımsson, Neal G Copeland, Nancy A Jenkins, and Robert N Eisenman. n.d. 'Mga, a Dual-Specificity Transcription Factor That Interacts with Max and Contains a T-Domain DNA- Binding Motif', 10.

Istaces, Nicolas, Marion Splittgerber, Viviana Lima Silva, Muriel Nguyen, Séverine Thomas, Aurore Le, Younes Achouri, et al. 2019. 'EOMES Interacts with RUNX3 and BRG1 to Promote Innate Memory Cell Formation through Epigenetic Reprogramming'. *Nature Communications* 10 (1): 3306. https://doi.org/10.1038/s41467-019-11233-6.

Janin, Joël, and Shoshanna J. Wodak. 1983. 'Structural Domains in Proteins and Their Role in the Dynamics of Protein Function'. *Progress in Biophysics and Molecular Biology* 42: 21–78. https://doi.org/10.1016/0079-6107(83)90003-2.

Jumper, John, Richard Evans, Alexander Pritzel, Tim Green, Michael Figurnov, Olaf Ronneberger, Kathryn Tunyasuvunakool, et al. 2021. 'Highly Accurate Protein Structure Prediction with AlphaFold'. *Nature* 596 (7873): 583–89. https://doi.org/10.1038/s41586-021-03819-2.

Kagiwada, Saya, Kazuki Kurimoto, Takayuki Hirota, Masashi Yamaji, and Mitinori Saitou. 2012. 'Replication-Coupled Passive DNA Demethylation for the Erasure of Genome Imprints in Mice'. *The EMBO Journal* 32 (3): 340–53. https://doi.org/10.1038/emboj.2012.331.

Kehler, James, Elena Tolkunova, Birgit Koschorz, Maurizio Pesce, Luca Gentile, Michele Boiani, Hilda Lomelí, et al. 2004. 'Oct4 Is Required for Primordial Germ Cell Survival'. *EMBO Reports* 5 (11): 1078–83. https://doi.org/10.1038/sj.embor.7400279.

Kennison, James A. 1995. 'THE POLYCOMB AND TRITHORAX GROUP PROTEINS OF *DROSOPHILA* : Trans-Regulators of Homeotic Gene Function'. *Annual Review of Genetics* 29 (1): 289–303. https://doi.org/10.1146/annurev.ge.29.120195.001445.

Kim, Shinseog, Ufuk Günesdogan, Jan J. Zylicz, Jamie A. Hackett, Delphine Cougot, Siqin Bao, Caroline Lee, et al. 2014. 'PRMT5 Protects Genomic Integrity during Global DNA Demethylation in Primordial Germ Cells and Preimplantation Embryos'. *Molecular Cell* 56 (4): 564–79. https://doi.org/10.1016/j.molcel.2014.10.003.

Kim, Yuna, Akio Kobayashi, Ryohei Sekido, Leo DiNapoli, Jennifer Brennan, Marie-Christine Chaboissier, Francis Poulat, Richard R Behringer, Robin Lovell-Badge, and Blanche Capel. 2006. 'Fgf9 and Wnt4 Act as Antagonistic Signals to Regulate Mammalian Sex Determination'. Edited by Hiroshi Hamada. *PLoS Biology* 4 (6): e187. https://doi.org/10.1371/journal.pbio.0040187.

Kispert, Andreas. 1995. 'The Brachyury Protein: A T-Domain Transcription Factor'. *Seminars in Developmental Biology* 6 (6): 395–403. https://doi.org/10.1016/S1044-5781(06)80003-4.

Koopman, Peter, John Gubbay, Nigel Vivian, Peter Goodfellow, and Robin Lovell-Badge. 1991. 'Male Development of Chromosomally Female Mice Transgenic for Sry'. *Nature* 351 (6322): 117–21. https://doi.org/10.1038/351117a0.

Kurimoto, Kazuki, Yukihiro Yabuta, Yasuhide Ohinata, Mayo Shigeta, Kaori Yamanaka, and Mitinori Saitou. 2008. 'Complex Genome-Wide Transcription Dynamics Orchestrated by Blimp1 for the

Specification of the Germ Cell Lineage in Mice'. *Genes & Development* 22 (12): 1617–35. https://doi.org/10.1101/gad.1649908.

Langmead, Ben, and Steven L Salzberg. 2012. 'Fast Gapped-Read Alignment with Bowtie 2'. *Nature Methods* 9 (4): 357–59. https://doi.org/10.1038/nmeth.1923.

Lawson, K. A., N. R. Dunn, B. A.J. Roelen, L. M. Zeinstra, A. M. Davis, C. V.E. Wright, J. P.W.F.M. Korving, and B. L.M. Hogan. 1999. 'Bmp4 Is Required for the Generation of Primordial Germ Cells in the Mouse Embryo'. *Genes & Development* 13 (4): 424–36. https://doi.org/10.1101/gad.13.4.424.

Lawson, K. A., and W. J. Hage. 2007. 'Clonal Analysis of the Origin of Primordial Germ Cells in the Mouse'. In *Novartis Foundation Symposia*, edited by Joan Marsh and Jamie Goode, 68–91. Chichester, UK: John Wiley & Sons, Ltd. https://doi.org/10.1002/9780470514573.ch5.

Leporcq, Clémentine, Yannick Spill, Delphine Balaramane, Christophe Toussaint, Michaël Weber, and Anaïs Flore Bardet. 2020. 'TFmotifView: A Webserver for the Visualization of Transcription Factor Motifs in Genomic Regions'. *Nucleic Acids Research* 48 (W1): W208–17. https://doi.org/10.1093/nar/gkaa252.

Lewis, E. B. 1978. 'A Gene Complex Controlling Segmentation in Drosophila'. *Nature* 276 (5688): 565–70. https://doi.org/10.1038/276565a0.

Lewis, Megan D., Sara A. Miller, Michael M. Miazgowicz, Kristin M. Beima, and Amy S. Weinmann. 2007. 'T-Bet's Ability To Regulate Individual Target Genes Requires the Conserved T-Box Domain To Recruit Histone Methyltransferase Activity and a Separate Family Member-Specific Transactivation Domain'. *Molecular and Cellular Biology* 27 (24): 8510–21. https://doi.org/10.1128/MCB.01615-07.

Li, H., B. Handsaker, A. Wysoker, T. Fennell, J. Ruan, N. Homer, G. Marth, G. Abecasis, R. Durbin, and 1000 Genome Project Data Processing Subgroup. 2009. 'The Sequence Alignment/Map Format and SAMtools'. *Bioinformatics* 25 (16): 2078–79. https://doi.org/10.1093/bioinformatics/btp352.

Love, Michael I, Wolfgang Huber, and Simon Anders. 2014. 'Moderated Estimation of Fold Change and Dispersion for RNA-Seq Data with DESeq2'. *Genome Biology* 15 (12): 550. https://doi.org/10.1186/s13059-014-0550-8.

Lowe, Matthew G., Ming-Ren Yen, Fei-Man Hsu, Linzi Hosohama, Zhongxun Hu, Tsotne Chitiashvili, Timothy J. Hunt, et al. 2022. 'EED Is Required for Mouse Primordial Germ Cell Differentiation in the Embryonic Gonad'. *Developmental Cell* 57 (12): 1482-1495.e5. https://doi.org/10.1016/j.devcel.2022.05.012.

Maatouk, Danielle M., Leo DiNapoli, Ashley Alvers, Keith L. Parker, Makoto M. Taketo, and Blanche Capel. 2008. 'Stabilization of β-Catenin in XY Gonads Causes Male-to-Female Sex-Reversal'. *Human Molecular Genetics* 17 (19): 2949–55. https://doi.org/10.1093/hmg/ddn193.

Maatouk, Danielle M., Lori D. Kellam, Mellissa R. W. Mann, Hong Lei, En Li, Marisa S. Bartolomei, and James L. Resnick. 2006. 'DNA Methylation Is a Primary Mechanism for Silencing Postmigratory Primordial Germ Cell Genes in Both Germ Cell and Somatic Cell Lineages'. *Development* 133 (17): 3411–18. https://doi.org/10.1242/dev.02500.

Madeira, Fábio, Matt Pearce, Adrian R N Tivey, Prasad Basutkar, Joon Lee, Ossama Edbali, Nandana Madhusoodanan, Anton Kolesnikov, and Rodrigo Lopez. 2022. 'Search and Sequence Analysis Tools Services from EMBL-EBI in 2022'. *Nucleic Acids Research* 50 (W1): W276–79. https://doi.org/10.1093/nar/gkac240.

Maeda, Ikuma, Daiji Okamura, Yuko Tokitake, Makiko Ikeda, Hiroko Kawaguchi, Nathan Mise, Kuniya Abe, Toshiaki Noce, Akihiko Okuda, and Yasuhisa Matsui. 2013. 'Max Is a Repressor of Germ Cell-Related Gene Expression in Mouse Embryonic Stem Cells'. *Nature Communications* 4 (1): 1754. https://doi.org/10.1038/ncomms2780.

Magnúsdóttir, Erna, Sabine Dietmann, Kazuhiro Murakami, Ufuk Günesdogan, Fuchou Tang, Siqin Bao, Evangelia Diamanti, Kaiqin Lao, Berthold Gottgens, and M. Azim Surani. 2013. 'A Tripartite Transcription Factor Network Regulates Primordial Germ Cell Specification in Mice'. *Nature Cell Biology* 15 (8): 905–15. https://doi.org/10.1038/ncb2798.

Margueron, Raphaël, and Danny Reinberg. 2011. 'The Polycomb Complex PRC2 and Its Mark in Life'. *Nature* 469 (7330): 343–49. https://doi.org/10.1038/nature09784.

Martello, Graziano, Toshimi Sugimoto, Evangelia Diamanti, Anagha Joshi, Rebecca Hannah, Satoshi Ohtsuka, Berthold Göttgens, Hitoshi Niwa, and Austin Smith. 2012. 'Esrrb Is a Pivotal Target of the Gsk3/Tcf3 Axis Regulating Embryonic Stem Cell Self-Renewal'. *Cell Stem Cell* 11 (4): 491–504. https://doi.org/10.1016/j.stem.2012.06.008.

Mathsyaraja, Haritha, Jonathen Catchpole, Brian Freie, Emily Eastwood, Ekaterina Babaeva, Michael Geuenich, Pei Feng Cheng, et al. 2021. 'Loss of MGA Repression Mediated by an Atypical Polycomb Complex Promotes Tumor Progression and Invasiveness'. *ELife* 10 (July): e64212. https://doi.org/10.7554/eLife.64212.

Matsui, Yasuhisa, and Kentaro Mochizuki. 2014. 'A Current View of the Epigenome in Mouse Primordial Germ Cells: EPIGENOME IN PRIMORDIAL GERM CELLS'. *Molecular Reproduction and Development* 81 (2): 160–70. https://doi.org/10.1002/mrd.22214.

Meng, Chenling, Jinyue Liao, Danfeng Zhao, Huihui Huang, Jinzhong Qin, Tin-Lap Lee, Degui Chen, Wai-Yee Chan, and Yin Xia. 2019. 'L3MBTL2 Regulates Chromatin Remodeling during Spermatogenesis'. *Cell Death & Differentiation* 26 (11): 2194–2207. https://doi.org/10.1038/s41418-019-0283-z.

Mikedis, Maria M, Yuting Fan, Peter K Nicholls, Tsutomu Endo, Emily K Jackson, Sarah A Cobb, Dirk G de Rooij, and David C Page. 2020. 'DAZL Mediates a Broad Translational Program Regulating Expansion and Differentiation of Spermatogonial Progenitors'. *ELife* 9 (July): e56523. https://doi.org/10.7554/eLife.56523.

Miller, Sara A., Albert C. Huang, Michael M. Miazgowicz, Margaret M. Brassil, and Amy S. Weinmann. 2008. 'Coordinated but Physically Separable Interaction with H3K27-Demethylase and H3K4-Methyltransferase Activities Are Required for T-Box Protein-Mediated Activation of Developmental Gene Expression'. *Genes & Development* 22 (21): 2980–93. https://doi.org/10.1101/gad.1689708.

Miller, Sara A., Sarah E. Mohn, and Amy S. Weinmann. 2010. 'Jmjd3 and UTX Play a Demethylase-Independent Role in Chromatin Remodeling to Regulate T-Box Family Member-Dependent Gene Expression'. *Molecular Cell* 40 (4): 594–605. https://doi.org/10.1016/j.molcel.2010.10.028.

Mirdita, Milot, Konstantin Schütze, Yoshitaka Moriwaki, Lim Heo, Sergey Ovchinnikov, and Martin Steinegger. 2022. 'ColabFold: Making Protein Folding Accessible to All'. *Nature Methods* 19 (6): 679–82. https://doi.org/10.1038/s41592-022-01488-1.

Miyauchi, Hidetaka, Hiroshi Ohta, So Nagaoka, Fumio Nakaki, Kotaro Sasaki, Katsuhiko Hayashi, Yukihiro Yabuta, Tomonori Nakamura, Takuya Yamamoto, and Mitinori Saitou. 2017. 'Bone Morphogenetic Protein and Retinoic Acid Synergistically Specify Female Germ-cell Fate in Mice'. *The EMBO Journal* 36 (21): 3100–3119. https://doi.org/10.15252/embj.201796875.

Mochizuki, Kentaro. n.d. 'Repression of Germline Genes by PRC1.6 and SETDB1 in the Early Embryo Precedes DNA Methylation-Mediated Silencing', 15.

Mochizuki, Kentaro, Jafar Sharif, Kenjiro Shirane, Kousuke Uranishi, Aaron B. Bogutz, Sanne M. Janssen, Ayumu Suzuki, Akihiko Okuda, Haruhiko Koseki, and Matthew C. Lorincz. 2021. 'Repression of Germline Genes by PRC1.6 and SETDB1 in the Early Embryo Precedes DNA Methylation-Mediated Silencing'. *Nature Communications* 12 (1): 7020. https://doi.org/10.1038/s41467-021-27345-x.

Molyneaux, Kathleen A., Jim Stallock, Kyle Schaible, and Christopher Wylie. 2001. 'Time-Lapse Analysis of Living Mouse Germ Cell Migration'. *Developmental Biology* 240 (2): 488–98. https://doi.org/10.1006/dbio.2001.0436.

Morris, Kevin J, and Anita H Corbett. 2018. 'The Polyadenosine RNA-Binding Protein ZC3H14 Interacts with the THO Complex and Coordinately Regulates the Processing of Neuronal Transcripts'. *Nucleic Acids Research* 46 (13): 6561–75. https://doi.org/10.1093/nar/gky446.

Murakami, Kazuhiro, Ufuk Günesdogan, Jan J. Zylicz, Walfred W. C. Tang, Roopsha Sengupta, Toshihiro Kobayashi, Shinseog Kim, Richard Butler, Sabine Dietmann, and M. Azim Surani. 2016. 'NANOG Alone Induces Germ Cells in Primed Epiblast in Vitro by Activation of Enhancers'. *Nature* 529 (7586): 403–7. https://doi.org/10.1038/nature16480.

Natsume, Toyoaki, Tomomi Kiyomitsu, Yumiko Saga, and Masato T. Kanemaki. 2016. 'Rapid Protein Depletion in Human Cells by Auxin-Inducible Degron Tagging with Short Homology Donors'. *Cell Reports* 15 (1): 210–18. https://doi.org/10.1016/j.celrep.2016.03.001.

Nicholls, Peter K., Hubert Schorle, Sahin Naqvi, Yueh-Chiang Hu, Yuting Fan, Yuting Fan, Yuting Fan, et al. 2019. 'Mammalian Germ Cells Are Determined after PGC Colonization of the Nascent Gonad.' *Proceedings of the National Academy of Sciences of the United States of America* 116 (51): 25677–87. https://doi.org/10.1073/pnas.1910733116.

Nichols, Jennifer, Branko Zevnik, Konstantinos Anastassiadis, Hitoshi Niwa, Daniela Klewe-Nebenius, Ian Chambers, Hans Schöler, and Austin Smith. 1998. 'Formation of Pluripotent Stem Cells in the Mammalian Embryo Depends on the POU Transcription Factor Oct4'. *Cell* 95 (3): 379–91. https://doi.org/10.1016/S0092-8674(00)81769-9.

Nishimura, Kohei, Tatsuo Fukagawa, Haruhiko Takisawa, Tatsuo Kakimoto, and Masato Kanemaki. 2009. 'An Auxin-Based Degron System for the Rapid Depletion of Proteins in Nonplant Cells'. *Nature Methods* 6 (12): 917–22. https://doi.org/10.1038/nmeth.1401.

Ogawa, Hidesato, Kei-ichiro Ishiguro, Stefan Gaubatz, David M. Livingston, and Yoshihiro Nakatani. 2002. 'A Complex with Chromatin Modifiers That Occupies E2F- and Myc-Responsive Genes in G_0 Cells'. *Science* 296 (5570): 1132–36. https://doi.org/10.1126/science.1069861.

Ohinata, Yasuhide, Hiroshi Ohta, Mayo Shigeta, Kaori Yamanaka, Teruhiko Wakayama, and Mitinori Saitou. 2009. 'A Signalling Principle for the Specification of the Germ Cell Lineage in Mice'. *Cell* 137 (3): 571–84. https://doi.org/10.1016/j.cell.2009.03.014.

Ohinata, Yasuhide, Bernhard Payer, Dónal O'Carroll, Katia Ancelin, Yukiko Ono, Mitsue Sano, Sheila C. Barton, et al. 2005. 'Blimp1 Is a Critical Determinant of the Germ Cell Lineage in Mice'. *Nature* 436 (7048): 207–13. https://doi.org/10.1038/nature03813.

Papaioannou, Virginia E. 2014a. 'The T-Box Gene Family: Emerging Roles in Development, Stem Cells and Cancer'. *Development* 141 (20): 3819–33. https://doi.org/10.1242/dev.104471.

———. 2014b. 'The T-Box Gene Family: Emerging Roles in Development, Stem Cells and Cancer'. *Development* 141 (20): 3819–33. https://doi.org/10.1242/dev.104471.

Pardo, Mercedes, Benjamin Lang, Lu Yu, Haydn Prosser, Allan Bradley, M. Madan Babu, and Jyoti Choudhary. 2010. 'An Expanded Oct4 Interaction Network: Implications for Stem Cell Biology, Development, and Disease'. *Cell Stem Cell* 6 (4): 382–95. https://doi.org/10.1016/j.stem.2010.03.004.

Parma, Pietro, Orietta Radi, Valerie Vidal, Marie Christine Chaboissier, Elena Dellambra, Stella Valentini, Liliana Guerra, Andreas Schedl, and Giovanna Camerino. 2006. 'R-Spondin1 Is Essential in Sex Determination, Skin Differentiation and Malignancy'. *Nature Genetics* 38 (11): 1304–9. https://doi.org/10.1038/ng1907.

Paula Dobrinić, Paula Dobrinić, Szczurek At, and Robert J. Klose. 2021. 'PRC1 Drives Polycomb-Mediated Gene Repression by Controlling Transcription Initiation and Burst Frequency'. *Nature Structural & Molecular Biology* 28 (10): 811–24. https://doi.org/10.1038/s41594-021-00661-y.

Pesce, Maurizio, Xiangyuan Wang, Debra J Wolgemuth, and Hans R Schöler. 1998. 'Differential Expression of the Oct-4 Transcription Factor during Mouse Germ Cell Differentiation'. *Mechanisms of Development* 71 (1–2): 89–98. https://doi.org/10.1016/S0925-4773(98)00002-1.

Popp, Christian, Wendy Dean, Suhua Feng, Shawn J. Cokus, Simon Andrews, Matteo Pellegrini, Steven E. Jacobsen, and Wolf Reik. 2010. 'Genome-Wide Erasure of DNA Methylation in Mouse Primordial Germ Cells Is Affected by AID Deficiency'. *Nature* 463 (7284): 1101–5. https://doi.org/10.1038/nature08829.

Qin, Jinzhong, Congcong Wang, Yaru Zhu, Ting Su, Lixia Dong, Yikai Huang, and Kunying Hao. 2021. 'Mga Safeguards Embryonic Stem Cells from Acquiring Extraembryonic Endoderm Fates'. *Science Advances* 7 (4): eabe5689. https://doi.org/10.1126/sciadv.abe5689.

Qin, Jinzhong, Warren A. Whyte, Endre Anderssen, Effie Apostolou, Hsu-Hsin Chen, Schahram Akbarian, Roderick T. Bronson, et al. 2012. 'The Polycomb Group Protein L3mbtl2 Assembles an Atypical PRC1-Family Complex That Is Essential in Pluripotent Stem Cells and Early Development'. *Cell Stem Cell* 11 (3): 319–32. https://doi.org/10.1016/j.stem.2012.06.002.

Quinlan, Aaron R. 2014. 'BEDTools: The Swiss-Army Tool for Genome Feature Analysis'. *Current Protocols in Bioinformatics* 47 (1). https://doi.org/10.1002/0471250953.bi1112s47.

Rafiee, Mahmoud-Reza, Julian A Zagalak, Sviatoslav Sidorov, Sebastian Steinhauser, Karen Davey, Jernej Ule, and Nicholas M Luscombe. 2021. 'Chromatin-Contact Atlas Reveals Disorder-Mediated Protein Interactions and Moonlighting Chromatin-Associated RBPs'. *Nucleic Acids Research* 49 (22): 13092–107. https://doi.org/10.1093/nar/gkab1180.

Rafiee, Mahmoud-Reza, Julian A Zagalak, Sviatoslav Sidorov, Sebastian Steinhauser, Karen Davey, Jernej Ule, and Nicholas M. Luscombe. 2020. 'SPACE Exploration of Chromatin Proteome to Reveal Associated RNA-Binding Proteins'. *BioRxiv*, July. https://doi.org/10.1101/2020.07.13.200212.

Ramírez, Fidel, Devon P Ryan, Björn Grüning, Vivek Bhardwaj, Fabian Kilpert, Andreas S Richter, Steffen Heyne, Friederike Dündar, and Thomas Manke. 2016. 'DeepTools2: A next Generation Web Server for Deep-Sequencing Data Analysis'. *Nucleic Acids Research* 44 (W1): W160–65. https://doi.org/10.1093/nar/gkw257.

Rha, Jennifer, Stephanie K. Jones, Jonathan Fidler, Ayan Banerjee, Sara W. Leung, Kevin J. Morris, Jennifer C. Wong, et al. 2017. 'The RNA-Binding Protein, ZC3H14, Is Required for Proper Poly(A) Tail Length Control, Expression of Synaptic Proteins, and Brain Function in Mice'. *Human Molecular Genetics* 26 (19): 3663–81. https://doi.org/10.1093/hmg/ddx248.

Richardson, Brian E., and Ruth Lehmann. 2010. 'Mechanisms Guiding Primordial Germ Cell Migration: Strategies from Different Organisms'. *Nature Reviews Molecular Cell Biology* 11 (1): 37–49. https://doi.org/10.1038/nrm2815.

Rikin, Amir, and Todd Evans. 2010. 'The Tbx/BHLH Transcription Factor Mga Regulates Gata4 and Organogenesis'. *Developmental Dynamics* 239 (2): 535–47. https://doi.org/10.1002/dvdy.22197.

Rudolph, Jan Daniel, and Jürgen Cox. 2019. 'A Network Module for the Perseus Software for Computational Proteomics Facilitates Proteome Interaction Graph Analysis'. *Journal of Proteome Research* 18 (5): 2052–64. https://doi.org/10.1021/acs.jproteome.8b00927.

Russ, Andreas P., Sigrid Wattler, William H. Colledge, Samuel A. J. R. Aparicio, Mark B. L. Carlton, Jonathan J. Pearce, Sheila C. Barton, et al. 2000. 'Eomesodermin Is Required for Mouse Trophoblast Development and Mesoderm Formation'. *Nature* 404 (6773): 95–99. https://doi.org/10.1038/35003601.

Saitou, M., and M. Yamaji. 2012. 'Primordial Germ Cells in Mice'. *Cold Spring Harbor Perspectives in Biology* 4 (11): a008375–a008375. https://doi.org/10.1101/cshperspect.a008375.

Saitou, Mitinori, Sheila C. Barton, and M. Azim Surani. 2002. 'A Molecular Programme for the Specification of Germ Cell Fate in Mice'. *Nature* 418 (6895): 293–300. https://doi.org/10.1038/nature00927.

Saitou, Mitinori, and Masashi Yamaji. 2010. 'Germ Cell Specification in Mice: Signalling, Transcription Regulation, and Epigenetic Consequences'. *REPRODUCTION* 139 (6): 931–42. https://doi.org/10.1530/REP-10-0043.

Sanjana, Neville E, Ophir Shalem, and Feng Zhang. 2014. 'Improved Vectors and Genome-Wide Libraries for CRISPR Screening'. *Nature Methods* 11 (8): 783–84. https://doi.org/10.1038/nmeth.3047.

Sato, Shun, Tomomi Yoshimizu, Eimei Sato, and Yasuhisa Matsui. 2003. 'Erasure of Methylation Imprinting Oflgf2r during Mouse Primordial Germ-Cell Development'. *Molecular Reproduction and Development* 65 (1): 41–50. https://doi.org/10.1002/mrd.10264.

Schuettengruber, Bernd, Henri-Marc Bourbon, Luciano Di Croce, and Giacomo Cavalli. 2017. 'Genome Regulation by Polycomb and Trithorax: 70 Years and Counting'. *Cell* 171 (1): 34–57. https://doi.org/10.1016/j.cell.2017.08.002.

Seisenberger, Stefanie, Simon Andrews, Felix Krueger, Julia Arand, Jörn Walter, Fátima Santos, Christian Popp, Bernard Thienpont, Wendy Dean, and Wolf Reik. 2012. 'The Dynamics of Genome-Wide DNA Methylation Reprogramming in Mouse Primordial Germ Cells'. *Molecular Cell* 48 (6): 849–62. https://doi.org/10.1016/j.molcel.2012.11.001.

Seki, Yoshiyuki, Katsuhiko Hayashi, Kunihiko Itoh, Michinao Mizugaki, Mitinori Saitou, and Yasuhisa Matsui. 2005. 'Extensive and Orderly Reprogramming of Genome-Wide Chromatin Modifications Associated with Specification and Early Development of Germ Cells in Mice'. *Developmental Biology* 278 (2): 440–58. https://doi.org/10.1016/j.ydbio.2004.11.025.

Seki, Yoshiyuki, Masashi Yamaji, Yukihiro Yabuta, Mitsue Sano, Mayo Shigeta, Yasuhisa Matsui, Yumiko Saga, Makoto Tachibana, Yoichi Shinkai, and Mitinori Saitou. 2007. 'Cellular Dynamics Associated with the Genome-Wide Epigenetic Reprogramming in Migrating Primordial Germ Cells in Mice'. *Development* 134 (14): 2627–38. https://doi.org/10.1242/dev.005611.

Sekido, Ryohei, Isabelle Bar, Véronica Narváez, Graeme Penny, and Robin Lovell-Badge. 2004. 'SOX9 Is Up-Regulated by the Transient Expression of SRY Specifically in Sertoli Cell Precursors'. *Developmental Biology* 274 (2): 271–79. https://doi.org/10.1016/j.ydbio.2004.07.011.

Sekido, Ryohei, and Robin Lovell-Badge. 2008. 'Sex Determination Involves Synergistic Action of SRY and SF1 on a Specific Sox9 Enhancer'. *Nature* 453 (7197): 930–34. https://doi.org/10.1038/nature06944.

Senft, Anna D., Elizabeth K. Bikoff, Elizabeth J. Robertson, and Ita Costello. 2019. 'Genetic Dissection of Nodal and Bmp Signalling Requirements during Primordial Germ Cell Development in Mouse'. *Nature Communications* 10 (1): 1089. https://doi.org/10.1038/s41467-019-09052-w.

Sharif, Jafar, Masahiro Muto, Shin-ichiro Takebayashi, Isao Suetake, Akihiro Iwamatsu, Takaho A. Endo, Jun Shinga, et al. 2007. 'The SRA Protein Np95 Mediates Epigenetic Inheritance by Recruiting Dnmt1 to Methylated DNA'. *Nature* 450 (7171): 908–12. https://doi.org/10.1038/nature06397.

Shen-Li, Hong, Rónán C. O'Hagan, Harry Hou, James W. Horner, Han-Woong Lee, and Ronald A. DePinho. 2000. 'Essential Role for Max in Early Embryonic Growth and Development'. *Genes & Development* 14 (1): 17–22. https://doi.org/10.1101/gad.14.1.17.

Showell, Chris, Olav Binder, and Frank L. Conlon. 2004. 'T-Box Genes in Early Embryogenesis'. *Developmental Dynamics* 229 (1): 201–18. https://doi.org/10.1002/dvdy.10480.

Skene, Peter J, and Steven Henikoff. 2017. 'An Efficient Targeted Nuclease Strategy for High-Resolution Mapping of DNA Binding Sites'. *ELife* 6 (January): e21856. https://doi.org/10.7554/eLife.21856.

Smits, Arne H., Pascal W. T. C. Jansen, Ina Poser, Anthony A. Hyman, and Michiel Vermeulen. 2013. 'Stoichiometry of Chromatin-Associated Protein Complexes Revealed by Label-Free Quantitative Mass Spectrometry-Based Proteomics'. *Nucleic Acids Research* 41 (1): e28–e28. https://doi.org/10.1093/nar/gks941.

Soding, J., A. Biegert, and A. N. Lupas. 2005. 'The HHpred Interactive Server for Protein Homology Detection and Structure Prediction'. *Nucleic Acids Research* 33 (Web Server): W244–48. https://doi.org/10.1093/nar/gki408.

Stielow, Bastian, Florian Finkernagel, Thorsten Stiewe, Andrea Nist, and Guntram Suske. 2018. 'MGA, L3MBTL2 and E2F6 Determine Genomic Binding of the Non-Canonical Polycomb Repressive Complex PRC1.6'. Edited by Luciano Di Croce. *PLOS Genetics* 14 (1): e1007193. https://doi.org/10.1371/journal.pgen.1007193.

Stott, D, A Kispert, and B G Herrmann. 1993. 'Rescue of the Tail Defect of Brachyury Mice.' *Genes & Development* 7 (2): 197–203. https://doi.org/10.1101/gad.7.2.197.

Sun, Jin, Jian Wang, Lin He, Yi Lin, and Ji Wu. 2015. 'Knockdown of Polycomb-Group RING Finger 6 Modulates Mouse Male Germ Cell Differentiation in Vitro'. *Cellular Physiology and Biochemistry* 35 (1): 339–52. https://doi.org/10.1159/000369700.

Sun, Xiaoyun, Ji Chen, Yanyong Zhang, Mumingjiang Munisha, Scott Dougan, and Yuhua Sun. 2018. 'Mga Modulates Bmpr1a Activity by Antagonizing Bs69 in Zebrafish'. *Frontiers in Cell and Developmental Biology* 6 (September): 126. https://doi.org/10.3389/fcell.2018.00126.

Sun, Yuhua, Wei-Chia Tseng, Xiang Fan, Rebecca Ball, and Scott T. Dougan. 2014. 'Extraembryonic Signals under the Control of MGA, Max, and Smad4 Are Required for Dorsoventral Patterning'. *Developmental Cell* 28 (3): 322–34. https://doi.org/10.1016/j.devcel.2014.01.003.

Surani, M. Azim. 2007. 'Germ Cells: The Eternal Link between Generations'. *Comptes Rendus Biologies* 330 (6–7): 474–78. https://doi.org/10.1016/j.crvi.2007.03.009.

Suzuki, Atsushi, Katsuhide Igarashi, Ken-ichi Aisaki, Jun Kanno, and Yumiko Saga. 2010. 'NANOS2 Interacts with the CCR4-NOT Deadenylation Complex and Leads to Suppression of Specific RNAs'. *Proceedings of the National Academy of Sciences* 107 (8): 3594–99. https://doi.org/10.1073/pnas.0908664107.

Suzuki, Atsushi, and Yumiko Saga. 2008. 'Nanos2 Suppresses Meiosis and Promotes Male Germ Cell Differentiation'. *Genes & Development* 22 (4): 430–35. https://doi.org/10.1101/gad.1612708.

Suzuki, Ayumu, Masataka Hirasaki, Tomoaki Hishida, Jun Wu, Daiji Okamura, Atsushi Ueda, Masazumi Nishimoto, et al. 2016. 'Loss of MAX Results in Meiotic Entry in Mouse Embryonic and Germline Stem Cells'. *Nature Communications* 7 (1): 11056. https://doi.org/10.1038/ncomms11056.

Syrjänen, Johanna Liinamaria, Luca Pellegrini, and Owen Richard Davies. 2014. 'A Molecular Model for the Role of SYCP3 in Meiotic Chromosome Organisation'. *ELife* 3 (June): e02963. https://doi.org/10.7554/eLife.02963.

Tachibana, Makoto, Jun Ueda, Mikiko Fukuda, Naoki Takeda, Tsutomu Ohta, Hiroko Iwanari, Toshiko Sakihama, Tatsuhiko Kodama, Takao Hamakubo, and Yoichi Shinkai. 2005. 'Histone Methyltransferases G9a and GLP Form Heteromeric Complexes and Are Both Crucial for Methylation of Euchromatin at H3-K9'. *Genes & Development* 19 (7): 815–26. https://doi.org/10.1101/gad.1284005.

Tanaka, Satomi S., Akihiro Nakane, Yasuka L. Yamaguchi, Takeshi Terabayashi, Takaya Abe, Kazuki Nakao, Makoto Asashima, Kirsten A. Steiner, Patrick P. L. Tam, and Ryuichi Nishinakamura. 2013. 'Dullard/Ctdnep1 Modulates WNT Signalling Activity for the Formation of Primordial Germ Cells in the Mouse Embryo'. Edited by Masaru Katoh. *PLoS ONE* 8 (3): e57428. https://doi.org/10.1371/journal.pone.0057428.

Tang, Walfred W. C., Toshihiro Kobayashi, Naoko Irie, Sabine Dietmann, and M. Azim Surani. 2016. 'Specification and Epigenetic Programming of the Human Germ Line'. *Nature Reviews Genetics* 17 (10): 585–600. https://doi.org/10.1038/nrg.2016.88.

Tatsumi, Daiki, Yohei Hayashi, Mai Endo, Hisato Kobayashi, Takumi Yoshioka, Kohei Kiso, Shinichiro Kanno, et al. 2018. 'DNMTs and SETDB1 Function as Co-Repressors in MAX-Mediated Repression of Germ Cell–Related Genes in Mouse Embryonic Stem Cells'. Edited by Osman El-Maarri. *PLOS ONE* 13 (11): e0205969. https://doi.org/10.1371/journal.pone.0205969.

Thorvaldsdottir, H., J. T. Robinson, and J. P. Mesirov. 2013. 'Integrative Genomics Viewer (IGV): High-Performance Genomics Data Visualization and Exploration'. *Briefings in Bioinformatics* 14 (2): 178–92. https://doi.org/10.1093/bib/bbs017.

Tosic, Jelena, Gwang-Jin Kim, Mihael Pavlovic, Chiara M. Schröder, Sophie-Luise Mersiowsky, Margareta Barg, Alexis Hofherr, et al. 2019. 'Eomes and Brachyury Control Pluripotency Exit and Germ-Layer Segregation by Changing the Chromatin State'. *Nature Cell Biology* 21 (12): 1518–31. https://doi.org/10.1038/s41556-019-0423-1.

Tsusaka, Takeshi, Kei Fukuda, Chikako Shimura, Masaki Kato, and Yoichi Shinkai. 2020. 'The Fibronectin Type-III (FNIII) Domain of ATF7IP Contributes to Efficient Transcriptional Silencing Mediated by the SETDB1 Complex'. *Epigenetics & Chromatin* 13 (1): 52. https://doi.org/10.1186/s13072-020-00374-4.

Uranishi, Kousuke, Masataka Hirasaki, Yuka Kitamura, Yosuke Mizuno, Masazumi Nishimoto, Ayumu Suzuki, and Akihiko Okuda. 2021. 'Two DNA Binding Domains of MGA Act in Combination to Suppress Ectopic Activation of Meiosis-Related Genes in Mouse Embryonic Stem Cells'. *Stem Cells* 39 (11): 1435–46. https://doi.org/10.1002/stem.3433.

Vainio, Seppo, Minna Heikkilä, Andreas Kispert, Norman Chin, and Andrew P. McMahon. 1999. 'Female Development in Mammals Is Regulated by Wnt-4 Signalling'. *Nature* 397 (6718): 405–9. https://doi.org/10.1038/17068.

Vincent, Stéphane D., N. Ray Dunn, Roger Sciammas, Miriam Shapiro-Shalef, Mark M. Davis, Kathryn Calame, Elizabeth K. Bikoff, and Elizabeth J. Robertson. 2005. 'The Zinc Finger Transcriptional Repressor Blimp1/Prdm1 Is Dispensable for Early Axis Formation but Is Required for Specification of Primordial Germ Cells in the Mouse'. *Development* 132 (6): 1315–25. https://doi.org/10.1242/dev.01711.

Wang, Hui, Elizabeth C Curran, Thomas R Hinds, Edith H Wang, and Ning Zheng. 2014. 'Crystal Structure of a TAF1-TAF7 Complex in Human Transcription Factor IID Reveals a Promoter Binding Module'. *Cell Research* 24 (12): 1433–44. https://doi.org/10.1038/cr.2014.148.

Wang, Xiaoyi, and Melissa E. Pepling. 2021. 'Regulation of Meiotic Prophase One in Mammalian Oocytes'. *Frontiers in Cell and Developmental Biology* 9 (May): 667306. https://doi.org/10.3389/fcell.2021.667306.

Wang, Yan, Hang Zhang, Haolin Zhong, and Zhidong Xue. 2021. 'Protein Domain Identification Methods and Online Resources'. *Computational and Structural Biotechnology Journal* 19: 1145–53. https://doi.org/10.1016/j.csbj.2021.01.041.

Washkowitz, Andrew J., Caroline Schall, Kun Zhang, Wolfgang Wurst, Thomas Floss, Jesse Mager, and Virginia E. Papaioannou. 2015. '*Mga* Is Essential for the Survival of Pluripotent Cells during Peri-Implantation Development'. *Development* 142 (1): 31–40. https://doi.org/10.1242/dev.111104.

Weber, Susanne, Dawid Eckert, Daniel Nettersheim, Ad J.M. Gillis, Sabine Schäfer, Peter Kuckenberg, Julia Ehlermann, et al. 2010. 'Critical Function of AP-2gamma/TCFAP2C in Mouse Embryonic Germ Cell Maintenance1'. *Biology of Reproduction* 82 (1): 214–23. https://doi.org/10.1095/biolreprod.109.078717.

Wehn, Amy K., Deborah R. Farkas, Carly E. Sedlock, Dibya Subedi, and Deborah L. Chapman. 2020. 'Functionally Distinct Roles for T and Tbx6 during Mouse Development'. *Biology Open* 9 (8): bio054692. https://doi.org/10.1242/bio.054692.

Western, Patrick S., Denise C. Miles, Jocelyn A. Van Den Bergen, Matt Burton, and Andrew H. Sinclair. 2008. 'Dynamic Regulation of Mitotic Arrest in Fetal Male Germ Cells'. *Stem Cells* 26 (2): 339–47. https://doi.org/10.1634/stemcells.2007-0622.

Yabuta, Yukihiro, Kazuki Kurimoto, Yasuhide Ohinata, Yoshiyuki Seki, and Mitinori Saitou. 2006. 'Gene Expression Dynamics During Germline Specification in Mice Identified by Quantitative Single-Cell Gene Expression Profiling1'. *Biology of Reproduction* 75 (5): 705–16. https://doi.org/10.1095/biolreprod.106.053686.

Yamaguchi, Shinpei, Kwonho Hong, Rui Liu, Li Shen, Azusa Inoue, Dinh Diep, Kun Zhang, and Yi Zhang. 2012. 'Tet1 Controls Meiosis by Regulating Meiotic Gene Expression'. *Nature* 492 (7429): 443–47. https://doi.org/10.1038/nature11709.

Yamaguchi, Shinpei, Kazuki Kurimoto, Yukihiro Yabuta, Hiroyuki Sasaki, Norio Nakatsuji, Mitinori Saitou, and Takashi Tada. 2009. 'Conditional Knockdown of *Nanog* Induces Apoptotic Cell Death in Mouse Migrating Primordial Germ Cells'. *Development* 136 (23): 4011–20. https://doi.org/10.1242/dev.041160.

Yamaguchi, Shinpei, Li Shen, Yuting Liu, Damian Sendler, and Yi Zhang. 2013. 'Role of Tet1 in Erasure of Genomic Imprinting'. *Nature* 504 (7480): 460–64. https://doi.org/10.1038/nature12805.

Yamaji, Masashi, Yoshiyuki Seki, Kazuki Kurimoto, Yukihiro Yabuta, Mihoko Yuasa, Mayo Shigeta, Kaori Yamanaka, Yasuhide Ohinata, and Mitinori Saitou. 2008. 'Critical Function of Prdm14 for the Establishment of the Germ Cell Lineage in Mice'. *Nature Genetics* 40 (8): 1016–22. https://doi.org/10.1038/ng.186.

Yeom, Y.I., G. Fuhrmann, C.E. Ovitt, A. Brehm, K. Ohbo, M. Gross, K. Hubner, and H.R. Scholer. 1996. 'Germline Regulatory Element of Oct-4 Specific for the Totipotent Cycle of Embryonal Cells'. *Development* 122 (3): 881–94. https://doi.org/10.1242/dev.122.3.881.

Ying, Ying, Xiaoxia Qi, and Guang-Quan Zhao. 2001. 'Induction of Primordial Germ Cells from Murine Epiblasts by Synergistic Action of BMP4 and BMP8B Signalling Pathways'. *Proceedings of the National Academy of Sciences* 98 (14): 7858–62. https://doi.org/10.1073/pnas.151242798.

Yokobayashi, Shihori, Ching-Yeu Liang, Hubertus Kohler, Peter Nestorov, Zichuan Liu, Miguel Vidal, Maarten van Lohuizen, Tim C. Roloff, and Antoine H. F. M. Peters. 2013. 'PRC1 Coordinates Timing of Sexual Differentiation of Female Primordial Germ Cells'. *Nature* 495 (7440): 236–40. https://doi.org/10.1038/nature11918.

Yoshikawa, Toshiyuki, Yulan Piao, Jinhui Zhong, Ryo Matoba, Mark G. Carter, Yuxia Wang, Ilya Goldberg, and Minoru S.H. Ko. 2006. 'High-Throughput Screen for Genes Predominantly Expressed in the ICM of Mouse Blastocysts by Whole Mount in Situ Hybridization'. *Gene Expression Patterns* 6 (2): 213–24. https://doi.org/10.1016/j.modgep.2005.06.003.

Yu, Guangchuang, Li-Gen Wang, Yanyan Han, and Qing-Yu He. 2012. 'ClusterProfiler: An R Package for Comparing Biological Themes Among Gene Clusters'. *OMICS: A Journal of Integrative Biology* 16 (5): 284–87. https://doi.org/10.1089/omi.2011.0118.

Yu, Guangchuang, Li-Gen Wang, and Qing-Yu He. 2015. 'ChIPseeker: An R/Bioconductor Package for ChIP Peak Annotation, Comparison and Visualization'. *Bioinformatics* 31 (14): 2382–83. https://doi.org/10.1093/bioinformatics/btv145.

Zagore, Leah L., Thomas J. Sweet, Molly M. Hannigan, Sebastien M. Weyn-Vanhentenryck, Chaolin Zhang, and Donny D. Licatalosi. 2018. 'Dazl Regulates Germ Cell Survival through a Network of PolyA-Proximal MRNA Interactions'. *BioRxiv*, February, 273292. https://doi.org/10.1101/273292.

Zernicka-Goetz, Magdalena, Samantha A. Morris, and Alexander W. Bruce. 2009. 'Making a Firm Decision: Multifaceted Regulation of Cell Fate in the Early Mouse Embryo'. *Nature Reviews Genetics* 10 (7): 467–77. https://doi.org/10.1038/nrg2564.

Zhang, Yong, Tao Liu, Clifford A Meyer, Jérôme Eeckhoute, David S Johnson, Bradley E Bernstein, Chad Nusbaum, et al. 2008. 'Model-Based Analysis of ChIP-Seq (MACS)'. *Genome Biology* 9 (9): R137. https://doi.org/10.1186/gb-2008-9-9-r137.

Zimmermann, Lukas, Andrew Stephens, Seung-Zin Nam, David Rau, Jonas Kübler, Marko Lozajic, Felix Gabler, Johannes Söding, Andrei N. Lupas, and Vikram Alva. 2018. 'A Completely Reimplemented MPI Bioinformatics Toolkit with a New HHpred Server at Its Core'. *Journal of Molecular Biology* 430 (15): 2237–43. https://doi.org/10.1016/j.jmb.2017.12.007.

Abbreviations

bHLH/Zip	basic helix loop helix leucine zipper domain
DNMT1/3A/3B	DNA methyltransferase 1/3A/3B
DUF	domain unknow function
E	Embryonic day
EPI	Epiblast
EpiLCs	Epiblast-like cells
ExE	Extra-embryonic ectoderm
H2A/H4R3me2s	H2A/H4 arginine 3 symmetrical methylation
H2AK199ub1	mono-ubiquitination of Lys 199 of H2A
H3K27me3	H3 lysine 27 trimethylation
H3K9me2	H3 lysine 9 dimethylation
ICM	inner cell mass
mESCs	mouse embryonic stem cells
MGA	MAX giant associated protein
ncPRC1.6	non-canonical Polycomb repressive complex 1.6
PE	primitive endoderm
PcG	Polycomb repressive complex
PGCLCS	PGC-like cells
PGCs	Primordial germ cells
TE	Trophectoderm
TET1/2/3	ten-eleven translocation
WGBS	whole genomic bisulfite sequencing

Curriculum Vitae

Erica Calabrese

Address	Mauerstraße 24, 37073, Göttingen, Germany
Email	erica.c99@hotmail.com
Phone	+49(0)1732731809

Education

PhD student at International Max Planck Research School for Genome Science

Affiliation	Georg-August-Universität, Department of Developmental Biology (GZMB), Göttingen, Germany
Dates	09/2018-Present
Group Leader	Dr. Ufuk Günesdogan

Master's degree in Molecular and Cellular Biology,
110/110 magna cum Laude (First class honours)

Affiliation	Alma Mater Studiorum, University of Bologna, Department of Pharmacy and Biotechnology (FaBiT) of University of Bologna, Bologna, Italy
Dates	10/2014-12/2016
Group Leader	Prof. Dr. Giovanni Perini
Final Thesis	"Role of MAX and MNT transcription factors in neuroblastoma biology"

Bachelor's degree in Biological Sciences ,100/110
(Second class honours upper division)

Affiliation	Alma Mater Studiorum, University of Bologna, Department of Pharmacy and Biotechnology (FaBiT) of University of Bologna, Bologna, Italy
Dates	10/2011-10/2014
Group Leader	Prof. Dr. Giovanni Venturoli
Final Thesis	"Dehydration affects the electronic structure of the primary electron donor in photosynthetic reaction centre"

Work experiences

	Research Technician
Affiliation	Gurdon Institute, Henry Wellcome Building of Cancer and Developmental Biology, Cambridge, United Kingdom
Dates	02/2018-07/2018
Group Leader	Prof. Dr. Azim Surani
Description	I was responsible for maintaining the laboratory organization and generating various common laboratory reagents (i.e. colture medium hESC/iPSC)

Conferences and Meeting

2022	Japan-UK Regulation through Chromatin Conference, United Kingdom "The context-dependent role of MGA during primordial germ cell development", poster presentation

Workshops

2022	Scientific Writing: "How to start" to "How to publish", Graduate Academy at Clausthal University of Technology, Clausthal-Zellerfeld, Germany.
2021	MaxQuant Summer School, Online, Germany.
2019	Sequence analysis of proteins and their post-translational modifications by electrospray ionization (ESI) mass spectrometry, Max Planck Institute for Multidisciplinary Sciences Bioanalytical Mass Spectrometry, Göttingen, Germany Introduction to R and RNA-seq, Georg-August-Universität, Göttingen, Germany. Learn to Analyze RNA-seq and ChIP-seq Data, Galaxy Course, NGS Integrative Genomics Core Unit (NIG) and the core Facility Medical Biometry and Statistical Bioinformatics (MBSB) Georg-August-Universität, Göttingen, Germany.

Language

First language	Italian, native proficiency
Second language	English, advanced proficiency
Third language	German, elementary proficiency